MODELLING AND EXPERIMENTAL STUDIES

OF

A CONTINUOUS EMULSION POLYMERIZATION REACTOR

by

Constantine Kiparissides, Dipl.Eng., M. Eng.

A Thesis

Submitted to the School of Graduate Studies

in Partial Fulfilment of the Requirements

for the Degree

Doctor of Philosophy

McMaster University

November, 1978

CONTINUOUS LATEX REACTOR-MODELLING AND EXPERIMENTAL STUDIES

To my best friend and wife

ZINA

DOCTOR OF PHILOSOPHY
(Chemical Engineering)

McMaster University
Hamilton, Ontario

TITLE: Modelling and Experimental Studies of a Continuous Emulsion Polymerization Reactor

AUTHOR: Constantine Kiparissides, Dipl.Eng. (Natl. Tech. University of Athens); M.Eng. (McMaster University)

SUPERVISORS: Dr. A.E. Hamielec, Dr. J.F. MacGregor

NUMBER OF PAGES: xxiii, 295

ABSTRACT

In continuous emulsion polymerization the commercially important phenomena of sustained oscillations and large start-up transient conversion overshoots have been observed by several investigators. Experimental studies have shown that the conversion, number of polymer particles and all other related properties often oscillate with time. In other words a steady state is never achieved. These oscillations can lead to emulsifier levels too small to adequately cover polymer particles with the result that excessive agglomeration and reactor fouling can occur. Furthermore, excursions to high polymer concentrations, due to the cycling behaviour of conversion can result in excessive branching and poor polymer processability. It is evident that this reactor behaviour is highly undesirable since it results in a continuously varying product quality.

In this thesis, the complex physical and chemical phenomena occurring in a continuous emulsion polymerization reactor are studied both experimentally and mathematically. Dynamic models suitable for prediction and on-line control studies are developed based on particle age distribution. On-line techniques are developed to measure some states of the control model and to monitor the reactor performance. These techniques are based on turbidity measurements and liquid exclusion chromatography. A multivariable stochastic control algorithm is developed

to control the pathological behaviour of continuous emulsion polymerization reactors and ensure a high productivity and product quality.

ACKNOWLEDGEMENTS

The author wishes to thank all those who contributed to this work. He is particularly indebted to:

His research directors, Drs. A.E. Hamielec and J.F. MacGregor for their encouragement and moral support throughout the course of this work.

Dr. S. Singh for his support on the experimental aspects of this work.

All members of the Control and Polymer Groups at McMaster University and in particular Mr. L.H. Garcia for their lively discussions.

Miss Veronica Komczynski for her care and patience in typing this thesis.

My parents for their affection and moral support.

Finally, I wish to express my gratitude to the Department of Chemical Engineering, McMaster University, for providing financial assistance.

TABLE OF CONTENTS

LIST OF FIGURES

LIST OF TABLES

NOMENCLATURE

A	(nxn) dynamic state matrix
A_m	total surface area of micelles, dm^2/ℓ-latex
$A_n(t,\tau)$	surface area of $n(t,\tau)$ class of polymer particles, dm^2/ℓ-latex
A_p	total surface area of polymer particles, dm^2/ℓ-latex
$\underset{\sim}{a}$	(7x1) vector of absorbance values
a_p	interfacial area of a particle, dm^2/particle
a_s	area occupied by an emulsifier mole dm^2/mole
B	control matrix
D_p	diffusion coefficient of monomeric radicals in the polymer particles, dm^2/sec
D_{pp}	particle diameter
DP_{max}	maximum degree of polymerization
d_m	density of monomer, gr/ℓ
d_p	density of polymer gr/ℓ
fk_d	effective rate coefficient of initiator decomposition, sec^{-1}
$f(t)$	net rate of particle nucleation, 1/sec-ℓ-latex
H	measurement matrix
I	initiator
$[I]_w$	initiator concentration, molecules/ℓ-latex

$[I]_{feed}$	initiator concentration in the feed, molecules/ℓ-latex
I_m	m^{th} order unity matrix
K	parameter in equations (2.51)-(2.52)
K	growth rate constant in equation (2.21)
k_a	capture rate constant equation (2.79)
k_{ab}	overall transport coefficient for radical transfer from the aqueous phase into polymer particles, dm/sec
$k_c(v,v',\sigma_p)$	coef. of coalescence between two particles of volumes v and v' with electric charge density of σ_p, ℓ/mole-sec
k_d	rate coefficient of initiator decomposition, sec^{-1}
k_{de}	the rate coefficient of radical escape from the polymer particles, sec^{-1}
k_{fm}	rate coefficient of chain transfer to monomer, ℓ/mole-sec
k_{ho}	rate coefficient of homogeneous nucleation, sec^{-1}
k_m	rate coefficient of micellar nucleation dm/sec
k_p	rate coefficient of polymer propagation, ℓ/mole-sec
k_{tw}	rate coefficient of termination in aqueous phase
k_v	volume of emulsion phase over the volume of aqueous phase, ℓ-latex/ℓ
L	critical diffusion length, dm
$\underset{\sim}{\ell}_i$	ith principal eigenvector
M	monomer
M_F	monomer concentration in the feed, mole/ℓ-latex

M_T	total monomer concentration in the reactant, mole/ℓ-latex
M_w	molecular weight of monomer
M_{wc}	saturation concentration of monomer in the water phase, mole/ℓ
m	partition coefficient of monomeric radicals between water and particle phase, equations (2.50)-(2.53)
m	ratio of refractive indices n/n_m, equations (3.9)-(3.10) (refractive index of particles/refractive index of suspending medium)
m_s	micelle
Na	Avogadro's number
N(t)	total number of particles at t, 1/ℓ-latex
N_q	number of particles with q radicals
$n(t,\tau)$	number of particles at time t which were born at time τ, 1/ℓ-latex
$n(t,\tau_i)$	number of particles at t which were born at τ_i
P(t)	total polymer property at time t
$p(t,\tau)$	a polymer property associated with particles of $n(t,\tau)$ class
$\bar{q}(t,\tau)$	average number of radicals per particle of class $n(t,\tau)$, molecules
$\bar{q}_i$	average number of radicals per particle of the ith generation, molecules
q_t	denotes the number of discrete particle generations
R	free radical

$[R]_{feed}$	free radical concentration in the feed stream, molecules/ℓ-latex
$[R]_w$	free radical concentration in the aqueous phase, molecules/ℓ-latex
R_w	variance covariance matrix for $\underline{w}(k)$
R_v	variance covariance matrix for $\underline{v}(k)$
r_t	total number of all particle $n(t,\tau)$ classes
$r(t,\tau)$	radical initiation rate corresponding to $n(t,\tau)$ class of particles
S_F	total emulsifier concentration in inflow, dm^2/ℓ-latex
S_T	total emulsifier concentration in the reactor, dm^2/ℓ-latex
S_{CMC}	critical micelle concentration
T	sampling time, sec
t	time, sec
$\underline{u}$	vector of manipulated variables
V_p	total polymer volume, ℓ/ℓ-latex
v_m	volume of a micelle
v_o	volume of a precipitated oligomer particle
$v(t,\tau)$	volume of a particle associated with the $n(t,\tau)$ class of particles, ℓ
$v_p(t,\tau)$	polymer volume of a particle, ℓ
$\bar{v}_{pi}$	average polymer volume for a particle of the ith generation,
x_c	monomer conversion at which monomer droplets disappear, 20%
x(t)	total monomer conversion

x_i	monomer conversion of the ith generation of particles
$\underset{\sim}{x}$	state vector
$\dot{\underset{\sim}{x}}$	time derivative of state vector
$\hat{\underset{\sim}{x}}(k/k)$	state estimate of $\underset{\sim}{x}$
$\underset{\sim}{y}$	vector of output variables
$\underset{\sim}{z}$	augmented state vector
α	k_t/Na in equation (2.21)
β	$(4\Pi)^{1/3}(3)^{2/3}\rho_A/(S)$ parameter in equation (2.21)
γ	$(4\Pi)^{1/3}(3)^{2/3}k_o$ parameter in equation (2.21)
$\Delta\tau_i$	time interval, sec
δ	$(1+D_w/D_p m)^{-1}$ parameter in (2.52)
ε	k_{ab}/k_m ratio
θ	mean residence time, sec
μ	k_{ho}/k_m ratio
$\mu(t,\tau)$	rate of particle volume growth associated with a particle of $n(t,\tau)$ class, ℓ/molecules-sec
$\mu_p(t,\tau)$	rate of polymer volume growth associated with a particle of $n(t,\tau)$ class
ρ_A	total rate of radical absorption in the particles molecules/ℓ-sec
ρ_i	the rate of radical production in the aqueous phase
σ_p	electric charge density in the surface of a particle
ϕ	monomer volume fraction in a particle
ψ	surface potential
$'$	denotes transpose of a matrix, e.g., ϕ'

denotes vector, e.g., $\underset{\sim}{w}$

denotes estimate, e.g., $\hat{\underset{\sim}{x}}(k/k)$

denotes derivative with respect to time, e.g., $\dot{\underset{\sim}{x}}$

CHAPTER 1

INTRODUCTION AND OBJECTIVES

This Chapter is provided as a guide to the variety of topics covered in this thesis since the subject being treated involves such a wide spectrum of complex techniques from the fields of polymerization, surface chemistry, mathematical modelling, on-line techniques for polymer characterization, and reactor design, as well as modern multivariable control theory. However, the ultimate objective of this study is to develop a multivariable stochastic control scheme to control the pathological behaviour of continuous emulsion polymerization reactors and ensure a high productivity and product quality.

Continuous stirred tank reactors typically have inherent advantages for large scale commercial production. High reaction rates and high molecular weight polymers, with good yields of an easily handled, low viscosity latex which is suitable for many direct applications, all lend favourably to the continuous process. In addition, minimum manpower and maintenance, easier operation and control, more consistent product quality, and higher throughputs provide incentives for a broader use of continuous systems in the polymer industry. Examples of polymers produced in this way include styrene-butadiene copolymer, polychloroprene and polyvinylchloride.

It is believed that in the near future other polymers such as polyvinyl-acetate and its copolymers, which are used as latices, may be produced commercially on large scale in continuous emulsion reactors. The feasibility of commerical production of polymer and copolymer latices in continuous reactors is closely related with the control of the polymer properties of the latex product. Such properties include the particle size distribution of polymer latex, average particle diameters, molecular weight distribution etc.

One very interesting feature of continuous emulsion polymerization reactors is the appearance of commercially important phenomenon of sustained oscillations. Experimental investigations of emulsion polymerization in CSTR's have shown that the conversion, number of polymer particles and all other related properties oscillate often widely with time. In other words a steady state is never achieved. These oscillations can lead to emulsifier levels too small to adequately cover polymer particles with the result that excessive agglomeration and reactor fouling can occur. Furthermore, excursions to high polymer concentrations, due to the cycling behaviour of conversion can result in polymers with excessive branching and poor processability. It is evident that this reactor behaviour is highly undesirable since it results in a continuously varying product quality.

It is thus our research aim to study both experimentally and mathematically the continuous emulsion polymerization, understand sufficiently the complex physical and chemical phenomena occurring in a continuous polymerizer and develop dynamic models suitable for prediction and control of latex reactors. Moreover, minicomputer control of the product quality

from a continuous latex reactor involves the development of on-line detectors for measuring some states of the control model or even the polymer particle size distribution. It is believed that this study can offer new reactor designs which will ensure a high standard of product quality and operation of reactor free of undesirable oscillations.

This thesis has been divided into eight Chapters which closely follow the chronological development and progress of this study.

In Chapter 2, a sufficiently detailed historical review of emulsion polymerization is presented. Different mathematical models concerning mainly the batch process are derived. Dynamic phenomena in continuous emulsion reactors that have been reported in the literature are discussed. Finally, a general mathematical framework based on population balance principles is developed to describe the emulsion polymerization process. An application of this model is given by deriving the integro-differential balances which describe the total latex properties in a continuous reactor (conversion, total number of particles etc.) and by considering that each latex particle can be identified by its age distribution function.

Chapter 3 reviews some of the most common analytical methods that are used to determine the particle size distribution or some average particle diameter of the latex. Turbidity spectra analysis and liquid exclusion chromatography appear to be suitable for on-line measurements. They are simple, fast, can be easily implemented and used as on-line detectors. An alternative approach to the interpretation of turbidity spectra and to relating them to the model states is presented. This method

uses strictly empirical regression models based on principal components of turbidity data.

In Chapter 4, extensive experimental results are presented. The effects of initiator, emulsifier concentrations, mean residence time and rate of agitation on the production rate of polyvinyl acetate latices in a CSTR are investigated. Domains of conditions which give rise to sustained oscillations or complete agglomeration of the product are mapped out. The effect of different start-up policies on reactor transients is investigated. This Chapter starts with a description of the experimental set-up and polymerization procedure.

In Chapter 5, the problem of fitting the simplified model to conversion data obtained from the reactor is discussed. The unknown kinetic parameters of the model are estimated using a non-linear estimation program. The existence of limit cycles (sustained oscillations) is theoretically studied and closed trajectories in the phase plane are drawn to indicate the existence of sustained oscillations.

In Chapter 6, turbidity and LEC measurements are shown to follow satisfactorily all reactor variations. Turbidity data obtained over a wide range of operating conditions are analyzed to give regression models which adequately predict conversion and polymer volume as a function of turbidity measurements.

In Chapter 7, control and start-up policies for continuous emulsion reactors are investigated. To derive a multivariable stochastic control algorithm for the reactor a linear state model is derived from the non-linear

one. Subsequently, a discrete model is obtained suitable for computer control. The optimal feedback control settings are obtained by minimizing a linear quadratic objective function. A new reactor design is proposed for implementation and on-line control of a continuous emulsion reactor.

Chapter 8 discusses the significance of this work and possible extensions of it.

This study is intended to provide the ground work for a series of future application studies on latex reactors which aim to improve the performance of such complex system and encourage, therefore, the application of modern control theory to industrial polymer reactors.

CHAPTER 2

ON THE MATHEMATICAL MODELLING OF EMULSION POLYMERIZATION REACTORS

2.1 Introduction

Emulsion polymerization often has significant advantages over homogeneous bulk or solution polymerization in commercial production of polymers. Aside from the obvious physical advantages when a polymer latex is the final product as in paints or other coatings, there are distinct processing advantages. For example, low viscosity and good temperature control can often be achieved in an emulsion polymerization when this is impossible in bulk. In addition, high molecular weight polymer can usually be produced at much higher reaction rates in an emulsion polymerization reactor than in a bulk polymerization. For these and other reasons, emulsion polymerization has become a multi-billion dollar/year processing operation in terms of sales.

In spite of the industrial importance of these reactors and the fact that emulsion polymerization has been studied seriously for 30 years, the complex kinetics inherent in the reaction scheme has long obscured details of the process. Even today there is disagreement among investigators regarding some of the mechanisms involved.

Most early workers in the field chose to use batch reactor equipment to investigate emulsion polymerization. However, batch reactors tend to be time variant, that is, transient phenomena are introduced. Continuous emulsion polymerization reactors may be operated at a truly "steady state" condition, thereby allowing easier control of the process. In addition, as production volumes increase and as more and more industrial processes become continuous, a more comprehensive analysis of emulsion polymerization becomes more important.

Industrial emulsion polymerization processes may be classified into two distinct groups according to the ultimate use of the latex product. In some processes, the latex is merely an intermediate product which in a later stage of production is coagulated to give the bulk polymer. Examples of this kind of emulsion process include the production of PVC, ABS, SBR, and neoprene rubber. The other group of emulsion processes produces latices which after suitable treatment are used as latices. The production of poly (vinyl acetate) and poly (ethyl acrylate) latex paints and adhesives are typical examples of this type of emulsion process.

There is available an enormous literature on emulsion polymerization; therefore, an exhaustive bibliography will not be presented, but instead an outline of the present state of the theories for emulsion polymerization and some examples of their predictive capabilities will be given. For a detailed bibliography on emulsion polymerization the reader can be referred to the excellent review papers of Min and Ray (1974), Ugelstad and Hansen (1976), Poehlein and Dougherty (1977).

2.2 Emulsion Polymerization

In section 2.2.1 a qualitative picture of emulsion polymerization is presented. A review of previous theoretical approaches of Harkins and Smith is given in sections 2.2.2 and 2.2.3, then these are compared with the nucleation theories of Roe and Fitch in section 2.2.4.

2.2.1 The Physical Picture

An emulsion polymerization recipe comprises four essential ingredients, namely dispersion medium, monomer, initiator and emulsifier.

Such a "recipe" might be 100 parts dispersion medium, 50 parts monomer, 2 parts emulsifier, and 0.1 part initiator. In general, the dispersion medium is water and the monomer must be only partially soluble in it. On the other hand, the initiator must dissolve in the dispersion medium and not in the monomer.

The initiator system used in emulsion polymerization depends on the polymerization temperature used. Dissociative initiators, such as potassium and sodium persulfate are commonly used when the polymerization occurs at moderate to high temperature, i.e. above $50^{o}C$.

The emulsifier consists of molecules which are hydrophobic at one end and hydrophilic at the other. Typical emulsifiers used in industrial formulations include sodium and potassium salts of saturated long-chain acids such as lauric acid and palmitic acid, and sodium n-alkyl sulfates like sodium lauryl sulfate. The emulsifier plays several roles during the polymerization. Firstly, it serves to stabilize the monomer droplets in

the dispersion medium. Secondly, according to the classic theory of emulsion polymerization mechanism the presence of emulsifier is essential for formation of polymer particles. Thirdly, the emulsifier serves to stabilize the polymer particles being formed during the polymerization. Without the presence of a suitable type and amount of emulsifier the polymer particles would coalesce and a stable dispersion would not be obtained.

Owing to attractive forces between their hydrophobic ends, the emulsifier molecules form aggregates, so called micelles, when their concentration exceeds a certain critical value, the critical micelle concentration, C.M.C. Since the interior milieu of micelles thus is strongly hydrophobic, they are able to dissolve a certain amount of monomer, a phenomenon which is often referred to as solubilization. Thus, the monomer can be found in three different loci, before the polymerization begins. The major part, typically more than 95% is present as 1-10μ monomer droplets. A considerably smaller amount is solubilized in the micelles, being 50-100Å in diameter. Finally, a certain amount of monomer is present as an actual solution in the aqueous phase.

In what follows the manner in which a number of workers have constructed models based on specific mechanistic assumptions is discussed.

2.2.2 Kinetics and Mechanism

Harkins (1947) was the first to propose a mechanism for emulsion polymerization. For the nucleation and the progression of polymerization, he assumed:

i. Free radicals are produced in the aqueous phase and are

captured by the micelles. The monomer in the stung micelle is polymerized, whereby the micelle is transformed into a polymer particle. Thus, the micelle is the principal locus for nucleation of polymer particles.

ii. The principal locus of polymer formation is the polymer particle swollen with monomer.

iii. The monomer droplets serve as reservoirs from which by diffusion through the aqueous phase monomer molecules are fed to the growing particles.

iv. Particle formation ceases after all uninitiated micelles disappear, the particles formed simply grow until all the monomer is depleted.

v. Propagation reaction in a polymer particle stops when another free radical enters to terminate the reaction. The particle then grows again when a new radical enters, etc.

According to this qualitative scheme, emulsion polymerization may be considered as involving three intervals (Figure 2-1). During interval I polymer particles are generated. Part of the micelles is used for nucleation of polymer particles and part of them disintegrates to deliver the emulsifier necessary for stabilization of the growing polymer particles. In general only a very small fraction of the micelles is used for particle nucleation. At the end of stage I all micelles are consumed, and the generation of polymer particles ceases. In typical emulsion polymerization the final number of particles per litre emulsion is of the order 10^{16}-10^{18}.

During interval II the polymer particles grow. Owing to a rapid diffusion of monomer from the monomer droplets into the polymer particles, the particles are saturated with monomer as long as the separate monomer

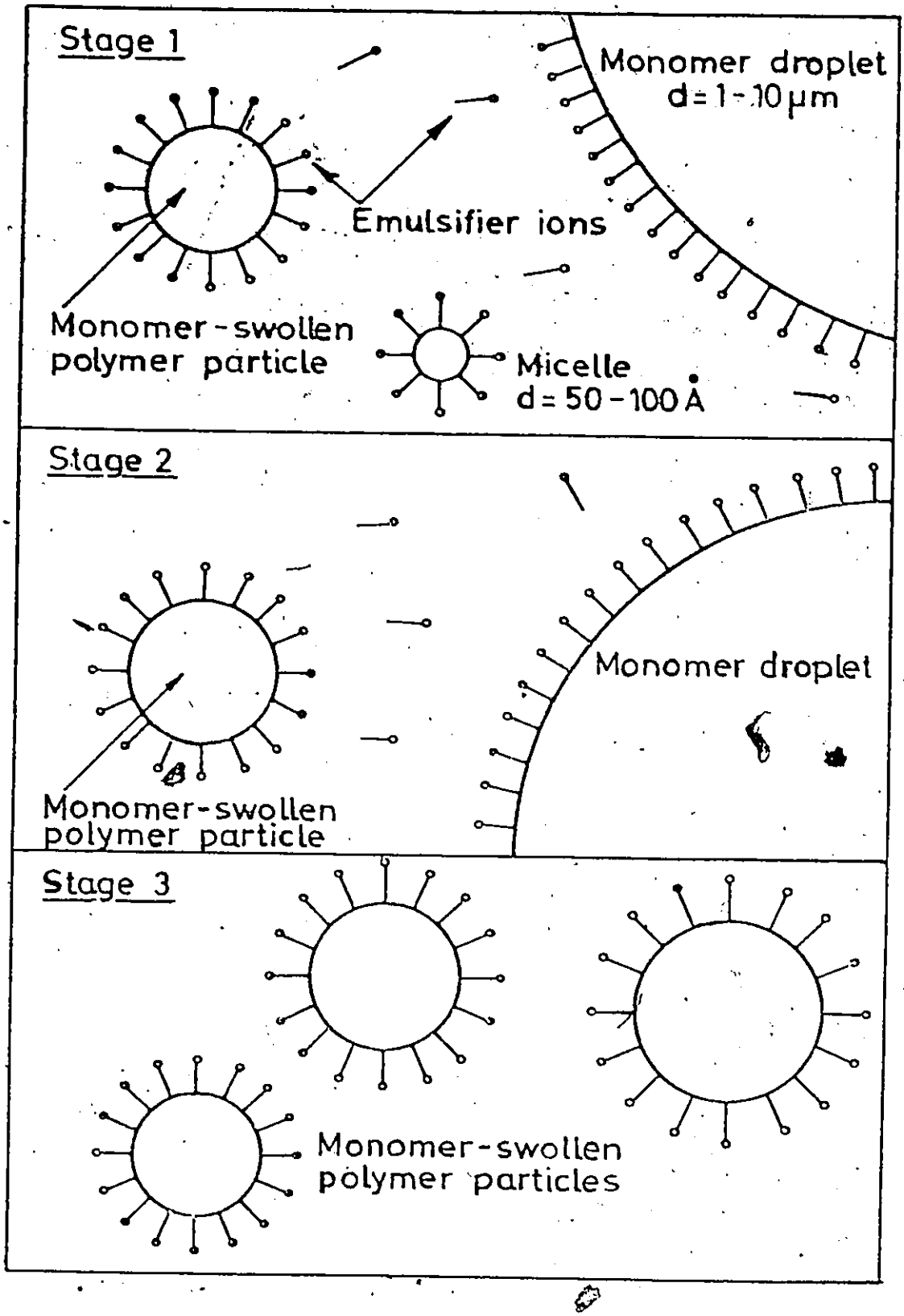

Figure (2-1) Schematic Representation of Emulsion Polymerization Mechanism

phase is present. Hence, the monomer-polymer ratio and therefore the monomer concentration within the particles remains constant. At the end of stage II the separate monomer phase vanishes.

In interval III the dispersion consists of only two phases, namely the water phase and the polymer phase (monomer-swollen polymer particles). If no new monomer is supplied to the particles, the concentration of monomer in the particles decreases steadily during this stage.

This very simple picture proposed by Harkins forms the basis for most of the quantitative theories to follow.

2.2.3 The Smith-Ewart Theory

Interval I. The kinetics of this stage is dependent upon the particle nucleation mechanism. The Smith-Ewart theory (1948) assumes nucleation in monomer-swollen soap micelles. The nucleation stops when all the micelles are consumed. The equation for the particle number may be derived in two ways which gives an upper and a lower limit for the particle number. The upper limit implies that only micelles can absorb free radicals, while the lower limit is calculated on the basis that both particles and micelles absorb radicals at a rate proportional to the surface area.

Upper Limit. The rate of particle generation is proportional to the rate of radical production from the initiator, ρ_i, (the symbols are defined in the nomenclature)

$$\frac{dN}{dt} = \rho_i \qquad (2.1)$$

This rate of particle nucleation is constant up to the time when the total area of polymer particles A_p is equal to the total surface area of soap, $a_s S$, where S is the total amount of soap in the system and a_s the specific area per unit amount of soap.

Lower Limit. In this case the particles are assumed to absorb radicals at a rate proportional to their surface area, A_p,

$$\frac{dN}{dt} = \rho_i\left(1 - \frac{A_p}{a_s S}\right) \tag{2.2}$$

The differential equations (2.1) and (2.2) may be easily solved (Ugelstad et al. (1976)) to give

$$N = k\left(\frac{\rho_i}{\mu}\right)^{.4} (a_s S)^{.6} \tag{2.3}$$

for the total number of polymer particles at the end of interval I, where k = .53 when radicals enter micelles only (upper limit), and k = .37 when radicals enter both micelles and particles in proportion to their respective total surface areas (lower limit). Equation (2.3) has been tested experimentally and in some cases has been found to fit experimental data well, especially for styrene and other water-insoluble monomers. On the other hand, equation (2.3) is in disagreement with experimental results obtained with vinyl chloride and vinyl acetate and actually it has been shown for these monomers that there is no effect of initiator concentration on N.

Interval II. The basic problem in emulsion polymerization is the determination of the average number of radicals per particle. Smith and Ewart (1948) applied the following recursion formula to calculate N_q, the number of

polymer particles having q radicals

$$\rho_A \frac{N_{q-1}}{N} + (q+1)k_d N_{q+1} + (q+2)(q+1)\left(\frac{k_t}{v}\right)N_{q+2}$$

$$= \rho_A \frac{N_q}{N} + qk_d N_q + q(q-1)\left(\frac{k_t}{v}\right)N_q \qquad (2.4)$$

where ρ_A is the total rate of radical absorption in the particles; k_d the rate "constant" for desorption of radicals from the particles; k_t the termination constant in the particles; N the total number of particles; and v the particle volume.

Equation (2.4) is obtained by setting $dN_q/dt = 0$. The terms on the left side give the rate of formation of particles containing q radicals, those on the right the rate of disappearance. Equation (2.4) is simplified for three different limiting cases:

Case 1. $\bar{q} << .5$ Under this condition $N_o >> N_1 >> N_{\bar{q}}$ and accordingly one has only to consider the first of the relations of equation (2.4),

$$N_1 k_d \simeq \rho_A \frac{N_o}{N} \qquad (2.5)$$

$$\rho_A \simeq k_d N_1 \simeq k_d N\bar{q} \qquad (2.6)$$

If termination in particles is dominating so that there is immediate termination when a radical enters a particle already containing a radical, then a steady state treatment gives

$$\rho_i = 2\left(\frac{\rho_A}{N}\right)N_1 \qquad (2.7)$$

Substituting ρ_A from equation (2.6) and recognizing that $N_1/N \approx \bar{q}$ gives

$$\bar{q} = \left(\frac{\rho_i}{2Nk_d}\right)^{\frac{1}{2}} \tag{2.8}$$

Case 2. $\bar{q} = .5$ This case, which is most generally known as the Smith-Ewart theory, considers that desorption may be neglected, which in turn, if termination in the water phase is negligible, implies that $\rho_A = \rho_i$. The solution for this case is also obvious and is treated in a large number of references for emulsion polymerization.

Case 3. $\bar{q} >> 1$ If desorption of radicals from the particles can be neglected, i.e., $\rho_A = \rho_i$, then the steady-state condition for this case is simply

$$\frac{\rho_A}{N} = 2\frac{k_t}{v}\bar{q}^2 \tag{2.9}$$

and

$$\bar{q} = \frac{(\rho_A V_p/2k_t)^{\frac{1}{2}}}{N} \tag{2.10}$$

where V_p, the total polymer volume, is equal with Nv.

Stockmayer's solution. The general solution of the Smith-Ewart equation (2.4) was first presented by Stockmayer (1957). His analytical solution, with some corrections by O'Toole (1965), takes the form

$$N_q = a^{q}2^{(b-1-3q)/2}\frac{I_{b+q-1}(a\sqrt{2})}{q!\,I_{b-1}(a)} \tag{2.11}$$

where $I_k(x)$ is the modified Bessel function of the first kind. This leads to the expression for the average number of radicals per particle as

$$\bar{q} = \frac{\sum_{q=0}^{\infty} qN_q}{N} = \begin{cases} \frac{1-b}{2} + \frac{a}{4}\frac{I_{b-2}(a)}{I_{b-1}(a)}, & \text{for } b \geq 1 \\ \frac{a}{4}\frac{I_b(a)}{I_{b-1}(a)} & \text{for } 0 < b \leq 1 \\ \frac{a}{4}\frac{I_o(a)}{I_1(a)} & \text{for } b = 0 \end{cases} \qquad (2.12)$$

where

$$a = \left(\frac{8V_p N_a \rho_A}{k_t N}\right)^{\frac{1}{2}}, \quad b = \frac{k_d a_p N_a}{k_t} \qquad (2.13)$$

The magnitude of the parameter, a, represents the relative importance of the initiation and chain termination mechanism, while the value of b represents the relative rate of radical desorption to radical termination.

If, as is usually the case, the rate of reaction, R_p, may be set equal to the rate of reaction within the particles,

$$R_p = -\frac{dM}{dt} = k_p [M]_p \bar{q} \frac{N}{N_a} \qquad (2.14)$$

where k_p is the propagation constant in the particles and $[M]_p$ is the

concentration of monomer in the particles.

O'Toole's treatment (eq. 2.12) gives a correct expression for $\bar{q}$ as a function of a and b whenever a is determined by ρ_A. It would clearly be preferable to have $\bar{q}$ expressed by the independent variable ρ_i, the rate of radical production in the aqueous phase. Ugelstad et al. (1967) derived a general method for calculation of $\bar{q}$ taking into account reabsorption of radicals into the particles and eventual contribution of termination in the aqueous phase. To achieve this they coupled the quasi-steady-state particle radical balance (eq. 2.4) to a quasi-steady-state radical balance in the aqueous pahse

$$\rho_A = \rho_i + \sum_{q=0}^{\infty} k_d N_q q - 2k_{tw}[R]_w^2 \qquad (2.15)$$

Although Ugelstad et al. calculated $\bar{q}$ numerically for this case, Min (1976) has shown that these results can be obtained analytically.

Modified Smith-Ewart Theory. In a series of papers Gardon (1968a,b) treated interval I and II of emulsion polymerization in detail. Gardon (1968a) solved numerically the nonsteady-state expression (2.4) for the number of particles containing $\bar{q}$ radicals without making the quasi-steady state assumption and neglecting radical desorption. However, his results clearly showed the validity of the quasi-steady state approximation because numerically his results were identical to those of Stockmayer (1957). Both of these results showed that due to the increase in the size of the polymer particles, $\bar{q}$ would increase with conversion so that both the rate of polymerization and average molecular weight would increase with

conversion in Interval II.

Katz and Saidel (1968),(1969) presented both a stochastic and deterministic model for the rate of polymerization and polymer size distribution in interval II. In an isothermal batch reactor they assumed, (i) all particles are the same size, (ii) a constant number of particles, and (iii) all the particles are homogeneous. When the rate of radical arrival is very small compared to its rate of termination, a particle contains either zero, or one growing polymer chain and the rate of radical arrival to particles can be considered as a stochastic process. At the other extreme, when the rate of radical arrival is much greater than its termination rate, many growing chains can coexist in a particle and a deterministic model is applicable since there is very little variation from particle to particle. These authors have also extended the stochastic approach in order to treat the case of more than one growing chain per particle.

Interval III. When the monomer disappears as a separate phase we pass into Interval III. In Interval III the monomer concentration steadily decreases with increasing conversion, and the particle volume decreases slightly due to contraction by polymerization. This interval deserves more attention largely because of the difficulty associated with a quantitative prediction of the variation of k_t and k_d and thereby of the average number of radicals per particle in this region. Alexander and Napper (1971) have divided this interval into three subintervals: (i) the period of continuous monomer supply to the reaction sites from the aqueous phase and monomer-rich

portion in the particle, (ii) the period of increasing internal viscosity of the particle causing diffusion of monomer to the propagation sites to become rate determining, and, (iii) the period of approach to the glass transition point of the polymer. During the last period, polymerization may virtually cease since the translational diffusion of monomer, and the segmental diffusion of polymer chain ends occur extremely slowly under such glassy conditions. Although some theories for the gel effect have been developed, a number of empirical relationships for the termination rate constant have been successfully applied in explaining relatively high conversion experimental batch emulsion and bulk polymerization data (Friis and Nyhagen (1973), Friis and Hamielec (1973)).

2.2.4 Homogeneous Nucleation

The validity of the Harkins and Smith-Ewart nucleation model has been strongly questioned, especially for water-soluble monomers, such as vinyl acetate, methyl methacrylate, and vinyl chloride. It is believed that nucleation in these systems occurs by precipitation of oligomeric chains formed by addition of monomer in the water phase. Such a mechanism has also been suggested for water-insoluble monomers. Roe (1968) was able to derive the same equation (2.3) as Smith and Ewart, without reference to the hypothesis of micellar particle initiation. In micellar systems initiation is possibly taking place by both mechanisms (Ugelstad et al. (1976)), and which mechanism is the dominant one is dependent upon the solubility of the monomer in water.

The idea of homogeneous particle nucleation originally invoked by Roe was further refined by Fitch and Tsai (1971) who suggested that particle generation depends on three processes as follows,

$$\frac{dN}{dt} = \rho_i - \rho_A - \rho_F \qquad (2.16)$$

where ρ_i is the radical initiation rate, ρ_A is the rate of absorption of radical oligomeric chains in polymer particles but not micelles, and ρ_F is the rate of particle coalescence. According to this model for particle generation, during the earliest stages of polymerization, soluble oligomeric free radicals exist in solution. These ultimately grow to some critical chain length whereupon they precipitate to form primary particles.

Fitch and Tsai set ρ_A, the rate of radical absorption proportional to the particle surface, and the expression for ρ_A becomes

$$\rho_A = \rho_i \, L \, \frac{A_p}{4} \qquad (2.17)$$

where L is the average diffusion distance of an oligomeric radical before precipitation. L is obtained from Einstein's diffusion law as

$$L = \left(2D_w \frac{DP_{max}}{k_p M_{wc}}\right)^{\frac{1}{2}} \qquad (2.18)$$

The values of L and D_w in equation 2.18 are of course average values since the oligomeric radical is continuously growing. If particle flocculation occurs only to a limited extent, the net rate of particle formation, f, will

be the difference between the rate at which radicals are formed, and the rate at which they are captured, and is given by

$$f = \rho_i (1 - \frac{A_p}{4/L}) \qquad (2.18)$$

It is interesting to note that equation (2.18) is similar to the Smith-Ewart equation (2.2) for particle generation. Gardon (1968b) and Gatta et al. (1969) have also derived similar expressions for the rate of particle generation.

Because the capture rate, ρ_A, is assumed to be determined by collision with the particle surface, equation (2.17), the theory is called the collision theory. However, it has been argued that the collision theory is incorrect and that the capture rate must be calculated from the diffusion theory as

$$\rho_A = k_a [R]_w = 4\pi D_w \sum_i r_i N_i [R]_w \qquad (2.19)$$

where D_w is the diffusion constant of radicals in the homogeneous medium. This expression is the same as applied by von Smoluchowski in the calculation of fast coagulation of uncharged colloidal particles and assumes that the diffusional path length is much greater than the particle size. From this equation, the free radical flux through unit area should be expected to be greater for smaller particles and micelles. The difficulty in applying the diffusion theory is that the concentration of radicals in water, $[R]_w$, must be known. Ugelstad and Hansen (1976) have proposed a model where the rate of change of the concentration of each oligomeric

radical is calculated as the difference between the formation rate from lower chains and the disappearance rate of propagation and capture in particles. In the case of styrene in emulsifier-free systems, they have shown that the critical chain length, j_{cr}, (the maximum number of monomeric units in an oligomer) may be as low as 5 and that oligomers lower than 4-mers are captured at much lower rate than 4-mers, so that the rate of capture is only determined by the $(j_{cr}-1)$-mers. If termination in the water phase is neglected,

$$\frac{dN}{dt} = \rho_i/(1 + k_c N/k_p[M]_w) \qquad (2.20)$$

For $k_c N/k_p[M]_w \ll 1$, this gives

$$\frac{dN}{dt} \simeq \rho_i(1-k_c/k_p[M]_w) \qquad (2.20a)$$

where k_c is the capture constant.

The rate of capture will here be relatively low, so that a high number of particles will be formed. These will be stable as long as enough emulsifier is present to stabilize them. Equation (2.20a) has the same form as equation (2.2), the Smith-Ewart lower limit which has been derived under the assumption that the collision theory is valid. Fitch and Shih (1975) have presented experimental particle generation data for dilute seeded latices which support the diffusion theory. However, at the present time, there is insufficient evidence to show the exclusive validity of either mechanism of radical capture for concentrated latices of commercial

interest and further experimental work is required.

2.3 Modelling of Continuous Emulsion Polymerization

In addition to batch reactors, for which most of the earlier theories were developed there are also semicontinuous and continuous reactors used for emulsion polymerization. The semicontinuous system involves a continuous feeding of monomer, or monomer with emulsifier after a part of the recipe has been charged. This technique gives certain advantages in altering the polymer structure and is more efficient in reactor utilization because the monomer can be added as fast as the heat of polymerization can be removed. This technique is widely used in the synthetic latex industry today. There are extensive experimental investigations on semicontinuous reactors, but there have been few theoretical treatments of this type of system; see Gerrens (1969) and Wessling (1968).

Continuous stirred tank reactors typically have inherent advantages for large scale commercial productions. Minimum manpower and maintenance, easier operation and control, more consistent product quality, and higher throughputs all lend favour to the continuous process. The early literature describes processes for continuous emulsion polymerization of SBR, poly (vinyl chloride) (PVC), and chloroprene rubber (CR). Continuous reactor systems are presently employed for the commercial production of SBR, NBR, CR, acrylonitrile-butadiene-styrene copolymer (ABS), PVC, and a number of other synthetic latices.

Although continuous reactor systems are widely used to produce

synthetic latices, most published research work on emulsion polymerization kinetics is based on batch reactor data. There are reasons for not employing continuous reactors for research. The equipment is usually more complex, more costly, and less flexible. Experimental run times are lengthened, and larger amounts of raw materials are consumed.

There have been a number of theoretical investigations published for continuous emulsion polymerization. The first significant work on the problem was presented by Gershberg and Longfield (1961). Omi et al. (1969), (1971) and Nomura et al. (1971) based their models on uniform particle size and Smith-Ewart case 2 kinetics. DeGraff and Poehlein (1971) developed a model to predict effluent particle size distribution from a continuous emulsion polymerization reactor. They coupled the residence time distribution in continuous well mixed vessels to the Stockmayer model to arrive at a model which gives the particle size distribution. The model of DeGraff and Poehlein gives good agreement with their data on styrene for long residence times. However, for short residence times the prediction is quite poor.

Stevens and Funderburk (1972) illustrated the use of the population balance in continuous emulsion polymerization. Their model was capable of predicting the overall particle size distribution leaving the reactor. Free radical desorption was ignored. However, the main shortcoming in their model was that the size dependent average number of free radicals per particle had to be calculated before obtaining solutions to their population balance equation. Recently Thompson and Stevens (1977) have used

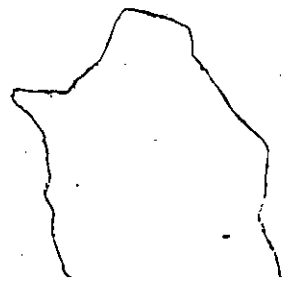

a new approach to model continuous emulsion polymerization. The Smith-Ewart recursion equation is incorporated directly as the "rate of formation" relation for polymer particles. As a result of this approach, the mechanism of free radical desorption from polymer particles is easily included, and finite termination rates in particles are allowed. Particle growth is incorporated in the model, and particle size distributions are obtained. Their complete model is given as

$$\frac{\partial N_q}{\partial t} + K\frac{\partial}{\partial v}(qN_q) = \frac{N_{qin}-N_q}{\tau} + \frac{\alpha}{v}[(q+2)(q+1)N_{q+2} - q(q-1)N_q] +$$

$$\beta v^{2/3}[N_{q-1}-N_q] + \frac{\gamma}{v^{1/3}}[(q+1)N_{q+1}-qN_q] \qquad (2.21)$$

(The symbols are defined in the nomenclature). By allowing q to take on non-negative integer values, the entire family of population balance equations can be realized. The results that they presented are based on the equations generated by letting q take on values from 0 to 5, and assuming that the reactor operates at steady state. However, they can not estimate the absolute number of particles unless the value of N_{To}, the number density of polymer particles at "zero size" is known for a given system. Moreover, for unsteady state operation of reactor (reactor transients, sustained oscillations) their model becomes unattractive and sensitive to termination of the infinite set of equations, (i.e. when q takes very large values).

It is clear from the brief discussion of this section that there have been a large number of isolated theories developed to model emulsion

polymerization systems. Furthermore, none of these is very general, nor does any of them provide a suitable framework for including the whole spectrum of mechanisms postulated for emulsion polymerization. However, in 1974 came the most general and extensive published work regarding mathematical modelling of emulsion polymerization in a fundamental review article by Min and Ray. After carefully reviewing the modelling efforts presented thus far, they proceeded to develop a model far more comprehensive than any previously formulated. These authors incorporated more mechanisms than ever presented elsewhere. Although they illustrated the model with a particular set of mechanisms, the framework is sufficiently general that it is straightforward to add the effects of specific mechanisms not mentioned. However, their model has not been tested extensively, especially under such severe conditions as steady state reactor multiplicity and limit cycling operation. The large number of parameters required to describe the variety of mechanisms incorporated in the model makes the use of this general framework difficult and unattractive. Nevertheless, Min and Ray's rigorous mathematical treatment gives a unique picture of the population balance approach and its application in emulsion polymerization.

In section 2.4, a mathematical model for the emulsion polymerization of vinyl acetate in a CSTR is derived by using mainly population balance principles invoked by Pis'men and Kuchanov (1971) and Min and Ray (1974). The approach taken by Min and Ray focuses on the size distribution rather than on the residence time or age distribution of particles.

The latter approach was taken by Gorber (1973) on modelling a continuous emulsion polymerizer for styrene. Dickinson (1976) extended Gorber's work to derive a mathematical model for the emulsion polymerization of styrene in a train of CSTR's. Dickinson's main difference compared to Min's approach (1976) was that he derived the population balances in terms of the total properties (i.e. total polymer volume, total number of particles etc.). That enabled him to recast the general integral partial differential equations into a system of integro-differential equations simplifying, thus, the numerical solution of the problem.

A similar approach based on age distribution function is taken in this thesis to model a CSTR for the emulsion polymerization of vinyl acetate. This model and a simplified one to be used for on-line control studies are described in section 2.5.

2.3.1 Dynamic Phenomena in CSTR's

Other work on CSTR systems include a number of papers dealing with multiple steady states, process dynamics and system stability. Matsuura and Kato (1967) predicted three steady states for an isothermal CSTR; Yamazaki and Ichikawa (1969) studied the effects of segregation on the dynamic response of a continuous flow chemical reactor; Goryusko and Vilesov (1971) studied the stability of a CSTR for the emulsion polymerization of vinyl chloride on the basis of homogeneous phase considerations; Gerrens et al. (1971) have shown experimental verification of theoretical predictions of multiple steady states. Brooks (1973) considered micelles

to be participating in two competing rate processes; the nucleation of new particles and dissolution into the aqueous phase. For a single CSTR, he developed the particle and micelles conservation equations. As Brooks noted, their form leads to the possibility of solutions which show the dependent variables oscillating with respect to time. Recently, Jaisinghani and Ray (1977) presented dynamic models for the continuous bulk polymerization of both methyl methacrylate and styrene monomers. In fact, according to their models, operating conditions can be determined under which multiple steady states and limit cycles might be observed as coupled phenomena.

The way in which continuous stirred tank emulsion polymerization reactors are started up can have a significant influence, not only on the transients before steady state is achieved, but also on the nature of the ultimate state obtained after all transient effects die out. An understanding of the transient behaviour of continuous reactors is important for start-up, for control, and possibly for planning continuous oscillatory operation. If a single CSTR is started empty or by adding initiator to a full vessel of inactive emulsion, a conversion overshoot is observed. The explanation of this phenomenon follows easily. The first free radicals generated are almost entirely utilized to form new particles. Since these particles do not grow rapidly to the steady-state size distribution, the radical efficiency in generating new particles remains high and the particle concentration passes its steady-state value. Eventually, however, these particles do grow and some leave the reactor. Hence the system converges to steady-state operation, usually within 3 to 5 mean residence times.

Gershberg and Longfield (1961) used a three stage reactor train where the system was started up from an empty state by pumping premixed emulsion into the first stage. They reported conversion overshoots in excess of 100% with a cyclic approach to steady operation. Nomura et al. (1971) on the other hand, filled their single reactor with monomer emulsion and started the continuous reaction period by simultaneously injecting initiator and pumping monomer emulsion plus initiator into the reactor. Overshoots in both conversion and polymer particle concentration were observed. Gorber (1973), using the same start-up procedure, also observed the initial conversion overshoot and gave some evidence of separate generation of new particles. Conversion overshoots were also detected by the author for the continuous emulsion polymerization of vinyl acetate and these are presented in Chapter 4.

Sustained Oscillations. In continuous emulsion polymerization the commercially important phenomena of sustained oscillations and steady-state multiplicity have been studied in carefully conducted laboratory experiments by Gerrens and Ley (1974), and Greene et al. (1976), for the monomers styrene, methyl methacrylate and vinyl acetate. However, steady-state multiplicity has not been observed for vinyl acetate as it probably does not exist. Although there is no published literature on the subject, it is known that oscillations occur in the continuous emulsion polymerization of chloroprene and styrene-butadiene copolymer on a commercial scale. These oscillations can lead to emulsifier levels too small to adequately cover polymer particles with the result that excessive agglomeration and fouling

can occur. Furthermore, for monomer systems where long chain branching occurs, excursions to high polymer concentrations, due to the cycling behaviour of conversion, can result in polymers with excessive branching and, therefore, poor processability.

One of the first theoretical attempts to explain sustained oscillations in continuous emulsion polymerization was done by Omi et al. (1969) for styrene monomer. Recently, Dickinson and Gall (1976) simulated the experimental results of Gerrens (1974) for the continuous emulsion polymerization of styrene, for both cases of sustained and damped oscillations. In their model, they considered a particle generation mechanism which depended on both the available free soap and the aqueous phase monomer concentration, and corrected for diffusion-controlled termination in the polymer particles by letting the termination constant, k_t, fall with conversion.

In an extensive experimental study in this thesis on the production of polyvinyl acetate latices in a CSTR, the related phenomena of sustained oscillations (in conversion, number and size of polymer particles) were observed. These results are discussed in Chapter 4. Using the theoretical models described in section 2.5, we are able to explain these oscillations over essentially the entire range of operation. Latex properties such as particle size distribution, total particle surface area, total number of particles and free soap concentration are accounted for in the models derived in the following sections. The unquestionable commercial importance of all the above properties for a latex product make such models useful for the

design and control of latex reactors.

2.4 The Population Balance Approach

As a means of beginning our model development, let us consider the case where the following polymerization and particle nucleation mechanisms take place in the reactor.

Initiation of radicals	$I \xrightarrow{k_d} 2R$
Particle nucleation via a micelle	$R + m_s \xrightarrow{k_m} P_1$
Homogeneous particle nucleation	$R + M \xrightarrow{k_h} P_1$
Entry of radicals into particles	$R + P_q \xrightarrow{k_{ab}} P_{q+1}$
Desorption of radicals from polymer particles	$P_q \xrightarrow{k_{de}} P_{q-1} + R$
Propagation in polymer particles	$P_q + M \xrightarrow{k_p} P_q$
Chain transfer to monomer	$P_q \xrightarrow{k_{fm}} P_q$
Termination in polymer particles	$P_q \xrightarrow{k_{tp}} P_{q-2}$

where P_q denotes a particle with q radicals and N_q is the number of particles P_q.

The basic assumptions made in modelling this reaction are:

(i) The reactor is uniformly mixed

(ii) The density change in the reaction mixture is negligible (liquid phase)

(iii) The extent of particle breakup is negligible

(iv) Particles can be generated by both micellar and homogeneous mechanisms.

(v) The monomer volume fraction in a particle, $\phi(t)$, is assumed to be independent of particle size.

In other words, monomer diffuses into particles independently of their size. Therefore, for a constant monomer feed concentration we have

$$\phi(t) = \phi_{sat} \; ; \quad x \leq x_c \tag{2.22}$$

when monomer drops are present, otherwise

$$\phi(t) = \frac{1-x}{1-x(1-d_m/d_p)} \; ; \quad x > x_c \tag{2.23}$$

in the monomer starved region. Although the model is developed by considering a particular set of mechanisms taking place in the reactor, one could treat other kinetic schemes in a completely similar way.

As can be seen in Figure 2-1, the macroscopic reactor is made up of an emulsion containing polymer particles, micelles, and monomer droplets suspended in a continuous aqueous phase. The mathematical description of this reactor involves a set of overall material balances. These include polymer particle population balances, monomer balances, micelle balances,

and material balances. Energy balances are not necessary, since heat transfer is generally rapid enough that the reactor is isothermal.

2.4.1 General Mathematical Framework

Each latex particle is characterized in this model by a vector $\underline{z} \equiv (z_1, z_2, \ldots z_s)$ which is a set of s physical quantities, whose numerical values will identify a given particle. Examples of state variables are particle size, age, number of radicals, number of dead or growing polymer chains etc. The fundamental quantity describing the population is the number density function, $n(\underline{z},t)$, which is regarded as a smooth function of $\underline{z}$ and t. The total number of particles, N(t) in the system is given by

$$N(t) = \int n(\underline{z},t)dV \qquad (2.24)$$

where dV is an infinitesimal volume in the state space of dimension s. The state of any given particle may change due to one reason or another. We are here referring to continuous changes in particle state in which the identity of the particle is preserved. Such changes in state can be frequently modeled by using fundamental conservation principles. The rate of change of a particle of state $\underline{z}$ is denoted by a vector function $\dot{\underline{z}}$, which may depend on $\underline{z}$ and variables associated with the continuous phase.

Let $f^+(\underline{z},t)dV$ (source function) be the rate of increase in the number of particles in a volume dV about $\underline{z}$ in the state space. Similarly we may define a sink function $f^-(\underline{z},t)$ so that the net generation rate $f(\underline{z},t)$ is given by

$$f(\underline{z},t) \equiv f^{+}(\underline{z},t) - f^{-}(\underline{z},t) \tag{2.25}$$

The population balance equation can now be readily written by invoking the continuity operator in the particle state space.

$$\frac{\partial}{\partial t} n(\underline{z},t) + \nabla \cdot \dot{\underline{z}} n(\underline{z},t) = f(\underline{z},t) \tag{2.26}$$

where ∇ is a $(\frac{\partial}{\partial z_1}, \frac{\partial}{\partial z_2} \ldots \frac{\partial}{\partial z_s})$ operator. Equation (2.26) has been derived by Hulburt and Katz (1964). It must be coupled with mass balance equations for continuous phase variables.

At this point, it must be pointed out that what has been accomplished is only the mathematical formulation of a rather simple accounting principle for particle number. However, the modelling and difficulty lies in identifying the nature of the functions $\dot{\underline{z}}$ and $f(\underline{z},t)$ for a given situation. This is illustrated in the modelling of the total particle size distribution in a continuous emulsion polymerization reactor.

Total Particle Size Distribution. Each latex particle is characterized by its volume v, Min (1976) and the number density function, $n(v,t)$, describes the particle population. For the particular set of mechanisms considered the particle size distribution takes the form after equation (2.26),

$$\frac{\partial n(v,t)}{\partial t} + \frac{\partial}{\partial v}(\bar{\mu}_q n(v,t)) = \frac{1}{\theta} n(v,t)_{feed} + k_h[R]_w \delta(v-v_o) +$$

$$k_m A_m [R]_w \delta(v-v_m) + \frac{1}{2} \int_o^v k_c(v-v',v',\sigma_p) n(v-v',t) n(v',t) dv' - \frac{1}{\theta} n(v,t)$$

$$-n(v,t) \int_o^{\infty} k_i(v,v',\sigma_p) n(v',t) dv' \tag{2.27}$$

where the first term in equation (2.27) represents the change of total number of particles with time and the second term represents the rate of change by volume increase of growing particles. On the other hand, the first, second, third and fourth term on the right hand side of equation (2.27) represent the rate of population change by inflow, the rate of new particle formation by oligomer precipitation, the rate of particle formation by micellar nucleation, and the rate of particle formation by coalescence respectively. Finally, the last two terms of equation (2.27) represent the rates of particle change by outflow and particle disappearance by coalescence. $k_c(v,v',\sigma_p)$ is the rate coefficient of coalescence between two particles of volumes v and v' with electric change density of σ_p. μ is the volumetric growth rate per radical in the particle and $\bar{q}$ is the average number of radicals per particle.

Similar partial-differential-integral equations can be derived from equation (2.26) for different state vectors $\underline{z}$. Therefore, for $\underline{z} \equiv (v,q)$ we get the radical number distribution, $n(v,q,t)$, which is a bivariate distribution. For $\underline{z} \equiv (v,q,m)$ we get the growing polymer molecular weight distribution, $n(v,q,m,t)$, and so on. However, the significant difficulties in the application of population balances are in the solution of the integro-differential equations, and in the identification of the expressions which describe particle behaviour.

2.4.2 Solution of Equations

Since frequently the leading moments of the number density function offers a satisfactory description of the population, it has been suggested

(Hulburt and Katz (1964), Argyriou et al. (1971), Min (1976)) that moment equations be directly obtained from the balance equation. Frequently, this leads to trouble either in the form of unclosed moment equations, equations with fractional moments, or those that simply do not directly yield moments. To overcome these difficulties, a Laguerre function expansion of the number density function, has been suggested by Hulburt and Katz (1964). The coefficients of the Laguerre function expansion are related to the integral moments of the distribution in a simple manner. However, as Ramkrishna (1971) has shown this procedure is equivalent to a particular application of the method of weighted residuals (MWR) to the solution of the population balance equation (PBE) (2.27). Subramanian and Ramkrishna (1971) further demonstrated the applicability of MWR to the solution of the PBE by analyzing the behaviour of a biological population. An excellent review of MWR has been given by Finlayson and Scriven (1966). Consider the solution of a scalar version of equation (2.26) (z scalar)

$$\frac{\partial n}{\partial t} + \frac{\partial}{\partial z}(\dot{z}n) = f(z;t) \tag{2.28}$$

with $0 < z < \infty \qquad t > 0; \qquad n(z,0) = g(z)$ (2.29)

In MWR the unknown distribution $n(z,t)$ is expanded in terms of a finite number of trial functions $\{\phi_i(z)\}$

$$n(z,t) = \sum_{i=1}^{N} c_i(t)\phi_i(z)$$

$$n(z,0) = \sum_{i=1}^{N} c_i(0)\phi_i(z) = g(z) \tag{2.30}$$

The $\{\phi_i(z)\}$ may preferably come from a complete set in an appropriate space to which $n(z,t)$ belongs (say $L_2[0,\infty)$ in this case). The trial functions have also been assumed to be time-independent although a more general formulation may eliminate this assumption.

The trial solution (2.30) is then substituted into equation (2.28) to obtain a residual function $R(z,t)$.

$$R(z,t) \equiv L\left(\sum_{i=1}^{N} c_i(t)\phi_i(z)\right) - f\left(\sum_{i}^{N} c_i(t)\phi_i(z),\ t\right) \tag{2.31}$$

where L represents the continuity operator in the left hand side of equation (2.28). Also

$$R(z,0) \equiv \sum_{i=1}^{N} c_i(0)\phi_i(z) - g(z) \tag{2.32}$$

The functions $\{c_i(t)\}$ together with their initial values $\{c_i(0)\}$ must be determined such that the residuals equations (2.31) and (2.32) are as close to zero as possible over the entire semi-infinite interval. The essence of MWR is to accomplish this by orthogonalizing the residuals with a set of functions $\{\psi_i(z)\}$ also preferably from a complete set in $L_2[0,\infty)$. Thus

$$\int_0^\infty R(z,t)\psi_i(z)dz = 0 \qquad i = 1,2,\ldots N \tag{2.33}$$

$$\int_0^\infty R(z,0)\psi_i(z)dz = 0 \tag{2.34}$$

Equations (2.33) will lead to a set of N ordinary differential equations

in $\{c_i(t)\}$ where initial conditions can be obtained from (2.34). The success of the method hinges on appropriate selection of the trial function $\{\phi_i\}$ and the weighting functions $\{\psi_i\}$. It is easy to show that when the trial functions $\{\phi_i\}$ are taken to be the Laguerre functions and the weighting functions are taken to be $\psi_i(z) = z^i$, then equations (2.33) reduce to the moment equations.

The choice of the trial function is a vital aspect of success with weighted residual techniques. A successful application of MWR technique for solving population balance equations has been demonstrated by Singh and Ramkrishna (1977). However, when the particle state variable is a vector, the resulting multivariate number density functions are likely to be much harder to solve for. This problem requires further investigation.

2.5 The Age Distribution Analysis

In this section, models of two levels of sophistication are developed; a comprehensive model which solves for the age distribution function of polymer particles, and a simplified one to be used for the control studies on the latex reactors. Both models adequately simulate experimental data after Greene et al. (1976) and these simulation results can be found in a paper by Kiparissides et al. (1978). In Chapter 5, experimental results obtained in this research (Chapter 4) are successfully fitted by the models and the unknown kinetic parameters of the simplified model are estimated.

2.5.1 Model Development

In deriving the differential equations, which describe the dynamic behaviour of the important latex properties, the age distribution function is used and this enables us to follow all variations in individual growth rates due to past and present reaction conditions. On the contrary, the approach given in section 2.4.1 is based on the volume of each latex particle. Particle growth rate is generally considered as a function of monomer concentration in the particle, particle size and rates of radical adsorption and desorption.

The basic assumptions made in modelling this reaction system are the same to those considered in section 2.4, as well as that the extent of particle flocculation is negligible.

In a continuous stirred tank reactor particles can be generated continuously leading to distributions of particle size and age. Let $f(t)$ denote the net rate of particle generation in the reactor, Figure 2-2. The function $n(t,\tau)d\tau$ is defined to be the number of particles in the reactor, at time t, which were born in the time interval $[\tau,\tau+d\tau]$, and for a well-stirred reactor, this number of particles is completely characterized by a single coordinate τ, the time it has spent in the vessel. The equation of motion ($\dot{Z}$, see equation 2.28) for a typical particle is simply that

$$\dot{Z} = \frac{d\tau}{dt} = 1 \qquad (2.35)$$

where t is the clock time. The particle phase space is just the τ-axis. With equation (2.35) the population balance equation (2.28) becomes

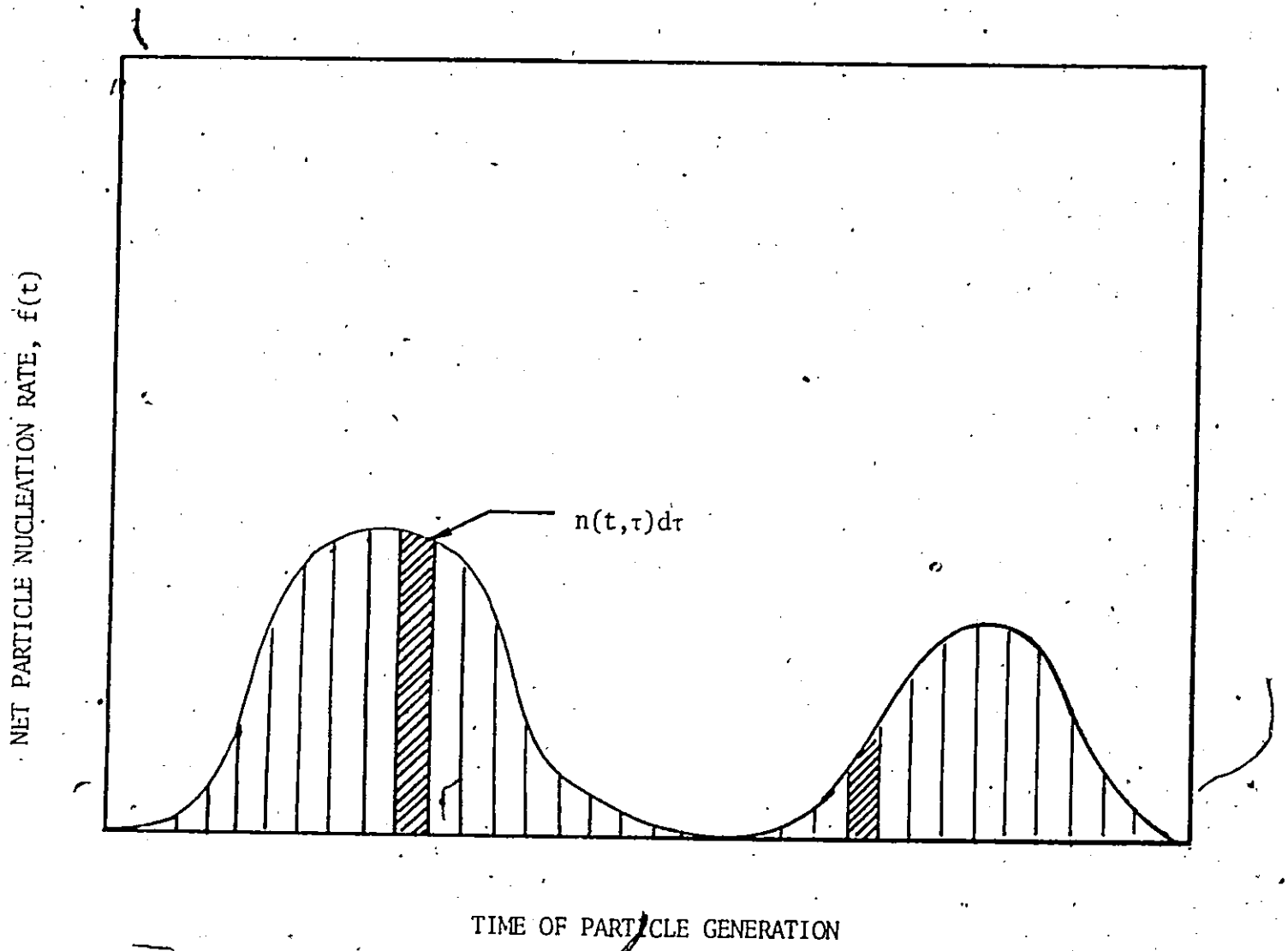

Figure (2-2) Net Particle Nucleation Rate, f(t), with respect to Birth Time, τ

$$\frac{\partial n(t,\tau)}{\partial t} + \frac{\partial n(t,\tau)}{\partial \tau} = \frac{-n(t,\tau)}{\theta} + f(t)\delta(t-\tau) \qquad (2.36)$$

where the Dirac function $\delta(t-\tau)$ indicates the time of appearance of a particular class of particles and θ is the mean residence time. The general solution of equation (2.36) is given by Hulburt and Katz (1964) and was obtained by using Fourier transforms and the concept of generalized functions. It may also be easily found by using Laplace transforms that

$$n(t,\tau) = f(\tau)e^{-(t-\tau)/\theta}; \quad \tau > t \qquad (2.37)$$

is the steady state solution of equation (2.36), and $(t-\tau)$ denotes the age of all particles in the reactor which were generated at some previous time interval $[\tau, \tau+d\tau]$ at a rate $f(\tau)$. In deriving equation (2.36), it is assumed that particle appearance in the reactor is due only to nucleation mechanisms.

We define now $p(t,\tau)$ to be some property of the latex, associated with the class of particles $n(t,\tau)d\tau$, then the total property for all particles in the reactor will be given by

$$P(t) = \int_{t_o}^{t} p(t,\tau)n(t,\tau)d\tau \qquad (2.38)$$

Using the general form of Leibnitz' rule for differentiating equation (2.38) and substituting equation (2.36) into the resulting equation we obtain

$$\frac{dP(t)}{dt} = \frac{-P(t)}{\theta} + f(t)p(t,t) + \int_{t_o}^{t} \frac{dp(t,\tau)}{dt}\, n(t,\tau)d\tau \qquad (2.39)$$

where the property p(t,t) is taken to be negligible for newly generated particles except where p(t,t) stands for number of particles.

2.5.2 The Total Property Balances

The differential equations, which describe the total properties of a latex in a continuous reactor, can be now derived directly from equation (2.39). Therefore, total property balances for number of particles, polymer volume, area of particles and conversion are written

$$\frac{dN(t)}{dt} = \frac{N(t)}{\theta} + f(t) \tag{2.40}$$

$$\frac{dV_p(t)}{dt} = -\frac{V_p(t)}{\theta} + \int_o^t \mu_R(t,\tau)\bar{q}(t,\tau)n(t,\tau)d\tau \tag{2.41}$$

$$\frac{dA_p(t)}{dt} = -\frac{A_p(t)}{\theta} + \frac{2}{3}(36\Pi)^{1/3}\int_o^t v(t,\tau)^{-1/3}\mu(t,\tau)\bar{q}(t,\tau)n(t,\tau)d\tau \tag{2.42}$$

$$\frac{dx(t)}{dt} = -\frac{x(t)}{\theta} + \frac{d_p}{M_F M_W}\int_o^t \mu_p(t,\tau)\bar{q}(t,\tau)n(t,\tau)d\tau \tag{2.43}$$

where $N(t) = \int_o^t n(t,\tau)d\tau$ is the total number of particles,

$V_p(t) = \int_o^t v_p(t,\tau)n(t,\tau)d\tau$ is the total polymer volume,

$A_p(t) = \int_o^t a_p(t,\tau)n(t,\tau)d\tau$ is the total particle area,

and $x(t)$ is the total conversion in the reactor at time t. $\mu(t,\tau)$ and $\mu_p(t,\tau)$ are the particle and the polymer volume growth rates per radical respectively, associated with a particle of the class $n(t,\tau)d\tau$.

The total volumetric growth rate of the polymer phase in a particle can be obtained from equation (2.44)

$$\frac{dv_p(t,\tau)}{dt} = \mu_p(t,\tau)\bar{q}(t,\tau) = \frac{k_p d_m}{Nad_p}\,\Phi(t)\bar{q}(t,\tau) \qquad (2.44)$$

and the total volume of a particle is given by

$$v(t,\tau) = \frac{v_p(t,\tau)}{1-\Phi(t)} \qquad (2.45)$$

Assuming spherical particles, the surface area of a single particle is given by

$$a_p(t,\tau) = (36\Pi)^{1/3}\, v^{2/3}(t,\tau) \qquad (2.46)$$

$\bar{q}(t,\tau)$ denotes the average number of radicals per particle, k_p, is the propagation rate constant, M_F is the feed monomer concentration, M_W, the molecular weight of monomer, Na is Avogadro's number and d_m, d_p are the monomer and polymer densities respectively. The average number of radicals in a particle of volume $v(t,\tau)$ up to relatively high conversions for vinyl acetate monomer can be estimated from equation (2.6) after Ugelstad and Hansen (1976) as

$$\bar{q}(t,\tau) = \frac{\rho_n}{k_{de}(t,\tau)n(t,\tau)d\tau} \qquad (2.47)$$

where ρ_n is the radical entry rate to the $n(t,\tau)d\tau$ class of particles. Assuming that termination takes place exclusively in polymer particles, a steady-state treatment gives

$$r(t,\tau) = 2\rho_n \bar{q}(t,\tau) = \frac{R_I A_n(t,\tau)d\tau}{A_p(t)} \qquad (2.48)$$

where $r(t,\tau)$ is the radical initiation rate corresponding to the $n(t,\tau)d\tau$ class of particles, $A_n(t,\tau)d\tau$ is the surface area of the $n(t,\tau)d\tau$ class of particles and R_I is the total initiation rate. In Appendix I, a general expression for the average number of radicals per particle, $\bar{q}$, is derived. Substituting equation (2.48) into equation (2.47) we obtain

$$\bar{q}(t,\tau) = \left(\frac{R_I}{2k_{de}(t,\tau)n(t,\tau)d\tau}\right)^{1/2} \left(\frac{A_n(t,\tau)d\tau}{A_p(t)}\right)^{1/2} \qquad (2.49)$$

where k_{de} is a desorption coefficient of radicals from polymer particles given by Nomura et al. (1976) as

$$k_{de}(t,\tau) = \left(\frac{12\, D_w\, \delta}{m\, D_{pp}^2}\right)\left(\frac{k_{fm}}{k_p}\right) = k'_{de}\, v^{-2/3}(t,\tau) \qquad (2.50)$$

where D_w is the diffusion coefficient of monomeric radicals in the water phase, D_{pp}, denotes the diameter of a particle, m is a partition coefficient

of monomeric radicals between water and particle phases and k_{fm} is the rate coefficient of chain transfer to monomer. Combining equation (2.49) with equations (2.37), (2.45), (2.50) and substituting the new equation into equation (2.44) the volumetric growth rate of the polymer phase in a particle can be written as

$$\frac{dv_p(t,\tau)}{dt} = \frac{K}{f(\tau)^{1/2}} e^{(t-\tau)/2\theta} (1-e^{-t/\theta}) v_p^{1/3}(t,\tau) \qquad (2.51)$$

where

$$K = \frac{k_p d_m}{N a d_p} \left(\frac{m k_p}{12 D_w \delta k_{fm}} f k_d [I]_{feed} \frac{A_n(t,\tau)}{A_p(t)}\right)^{1/2} \left(\frac{6}{\pi}\right)^{1/3} \Phi(t)^{1/3} (1-\Phi(t))^{-1/3} \qquad (2.52)$$

$$\delta = \left(1 + \frac{D_w}{D_p m}\right)^{-1} \qquad (2.53)$$

$$[I]_w = \frac{[I]_{feed}(1-e^{-t/\theta})}{(1+k_d\theta)} \qquad (2.54)$$

D_p is the diffusion coefficient of monomeric radicals in the polymer particles and k_d is the rate constant for initiator decomposition. To derive equation (2.51) we used the fact that the start-up procedure, to be considered later, consists of filling the reactor with degassed water prior to introducing any feed streams.

The extension of the above developed equations to more than one reactor is straightforward. However, the complexity of the resulting

equations can lead to some numerical difficulties during solution.

2.5.3 Initiator, Oligomeric Radicals and Emulsifier Balances

The aqueous phase initiator and oligomeric radicals balances can be written

$$\frac{d[I]_w}{dt} = \frac{1}{\theta}([I]_{feed} - [I]_w) - k_d[I]_w \tag{2.55}$$

$$\frac{d[R]_w}{dt} = \frac{1}{\theta}([R]_{feed} - [R]_w) + 2fk_d[I]_w - k_{ab}A_p[R]_w k_v$$

$$k_m A_m[R]_w k_v - k_h[R]_w - k_{tw}[R]_w^2 + \int_o^t k_{de} n(t,\tau)\bar{q}(t,\tau)d\tau \tag{2.56}$$

Deriving equation (2.56), it was assumed that the rate of radical capture is proportional to the total surface available for radical capture (Smith-Ewart (1948), Gardon (1968b) and Fitch and Tsai (1971).

However, a mass balance equation in which the radical capture would be proportional to the radius (Ugelstad et al. 1976) of particles or micelles could equally be used.

$[I]_{feed}$, $[R]_{feed}$ are the initiator and radical concentrations in the aqueous phase in the reactor. The third term on the right of equation (2.56) represents the rate at which radicals are captured by polymer particles, and it is proportional to the total particle area, A_p, and the radical concentration $[R]_w$. k_{ab} is an overall transport coefficient for radical

transfer from the aqueous phase into polymer particles.

The next term in equation (2.56) represents the rate at which polymer particles are generated by the micellar mechanism. A_m is the free coverage area of micelles given by

$$A_m = S_T - S_{CMC} - A_p \qquad (2.57)$$

where S_{CMC} is the critical micelle concentration converted in dm^2/ℓ-emulsion and S_T is the total emulsifier concentration in dm^2/ℓ-emulsion given by

$$\frac{dS_T}{dt} = \frac{1}{\theta}(S_F - S_T) \qquad (2.58)$$

S_F is the emulsifier concentration in the feed.

The term $k_h[R]_w$ stands for the rate of homogeneous nucleation of particles. This means that polymer particles can be generated even though micelles do not exist. However, according to Fitch (1971), the rate of homogeneous generation of particles should be allowed to tend towards zero when the rate of radical capture by the existing polymer particles becomes greater than the rate of initiation of radicals. Therefore, the rate constant, k_h, can be equated with the term $k_{ho}(1 - \frac{A_p}{4} L)$, where L is now defined, after Fitch, as the distance which a growing radical will diffuse before it precipitates out to form a primary particle, and it is obtained from Einstein's diffusion law, equation (2.18).

Finally the last term in equation (2.56) denotes the total desorption rate of radicals from the polymer particles.

Thus, according to our proposed kinetic model the total rate of particle nucleation may be written as

$$f(t) = k_m A_m [R]_w k_v + k_{ho}(1 - \frac{A_p}{4} L)\ [R]_w \qquad (2.59)$$

where k_m and k_{ho} are rate coefficients of particle nucleation by micellar and homogeneous mechanism respectively and the constant, k_v, represents the volume of emulsion phase over the volume of aqueous phase, ℓ- emulsion/ℓ.

It is interesting to note that according to equation (2.59) particles will be generated even though micelles are not present, and homogeneous nucleation of particles will cease only when the term $(1 - \frac{A_p}{4} L)$ becomes less than or equal to zero.

Equation (2.56) may be simplified by applying a stationary state hypothesis to the monomeric and oligomeric radicals and assuming that $[R]_{feed} \simeq 0$

$$[R]_w = \frac{\rho}{k_{ab} A_p k_v + k_m A_m k_v + k_h + 1/\theta} \qquad (2.60)$$

where ρ is equal to $R_I + \int_0^t k_{de} n(t,\tau) \bar{q}(t,\tau) d\tau$.

Therefore, by neglecting the term $1/\theta$ in equation (2.60) since it is very small ($\sim 10^{-4}$) compared to the other terms, the net particle generation rate, equation (2.59), can be written as

$$f(t) = \frac{\rho}{1 + \varepsilon \frac{A_p}{A_m} + \frac{\mu(1-A_p L/4)}{k_v A_m}} + \frac{\rho}{1 + k_v \frac{\varepsilon A_p}{\mu(1-A_p L/4)} + \frac{k_v A_m}{\mu(1-A_p L/4)}} \qquad (2.61)$$

where ε is defined to be the ratio, $\frac{k_{ab}}{k_m}$ and μ the ratio $\frac{k_{ho}}{k_m}$. These parameters ε and μ can be estimated from conversion and particle size distribution data collected from the reactor.

Equations (2.37), (2.40-43), (2.51-58) and (2.61) represent a general enough model form. Solution of these equations with the proper initial conditions will give information for the most important latex properties (e.g., conversion, total particle area, free emulsifier concentration, etc.), as well as the particle size distribution at any time t.

2.5.4 Application of Model Equations

To simulate our experimental data the complex system of integro-differential equations (2.40-43) must be solved according to the start-up procedure which consisted of filling the reactor with degassed water prior to introducing any feed streams. To simplify the numerical calculations the integral terms in equations (2.40-43) are replaced by equivalent summation terms over a finite number of time intervals, $\Delta\tau_i$, $i = 1, 2, \ldots, r_t$ (see Figure 2-2) yielding

$$\frac{dN(t)}{dt} = -\frac{N(t)}{\theta} + f(t) \tag{2.62}$$

$$\frac{dV_p(t)}{dt} = -\frac{V_p(t)}{\theta} + \sum_{i=1}^{r_t} K\, v_p^{1/3}(t,\tau_i)\, n^{1/2}(t,\tau_i)\, \Delta\tau_i \tag{2.63}$$

$$\frac{dA_p(t)}{dt} = -\frac{A_p(t)}{\theta} + \frac{2}{3}(36\pi)^{1/3}(1-\phi(t))^{-2/3} \sum_{i=1}^{r_t} K\, n^{1/2}(t,\tau_i)\, \Delta\tau_i \tag{2.64}$$

$$\frac{dx(t)}{dt} = -\frac{x(t)}{\theta} + \frac{d_p}{M_T M_W} \sum_{i=1}^{r_t} K v_p^{1/3}(t,\tau_i) n^{1/2} \omega(t,\tau_i) \Delta\tau_i \quad (2.65)$$

with the number of particles in the i^{th} class of particles $(\tau_i, \tau_i + \Delta\tau_i)$ given by

$$n(t,\tau_i)\Delta\tau_i = f(\tau_i)\Delta\tau_i \, e^{-(t-\tau_i)/\theta} \quad (2.66)$$

The polymer volume $v_p(t,\tau_i)$ of a particle in equations (2.63) and (2.65) associated with the i^{th} class of particles over a short time interval (t_{j-1},t_j) is obtained by integrating equation (2.51) over that interval to give

$$v_p(t_j,\tau_i) = \left[v_p(t_{j-1},\tau_i)^{2/3} + \frac{2}{3}\frac{K}{f(\tau_i)^{1/2}} \int_{t_{j-1}}^{t_j} e^{(t-\tau_i)/2\theta}(1-e^{-t/\theta})dt\right]^{3/2} \quad (2.67)$$

To solve this system of equations (2.62-65) over the time period (t_{j-1},t_j) all summation terms are originally evaluated at time t_{j-1} and then the system of four differential equations is solved from t_{j-1} to t_j (iteration one). With the new values of variables obtained from iteration one, the summation terms are computed again and the solution of differential equations is repeated. Under this iterative scheme convergence of the solution is achieved relatively fast (two or three iterations). The particle size distribution at any time t is found by plotting the frequency ratio $n(t,\tau)d\tau/N(t)$ for each class of particles against the particle size of that class given by equation (2.67):

2.5.5 Simplified Model

When particle generation occurs only during certain periods of time and these periods of particle generation are sufficiently short, as in the case for an emulsion system under sustained oscillation conditions, one can make the assumption that only one class of particles $n(t,\tau)d\tau$ is generated for each discrete period of particle nucleation. By lumping all the particles in each generation into a single class the summation terms in equations (2.62-65) can be replaced by equivalent average values for that class. For example the average volume of the i^{th} particle generation may be approximated by the average value

$$v_p(t,\tau_i) = \bar{v}_{pi}(t) = \frac{V_{pi}(t)}{N_i(t)} \tag{2.68}$$

Therefore, the dynamic equations (2.62-65) can be approximated by a set of differential equations describing the development of each particle generation "i" in the reactor (where the summations have been replaced by the single average values for that generation):

$$\frac{dN_i(t)}{dt} = -\frac{N_i(t)}{\theta} + f(t) \tag{2.69}$$

$$\frac{dV_{pi}(t)}{dt} = -\frac{V_{pi}(t)}{\theta} + \frac{k_p d_m}{N a d_p} \Phi(t)\ \bar{q}_i(t)\ N_i(t) \tag{2.70}$$

$$\frac{dx_i(t)}{dt} = -\frac{x_i(t)}{\theta} + \frac{k_p d_m}{M_I M_w} \Phi(t)\ \bar{q}_i(t)\ N_i(t) \tag{2.71}$$

$$A_{pi}(t) = (36\Pi)^{1/3} (\bar{v}_{pi}(t))^{2/3} N_i(t) \qquad (2.72)$$

where N_i, V_{pi}, x_i, A_i, $\bar{q}_i$ denote the total number of particles, total polymer volume, total conversion, total particle area and average number of radicals per particle of the i^{th} generation of particles. When two or more particle generations have been formed in the reactor the total properties of the latex product at the exit of the reactor will be given by

$$x(t) = \sum_{i=1}^{q_t} x_i(t), \quad V_p(t) = \sum_{i=1}^{q_t} V_{pi}(t), \quad N(t) = \sum_{i=1}^{q_t} N_i(t),$$

$$A_p(t) = \sum_{i=1}^{q_t} A_{pi}(t) \qquad (2.73)$$

where q_t denotes the number of discrete particle generations which have been appeared in the reactor until time t.

In deriving equation (2.73) it is assumed that the total particle area in the reactor can be approximated by the sum of the areas of all discrete particle generations. This assumption is valid as long as the reactor operates under sustained oscillations and narrow particle generations appear every 5-7 mean residence times apart.

However, for the steady-state case where particles are continuously formed, an infinite number of particle generations should be considered to calculate the particle area according to equation (2.73).

To simplify this calculation the total particle area, A_p, is approximated by the following expression

$$A_p = (36\Pi)^{1/3} \left(\frac{V_p}{N}\right)^{2/3} N \qquad (2.74)$$

where V_p is the total polymer volume in the reactor given by equation (2.70) after replacing $\bar{q}_i$ and N_i by an overall average number of radicals, $\bar{q}$, and the total number of particles, N, from equation (2.69) respectively.

Equation (2.74) can be considered as only an approximation of equation (2.73) and it will hold better for narrow particle size distributions. Nomura et al. (1971) made a similar assumption for A_p on modelling a CSTR for the emulsion polymerization of styrene.

This simplified model was also numerically solved and the results obtained were found to agree quite well with those of the more comprehensive model. Due to the simple form of this approximate model, numerical calculations are shorter. In addition, equations (2.69-72) can be recast to the usual state space form

$$\dot{\underset{\sim}{x}}(t) = A\, \underset{\sim}{x}(t) + B\, \underset{\sim}{u}(t) \qquad (2.75)$$

when we are dealing with the control problem in Chapter 6.

Equations (2.69-72) were also solved numerically for the case of a batch reactor. Experimental results obtained by Friis (1973) and Keung (1974) were successfully simulated and the results of the simulation are shown in Appendix II. It is interesting to note that using the concept of discrete period for particle nucleation we were able to predict the particle size distribution in a batch reactor and compared it successfully with the distribution obtained by Keung using electron microscopic analysis.

2.6 Conclusions

So far, we have reviewed the different emulsion polymerization theories and models which have been used to describe and predict the complex physical and chemical phenomena occurring in an emulsion polymerization reaction. At this point, the reader can appreciate the problems involved in formulating adequate dynamic models which can be used for prediction and control studies.

Furthermore, in continuous emulsion polymerization systems reactor multiplicity and limit cycles phenomena should be considered in any modelling development. This seems to complicate more any modelling work on continuous systems.

Nevertheless, we have tried to present here different models based mainly on population balance equations and discuss existing techniques for solving these equations. It is clear, however, that a general solution for these population balance equations is too difficult and, therefore, particular solutions should be obtained for an emulsion system based on realistic assumptions and judgement. Such an approach has been taken in deriving the models in section 2.5.

There, two levels of models are presented; a comprehensive one which uses the age distribution of particles and a simplified model which accounts for discrete nucleation periods. In both models it is considered that polymer particles are generated by both micellar and homogeneous mechanisms. Formulating the net particle generation rate we have introduced two parameters which can be estimated from experimental data. The ability

of the general model to provide reactor simulations by specifying reactor operating conditions will be demonstrated through the simulation of our experimental results in Chapter 5. However, to study the problem of on-line control of a continuous latex reactor and find an optimal control policy, the approximate model should be used.

CHAPTER 3

ON-LINE TECHNIQUES AND MEASUREMENTS

3.1 Introduction

The measurement of particle and particle size distribution (PSD) is one of the most necessary tasks for characterizing a latex, a powdered material, or any suspension. The importance of this physical characteristic of a system is readily realized when one examines the chemical and physical properties controlled by particle size and size distribution. From a practical viewpoint, the particle size of a resin used, for example, in a coating paint or plastisol can be critical, and if the resin PSD contains particles with a diameter approaching the thickness of the coating, a streaky non-uniform film results. Thus, control of particle size by means of reproducible and accurate (and fairly simple) analysis is of primary importance.

As mentioned in Chapter 1, one of the objectives of the present work was the development of practical on-line techniques for the measurement of polymer particle size, total polymer volume and conversion. These techniques should be simple, accurate and fast enough to be used as on-line control measurements. Proper measurement at least some of the model's states (conversion, polymer volume, number of particles) is required to

achieve our control objectives.

From all techniques available for the measurement of particle size distribution, light transmission (LT) and liquid exclusion chromatography (LEC) appear to be the most practical and quickest ones for on-line control studies. Analysis time can be less than five minutes for both methods and they can be easily implemented for on-line measurements.

Various particle size measurements are briefly reviewed in section 3.2. Then, in section 3.3 a critical discussion of turbidity spectra analysis is presented. A statistical approach is developed in section 3.3.4 to correlate directly turbidity measurements with the states of the simplified model (equation 2.75). A description of LEC technique is given in section 3.4.

3.2 Some Methods of Particle Size Measurement

Much of the literature dealing with particle size measurements fails to analyze the spectrum of techniques as to their advantages and shortcomings, their principle, the kind of data obtained, and the applicability of given analytical techniques to the problem at hand. However, Collins et al. (1975) in a review article critically examined various particle size measurement techniques using the above criteria.

Some of the most important problems in particle size technology are summarized below.

(i) Ultimate particle size versus agglomerate size. If, for example, one is interested in the effect of particle size on viscosity, a measurement

of the ultimate size is of little value. However, if one is studying the growth of latex particles in emulsion polymerization then agglomerate size would be of little interest.

(ii) Particle shape. Most particles are a bit like humans, that is, no single number will adequately describe their physical dimensions. While microscopic methods enable some choice in the matter of defining a diameter, most methods do not. In light scattering, Brownian motion causes a spherical volume to be swept out by the particle and thus "time average sphere" is the basis of the diameter taken for the particle.

(iii) Particle Size Distribution. Once having decided on an appropriate measure for the diameter of the particle, one must next consider the distribution of particle sizes present. If the particles are all the same size a single number will suffice to describe the system; however, in a real situation this is never the case. "Average" diameters are usually used to describe a given particle population even when full distribution data is available. The main reasons for using particle size averages are:

a) They are convenient and simple

b) They lend themselves to numerical analysis

c) Some methods only give an average diameter.

The most familiar averages are;the number average which is defined as:

$$D_n = \frac{\Sigma n_i D_i}{\Sigma n_i} = \frac{\text{Number of particles of } D_i}{\text{Total number of particles}} \qquad (3.1)$$

The surface average is defined as:

$$D_s = \frac{\Sigma n_i D_i^3}{\Sigma n_i D_i^2} = \frac{\text{Total volume of particles}}{3(\text{Total particle surface})} \qquad (3.2)$$

This average is of interest in latex technology since it can be easily obtained by soap titration.

The weight average is defined as:

$$D_w = \frac{\Sigma n_i D_i^4}{\Sigma n_i D_i^3} = \frac{\Sigma w_i D_i}{\Sigma w_i} \qquad (3.3)$$

It is of importance primarily since many light scattering methods give a value close to it.

The volume average is equivalent to:

$$D_v = \left(\frac{\Sigma n_i D_i^3}{\Sigma n_i}\right)^{1/3} \qquad (3.4)$$

It is obtained from the flow ultramicroscope and similar devices which count the particles per unit volume of a suspension. It should be borne in mind that if distribution data is available then it is possible to compute any of the particle size averages.

A brief description of some "average" particle size measurement methods of their advantages and limitations is given in Table 3-1.

Methods used to obtain the particle size distribution vary from the direct microscope analysis to the indirect methods that depend on intrinsic or optical properties of the particles themselves. Techniques

Table 3-1 Some Methods Used for the Measurement of an Average Particle Size

Method	Principle	Advantages	Limitations	Application Range
1. Light Transmission	Measurement of transmitted monochromatic light which at a given concentration is a function of particle size and refractive index	-Method rapid, simple -Small sample -Values obtained useful for quality control	-Concentration should be known accurately -Presence of large particles will give high results -Sensitive to small changes in ratio of refractive indices(m)	Size determinations in the range of 500-3000Å
2. Dissymetry	The intensity of scattered light is measured at 45° and 135°	-Relatively simple -Relative concentrations need be known	-Multivalued answers above 2000Å -m, must be known	Size diameters to 2000Å
3. Maximum-Minimum Technique	Light intensity is measured as a function of angle and the angles of max and min intensity are noted.	-Concentrations need not be accurately known -Very high accuracy -A qualitative estimate of polydispersity can be obtained	-Expensive spectrophotometer must be used -Easy to miss an angle of max. intensity -m, must be known accurately -sensitive to polydispersity	The present lower limit is 2200Å

4. Forward Angle Ratio	The intensity of scattered light at various angles is measured and the ratio of intensities at five degree intervals computed	-Relative concentration need be known -Not very sensitive to m -Range from 500 to 5000Å	-Expensive spectrophotometer must be used	Useful to much larger particle diameter up to 5000Å
5. Flow Ultramicroscope	A highly dilute suspension is pumped through a glass tube. The tube is illuminated by an intense narrow band of light. As a particle passes through it appears as a flash of light through a microscope	-Method relative rapid -Accurate and reproducible -Detection of agglomerates -No calibration by means of a standard	-It is not available commercially -Total solids must be known with high precision -Too large diameters if the suspensions have a tendency to agglomerate	Measuring the particle diameter of any material larger than 500Å.

for measuring particle size distribution in the submicron range tend to be either time consuming, inaccurate or limited to a portion of the total size range.

Electron Microscope. The electron microscope with its greater resolution is useful in sizing particles below 10,000Å. Resolution on modern instruments is of the order of 2-7Å. A drop of highly dilute suspension (10^{-3}-10^{-5} gm/ml) is placed on a collodion coated screen of about 200 mesh and allowed to dry. The dried specimen is then examined in the microscope and particles photographed, and from the magnification employed the number average particle size can be computed. Diameter averages other than number average can also be obtained by integrating the histogram.

One of the main problems in electron microscopy is the difficulty in obtaining a representative sample. Since 1-2 thousand particles are generally counted the magnitude of the problem is apparent. Another problem with the electron microscope is that the temperature of the sample can reach as high as 200°C. Under these conditions PVC latexes, for example, will shrink and give diameters about 20% too low. Furthermore, PVAc and other soft latices should be treated with a special hardening technique before particles will be photographed. This treatment can alter the original particle dimensions; therefore, the final particle averages.

Above all this method is time consuming, expensive and obviously not an on-line technique.

Joyce Loebl Disc Centrifuge. The principle of the Joyce Loebl Disc Centrifuge system combines that of sedimentation with centrifugation. The Joyce-Loebl

instrument depends on the centrifugation of suspension for a time t and then sampling the suspension at a given distance into the fluid where Stokes' Law predicts the presence of particles smaller than a given diameter and measuring the concentration. From this data a distribution graph of particle diameter against percentage cumulative weight under size can be obtained.

The Disc Centrifuge allows analysis of particles, depending on their density, ranging from 30μ down to 0.01μ. This method is difficult to use with particles smaller than 1000Å because the analysis time becomes too long considering the stability of the instrument.

3.3 Turbidity Spectra Analysis for Measurement of PSD

3.3.1 Turbidity Spectra

Light transmission has been a standard method for the measurement of colloidal spherical particles. The fundamental theory was developed by Mie. Heller and his coworkers in a series of papers (Heller and Pangonis (1957), Wallach et al. (1961) and Stevenson et al. (1961)) outlined the theory which gave size distribution curves in heterodisperse systems of nonabsorbing colloidal spheres from measurements of turbidity spectra. The assumption was made that the unknown PSD followed a distributional form commonly found in emulsion systems. Maron et al. (1963) applied the method to measure polydisperse polybutadiene-styrene particles. Gledhill (1961) described a method for constructing a graphical calibration grid for a system of known optical constants and known distributional form, from which the

weight mean diameter and standard deviation of the distribution corresponding to observed turbidity measurements could be read directly. The particle size distribution constants obtained by that method agreed with those determined from electron-microscopic analysis.

However, as Maxim et al. (1969) indicated in their publication, the turbidity spectra method, though very attractive because of the simplicity of the experimental technique, should not be used alone for particle size analysis and hence cannot be considered a routine procedure. In their work, they assumed that the distribution followed the function below, which presumably is commonly found in emulsion latices:

$$Cf(r) = (r-r_o)\exp(-(r-r_o)/s)^3 \quad \text{for } r > r_o \tag{3.5}$$

where C is a normalized constant, r_o is the radius of the smallest particles present, and s is a parameter describing the width of the distribution. To obtain estimates of the parameters r_o and s, they used a non-linear least squares method and drew the 99% joint confidence region for the parameters. Looking at the long narrow shape of that likelihood contour they correctly concluded that the actual distribution could fall anywhere within that envelope (an infinite number of alternative distributions). In other words a unique distribution could not be obtained. In their conclusions, they stated that matching experimental and theoretical curves to determine appropriate parameter values might result in multivalued solutions.

However, if results of this turbidimetric determination can at least specify a family of alternative distributions, then by combining this method

with some other technique for measuring a given moment of the distribution, we should be able to satisfactorily specify a unique member of this family. The use of LEC as a complementary technique could solve the problem of on-line determination of PSD.

The advantages and shortcomings of the turbidimetric determination should have become clear from the discussion so far. Next the underlined theory and quantitative equations which relate the turbidity to a PSD are developed.

3.3.2 Turbidity Theory

In the absence of multiple scattering and for a monodisperse spherical suspension the turbidity, τ, is related to particle number and diameter as follows:

$$\tau = N \frac{\pi D^2}{4} K\left(\frac{D}{\lambda_m}, \frac{n}{n_m}\right) \tag{3.6}$$

where N is the number of particles/liter, D is the particle diameter, $K\left(\frac{D}{\lambda_m}, \frac{n}{n_m}\right)$ is the extinction coefficient readily calculated as a function of D/λ_m and n/n_m using the Mie theory. λ_m is the wavelength of light in the suspending medium; n and n_m are the refractive indices of the particle and suspending medium correspondingly. The turbidity is found by measuring the intensity of transmitted light with a spectrophotometer and using the following equation:

$$\tau = \frac{1}{\ell} \ln(I_o/I) \tag{3.7}$$

where I_o is the intensity of the primary beam, I is the intensity of the transmitted beam and ℓ is the path length of the detector cell. For a polydisperse suspension of spheres equation (3.6) becomes an integral equation of the form:

$$\tau = N \int_o^\infty K\left(\frac{D}{\lambda_m}, \frac{n}{n_m}\right) \frac{\pi D^2}{4} f(D)dD \qquad (3.8)$$

In principle, measurement of τ as a function of wavelength should permit one to determine N, the number of particles per liter and f(D), the normalized frequency distribution of particle diameter. There are, of course, some limitations to this approach and, specifically, for values of alpha ($\alpha = \frac{\pi D}{\lambda_m}$) less than unity when the Rayleigh scattering theory gives the extinction coefficient analytically as

$$K = \frac{8}{3}\left(\frac{m^2-1}{m^2+2}\right)^2 \alpha^4 \qquad (3.9)$$

Substituting equation (3.9) into (3.8) one obtains

$$\tau = \frac{2\pi^5}{3\lambda_m^4}\left(\frac{m^2-1}{m^2+2}\right)^2 N \int_o^\infty D^6 f(D)dD \qquad (3.10)$$

The concentration of particles can be expressed as

$$c = \frac{\pi d_p N}{6} \int_o^\infty D^3 f(D)dD \qquad (3.11)$$

Dividing equation (3.10) by (3.11) we obtain

$$\frac{\tau}{c} = \text{Con.} \frac{\int_0^\infty D^6 f(D)dD}{\int_0^\infty D^3 f(D)dD} = \text{Con.}\ \bar{D}_w^{-3} \qquad (3.12)$$

where $\bar{D}_w$ is a turbidity weight average particle diameter.

It is clear that for a polydisperse suspension in the Rayleigh scattering regime, the use of different wavelengths will not provide additional information. Indeed it is necessary to know both τ and c to obtain a measure of $\bar{D}_w$. In the Mie scattering regime ($1.0 < \alpha < 10.0$) the dependence of the extinction coefficient on α is more complex and in principle it should be possible to obtain both the particle number and size distribution through measurements of turbidity as a function of wavelength. However, without prior knowledge of the shape of the particle size distribution, it is almost impossible to find a unique distribution function. Moreover, even if we know the distributional form of the unknown distribution it is very difficult to avoid multivalued solutions for the parameters. However, for purposes of control of polymer particle number and size distribution it may not be necessary to know the precise distribution. The establishment of desirable time trajectories for particle number and D_n and D_w should be adequate to ensure that the specifications of the final latex product can be attained. A technique for solving directly for the moments of the unknown PSD is now developed.

3.3.3 The Method of Moments

One of the main problems with the turbidimetric technique to determine the PSD of a latex product is that the form of the unknown PSD must

be assumed. To overcome this problem according to our proposed technique the term $K(\frac{D}{\lambda_m},\frac{n}{n_m})\frac{\pi D^2}{4}$ in equation (3.8) is approximated with a polynomial of the form

$$K(\frac{D}{\lambda_m},\frac{n}{n_m})\frac{\pi D^2}{4} \simeq \sum_{i=0}^{p} C_{i\lambda} D^i \qquad (3.13)$$

To estimate values for the $C_{i\lambda}$ coefficients at a given wavelength (e.g. $\lambda = 6000\text{Å}$), we first generate values for the $K\frac{\pi D^2}{4}$ term using a program developed by Dave (1968) at IBM. Then, estimates for the polynomial coefficients, $C_{i\lambda}$, are obtained from a least squares routine. The order of polynomial approximation, p, is chosen to give what is considered to be an adequate fit of the data. In Table 3-2, the function, $K\frac{\pi D^2}{4}$, is compared with the polynomial approximation of equation (3.13). The agreement is good. Table 3-3 gives the values of the polynomial coefficients, $C_{i\lambda}$ for different wavelengths.

Equation (3.13) can be now substituted into equation (3.8) which becomes

$$\tau_\lambda \simeq N \int_0^\infty (\sum_{i=0}^{p} C_{i\lambda} D^i) f(D)\,dD \qquad (3.14)$$

By recalling the definition of the "i" moment of a distribution,

$$J_i = \int_0^\infty D^i f(D)\,dD \qquad (3.15)$$

equation (3.14) can be written in terms of the moments of the unknown

Table 3-2

Exact and Approximate Values of $\frac{K\Pi D^2}{4}$ Function (equation (3.13)) for Different Values of D(λ = 5000 Å)

D in nm	$\frac{K\Pi D^2}{4}$	$\sum_{i=1}^{7} C_{i\lambda} D^i$	D in nm	$\frac{K\Pi D^2}{4}$	$\sum_{i=1}^{7} C_{i\lambda} D^i$
40	$.1844\ 10^2$	$.6047\ 10^3$	440	$.3995\ 10^7$	$.4003\ 10^7$
80	$.1064\ 10^4$	$.1682\ 10^4$	480	$.5757\ 10^7$	$.5753\ 10^7$
120	$.1012\ 10^5$	$.9612\ 10^4$	520	$.8014\ 10^7$	$.8004\ 10^7$
160	$.4400\ 10^5$	$.4082\ 10^5$	560	$.1084\ 10^8$	$.1084\ 10^8$
200	$.1239\ 10^6$	$.1205\ 10^6$	600	$.1432\ 10^8$	$.1433\ 10^8$
240	$.2776\ 10^6$	$.2823\ 10^6$	640	$.1856\ 10^8$	$.1857\ 10^8$
280	$.5578\ 10^6$	$.5672\ 10^6$	680	$.2366\ 10^8$	$.2364\ 10^8$
320	$.1026\ 10^7$	$.1023\ 10^7$	720	$.2965\ 10^8$	$.2964\ 10^8$
360	$.1717\ 10^7$	$.1707\ 10^7$	760	$.3661\ 10^8$	$.3664\ 10^8$
400	$.2675\ 10^7$	$.2678\ 10^7$	800	$.4474\ 10^8$	$.4474\ 10^8$

Table 3-3

Numerical Values of the Coefficients $C_{i\lambda}$ at Different Wavelengths

λ(nm)	C_0	C_1	C_2	C_3	C_4	C_5	C_6
650	$-.2402\ 10^{5}$	$.8592\ 10^{2}$	$-.7382\ 10^{-1}$	$.1668\ 10^{-4}$	$.3421\ 10^{-8}$	$.3685\ 10^{-12}$	$-.1949\ 10^{-16}$
600	$.6314\ 10^{4}$	$-.2718\ 10^{2}$	$.4006\ 10^{-1}$	$-.3213\ 10^{-4}$	$.1453\ 10^{-7}$	$-.5434\ 10^{-12}$	$.1016\ 10^{-16}$
550	$-.1633\ 10^{5}$	$.6029\ 10^{2}$	$-.5034\ 10^{-1}$	$.4197\ 10^{-5}$	$.9376\ 10^{-8}$	$.7939\ 10^{-13}$	$-.1479\ 10^{-16}$
500	$-.7145\ 10^{3}$	$.3424\ 10^{1}$	$.5138\ 10^{-2}$	$-.2031\ 10^{-4}$	$.1684\ 10^{-7}$	$-.4064\ 10^{-12}$	$-.3933\ 10^{-17}$
450	$-.8700\ 10^{4}$	$.3535\ 10^{2}$	$-.2936\ 10^{-1}$	$-.7906\ 10^{-5}$	$.1826\ 10^{-7}$	$-.2665\ 10^{-12}$	$-.1749\ 10^{-16}$
400	$-.2256\ 10^{4}$	$.1048\ 10^{2}$	$-.3606\ 10^{-2}$	$-.2269\ 10^{-4}$	$.2730\ 10^{-7}$	$-.7531\ 10^{-12}$	$-.1604\ 10^{-16}$
350	$.1280\ 10^{5}$	$-.5110\ 10^{2}$	$.6515\ 10^{-1}$	$-.6022\ 10^{-4}$	$.4526\ 10^{-7}$	$-.2002\ 10^{-11}$	$-.1368\ 10^{-18}$

distribution as

$$\tau_\lambda = N(C_{o\lambda}J_o + C_{1\lambda}J_1 + \ldots + C_{p\lambda}J_p) \qquad (3.16)$$

To eliminate the dependence of τ_λ in equation (3.16) from the number of particles, N, equation (3.16) is divided by an arbitrary turbidity value, τ^*_λ, taken within the range of turbidity spectra (6500 to 3500Å). Therefore,

$$g_\lambda = \frac{\tau_\lambda}{\tau^*_\lambda} = \frac{\sum_{i=0}^{p} C_{i\lambda}J_i}{\sum_{i=0}^{p} C^*_{i\lambda}J_i} \qquad (3.17)$$

Equation (3.17) relates the unknown moments of the distribution, J_i, with the known ratios, g_λ. By recalling that the zero moment of any normalized function is equal to 1, equation (3.17) can be rewritten as

$$(C_{1\lambda}-g_\lambda C^*_{1\lambda})J_1 + (C_{2\lambda}-g_\lambda C^*_{2\lambda})J_2 + \ldots = -(C_{o\lambda}-g_\lambda C^*_{o\lambda}) \qquad (3.18)$$

To estimate the first p moments of the unknown distribution, f(D), equation (3.18) can be applied at (p-1) different wavelengths and the resulting system of simultaneous algebraic equations solved for the unknown moments. A least squares solution can be used if more than (p-1) measurements are used.

The proposed method is simple and the number average, D_n, and weight average particle diameter, D_w, are easily calculated in terms of the computed moments as,

$$D_n = J_1 \quad \text{and} \quad D_w = J_4/J_3.$$

The determination of the unknown PSD is based on the assumption that a given distribution can be represented analytically with the use of a given set of moments. For the representation of a distribution from its moments, the Laguerre polynomial expansion or the Hermite polynomial expansion can be applied. Any normalized distribution function can be represented with its moments (Hulbert and Katz (1964), Hamielec and Ray (1969), Min (1976)) as

$$f(D) = \frac{1}{\Gamma(\beta+1)} \exp(-D) D^{\beta} \sum_{n=0}^{N_{max}} C_n^{\beta} L_n^{\beta}(D) \qquad (3.19)$$

where the base distribution is the gamma distribution and is modified further with an increasing number of moments. The coefficients, C_n^{β}'s reflect the moment information as

$$C_n^{\beta} = \sum_{j=0}^{n} (-1)^j \frac{(n_j)\beta!}{\Gamma(\beta+j+1)} J_j \qquad (3.20)$$

and the generalized Laguerre polynomial, $L_n^{\beta}(D)$, is

$$L_n^{\beta}(D) = \frac{\exp(D) D^{-\beta}}{n!} \frac{d^n}{dD^n} \{\exp(-D) D^{n+\beta}\} = \sum_{j=0}^{n} (-1)^j \binom{n+\beta}{n-j} \frac{D^j}{j!} \qquad (3.21)$$

where β is a free parameter to be determined. The value of β is determined so as to provide a fast convergence of the series in equation (3.19), and is chosen such that the only distribution which can be obtained from its first two moments J_1 and J_2 (information on a mean and a variance), is a family of the gamma distribution.

$$f(D) = \frac{1}{\Gamma(\beta+1)} \exp(-D) D^{\beta} \qquad (3.22)$$

By determining β in this way the normalized distribution function, $f(D)$, is represented with its moments as equation (3.19) with $C_0^{\beta} = 1$ and $C_1^{\beta} = C_2^{\beta} = 0$.

3.3.4 Principal Component Regression on Turbidity Data

An alternative approach to the interpretation of the turbidity spectra and to relating them to the model states (polymer volume, etc.) is to use strictly empirical regression models. That is, rather than building on the theoretical relationship of equation (3.8), one can develop empirical regression models for a particular system which will enable one to predict the polymer volume (and perhaps the number of particles) at different times from the measured turbidity curves (Figure 3-1). In order to extend the maximum amount of information from these curves while using a minimum number of regression variables and parameters, one can use principal components.

If the turbidity curves are represented by a vector of observations $\underline{X}_i(\lambda)$ taken at a number of discrete wavelengths, the principal components will be linear combinations of these measurements which have special properties. For example, the first principal component is the normalized linear combination with maximum variance, while the second principal component is that linear combination, orthogonal to the first one that has the next largest variance, etc. These principal components are the characteristic vectors of the covariance matrix of the $\underline{X}_i(\lambda)$ vectors. The corresponding characteristic values are their variances (Anderson (1958)). The use of

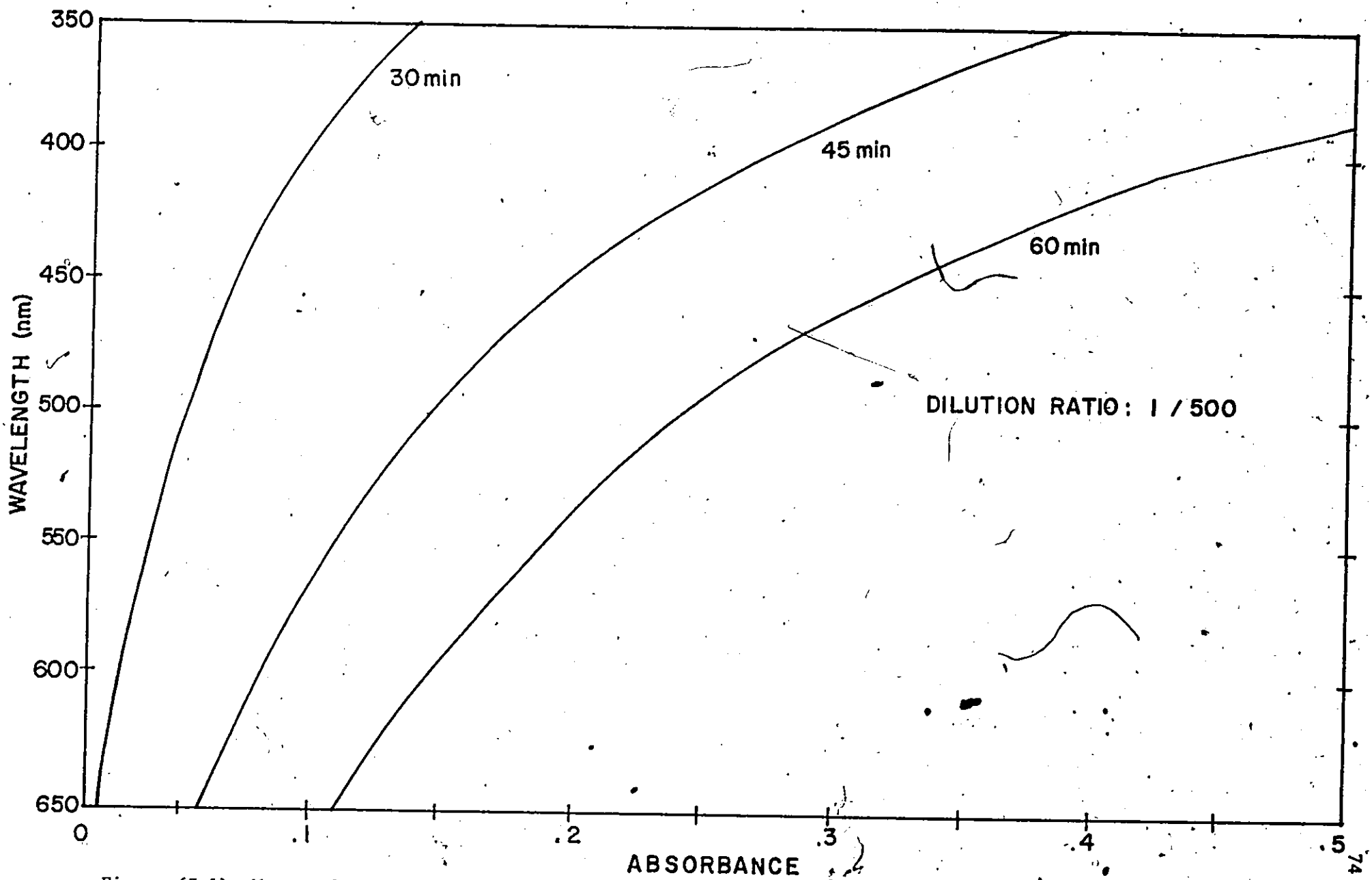

Figure (3-1) Measured Turbidity Curves at Different Reaction Times

principal components here is to reduce the dimensionality of the prediction variable space from an infinite dimensional one (a continuous turbidity curve) to one defined by a small number of orthogonal independent variables (linear combinations of the spectral measurements) which essentially contain most of the information of the original space. An example of the use of principal component regression is given by Sylvestre et al. (1974) in a spectrophotometric study of a simple reversible chemical reaction.

In Chapter 6 the principal component analysis is applied to obtain regression equations which adequately predict conversion, total polymer volume as a function of turbidity values.

3.4 Liquid Exclusion Chromatography

For over a decade, gel permeation chromatography (GPC) has been used extensively for the separation of polymer molecules according to their size in solution. Recently, this technique has been adopted for analogous separation of colloidal dispersions according to size (Small (1974), Small et al. (1976), Coll et al. (1975), Gaylor et al. (1975)).

There are two complementary approaches to the use of size exclusion chromatography to separate particle suspensions according to size. The more powerful technique called liquid exclusion chromatography (LEC) utilizes porous packing and relies mainly on steric exclusion from the pores of the packing for size separation. The other called hydrodynamic chromatography (HDC) mainly developed by Small (1974), utilizes non-porous packing and relies mainly on the velocity profile in the interstitial regions

for size separation. These two complementary approaches cover particle diameter ranges from 10-5000Å (LEC) and 3000-20,000Å (HDC). In LEC there is no limit to how small the particle to be separated can be. The upper limit is a result of a greatly reduced diffusion coefficient for large particles, and is probably about 4000Å. On the other hand, there appears to be a practical lower limit for HDC, Mori (1974). The upper limit on particle diameter is probably several microns and can be increased by increasing the diameter of the packing particle.

Krebs and Wunderlich (1971) were the first to succeed in separating polymethylmethacrylate and polystyrene latex particles using silica gel having very large pores (500-50,000Å). More recently, Gaylor et al. (1975) and Coll et al. (1975) developed LEC further by suitable selection of emulsifier and electrolyte concentrations to optimize resolution. The basic separating mechanisms in LEC and in HDC are discussed in the following section.

3.4.1 Separation Mechanisms

Figure 3-2 shows schematically the difference between the separating mechanisms for LEC and HDC. A bed packed with porous or non-porous particles presents the particles suspended in the carrier liquid with a tortuous path through a large number of capillary-like tunnels. Larger particles are excluded from regions near the capillary walls where axial velocities are small and on the average experience higher velocities and shorter residence times in the bed. With porous packing smaller suspended particles can also

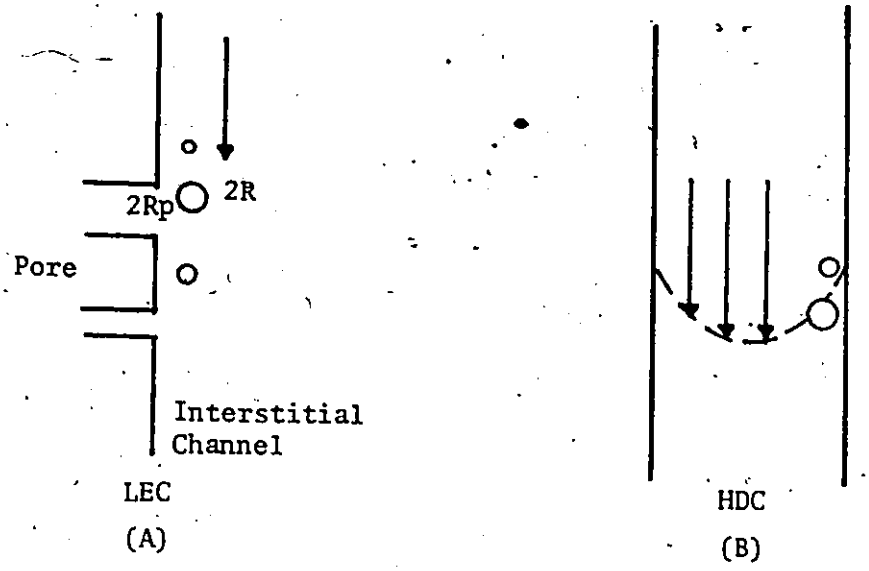

Figure (3-2) Diagrammatic Representation of the Mechanisms of Separation by Liquid Exclusion Chromatography LEC) Hydrodynamic Chromatography (HDC)

diffuse into the pores giving a second and more efficient mechanism of retardation and size separation. It has been suggested that the flow pattern of the liquid in the interstitial channels also plays an important role in separation, (DiMarzio et al. (1969)).

A most important problem in the chromatography of lyophobic sols is the tendency for adsorption on the packing material. It is, therefore, essential that the carrier liquid contain a stabilizing agent such as an anionic surfactant. In the investigation made by Coll et al. (1975) with porous glass packing, it was necessary to use surfactant and electrolyte. The surfactant was used to prevent adsorption and the electrolyte to suppress the electrical double layer so as to prevent it from filling the pores. In the absence of electrolyte the latex particles were virtually excluded from all the pores.

McHugh (1977) first investigated the use of UV spectrophotometer and the Mie theory as a detector for HDC. This subject has been studied in some detail by Singh and Hamielec (1977) and Singh (1977). They have derived correction factors for axial dispersion for a general detector whose signal is proportional to the number of particles times particle diameter to the power gamma (γ) where γ varies from zero to six. This general detector includes a turbidimeter ($\gamma=6$) and a refractometer ($\gamma=3$). They concluded that LEC is sufficiently rapid for the off-line monitoring of latex particle growth in emulsion polymerization. With some modification it could be used in an on-line mode as a sensor for reactor control. However, the present state of LEC does require the development of a proper method for the

complete extraction of a PSD from a chromatograph peak profile.

3.5 Other On-line Techniques

Up to this time, we have seen different techniques which are available for measuring the particle size of aqueous dispersions of materials having diameters considerably smaller than the wavelength of visible light. From those techniques discussed turbidity spectra analysis and LEC appear to be the most favourable ones. This is mainly due to the following reasons:

(i) Relatively inexpensive equipment is required.

(ii) They are simple and rapid.

(iii) They can be easily implemented as on-line techniques.

(iv) Their accuracy and efficiency can be increased if both techniques are used in a complementary way.

There are several other techniques which can be used as on-line methods for measuring some of the states of the control model (conversion, number of particles, soap concentration etc.). Gas chromatography analysis can be used on-line for measuring conversion and conductivity or pH-measurements can be related to the free soap concentration or the total interfacial area of polymer particles. Conductivity could be high during the early stages of polymerization because soap is present in micellar form producing better electrical transport than after it has become primarily attached to more bulky latex particles. Beyond the CMC, the conductivity decreases. Conductivity remains relatively high in these systems because of the salts other than soap which are present. However, the soap

is by far the highest concentration of ionizable salt present and its bonding in a less mobile form to the growing polymer particles causes a considerable decrease in conductivity. Surface tension measurements also can be used to follow and detect the critical micelle concentration and free soap variations.

3.6 Conclusions

Several techniques used for measuring some "average" particle diameter or PSD have been discussed. From the methods described, turbidity spectra analysis and liquid exclusion chromatography appear to have some specific advantages over other techniques. They are simple, rapid and can be used as on-line detectors.

A new technique for calculating the leading moments of an unknown distribution from a series of turbidity measurements has been developed. A statistical method has also been described which directly correlates the turbidity measurements with the states of our control model.

Application and results of the last two techniques are given in Chapter 6 of this thesis.

CHAPTER 4

EXPERIMENTAL STUDIES

4.1 Introduction

To test the comprehensive and approximate models developed (section 2.5) for the continuous emulsion polymerization of vinyl-acetate, a series of experiments was carried out with different initiator (I) and emulsifier (S) concentrations, for different residence times θ and rates of agitation, (r.p.m.). The effect of these variables on the production rate of polyvinyl acetate latices in a CSTR was investigated over a wide range of operating conditions. The related phenomena of sustained oscillations (in which the conversion and number of particles oscillate widely with time), as well as particle agglomeration were observed in numerous runs. Domains of conditions which gave rise to sustained oscillations or complete agglomeration of the product were experimentally mapped out. Different start-up policies were attempted to find out their effects on reactor transients and steady state levels.

On and off-line turbidity measurements from a scanning spectrophotometer were successfully used to follow the reactor variations. Off-line conversion measurements were done gravimetrically. To monitor the latex particle growth rate and changes in particle size distribution an LEC technique was successfully employed.

A description of the experimental set-up is given in section 4.2. Then, in the following sections, experimental results collected under different operating conditions are presented and critically discussed.

4.2 Experimental Procedure

4.2.1 Materials and Reactor Layout

The chemicals used in this study were vinyl acetate, emulsifier, initiator and water. The vinyl acetate was obtained from CIL in 5 gallon drums. The monomer was distilled to remove the inhibitor and kept in a refrigerator before use. The emulsifier used was sodium lauryl sulphate (Product No. 30175) obtained from BDH Chemicals. Laboratory grade potassium persulfate of 99.7% purity was obtained from Fisher Scientific Co. and was used as initiator. These chemicals were used without further purification. Distilled water was used as the dispersion medium and solvent for the initiator. Two grades of nitrogen used were an L-grade (99.5%) and a certified grade (99.99%). Nitrogen was used to purge the initial reaction mixture and raw materials. It was found that different rate data were obtained when using different nitrogen grades. For the final experimental runs a certified nitrogen grade was used. Traces of oxygen were removed by bubbling the nitrogen gas through a 5% pyrogallol solution in 2N NaOH.

Reactor Layout. A schematic diagram of the reaction apparatus is shown in Figure 4-1. Two storage tanks were used for the raw material. Both tanks made from polyethylene were blanketed with nitrogen to prevent oxygen retardation. The first tank containing the monomer (4 parts), water (7 parts) and

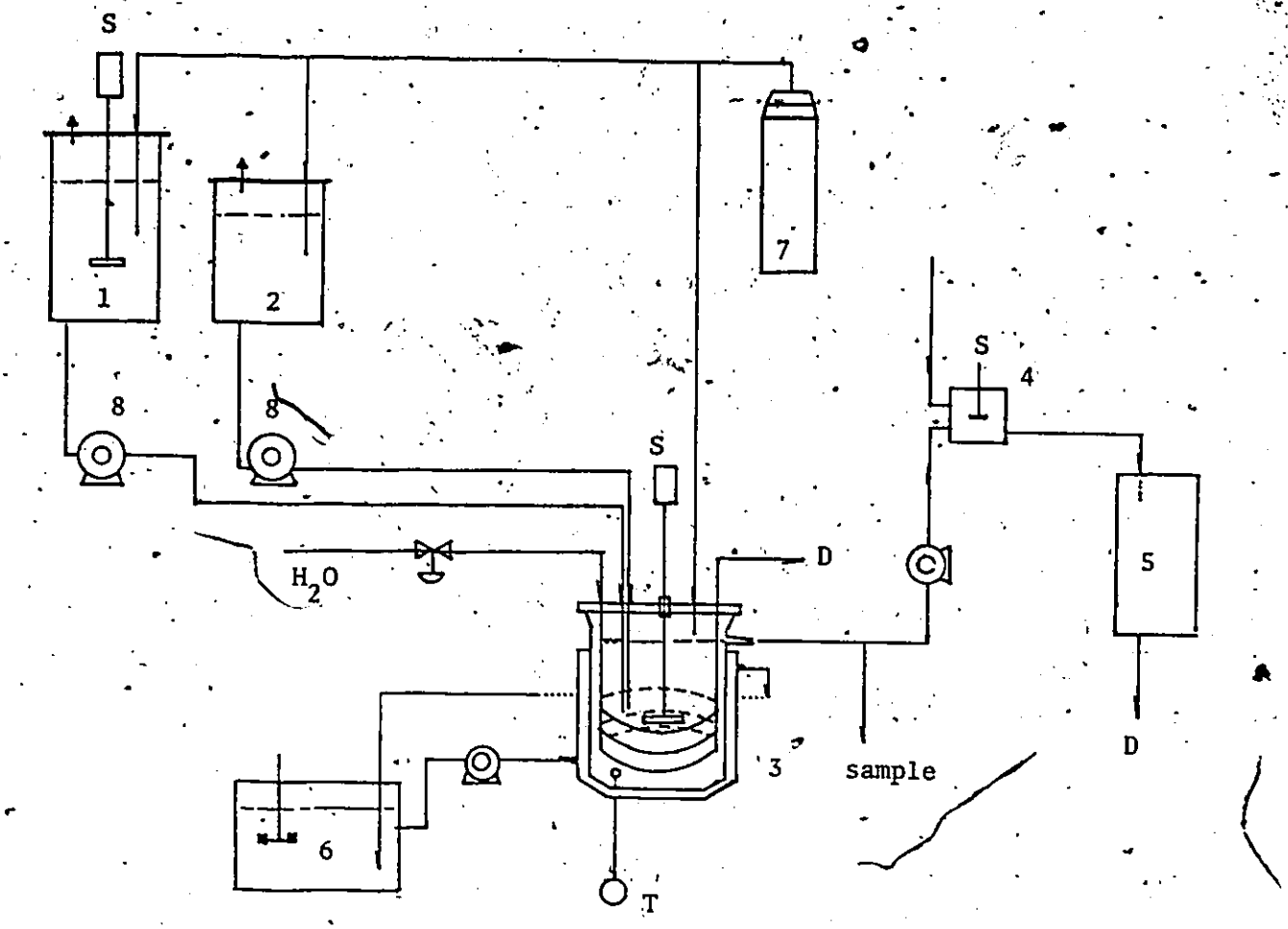

Figure (4-1) Schematic Diagram of the Reactor Set-up

1 - Storage Tank (Monomer, water, soap)
2 - Storage Tank (Water, initiator)
3 - Reactor
4 - Dilution Vessel
5 - DU Spectrophotometer
6 - Constant Temperature Bath
7 - Nitrogen supply
8 - Constant flow rate pumps
S - Stirrer
D - Drain

surfactant had a 5 gallon capacity and was stirred by a flat blade paddle. The smaller storage tank containing the rest of the recipe's water (3 parts) and the total amount of initiator had a 2 gallon capacity. The two separate feeds were fed to the reactor at constant rate by an MPL-micro duplex pump through polyethylene tubing. The reactor was a two liter, jacketed glass kettle with an overflow arm attached to its side to give a reactor volume of 1.2 ℓ at 320 r.p.m. The lid contained four ground joint connectors. The joint in the center contained the stirring rod. The other three joints contained the feed lines, condenser, inlet and outlet water flow lines, a thermometer, a thermocouple and the nitrogen purge line. The reactants were stirred using a flat blade, paddle type stirrer driven by a CAFRAMO model variable speed motor. The stainless steel cooling coil inside the reactor provided baffling to ensure proper mixing.

The reactor was designed so that it could be disassembled and re-assembled very easily to facilitate cleaning.

To keep a constant temperature in the reactor (50±.5°C) two different water streams, a cold and a hot one, were used. A heating bath was used to maintain the temperature of the hot stream at about 65°C. A high flow rate centrifugal pump was used for the circulation of the hot stream through the reactor jacket. The cold stream at about 40°C was flowing through a stainless steel coil, which was merged inside the reactor. To maintain a constant temperature in the reactor a simple feedback control loop was designed. This was accomplished by inserting a copper-constantan thermocouple in the reactor. An ACROMAG transmitter was used to convert a millivolt signal from the

thermocouple into a 10-50 mA input signal to a Proportional-Integral Foxboro electronic controller (model 62H). The controller's output, a 10-50 mA signal, after proper conversion into 1-9 volts signal was fed to a pressure-voltage transducer. The pneumatic output of the transducer (3-15 psig) could actuate a diaphragm control valve to regulate the flow rate of the cold stream.

The effluent emulsion product was divided into two streams. One stream after proper dilution with distilled water (100 to 500 times) was allowed to continuously flow into a Beckman DU spectrophotometer for turbidity measurements. Off-line turbidity measurements were also obtained every 10-20 min. Detailed instructions for the operation of the spectrophotometer are given in the Beckman manual. Samples for conversion and LEC measurements were collected from the second stream at regular time intervals (15 or 20 min.).

4.2.2 Polymerization Procedure

For all experiments, the emulsion recipe comprised 1000 ml H_2O, 400 ml of vinyl acetate and varying amounts of initiator (0.005-0.03 mole/ℓ-H_2O) and emulsifier (0.01-0.06 mole/ℓ-H_2O). The initiator was predissolved and the solution was purged with nitrogen for one hour before the reaction was started, as well as, during the experiment. The monomer, emulsifier and part of the recipe's total water (70%) were originally charged into the storage tank and stirred at a constant 600 r.p.m. under a nitrogen atmosphere for one hour so that a uniform emulsified mixture was obtained. The reactor start-up

consisted of filling the reactor with distilled water prior to introducing any feed streams. Then the nitrogen purge system was turned on, and the system was brought up to the reaction temperature (50°C), and the stirrer was adjusted to a speed of 320 r.p.m. After about one hour, the duplex micro-pump was turned on and the two separate streams were fed at constant rate into the reactor. At the same time the reactor nitrogen purge system was turned off. The continuous overflow was driven into a 5 gallon drum which contained a concentrated solution of hydroquinone (HDQ) for quenching the polymerization.

The conversion samples were obtained at frequent intervals by collecting about 5-10 ml of latex in a vial. The sample temperature was adjusted to about 10°C and then about 1 ml of it was transferred into a preweighed glass dish which was immediately weighed. After weighing the sample, 1-2 drops of a diluted solution of HDQ were added to avoid any further reaction. Then the dish was put into a vacuum oven at 25°C to dry to constant weight. The rest of the sample was kept at about 10°C and was used for off-line turbidity measurements, LEC analysis and for conversion replicates.

In a batch reactor the most common measurement is the conversion which is defined as the weight of polymer formed per weight of initial monomer present. In a match flow CSTR, that is when the feed and the initial reactor recipes are identical, the conversion can be defined in a similar manner to a batch reactor. However, if the feed and initial reactor concentrations are not identical another type of conversion definition must be formulated.

The concentration of monomer in all forms in the reactor, M_T(gr/ℓ-latex), can be obtained from

$$M_T = d_p V_p + M_{dr} + M_p + M_d \tag{4.1}$$

and must satisfy the equation

$$\frac{dM_T}{dt} = \frac{M_F - M_T}{\Theta} \tag{4.2}$$

where M_{dr}, M_p, M_d, M_F are: the monomer concentration in the monomer droplets, polymer particles, aqueous phase and feed respectively. d_p is the polymer density.

For a constant monomer feed concentration, M_F, the solution to equation (4.2) can be easily obtained as

$$M_T = M_F + e^{-t/\Theta}(M_{TO} - M_F) \tag{4.3}$$

where M_{TO} is the initial monomer concentration in the reactor.

Conversion, x, is then defined as the weight of polymer formed per weight of total monomer present, equation (4.3). In other words, x is calculated from equation (4.1) as

$$x = \frac{M_T - M_{dr} - M_p - M_d}{M_T} = \frac{d_p V_p}{M_T} \tag{4.4}$$

A total of 37 experimental runs were completed during the course

of this study. The effects of initiator, emulsifier concentration, residence time, stirring rate and the presence of impurities on the rate of polymerization were studied and the results are shown and discussed in the following pages. It should be kept in mind, however, that vinyl acetate emulsion polymerization is an extremely complex heterogeneous process. In the past, a large amount of research has been done to elucidate the effect of these variables on the rate of polymerization. However, the experimental results are very often contradictory.

4.3 Experimental Results

4.3.1 The Effect of Initiator and Emulsifier on Rate of Polymerization

Conversion and turbidity measurements have been tabulated and given in Appendix III. The effects of initiator and emulsifier variables on the rate of polymerization were investigated by designing a 2^2 factorial design. Two such factorial designs were performed each at a different mean residence time. The rate of agitation remained constant (320 r.p.m.) for all these experiments. Thus, for a 30 min. mean residence time we ran four experiments by taking all combinations of 2 levels of initiator (I = 0.005 and I = 0.01 mole/ℓ), with the 2 levels of emulsifier (S = 0.01 and S = 0.06 mole/ℓ). For a 20 min. mean residence time the 2 initiator levels were (I = 0.01 and I = 0.02 mole/ℓ) and the emulsifier levels (S = 0.01 and S = 0.04 mole/ℓ). Figures 4-2, 4-3, 4-4 and 4-5 show conversion versus time curves at different initiator-emulsifier concentrations. Qualitatively it can be observed that sustained oscillations appear at low emulsifier

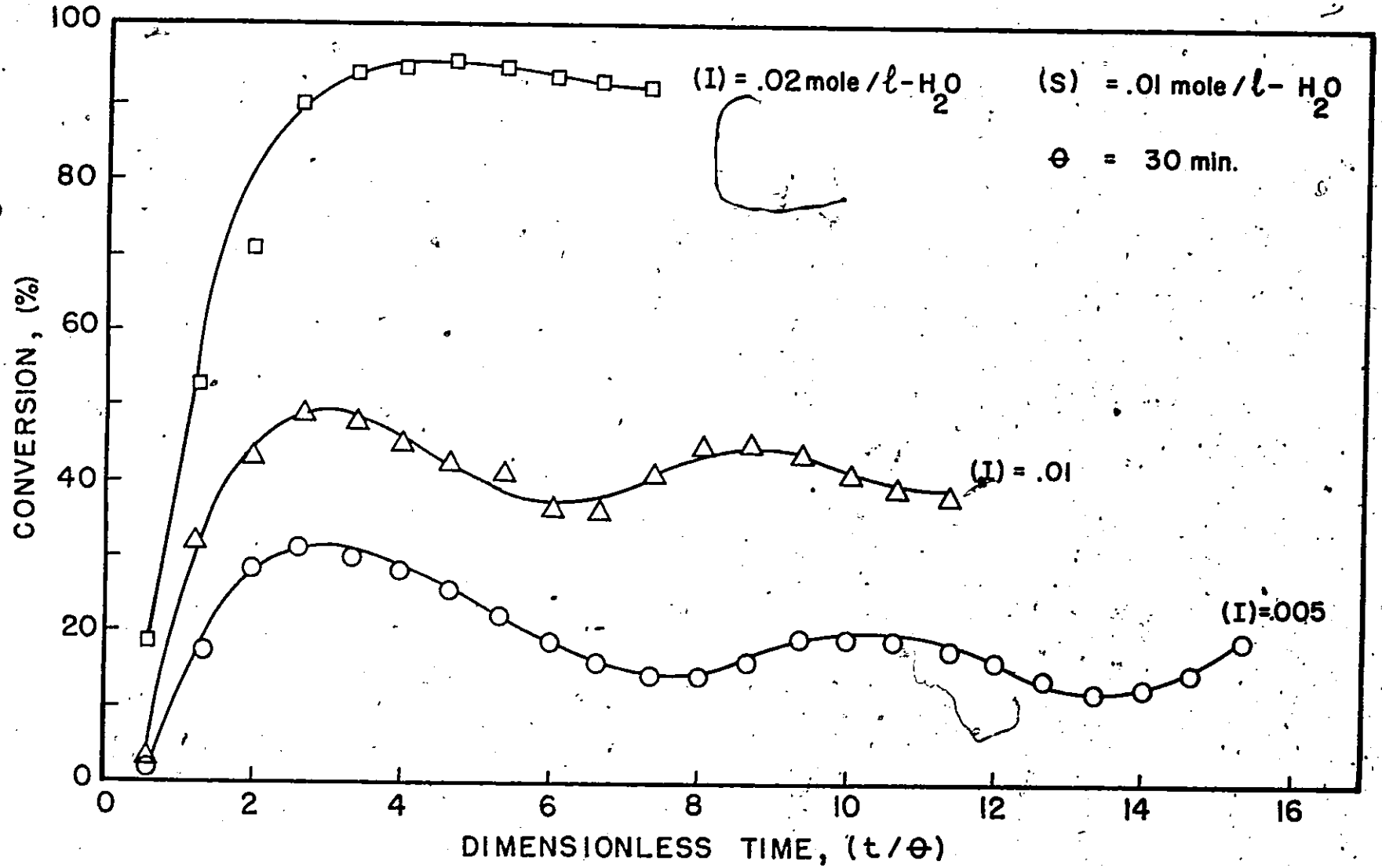

Figure (4-2) Conversion-Time Histories for Different Initiator Concentrations (T = 50°C, M/W = 4/10, r.p.m. 320)

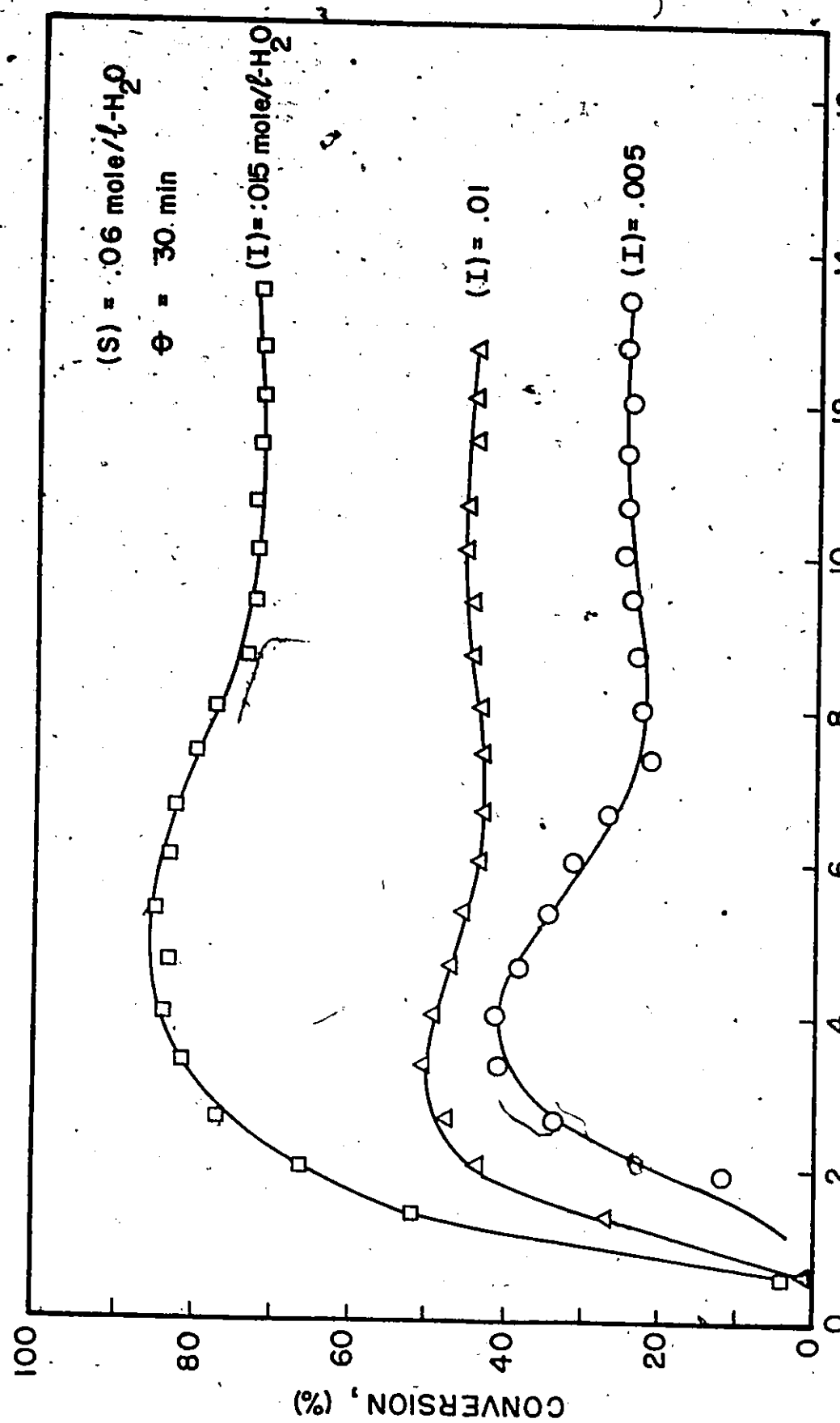

Figure (4-3) Steady-State Conversion-Time Histories for Different Initiator Concentrations (T = 50°C, M/W = 4/10, r.p.m. 320)

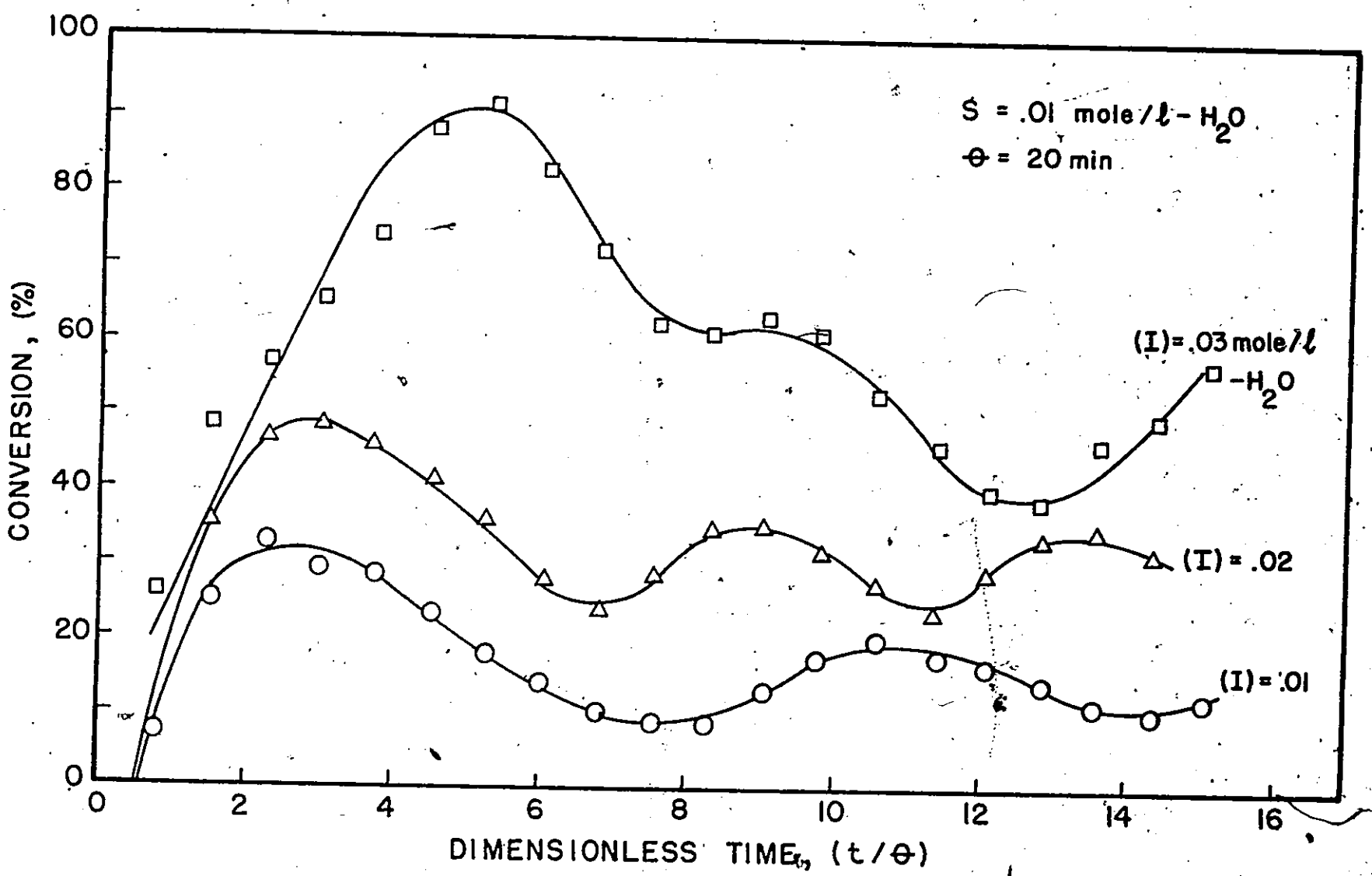

Figure (4-4) Conversion-Time Histories for Different Initiator Concentrations (T = 50°C, M/W = 4/10, r.p.m. 320)

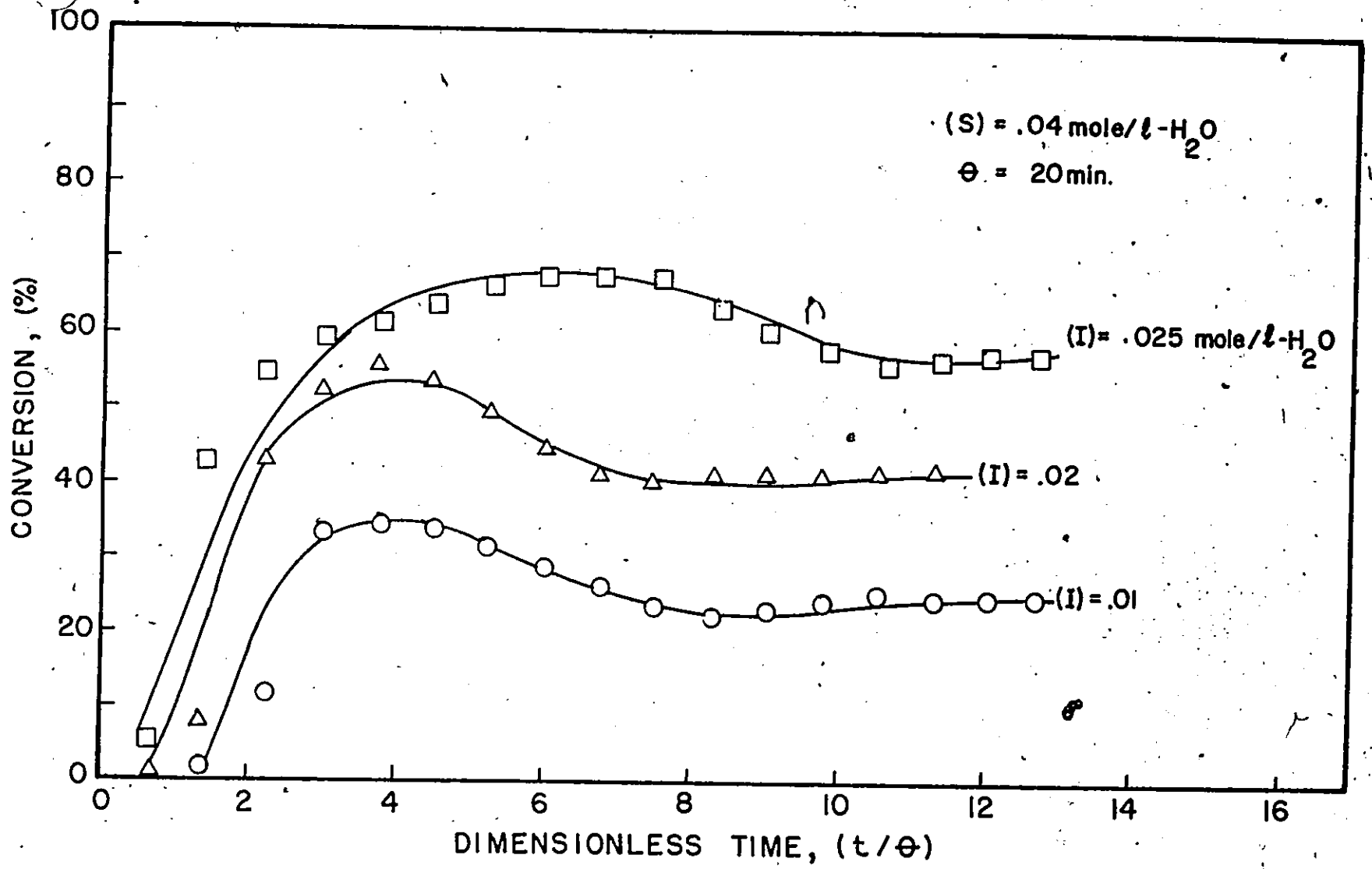

Figure (4-5) Steady-State Conversion-Time Histories for Different Initiator Concentrations (T = 50°C, M/W = 4/10, r.p.m. 320)

concentrations. On the other hand, a steady state value is obtained for high emulsifier concentrations.

The oscillating behaviour of conversion can be explained as follows. At the beginning of the reaction a rapid generation of a large number of particles occurs, leading to formation of a large particle surface area. This new surface area is rapidly covered with emulsifier. The rate of surface coverage exceeds the feed rate of fresh emulsifier to the reactor, and the reactor is depleted of free emulsifier. This leads to a period where particle generation rate is lower or even zero. The duration of this period depends on the feed rate of emulsifier and the residence time of polymer particles. When no new particles are being generated in the reactor the number of particles decreases because of wash-out of existing particles. Therefore, the consumption rate of emulsifier in covering the surface area of the growing particles decreases. Eventually the feed of emulsifier exceeds the consumption rate for surface coverage and emulsifier is again available for particle generation. This mechanism will lead to formation of discrete particle populations and fluctuations in polymerization rate and conversion. It is clear, therefore, that under many operating conditions in a CSTR with emulsion polymerization, oscillations will prevail with steady state being impossible to achieve.

A complete analysis of the limit cycle phenomena which occur in a continuous stirred tank emulsion polymerization reactor is given in Chapter 5 of this thesis.

The effect of initiator concentration on the conversion in a CSTR is also shown in Figure 4-6a for two different values of mean residence time. Conversion can be directly related to rate of polymerization (R_p) by the following equation

$$R_p = \frac{x \cdot [M]_F}{\theta} \qquad (4.5)$$

where x is the fractional conversion of monomer to polymer and $[M]_F$ is the monomer concentration in the mixed feed stream. An analysis of the data shown (Figure 4-6a) yields the rate of polymerization to be approximately proportional to the initiator concentration. This is in good agreement with the findings in the literature (Greene et al. (1976), Min and Ray (1974)).

Figure 4-6b shows the influence of emulsifier concentration on reactor conversion at two levels of initiator at 30 min. mean residence time. It appears that emulsifier concentration has a negligible effect on the rate of polymerization, ($R_p \propto (S)^{0.05}$). This is not in disagreement with recent investigations reported in the literature. In fact, Friis (1973) reported that the rate of polymerization was proportional to the 0.12 power of emulsifier concentration for a batch reactor and Litt et al. (1970) reported a zero effect. Greene et al. (1976) found that the polymerization rate was proportional to the 0.10 power of emulsifier concentration for a CSTR.

4.3.2 The Effect of Stirring and Impurities on the Emulsion Polymerization of Vinyl-acetate

Stirred tank reactors are widely used for emulsion polymerization on an industrial scale. It is often observed that the reaction rate and

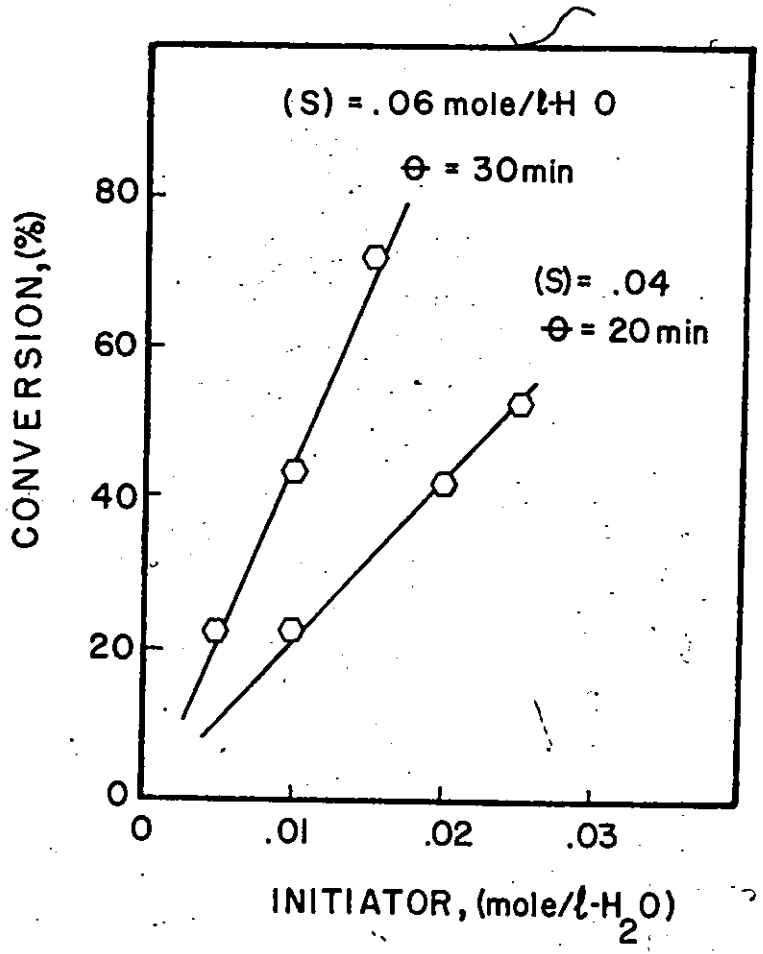

Figure (4-6a) The Effect of Initiator Concentration on the Steady-State Conversion Value (T = 50°C, M/W = 4/10, r.p.m. = 320)

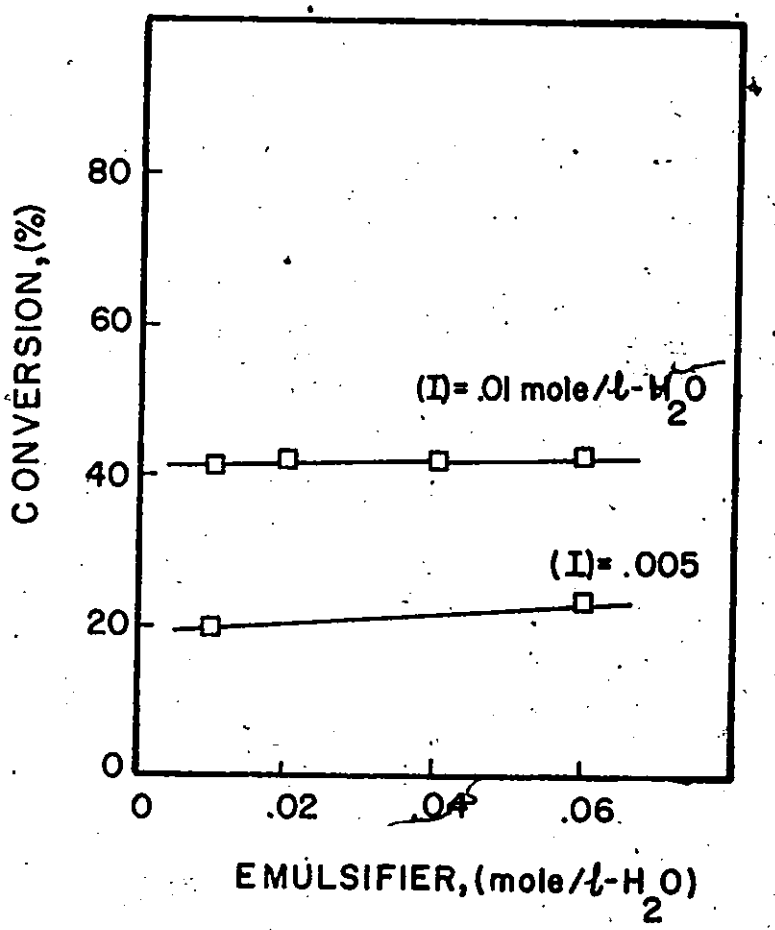

Figure (4-6b) The Effect of Emulsifier Concentration on the Steady-State Conversion Value (T = 50°C, M/W = 4/10, r.p.m. = 320, θ = 30 min)

the quality of the polymer produced are affected by the stirring conditions, but as this effect is very complicated it has not been well understood. Therefore, from the standpoint of reactor design and reactor scale-up, it is very important to know what kind and degree of stirring is required for emulsion polymerization.

Shunmukham et al. (1951) studied the effect of stirring on the emulsion polymerization of styrene and concluded that violent agitation diminished the polymerization rate. Schoot (1951) criticized Shummukham's results because the agitation effects that he observed might have been due to traces of oxygen contained in the nitrogen atmosphere under which the reaction was carried out. Evans et al. (1961) reported that the emulsion polymerization of vinylidene chloride was affected by stirring from the very beginning of the reaction, and they suggested two factors to interpret their results. The first was the effect on the reduction of the emulsifier effective for the formation of polymer particles caused by the adsorption of emulsifier molecules onto monomer droplets finely dispersed by stirring. The other was the effect upon monomer transport from monomer droplets to polymer particles.

However, Omi et al. (1969) came to the contrary conclusion that emulsion polymerization of styrene was not affected by stirring, as long as emulsification conditions were the same. They considered that stirring influenced the reaction only through the first of the above factors suggested by Evans.

As mentioned above, their conclusions were derived only from

observations of the reaction rate without determining other physical factors which might have enabled them to further test their hypotheses. Their conclusions appear to be inconsistent with each other.

Nomura et al. (1972) studied the effects of stirring in more detail and found that three factors were important in carrying out emulsion polymerization.

(i) Stirring significantly affected the course of reaction in the presence of an imperfectly purified nitrogen atmosphere.

(ii) At higher stirring speeds, polymer particles coagulated and coalesced. At lower stirring speeds, the reaction rate was controlled by the monomer transport rate from monomer droplets to the aqueous phase.

(iii) Stirring contributed to the reduction of the number of micelles because emulsifier molecules were adsorbed onto the surfaces of monomer droplets finely dispersed by the stirring. At low emulsifier concentrations near the critical micelle concentration, that effect could not be neglected.

From all the above mentioned facts it becomes clear that the rate of polymerization can be significantly affected by the rate of agitation and the presence of impurities. The effects of the above factors on the rate of polymerization were experimentally investigated and the results obtained are discussed next.

Figure 4-7 shows the effect of agitation rate on the conversion. Both experiments were carried out under the same initiator and emulsifier concentrations. The mean residence time was 30 min. and the steady state value of conversion at 320 r.p.m. (our usual agitation rate) was 43%,

Figure 4-6b. In the first case (curve 1) the agitation rate decreased from 320 r.p.m. to a new value 220 r.p.m. at time t = 360 min. That step change in agitation rate resulted in a 2.5% increase of the conversion. On the other hand, a step increase of the agitation rate from 320 r.p.m. to 500 r.p.m. and then to 420 r.p.m. resulted in a large decrease of the conversion and in a subsequent increase (Figure 4-7). The effect of stirring rate on the steady state value of conversion is also shown in Figure 4-8. The initiator concentration was equal to 0.01 mole/ℓ and the emulsifier concentration was 0.06 mole/ℓ. In all those experiments a certified grade of nitrogen was used for purging the raw materials and the initial reaction mixture. Traces of oxygen were removed by bubbling the N_2 gas through a 5% pyrogaloll solution in 2N NaOH and then through a silica-gel column for drying.

Fitch and Tsai (1971) have examined homogeneous particle formation from water solutions of MMA. They propose a mechanism which involves flocculation and/or stabilization of oligomeric radicals which are formed in the water phase. The data shown in Figures 4-7 and 4-8 are in qualitative agreement with Fitch's theory since a shear field would tend to promote flocculation, thus reducing the number of particles formed.

Moreover, an intense shear field would also increase the mechanical and surface coagulation, therefore reducing the total number of polymer particles and consequently the polymerization rate. The kinetics of coagulation of colloidal solutions of hydrophobic particles coagulated by stirring or by bubbling N_2 through them have been studied by Peters and Heller (1970), Heller and Peters (1970). They found that the rate of

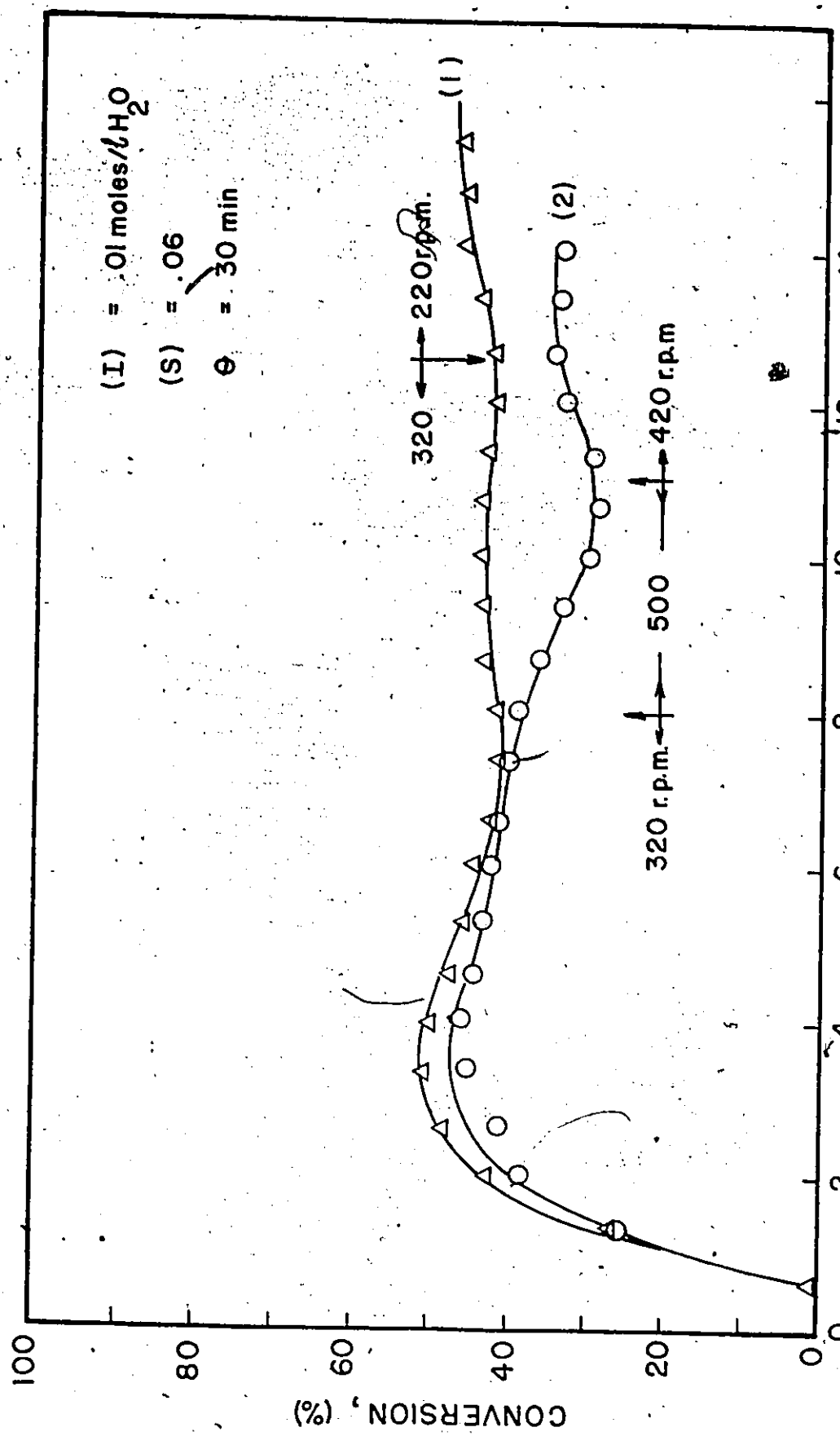

Figure (4-7) The Effect of Agitation Rate on the Conversion ($T = 50^{o}C$, $M/W = 4/10$)

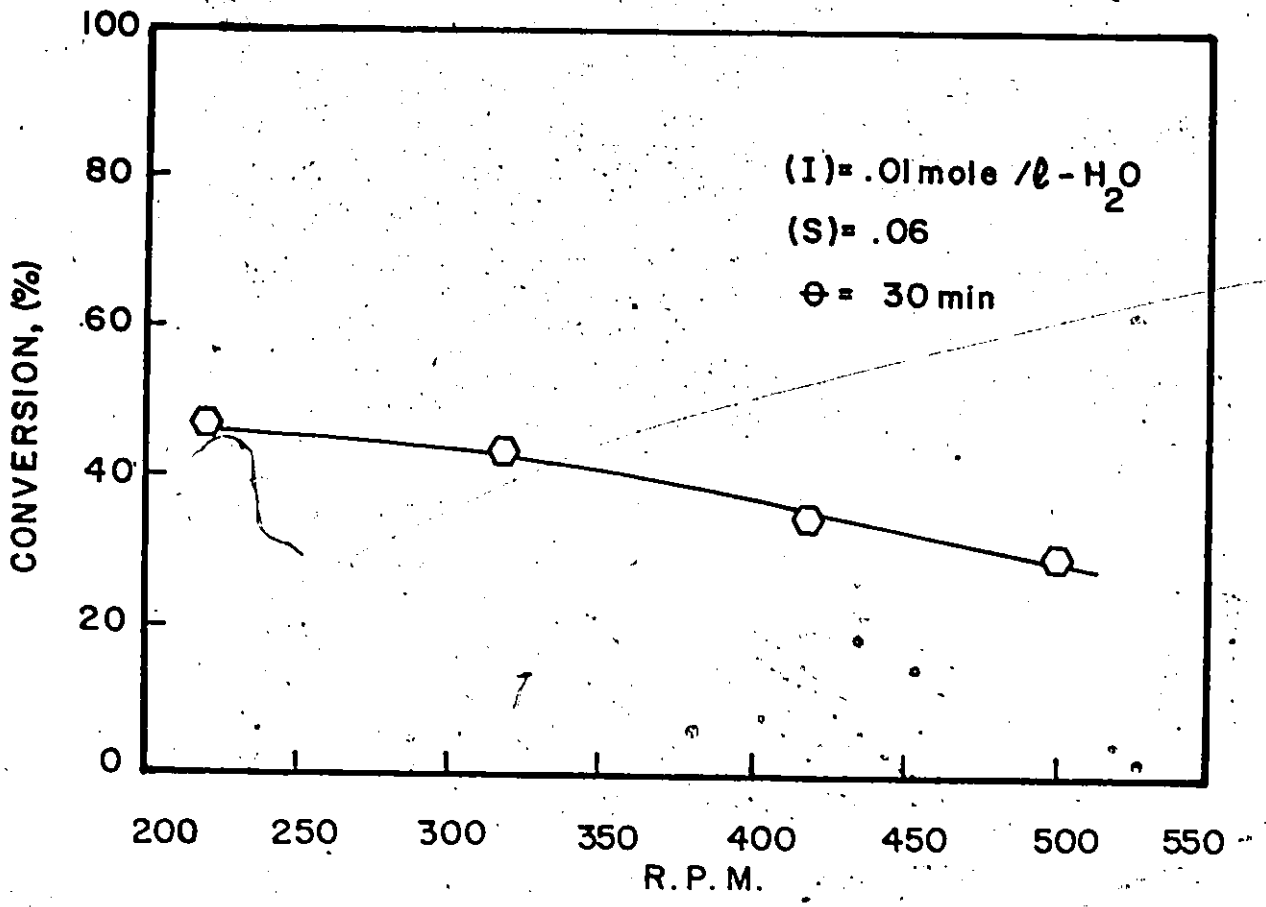

Figure (4-8) Relationship between Steady-State Conversion Value and r.p.m. (T = 50°C; M/W = 4/10)

mechanical and surface coagulation increased strongly with the ratio (S/V), S being the liquid-air surface generated by stirring and V is the volume of colloidal solution. This type of coagulation was found to conform very satisfactorily to the following rate equation

$$-\frac{dc}{dt} = k_o \frac{S}{V} \frac{c^2}{(k_1+k_2c)^2} \qquad (4.6)$$

where c is the bulk concentration of uncoagulated colloid; t is the time of bubbling or stirring; k_o is the rate constant for a bimolecular surface reaction. k_1 and k_2 are the two constants of the Langmuir isotherm which is assumed to govern the distribution of colloid between bulk and surface.

However, in addition to a possible coagulation at surfaces, agitation may also bring about a coagulation in bulk. This appears conceivable since mechanical coagulation by stirring might be accompanied by turbulent flow. The local excess kinetic energy imparted upon particles within a vortex and the simultaneous and temporary strong deformation of the electrostatic double layer could lead to a mutual approach of particles to less than the critical distance at which the potential energy curve reaches its maximum, in other words, to a distance at which predominance of the London dispersion forces leads to aggregation.

As we have already seen, by increasing the agitation rate a larger liquid-air interface is generated. This clearly increases the possibility of an oxygen-free radical reaction which subsequently reduces the number of radicals, hence the polymerization rate falls.

Another possible mechanism responsible for the observed decrease of conversion with an increasing amount of agitation is believed to be a transfer of emulsifier to the increased surface area of the smaller monomer droplets resulting from the more vigorous agitation. The removal of emulsifier to the monomer reduces the number of micelles formed, hence the number of polymer particles and the polymerization rate falls in accord with the Smith-Ewart theory. However, in the case of vinyl-acetate emulsion polymerization, monomer droplets disappear at 20% of conversion; therefore, above this relatively low conversion value monomer droplets do not exist and the above theory of the removal of emulsifier to the monomer does not hold.

Figure 4-9 shows the effect of violent agitation on the conversion. Experimental conditions ($I = 0.02$ mole/ℓ, $S = 0.04$ mole/ℓ, $\Theta = 20$ min, N_2; certified grade) were kept the same for both runs. However, an intensive agitation (560 r.p.m.) resulted in a longer induction period and later after about 6 mean residence times in a dramatic decrease of the rate of polymerization.

Presence of oxygen traces and the large liquid-air interface area generated by the violent stirring probably played important roles during the experiment. In addition, the intense shear field increased the mechanical surface and bulk coagulation reducing the total number of particles and polymerization rate.

Figure 4-10 and 4-11 show the effect of N_2 impurities on the conversion. A significant decrease in conversion was observed when an imperfectly purified nitrogen was used for the continuous purging of the

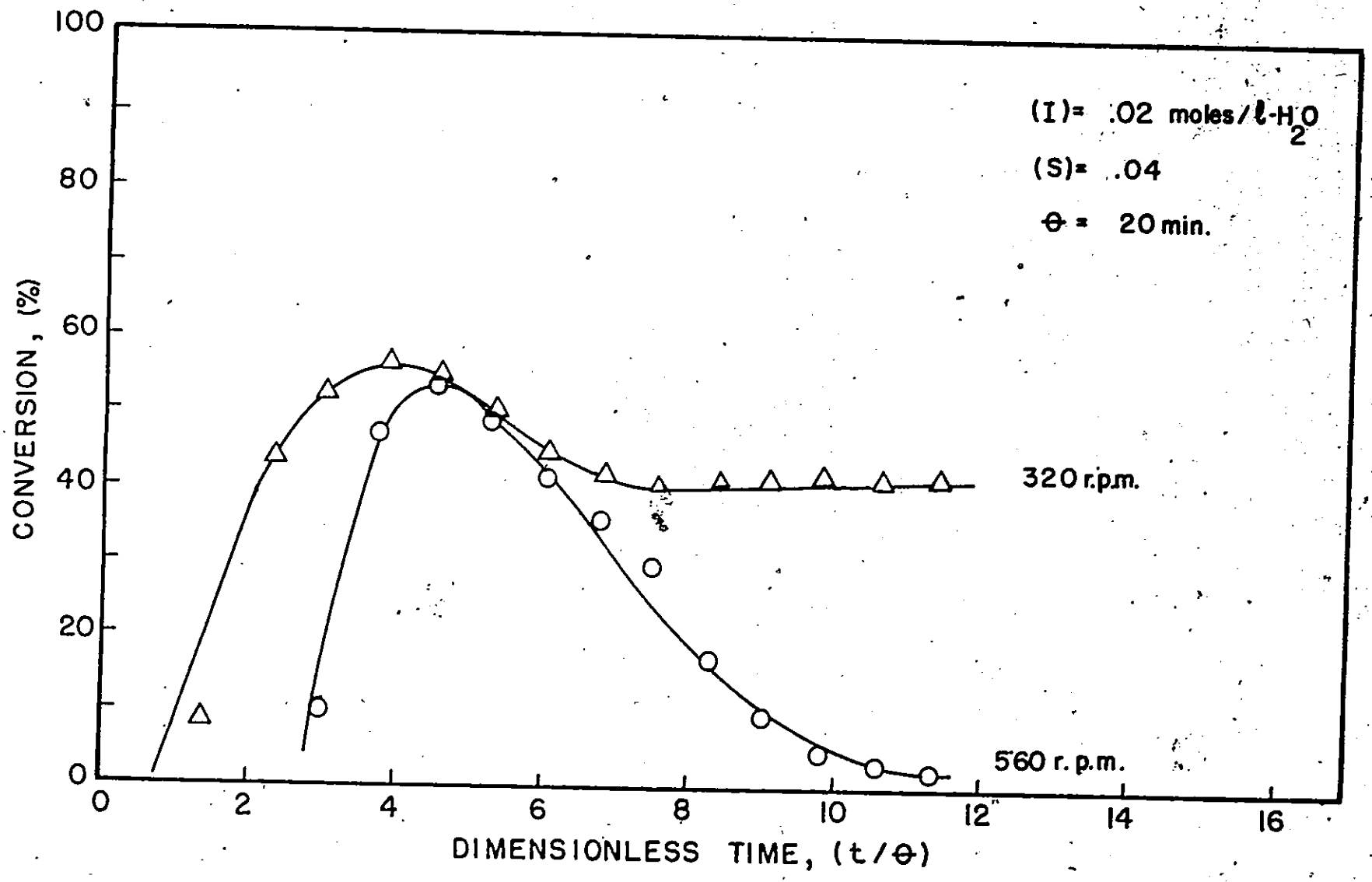

Figure (4-9) The Effect of Stirring on the Rate of Polymerization (T = 50°C, M/W = 4/10)

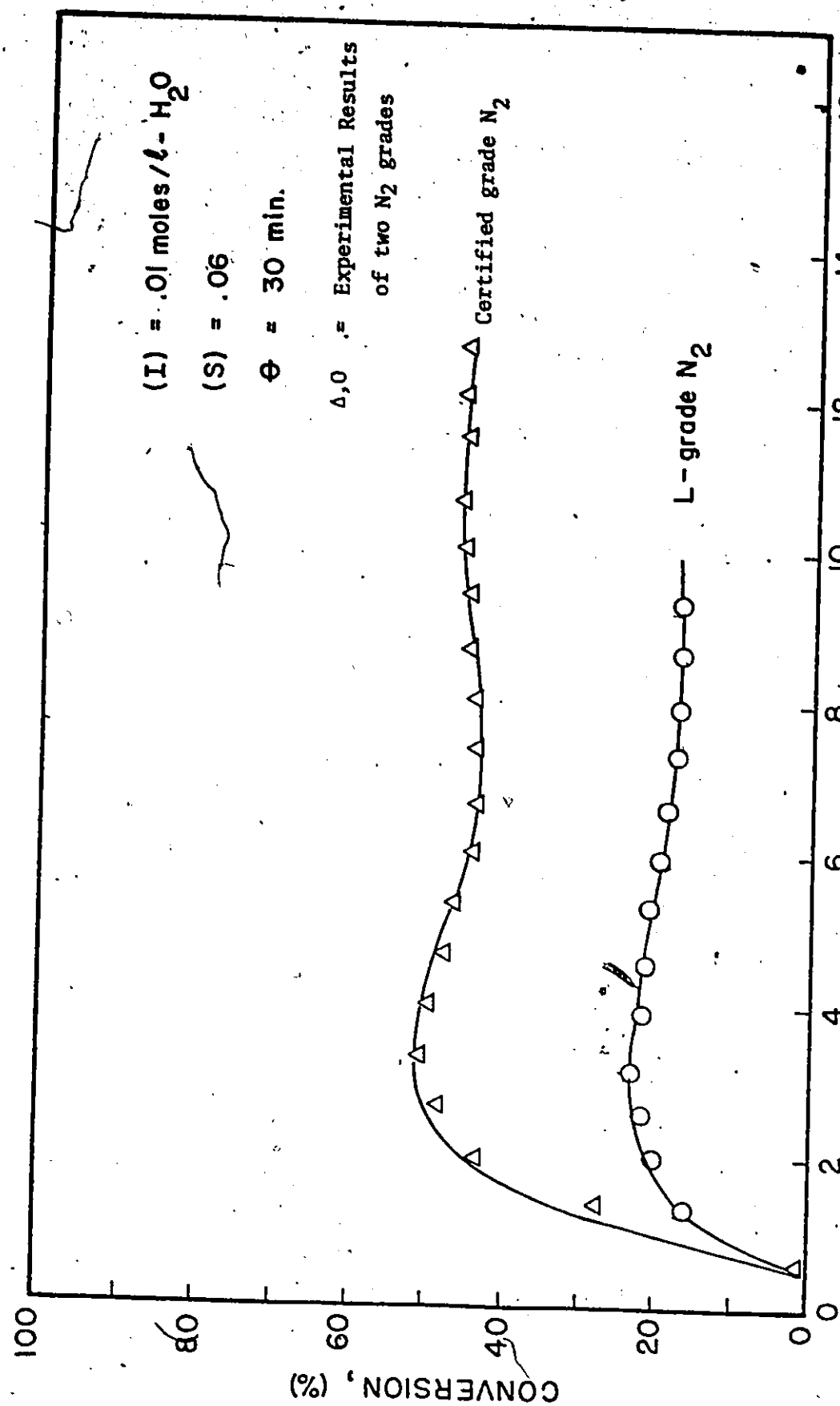

Figure (4-10) The Effect of Dissolved Impurities on the Steady-State Conversion Value ($T = 50^oC$, M/W = 4/10, r.p.m. = 320)

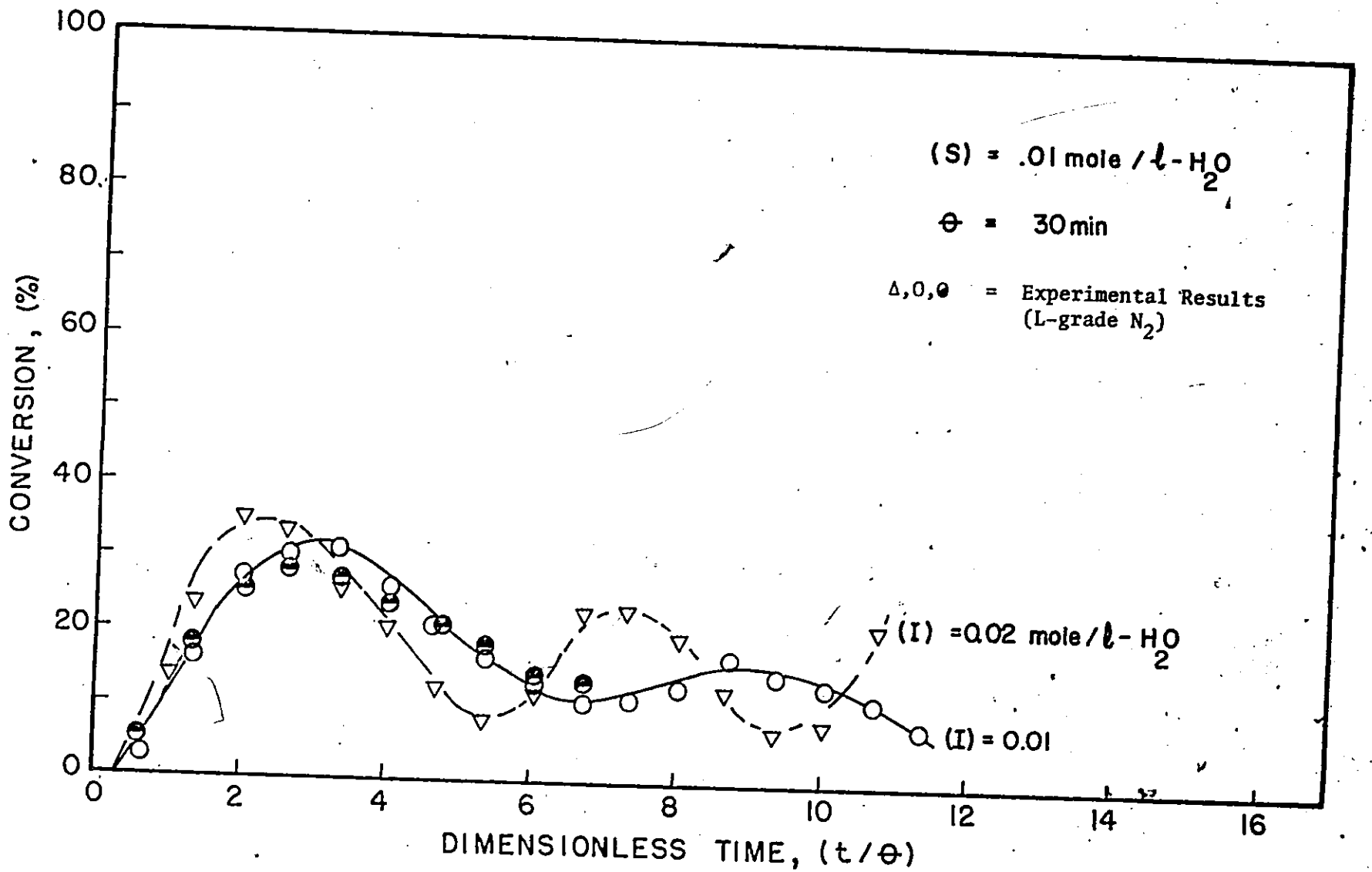

Figure (4-11) The Effect of Dissolved Impurities on the Rate of Polymerization (T = 50°C, M/W = 4/10, r.p.m. = 360)

reaction mixture. The results shown in Figure 4-10 were obtained under the same I = 0.01 mole/ℓ, S = 0.06 mole/ℓ and Θ = 30 min. However, lower conversion values were found when nitrogen (L-grade 99.5%) was continuously bubbled through the reaction mixture. Similarly, sustained oscillations obtained under continuous N_2 purging were of lower amplitude compared to those of Figure 4-2 obtained under the same initiator (I = 0.01 and I = 0.005 mole/ℓ) and emulsifier (S = 0.06 mole/ℓ) levels, but purging only the initial reaction mixture with a highly purified N_2.

4.3.3 Stability of the Latex and Reactor Fouling

Polymeric latices are lyophobic colloids. Normally they are stabilized by electrical repulsion between latex particles, arising from adsorbed soap anions or chemically attached anions. Another possibility is steric stabilization, for example by non-ionic surfactants.

A latex can be destabilized, and coagulated, in many different ways:

1. Addition of electrolyte
2. Mechanical agitation
3. Freezing and thawing
4. Addition of organic solvent, etc.

In many latex applications, premature coagulation is most undesirable; hence, stability (electrolytic stability, mechanical stability) is a major goal. On the other hand, emulsion polymerization is an important method of producing elastomers and plastics, which must be recovered from the aqueous latex by coagulation. We must therefore concern ourselves with both coagulation and its prevention.

The central theory of lyophobic colloid stability was developed by Deryaguin-Landau-Verwey-Overbeek (DLVO) and is concerned with the stability of an identical particle system (Verwey and Overbeek, 1949). Recent work regarding both attraction and repulsion interaction in heterogeneous systems makes it possible to determine the rate of coalescence for heterogeneous particles on the basis of DLVO theory.

Application of Fuchs' equation (1934), which gives the rate of collision for identical particles, to a heterogeneous system results in the following equation

$$\frac{\partial c_i}{\partial t} = D_{ij}\nabla^2 c_i - B_{ij}\,\mathrm{div}(F_{ij}c_i) \qquad (4.7)$$

where c_i is the concentration of particles of a_i radius.

For two different particles of radii a_i and a_j the diffusivity, D_{ij} can be defined,

$$D_{ij} = D_i + D_j = \frac{kT}{\eta 6\pi}\left(\frac{1}{a_i} + \frac{1}{a_j}\right) \qquad (4.8)$$

where η is the viscosity of the medium, k is the Boltzmann constant and T is the absolute temperature.

B_{ij} is the mobility constant of particles in a force gradient field and may be assumed as

$$B_{ij} = \frac{D_{ij}}{kT} \qquad (4.9)$$

F_{ij} is the interacting force between two different particles and is given as

$$F_{ij} = -\frac{dV_{ij}}{dr} \tag{4.10}$$

where V_{ij} is the total interaction potential between the ith and jth particles and includes all terms for energy repulsion and attraction.

Hogg et al. (1966) derived an expression for energy of repulsion between two particles with different size and potential and with constant surface potential as

$$V_{ij}^{R.} = \frac{\delta a_i a_j}{4(a_i+a_j)} \left[2\psi_i\psi_j \ln\left\{\frac{1+\exp(-k'H_o)}{1-\exp(-k'H_o)}\right\} + (\psi_i^2+\psi_j^2)\ln\{1-\exp(-2k'H_o\}\right] \tag{4.11}$$

The van der Waals energy of attraction between the same particles is given as

$$V_{ij}^{A} = -Aa_i a_j/6(a_i+a_j)H_o \tag{4.12}$$

where H_o is the closest distance between particle surfaces, δ, k', ψ are the dielectric constant, Debye reciprocal length, and surface potential respectively. A is the Hamaker constant for the interaction of polyvinyl acetate particles in water and is equal to $.54 \times 10^{-20}$ J (Dunn and Chong (1970)).

Overbeek (1949) defined the collision fraction, 1/W, which was named the stability ratio, as the fraction of collisions happening among

the particles which have overcome the repulsive interaction energy barrier. Hence when there is no energy barrier the collision fraction becomes 1/W = 1. The collision fraction is obtained as

$$\frac{1}{W} = \frac{1}{(a_i+a_j)\int_{a_i+a_j}^{\infty} \frac{1}{r^2} \exp(V_{ij}/kT)dr} \simeq 2k'(a_i+a_j)\exp(-V_{ijmax}/kT) \tag{4.13}$$

Thus the rate of particle coalescence can be written as

$$\frac{dc_{ij}}{dt} = (D_{ij}\ c_i c_j)\ \frac{1}{W} \tag{4.14}$$

where the coefficient of coalescence rate, D_{ij}, is based on diffusion only. Equation (4.14) indicates that the rate of coalescence is a product of the diffusional collision of particle times the collision fraction due to the interaction energy barrier. Substituting the values of D_{ij} and 1/W in equation (4.14) from equations (4.8) and (4.13), finally one can get

$$\frac{dc_{ij}}{dt} = c_i c_j \frac{4kT}{3\eta\Pi} \frac{1}{(a_i a_j)} (a_i+a_j)^2 \{(a_i+a_j)k'\exp(-V_{ijmax}/kT)\} \tag{4.15}$$

Since $a_i+a_j = \frac{1}{k'}$ for $V_{ijmax} = 0$, in order for the collision fraction to be one it is assumed that for $V_{max} > 0$

$$(a_i+a_j)^3 = E_f \frac{1}{k'^3} \tag{4.16}$$

where E_f is a lumping parameter for the agitation effect and an adjustment of the DLVO's approximation equation (4.13), then

$$\frac{dc_{ij}}{dt} = \frac{4kTE_f}{3\eta\pi k'^2}\left(\frac{1}{a_i a_j}\right)\exp(-V_{ijmax}/kT)c_i c_j \qquad (4.17)$$

Therefore, the rate coefficient of coalescence, k_c, based on the DLVO theory results in

$$k_c(a_i,a_j,\sigma_p) = \left(\frac{4kT}{3\eta\pi}\right)\left(\frac{E_f}{k'^2}\right)(a_i a_j)^{-1}\exp(-V_{ijmax}/kT) \qquad (4.18)$$

The double layer thickness, $1/k'$, is given (Adamson 1967)

$$k' = \left(\frac{8\pi c_T Na\, Z_o^2 e^2}{\delta\, kT}\right)^{\frac{1}{2}} \qquad (4.19)$$

where c_T is the total ionic strength of the medium, Z_o is valence of emulsifier molecule, e is electron charge, and δ is dielectric constant of medium. The maximum overall interaction barrier, V_{ijmax} may be determined by both the electrostatic potential energy for repulsion and attraction. Min (1974) used the surface potential, ψ_o, to determine the overall interaction energy. Since the surface potential ψ_o is linearly dependent upon the charge density, σ_p, on the surface of the particle, V_{ijmax} can be related to the charge density on the surface as

$$V_{ijmax} = B\psi_o^2 \qquad (4.20)$$

where B is the Davies constant (B = .24 cal/mV^2-mol in

in Min(1974)), and the surface potential, ψ_o, is obtained from the relation (Adamson, 1967).

$$\psi_o = \left(\frac{2kT}{Ze}\right) \sinh^{-1} \left(\frac{1}{k'}\left(\frac{2\Pi Ze}{\delta kT}\right)\sigma_p\right) \qquad (4.21)$$

while the surface charge density, σ_p, is determined as

$$\sigma_p = \frac{e_e(S_T - S_{CMC} - A_m - A_d)/a_e + G_s}{A_p} \qquad (4.22)$$

where e_e is the electric charge end group of one emulsifier molecule in e.s.u., a_e is the surface coverage by end group of one emulsifier molecule and G_s is the total charge of end groups on the surface of a particle.

Dunn and Chong (1970) have used the Poisson-Boltzmann equation to relate the surface potential, ψ_o, to the surface density, σ_p. Equation (2.27) in Chapter 2 includes expressions for the rate of formation and disappearance of particles by coalescence.

From equation (4.17) it can be seen that the rate of coalescence for two different classes of particles is proportional to the particle concentrations c_i, c_j, parameter E_f and the reciprocal of particle radii a_i^{-1} and a_j^{-1}. Moreover, an increase in the total ionic concentration, c_T, will result in an increase of the coalescence coefficient, k_c, and consequently of the rate of coalescence.

When electrical barriers exist between particles in a heterodispersed system, computations over a wide range of conditions have shown that small

particles may preferentially flocculate with themselves or with larger particles at rates that are 10 to 50 orders of magnitude faster than those of particles 10 times larger.

Bierman (1955) extended the Verwey-Overbeek theory for coalescence to non-identical particles and showed that those colloids which are most different in size will have the greatest chance of attracting and hence coagulating. One will obtain therefore a precipitation of those colloids falling at the tail ends of the distribution curve, leaving the colloids in the middle of this curve. The accelerated rapid coagulation in a mixture of large and small particles has been observed in a number of cases, i.e. in the coagulation of two sizes of Dow latex particles (Mathews et al. (1970)).

Catastrophic agglomeration occurred spontaneously several times during our experimental studies. Figure 4-12 shows typical conversion-time curves obtained at three different runs. Emulsifier concentration was 0.01 mole/ℓ and the mean residence time was equal to 30 min. Initiator concentration was equal to 0.015 mole/ℓ (one run) and 0.02 mole/ℓ (two runs). Experimental points, circles (O) and triangles (Δ) in Figure 4-12 indicate the high level of reproducibility in our experimental results. Complete agglomeration (reactor fouling) occurred at about 7-8 mean residence times after the reactor start up for both runs. A photograph taken after the fouling of the reactor Figure 4-13, shows clearly the extent of particle agglomeration. Large aggregates of polymer particles have formed a soft, sticky, highly porous mass which covers completely the cooling coil, agitator and feed lines.

In order to determine the time of appearance of those visible clusters

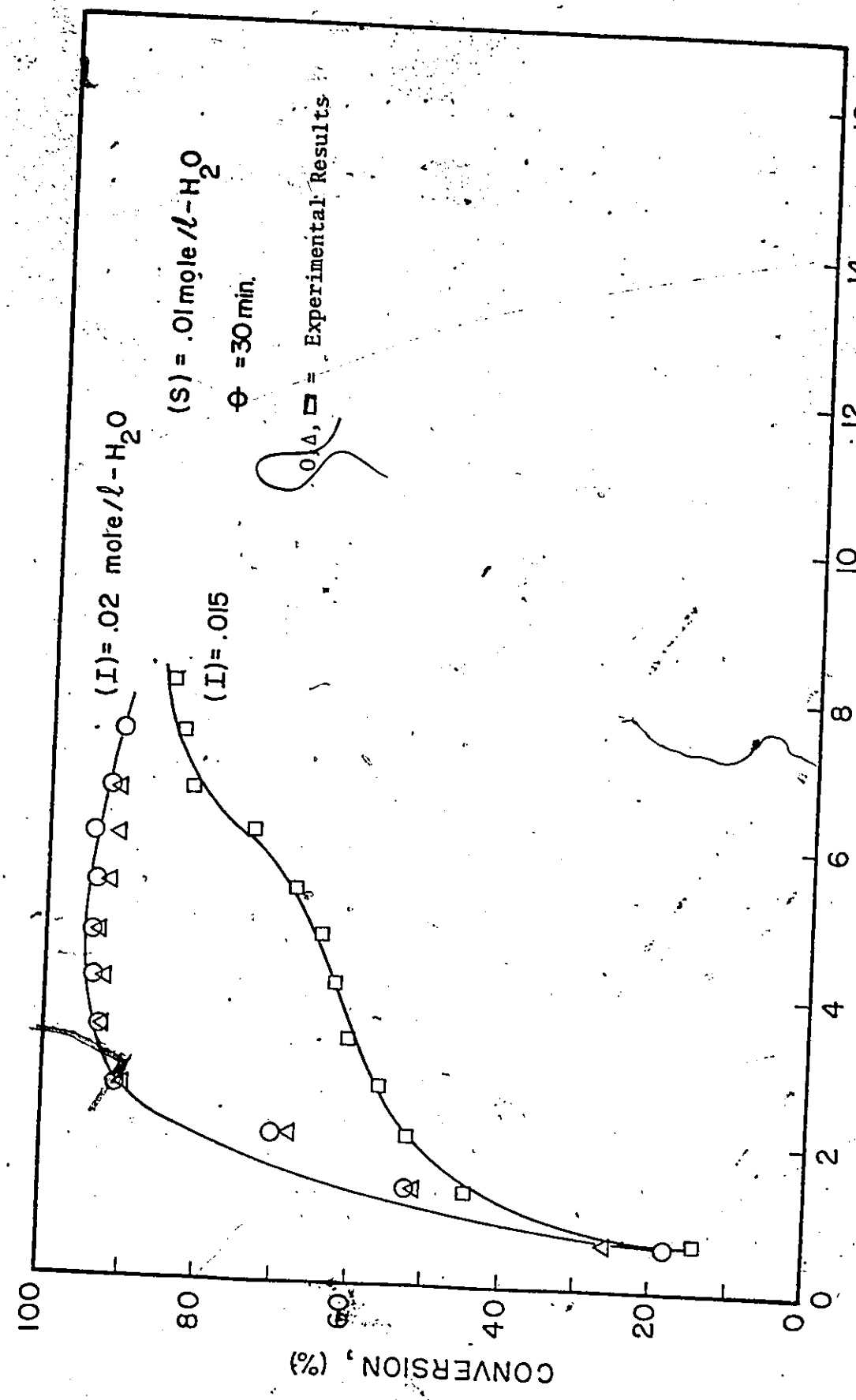

Figure (4-12) Reactor Fouling (T = 50°C, M/W = 4/10, r.p.m. = 320)

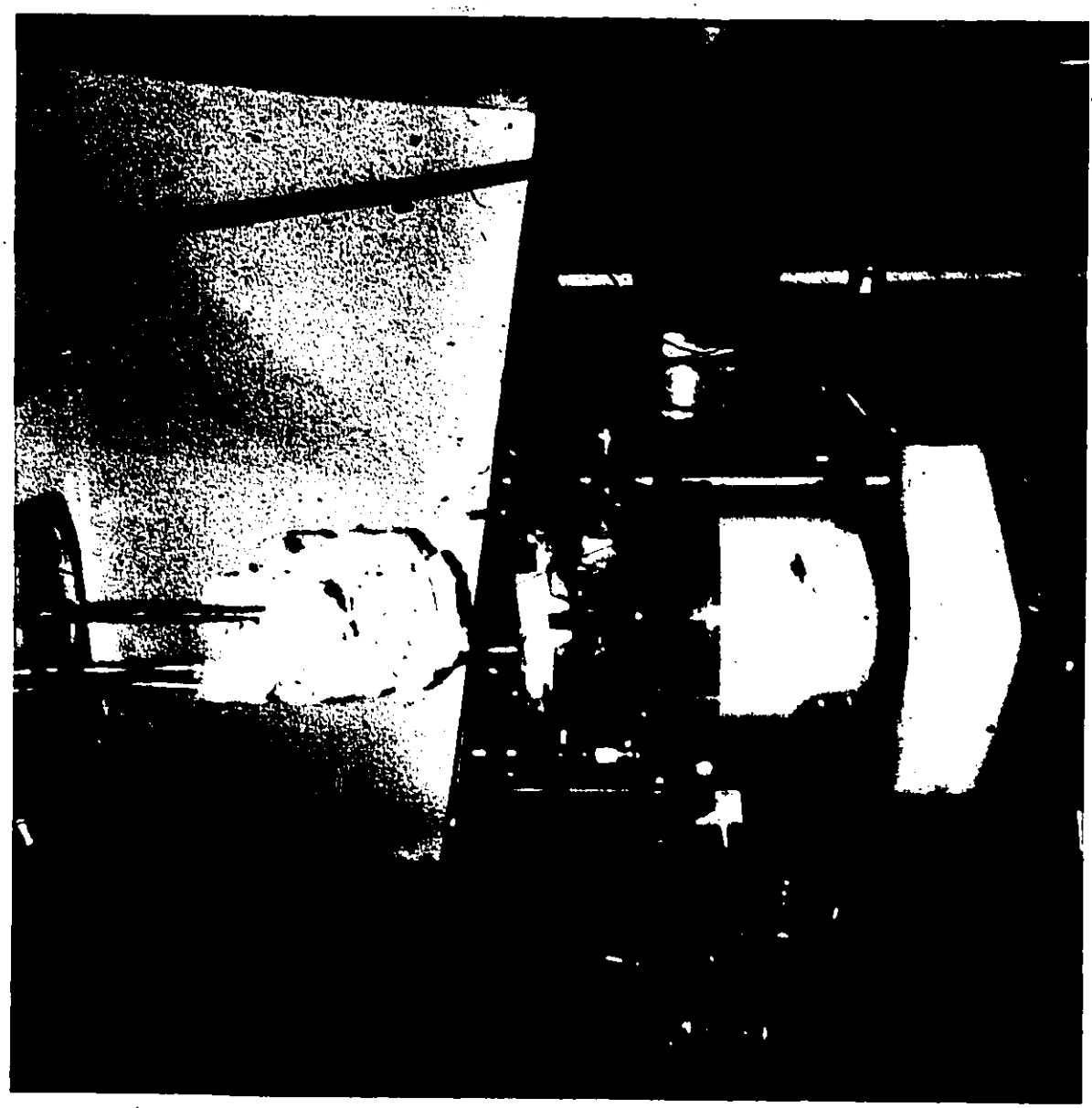

Figure (4-13) Catastrophic Agglomeration (T = 50°C, M/W = 4/10, r.p.m. 320)

of particles a third experiment was performed under identical conditions. During that run the reactor lid was opened at regular time intervals of 15-20 minutes to check for possible agglomerates on the stainless-steel coil, agitator rod or in the space between reactor wall and coil. However, large aggregates of particles were not observed until the time when a rapid particle agglomeration started and 10-15 minutes later a soft particle mass was formed again. It was found, therefore, that massive agglomeration occurred during a relatively short time period (10-20 min) and was closely related to the appearance of a second class of particles.

It is interesting to note that under the same low emulsifier concentration S = 0.01 mole/ℓ but for lower initiator concentrations, I = 0.005 - 0.01 mole/ℓ particle agglomeration was not observed and sustained oscillations in conversion were obtained (Figure 4-2).

Thus, it can be concluded that a high ionic strength of the medium, c_T, because of the high initiator concentration (I = 0.015-0.02 mole/ℓ) and the existence of large and small particles together (first and second class of particles) were probably the main reasons for the observed excessive particle agglomeration, equation (4.19). Moreover, a low surface charge density, σ_p, equation (4.22) could diminish the repulsive energy barriers between particles, therefore increase the rate of particle collision.

In addition, mechanical and surface coagulation might have contributed to the total rate of particle coalescence (see the effect of agitation parameter, E_f, in equation 4.17).

4.3.4 Reactor Start-up Induction Period

As mentioned in section 2.3.1, the way in which continuous stirred tank emulsion polymerization reactors are started up can have a significant influence, not only on the transients before steady state is achieved, but also on the nature of the ultimate state obtained after all transient effects die out.

Excursions into very high conversion regions because of the conversion overshooting and oscillatory behaviour are usually unacceptable in commercial reactor trains, and thus control and start-up policies for continuous reactor trains are investigated in Chapter 7. Control algorithms are developed and applied to the problem of achieving steady state conversion in the shortest possible time with a minimum overshoot.

Our standard way of starting up the reactor consisted of filling the reactor with distilled degassed water prior to introducing any feed streams. Conversion overshootings were detected in most experiments and are shown in Figures 4-2 through 4-6. To find out the effect of different start-up policies on the reactor transients and the final steady state achieved, different start-up methods were tried.

Figure 4-14 shows experimental data collected for two different start-up policies. Initiator, emulsifier concentrations and mean residence time, were kept identical for both runs. Run (15) was done accordingly to our usual start-up method. However, for run (3) the reactor start-up procedure was different. During that run (3) the reactor was originally filled with the emulsion recipe right from the beginning. Then

it was run as a batch reactor for one residence time (θ = 30 min) prior to introducing the feed streams. It can be seen that under that start-up policy an initial overshoot was obtained. Later, after the introduction of the feed streams conversion temporarily decreased and then started increasing to the same steady state value as run (13).

Figure 4-15 shows the effect of a different start-up policy in the case of a run having sustained oscillations. Again all experimental conditions were kept identical for both runs. However, the start-up policy for run (37) was as follows. Initially the reactor was charged with all the required raw materials except the initiator, and their concentrations were made equal to those in the feed streams. Then the temperature of the reaction mixture was brought to 50^{o}C and consequently polymerization started by feeding the raw material from the storage tanks and simultaneously injecting an aqueous initiator solution into the reactor in order to make the initiator concentration in the reactor equal to that in the feed streams. Run (37), Figure 4-15, appears to present a larger initial overshoot but it seems to approach the sustained oscillations obtained under the standard start-up method run (27). The slight phase different in the oscillations is simply due to a different initial induction period.

From the results presented we may conclude that different start-up policies do not change the ultimate steady state achieved under identical experimental conditions for the emulsion polymerization of vinyl acetate in a CSTR.

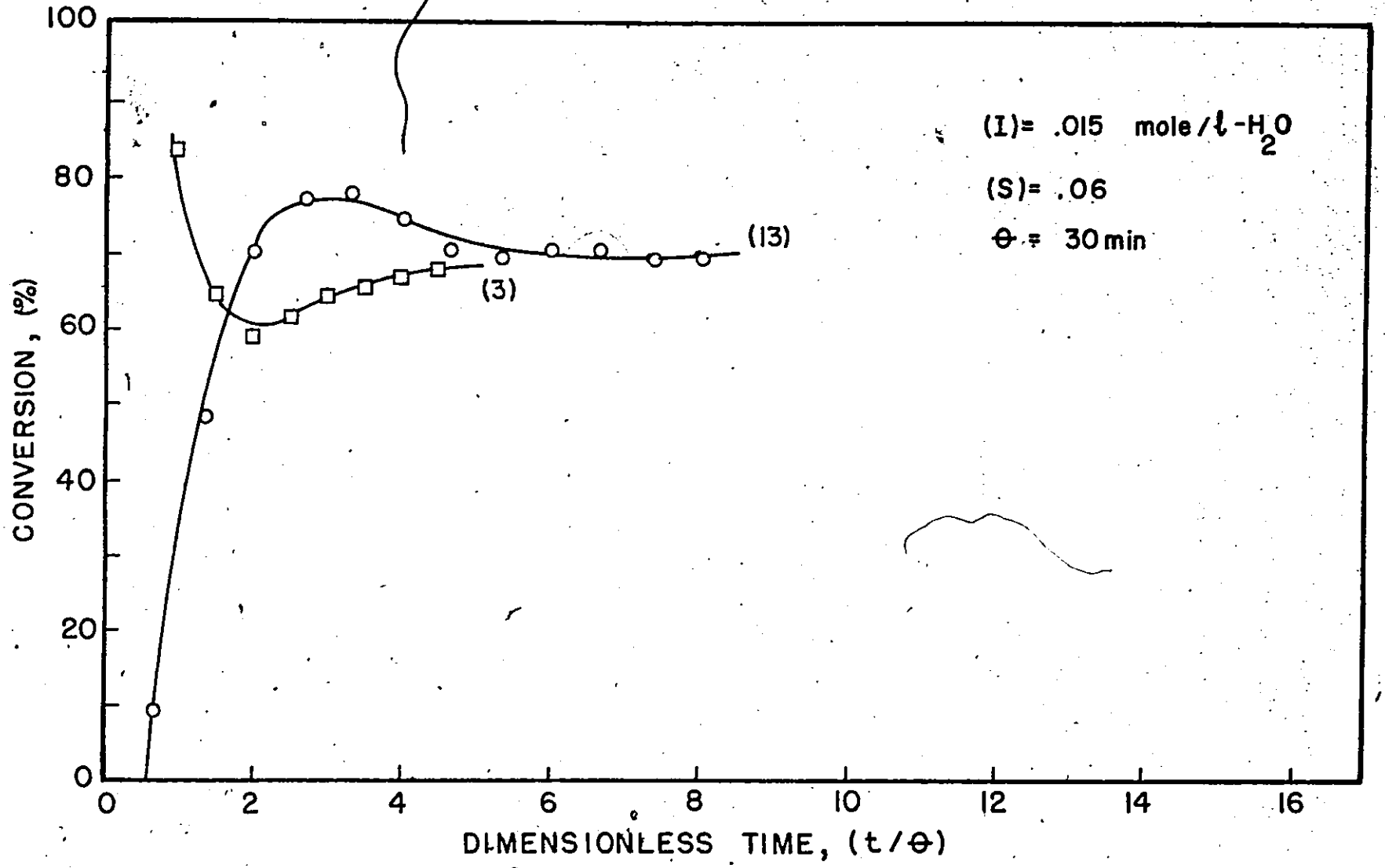

Figure (4-14) Different Reactor Start-ups (T = 50°C, m/W = 4/10, r.p.m. 320)

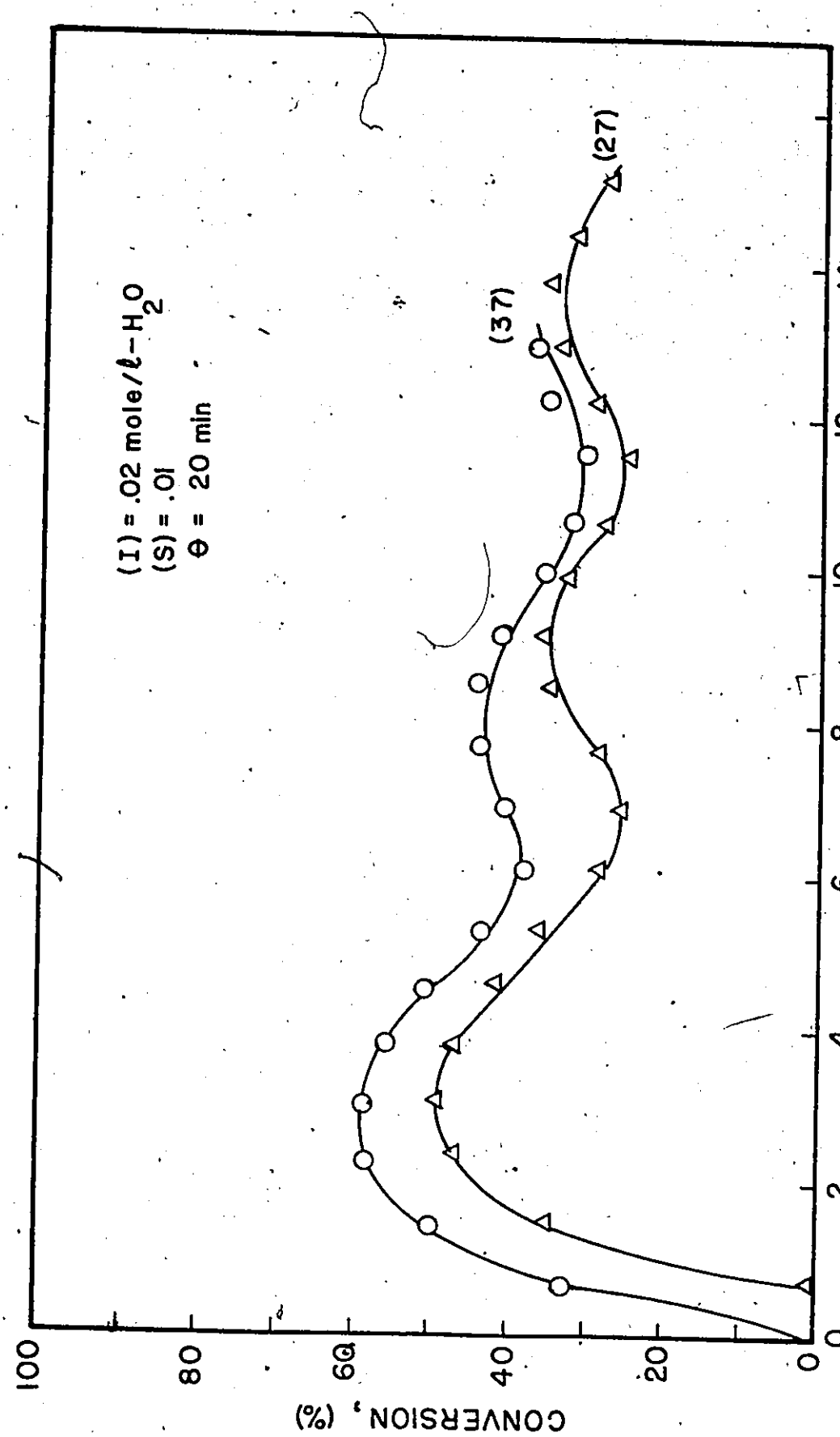

Figure (4-15) The Effect of Reactor Start-up on the Conversion (Sustained Oscillations, T = 50°C, M/W = 4/10, r.p.m. = 320)

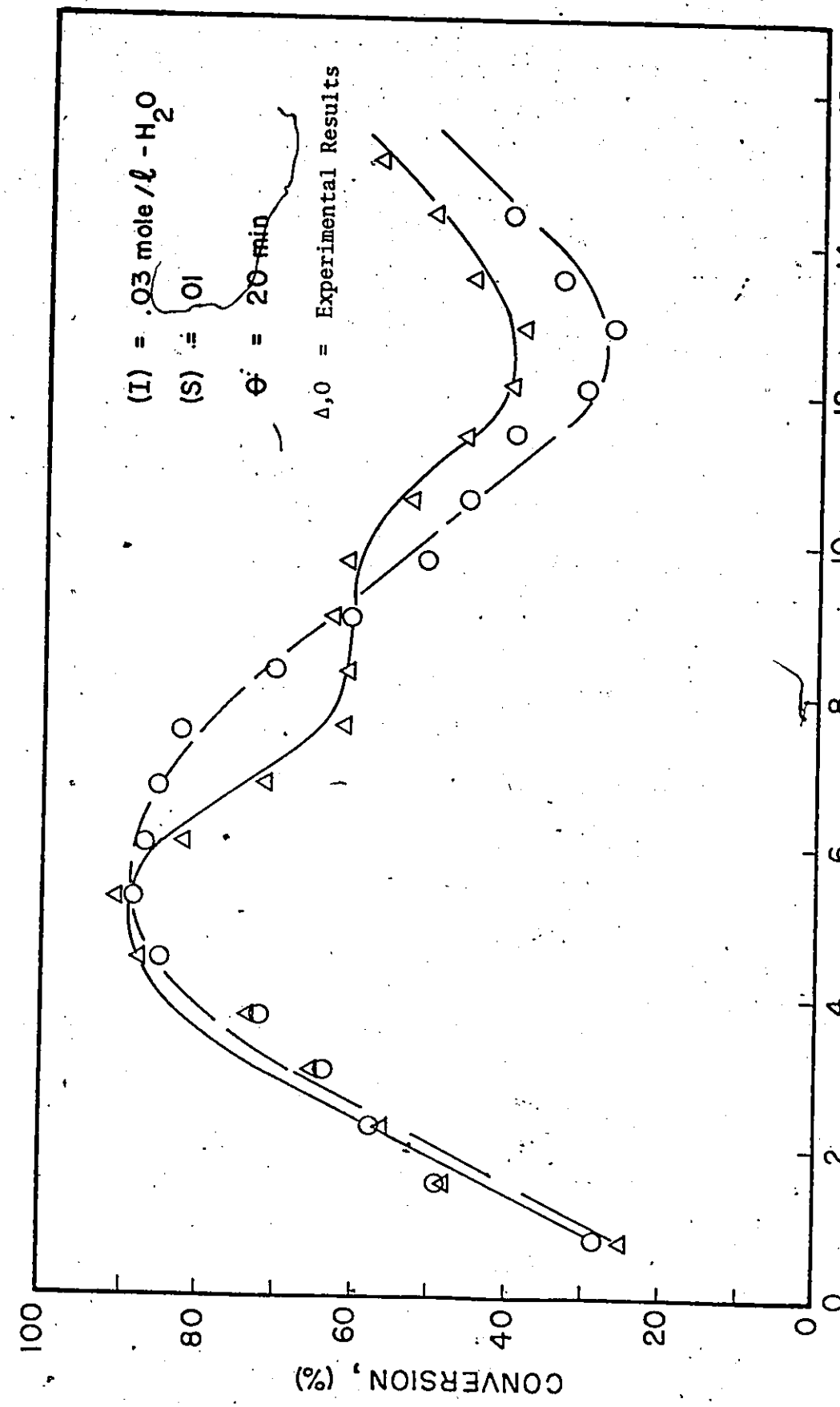

Figure (4-16) Conversion-Time Histories Showing the Reproducibility of the Experimental Measurements
($T = 50^oC$, $M/W = 4/10$, r.p.m. = 320)

Another rather undesirable feature we encountered during our experimental investigations was the existence of induction periods before the polymerization started. In other words the reaction could not start as soon as the feed streams were introduced to the emulsion system. The length of those periods could vary with different experimental conditions and especially with the rate of agitation. Rapid agitation prolonged the induction period for reasons already discussed in section 4.3.2. Usually induction periods could last for approximately one mean residence time. It is believed that these long periods are closely related with the start-up method being employed. The initial charge of the reactor with distilled water (from the tub) and the subsequent purging procedure for the removal of dissolved oxygen probably did not remove all the oxygen or other impurities dissolved in the "distilled" water. Moreover, the reactor system was not continuously purged with nitrogen during the reaction for the following reasons. First, it was found that imperfectly purified nitrogen could inhibit the reaction rather than protect it. Secondly, since a continuous overflow system was used to give a constant reactor volume, a positive nitrogen atmosphere would result in a continuous nitrogen flow through the attached overflow arm and consequently in a continuous stripping of the monomer from the surface of the emulsion system (VAc-b.p. 76°C, reaction temp. 50°C). Thus, these impurities had a significant effect on the initial efficiency of the initiator radicals. Because of the original low concentration (initiator concentration reached its final value exponentially) all newly generated radicals by the

decomposition of initiator were mainly consumed by reacting with existing impurities. However, as the initiator concentration increased more radicals were generated at a rate which significantly exceeded the rate of disappearance of radicals by reacting with impurities; therefore, free radicals became available to start the polymerization. This could explain the low initiator efficiency at the beginning of the polymerization and the larger one later as the concentration of dissolved impurities decreased with time and the initiator concentration reached its final value. This can be also seen from Figures 4-14 and 4-15 where under a different start-up method (high initial initiator concentration), an induction period was not observed. In Figure 4-16 a high initiator concentration ($I \geq 0.03$ mole/ℓ) in the feed reduced significantly the induction period although the reactor started initially filled with "distilled" water.

It should be noted, however, that the reproducibility of our experimental results has been consistent and high even under those extreme start-up conditions (Figures 4-11, 4-12, 4-16).

4.4 Conclusions

In this chapter experimental results obtained under a variety of operating conditions have been presented and critically discussed.

The effects of initiator, emulsifier and residence time on the rate of polymerization were investigated. Mean residence time and emulsifier concentration showed a negligible effect on the rate of

polymerization. On the other hand the rate of polymerization was found to be proportional to the initiator concentration. These results are in good agreement with those reported in the literature.

The effects of agitation rate and the presence of impurities on the rate of polymerization were also studied. The results of this study can be summarized as follows:

(i) Stirring can significantly affect the course of the polymerization in the presence of dissolved impurities and imperfectly purified nitrogen atmosphere.

(ii) Stirring can reduce the number of micelles.

(iii) At higher stirring speeds, oligomers and polymer particles coalesce.

(iv) Mechanical and surface coagulation is increased by rigorous agitation.

(v) A strong shear field can deform the electrostatic double layer of the particles.

(vi) An increasing amount of stirring increases the free liquid-air interface area and the oxygen contact with the bulk of the reaction mixture.

In section 4.3.3, reactor fouling and stability of a latex were examined in relation with the DLVO theory. It was found that surface charge density, σ_p, the electrolyte concentration, C_T, the reciprocal of the particle radii a_i^{-1}, a_j^{-1}, and an agitation parameter E_f, could affect the stability of the latex product. A high initiator concentration

with simultaneous presence of small and large particles could dramatically increase the coagulation rate.

Different reactor start-up policies did not change the ultimate steady state achieved. Induction periods were closely linked with the presence of impurities and oxygen traces.

It is believed that our extensive experimental work has given some insight into the complex kinetic mechanisms of the continuous emulsion polymerization and greatly improved our understanding of the process.

CHAPTER 5

PARAMETER ESTIMATION AND SIMULATION STUDIES

5.1 Introduction

Models of two levels of sophistication have been developed in Section 2.5. A comprehensive model which solves for the age distribution function of polymer particles, and a simplified model which neglects the effect of particle size distribution. The latter model should find use for the on-line control of latex reactors (Chapter 7). Conversion data obtained over a wide range of experimental conditions (Chapter 4) are used to estimate the parameters in the simplified model prior to its use for dynamic studies and on-line control of the reactor.

Conversion-time histories obtained under a variety of different conditions are successfully simulated by both models. Predictions of the comprehensive model concerning particle size distribution are found to be in good agreement with LEC measurements and experimental results reported by Gerrens (1974).

The existence of a limit cycle (sustained oscillations) is shown to be associated with a closed trajectory in the phase plane of the system. The existence of such closed trajectories has been linked with the behaviour of the sum $(\frac{\partial X}{\partial x} + \frac{\partial Y}{\partial y})$ where $\dot{x} = X(x,y)$ and $\dot{y} = Y(x,y)$ provide a description of the system behaviour (Bendixsons's theorem).

5.2 Parameter Estimation and Model Fitting

The reactor non-linear differential equations (2.69-2.72) and the associated initiator radicals and emulsifier balances contain several parameters which must be estimated from data collected on the reactor. In this section we discuss briefly the parameter estimation problem and show how the model can be used to fit the reactor data.

5.2.1 Least Squares Estimation

Least squares parameter estimation in systems where a single response is measured is a well known procedure. Justification for this method relies on the assumption that the measurement errors are independent, normally distributed random variables, with zero mean and constant variance. The least squares criterion for single response systems can be derived using a Bayesian approach. Box and Draper (1965) have used a Bayesian approach to obtain a multivariate criterion to be minimised, when estimating common parameters in multiresponse systems. They showed that one can obtain unbiased estimates of the parameters by minimising the determinant,

$$J(\underset{\sim}{\theta}) = \left| \sum_{i=1}^{N} \underset{\sim}{E}_i(\underset{\sim}{\theta}) \underset{\sim}{E}_i'(\underset{\sim}{\theta}) \right| \qquad (5.1)$$

where $\underset{\sim}{\theta}$ is the vector of the unknown parameters and $\underset{\sim}{E}_i$ is the vector of residuals for the i^{th} data set. The $\underset{\sim}{E}_i$ are the residuals obtained when the model predictions are subtracted from the measured responses.

$$\underline{E}_i = \underline{x}(t_i) - \underline{y}(t_i) \qquad (5.2)$$

Equation (5.1) represents the multivariable generalisation of the single response least squares criteria. The determinant $J(\underline{\theta})$ may be minimized by several of the available optimization techniques (gradient, direct search, etc.)

In Section 2.5.5, we derived a non-linear model with respect to the total number of particles, N, polymer volume, V_p, and conversion, x. However, from the experimental results obtained, namely conversion and turbidity data, only conversion measurements can give us direct information for one of the model's states. Of course, turbidity measurements contain information about the other two states of the model, N and V_p. However, retrieval of these two states from turbidity data implies knowledge of the conversion, x. This means that turbidity measurements are not completely independent of conversion measurements; therefore, inclusion of turbidity response will hardly improve the estimates of the model's parameters. Moreover, minimization of the determinant, $J(\underline{\theta})$, for the multiresponse case will likely increase the already large computation time which is required for the minimization of a single response least squares criterion.

One of the main difficulties involved in the least squares estimation procedure is how to carry out successfully the optimization of $J(\underline{\theta})$ for a highly non-linear model. Because of the complex nature of the model solutions, local optima can be expected to be encountered,

hence the choice of initial guesses for the unknown parameters is important. In addition, one serious problem arises related to the stability of the deterministic model. Slightly different initial conditions can result in entirely different responses, i.e. a steady-state response or a limit cycle behaviour. Of course, difficulties can be encountered with the numerical schemes and with roundoff. In the Runge-Kutta and other numerical difference schemes, numerical instability can arise if certain stability criteria are violated.

To obtain least squares estimates of the parameters entering non-linearly into the mathematical model an iterative technique is used; the estimates at each iteration are obtained by a method due to Marquardt (1963) which combines the Gauss (Taylor series) method and the method of steepest descent.

The idea behind this method is based on the following observations. The method of steepest descent often works well on the initial iterations, but the approach to the minimum grows progressively slower. On the other hand, the method of Gauss works well when the minimum of J is near, but often gives trouble on the initial iterations. The non-linear least squares routine (UWHAUS), which was used for the parameter estimation, shares with the steepest descent method the ability to converge from a region far from the minimum, and like the method of Gauss, should converge rapidly once the vicinity of the minimum is reached.

5.2.2 Parameters for Estimation

An examination of the differential equations developed in Section 2.5 to model the latex reactor shows that there are quite a few parameters or groups of parameters which require estimation. One can identify seven such parameters.

(1) $\epsilon = \frac{k_{ab}}{k_m}$ - the ratio of the transport coefficient for radical transfer from the aqueous phase into polymer particles over the rate coefficient for micellar nucleation.

(2) $\mu = \frac{k_{ho}}{k_m}$ - the ratio of the rate coefficient for homogeneous nucleation over the rate coefficient for micellar nucleation

(3) $L = (\frac{2D_w DP_{max}}{k_p M_{wc}})^{\frac{1}{2}}$ is defined as the distance which a growing radical will diffuse before it precipitates out to form a primary radical.

(4) D_w - the diffusion coefficient of monomeric radicals in the water

(5) S_{CMC} - the critical micelle concentration

(6) fk_d - effective rate coefficient of initiator decomposition

(7) $\delta = (1 + D_w/D_p m)^{-1}$ - parameter in equation (2.50).

There are of course a whole series of parameters associated with the kinetics of the reaction system. However, these parameters are considered "well-known" and can be obtained from the literature or previous kinetics studies done at McMaster University. Moreover, it was found that the simulation results were relatively insensitive to small changes in those parameters; therefore, precise estimates were not

required. Numerical values of all kinetic parameters used in the simulation studies are given in Appendix IV.

Before we proceed with the parameter estimation problem some interesting remarks concerning the seven unknown parameters should be made. From previous simulation studies it was found that the numerical value of the ratio, μ, was very close to one (Kiparissides et al. (1978)). It was then assumed that the rate coefficients for micellar and homogeneous particle nucleation should not significantly differ and a precise estimate of μ was not required. It was further shown in a series of simulation studies that small variations in L, D_w, S_{CMC}, and fk_d could be accounted for by small adjustments in the final estimates of the parameters ϵ and δ'. This would appear to be reasonable since all these parameters in some way affect the total radical concentration and ultimately the total nucleation rate. Therefore, "known" values from the literature were considered for the parameters L, D_w, fk_d and S_{CMC} (Appendix IV). These values were subsequently used throughout the simulation studies.

Thus, the primary estimation problem was reduced to two important parameters $\epsilon = \frac{k_{ab}}{k_m}$ and δ' for which a further discussion is given next.

Smith and Ewart proposed two idealized situations for the generating process of polymer particles. In the first idealized situation, it is supposed that the initiator radicals generated in the water phase are all captured by the micelles and do not enter the particles as long as the micelles are present, then

$$\epsilon = \frac{k_{ab}}{k_m} = 0 \qquad (5.3)$$

In the second idealized situation, it is supposed that a given interfacial area of the micelles and of the polymer particles always has the same effectiveness in collecting initiator radicals. Then ε is

$$\varepsilon = \frac{k_{ab}}{k_m} \propto \left(\frac{D_{pp}}{D_m}\right)^2 \sim 10^4 \qquad (5.4)$$

where D_{pp} and D_m denote the average diameters of polymer particles and micelles, respectively. However, there exists an intermediate situation between the two idealized situations of Smith and Ewart. According to Fick's law, k_{ab} and k_m obey the following relations, respectively.

$$k_{ab} = 2\pi D_w D_{pp}; \quad k_m = 2\pi D_w D_m \qquad (5.5)$$

In this case, ε is

$$\varepsilon = \frac{k_{ab}}{k_m} \propto \frac{D_{pp}}{D_m} \sim 10^2 \qquad (5.6)$$

The parameter ε is estimated later from experimental conversion data and is found to take values of the order 5 to 10^4 for emulsifier concentrations varying from 0.01 to 0.06 mole/ℓ. It should be noted that estimated values of ε are larger than 1 which means that there is a greater difficulty of radical entry into the micelles than into the polymer particles. This may be due to the following factors.

(i) One is that the energy barrier against the entry of the initiator radicals into the polymer particles is different.

(ii) Another is that the radicals, having entered the micelles, may escape again too rapidly to cause initiation because the micelle has too small a volume and are less viscous than the polymer particles.

(iii) Finally, a continuous increase of the emulsifier concentration should not imply a boundless increase of the total number of polymer particles, which means that the effectiveness of micelles in generating particles should decrease. The latter hypothesis is in agreement with experimental results reported by Dunn and Chong (1970). They actually showed that the curve relating surfactant concentration and the number of particles finally formed passed through a maximum, after which the number of particles started decreasing with increasing emulsifier concentration.

Moreover, a large increase in the surfactant concentration may result in an increase of the rate coefficient of coalescence, k_c, according to DLVO theory yielding therefore a higher capture rate of radicals by existing polymer particles. In a recent publication by Hansen and Ugelstad (1978) an alternative explanation is given for the assumed higher rate of absorption of radicals by polymer particles. Their explanation is not based upon any difference in the rate of absorption of radicals between the micelles and particles of the same size but upon a much higher rate of absorption of radicals in small particles already containing a radical.

It is clear from the above discussion that a functional relationship between the parameter, ϵ, and surfactant concentration, S, should exist. Parameter estimation subsequently showed that such a relationship

could be identified and had the following form: $\ell n\varepsilon = f(S)$. In Figure 5-1, the estimated values of $\ell n\varepsilon$ are plotted against the surfactant concentration (S) for different experimental runs. The asymptotic behaviour of $\ell n\varepsilon$ near the extremes of the independent variable (S) suggested that the continuous functional relationship ($\ell n\varepsilon = f(S)$) could be approximated by the two asymptotes, Figure 5-1,

$$\ell n\varepsilon = \theta_o + \theta_1(S-S_o); \quad S \leq S_o \tag{5.7}$$

$$\ell n\varepsilon = \theta_o + \theta_2(S-S_o); \quad S \geq S_o \tag{5.8}$$

Equations (5.7) and (5.8) include three unknown parameters to be estimated from experimental conversion data. It is obvious that, given more information, other empirical models could equally well be proposed to describe the $\ell n\varepsilon = f(S)$ relationship.

In deriving equation (2.50), which gives the desorption coefficient k_{de} of radicals from polymer particles, it was assumed that the value of δ was equal to one, after Nomura et al. (1971). However, in a recent publication Nomura and his coworkers (1976) noticed that the value of δ was uncertain and only heuristically taken equal to one. However, as Friis and Nyhagen (1973) showed there was a relative decrease in the diffusion coefficient, D_p, of monomeric radicals in the polymer particles, up to 100% in the conversion interval 0% to 90%. This was not unreasonable. In an investigation of the diffusion of water through swollen polymer membranes, Peterlin et al. (1971) have found a similar decrease in the diffusion coefficient in going from a highly swollen to a dry membrane.

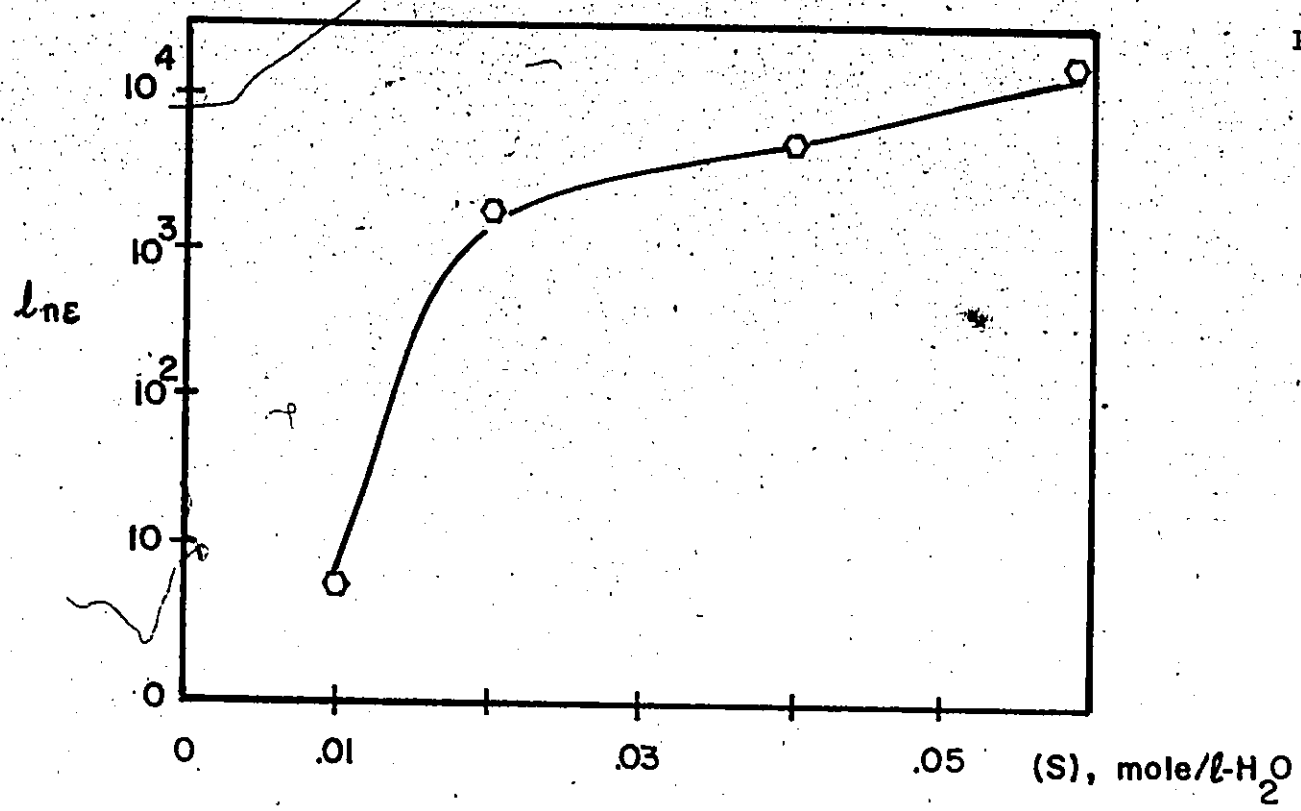

Figure (S-1) Relationship between ℓnε and Emulsifier Concentration

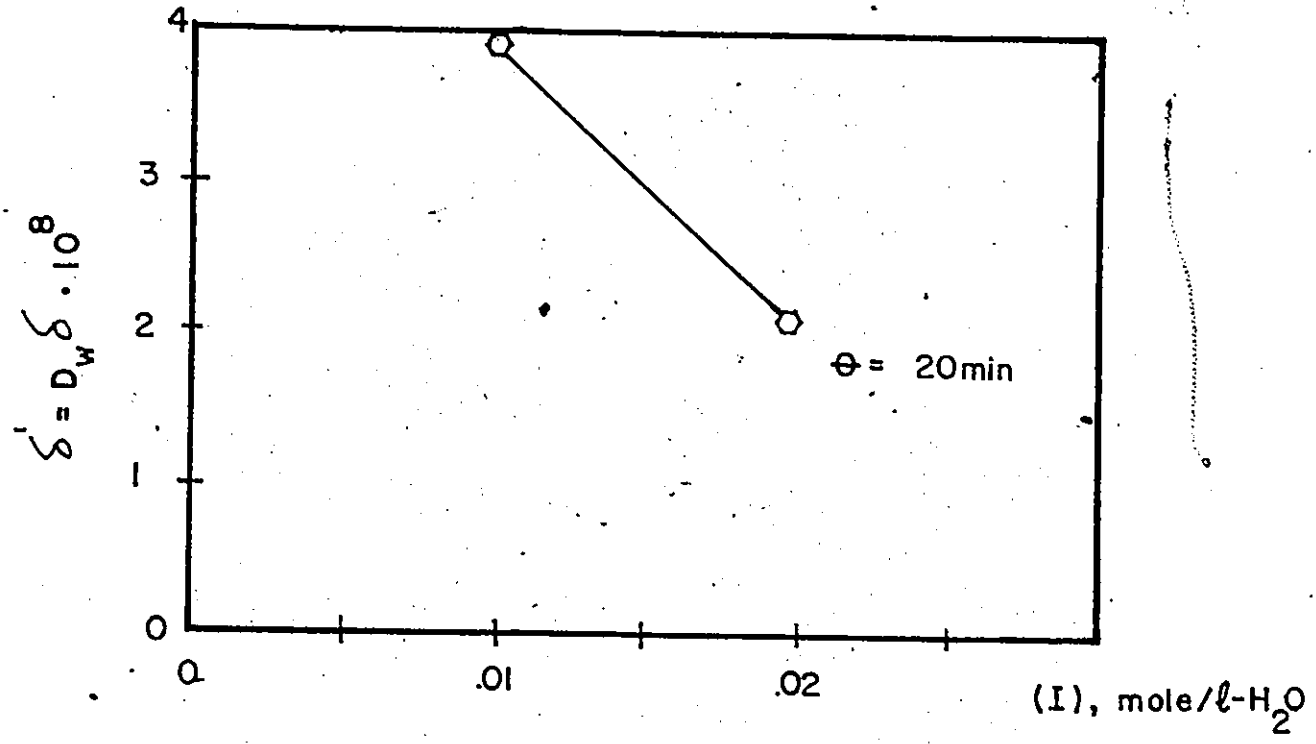

Figure (5-2) Relationship between the Parameter δ' and Initiator Concentration

That suggested that the term $D_w/D_p m$ in the expression for δ could easily exceed one resulting therefore in a smaller than one value for δ.

Moreover, according to the Stokes-Einstein equation the value of D_w can decrease depending upon the value of the coefficient of sliding friction B_{AB} (Bird et al. (1960)). It might be assumed that a similar decrease on D_w can be caused by an increase of initiator concentration according to the DLVO theory. To model the effects of initiator concentration on the parameters δ and D_w a new parameter, δ', was defined as a function of initiator concentration. Then, from the estimates of δ obtained from experimental runs at different initiator concentrations, it was found that δ' followed a linear relationship with initiator concentration (I), (Figure 5-2).

$$\delta' = \theta_3^{\infty} + \theta_4 \ (I) \qquad (5.9)$$

Therefore, the problem of estimating the parameters ε and δ' was recasted into that of estimating the new defined parameters $\underline{\theta} = (\theta_o, \theta_1, \theta_2, \theta_3, \theta_4)'$. This estimation problem is discussed next.

5.2.3 Fitting the Simplified Model to Experimental Data

A non-linear least squares routine (UWHAUS) was used to estimate the five unknown parameters, $\underline{\theta}$. Because of the complex nature of the solutions of the model and the non-linearity of the estimation surface, extra care was taken in determining initial values for the parameters. Preliminary fits of individual experimental runs were used to determine

the effects of the unknown parameters, θ, on the model's responses, and to obtain reasonable initial estimates. For the final estimation conversion data from ten different runs were used. Table 5-1 gives the number of conversion measurements and experimental conditions for each run. A total number of 185 conversion measurements were used for the estimation.

It is evident that a large computational effort and considerable computer time was involved in fitting these experimental data. To obtain the residuals for one iteration of UWHAUS routine the model had to be numerically solved 80 times approximately (8 times for each run). The numerical solution of the model's differential equations usually had to be carried out over a long reaction time (5-7 hours) for each run. This required approximately 70 secs CPU time on a CDC 6400. Therefore, one iteration required about 6000 secs CPU time.

Fortunately, the estimation program converged on the parameters at the end of the third iteration. Iteration stopped when relative change in each parameter was less than 1×10^{-3}. The final sum of squares after regression was equal to .9213. The total CPU time used was 19608 secs. The parameter estimates and all relative statistics are given in Table 5-2.

In Figures 5-3 to 5-7, conversion, number of polymer particles, total particle surface area, and free soap concentration are plotted against dimensionless time, (t/θ). These Figures have been arranged in the same order with the experiments of Table 5-1 used for the parameter estimation. In each Figure two different runs are plotted for comparison

Table 5-1

Experiments Used for the Parameter Estimation

	Run	Emulsifier Concentration mol/ℓ	Initiator Concentration mol/ℓ	Mean Residence time, min	Number of Data Points
1	15	0.01	0.01	30	17
2	20	0.01	0.005	30	23
3	19	0.06	0.01	30	18
4	23	0.06	0.005	30	17
5	24	0.04	0.01	30	18
6	25	0.02	0.01	30	18
7	26	0.01	0.01	20	20
8	27	0.01	0.02	20	17
9	28	0.04	0.01	20	20
10	29	0.04	0.02	20	17

Table 5-2

Parameter Estimates and Associated Statistics

Parameter Values via Regression

$\hat{\theta}_3$	$\hat{\theta}_4$	$\hat{\theta}_0$	$\hat{\theta}_1$	$\hat{\theta}_2$
6.30	489.90	7.20	558.6	58.03

Individual Confidence Limits for each Parameter (Linear Hypothesis)

6.39	499.00	7.33	570.80	76.25
6.21	480.80	7.07	546.40	39.80

Correlation Matrix

1.00				
.5762	1.000			
-.0443	-.4052	1.00		
-.3654	.2260	-.8537	1.000	
-.1037	.1778	-.3029	.3302	1.000

Variance of Residuals .0051 (180 D.F.)

reasons. In what follows simulation results obtained for oscillation and steady-state runs are successively discussed.

Conversion-time histories for the case of sustained oscillations are shown in Figures 5-3a and 5-6a. Circles (O) and triangles (Δ) represent experimental points while solid lines indicate the model's predictions. It is evident that there is generally a good agreement between the experimental and predicted values. However, in Figure 5-6a there seems to exist some discrepancy between experimental and predicted results. In fact, experimental oscillations appear with a higher frequency (smaller period) than the predicted ones. This difference might be explained by the fact that limited agglomeration takes place at higher initiator (I = 0.02 mole/ℓ) and low emulsifier concentration (S = 0.01 mole/ℓ) resulting in an actual decrease of the total number of polymer particles. This again results in a shorter washout period and a more frequent appearance of discrete particle generations. However, the model's limitations and experimental errors should always be kept in mind in studying these results.

Figures 5-3b and 5-6b show how the total number of polymer particles changes with time for the runs in which oscillations occur. Periodic nucleation of particles occurs almost every 6 to 8 mean residence times, and formation of polymer particles takes place in short time periods of about 0.1 to 0.4 residence times. The total particle area is plotted versus time in Figures 5-3c and 5-6c. It can be easily seen that both variables follow a similar limit cycle behaviour. Similarly, the free soap concentration shows an oscillatory behaviour in Figures 5-3d and 5-6c.

The latter Figures indicate that the reactor is substantially depleted of soap for long periods of time. Therefore, polymer particles are not adequately covered by emulsifier which could result in particle flocculation or even reactor fouling.

According to our proposed particle nucleation model (Section 2.5.2), sustained oscillations are mainly caused by the particle formation mechanisms. Thus, in periods where either of the terms A_m or k_h are greater than zero, then according to equation (2.59) rapid generation of particles occurs leading to the formation of a large surface area and the subsequent depletion of free emulsifier. The reactor is thus depleted of micelles and micellar nucleation ceases. Furthermore, as the total number of particles increases the rate of radical capture into polymer particles becomes larger than the rate of radical production and homogeneous nucleation stops. This finally leads to a long period during which particles are not generated. The duration of this period depends on the feed rate of emulsifier and the residence time of polymer particles. However, as the washout of existing particles continues emulsifier concentration starts to build up (Figures 5-3d and 5-6d) to the point when a new generation of polymer particles is formed. This periodic nucleation leads to the formation of discrete particle populations (Figures 5-3b and 5-6b) with concomitant oscillations in polymerization rate, conversion and other related properties.

Conversion-time histories for the case of steady-state reactor operation are shown in Figures 5-4a, 5-5a and 5-7a. Cirlces (o) and

triangles (Δ) represent the experimental results while the solid lines indicate the predicted values. There is a fine agreement between experimental and predicted results.

Figures 5-4b, 5-5b, and 5-7b show how the total number of polymer particles changes for a steady state reactor performance. There is initially a large overshoot in the number of polymer particles being formed, resulting in a large surface area (Figures 5-4c, 5-5c and 5-7c) and a subsequent surfactant depletion (Figures 5-4d, 5-5d, and 5-7d). This leads to a period where particles are not formed. However, soon the free emulsifier concentration exceeds the CMC, and a continuous particle nucleation begins. This almost constant particle nucleation rate results in a constant polymerization rate and consequently a steady state reactor operation. Similar profiles for conversion, number of polymer particles and emulsifier concentration have been reported by Nomura et al. (1971) for the steady-state operation of a continuous emulsion polymerization reactor for styrene.

From the simulation results presented it can be seen that our simplified model has enough power in predicting conversion-time histories, number of polymer particles, free surfactant concentration etc., over a wide range of operating conditions covering both cases of sustained oscillations and steady-state reactor operation.

This model will find further use in the optimal control of a latex reactor, which is treated in Chapter 7.

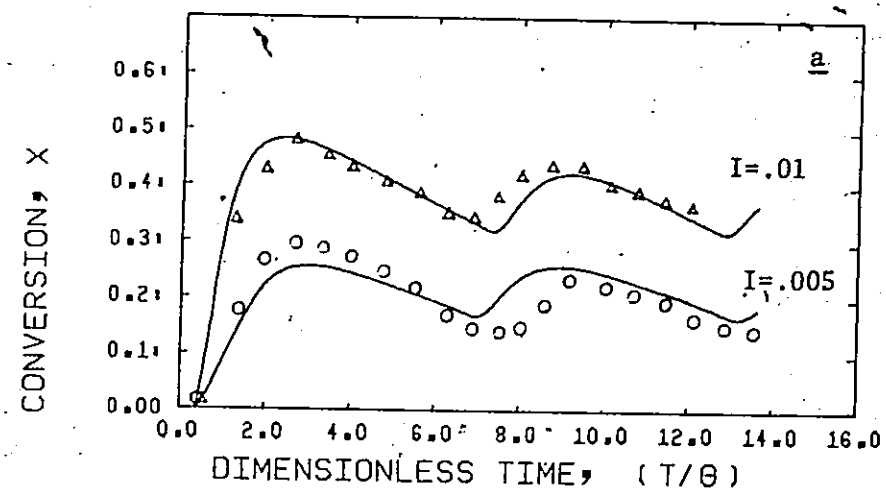

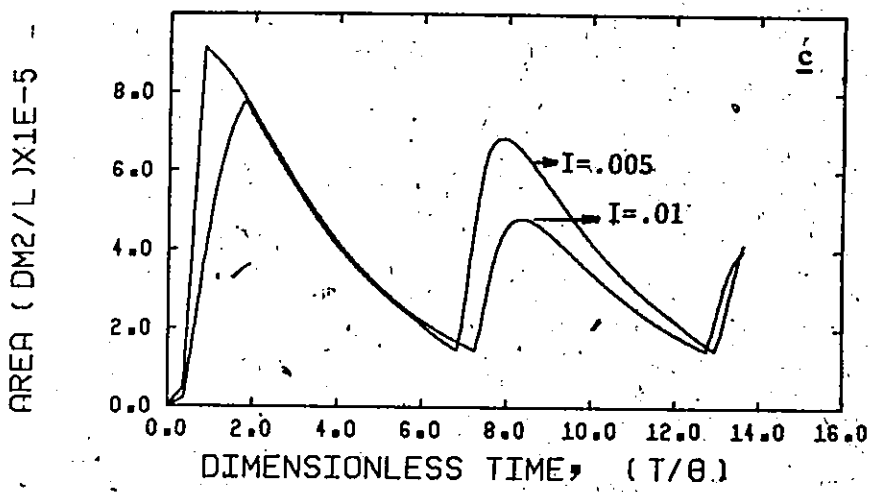

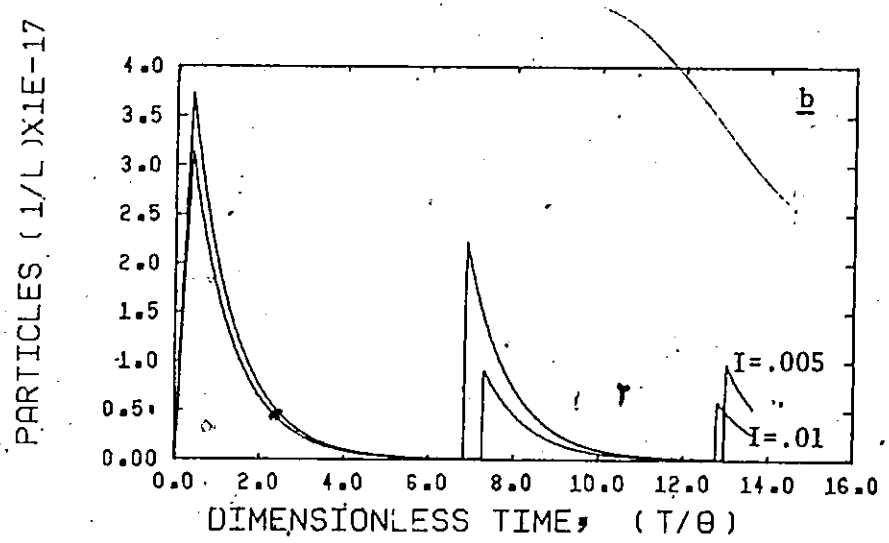

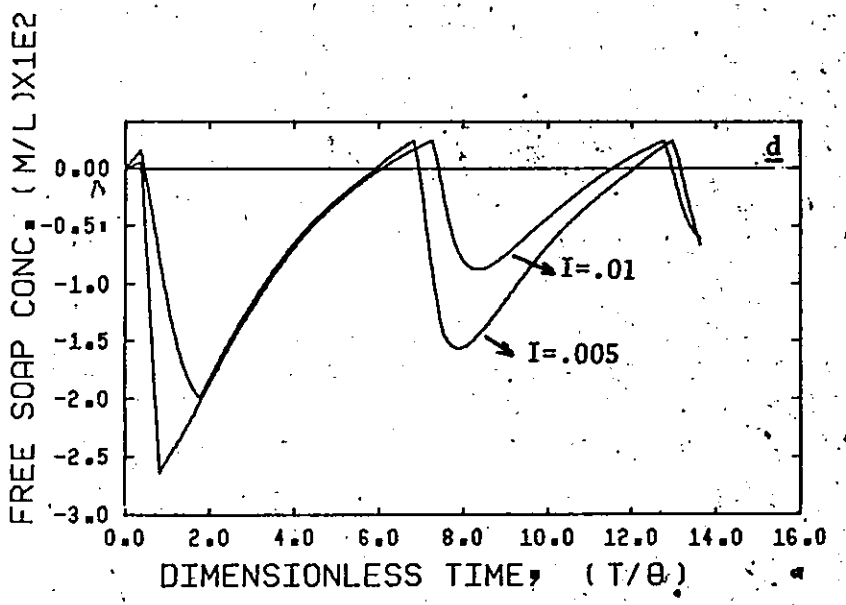

Figure (5-3) Simulation Results ((S) = .01 mole/ℓ-H_2O, T = 50°C, M/W = 4/10, r.p.m. = 320)

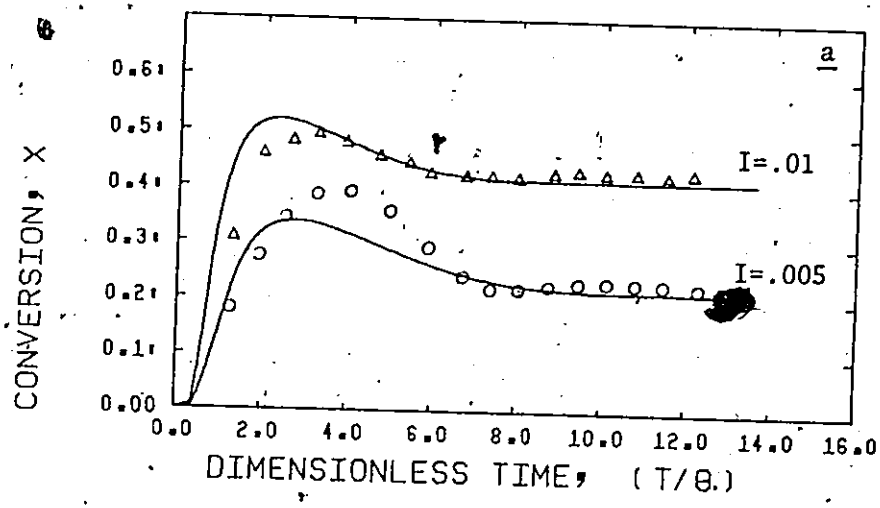

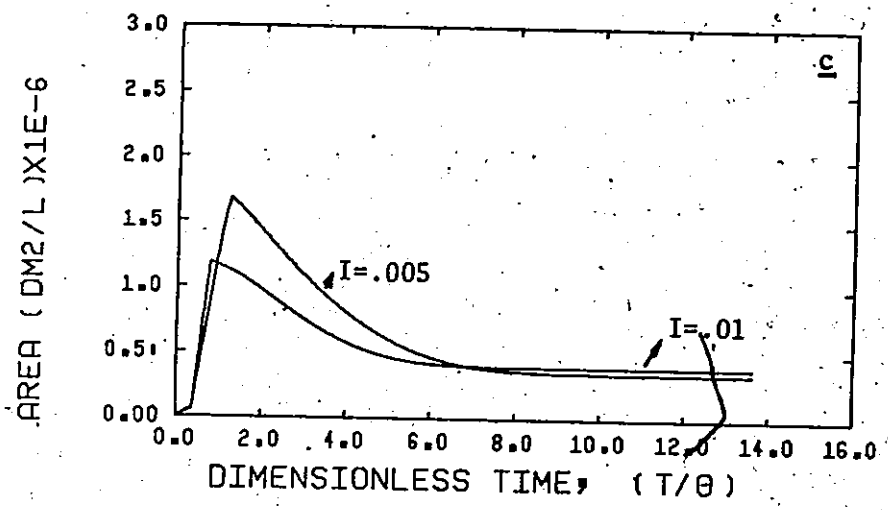

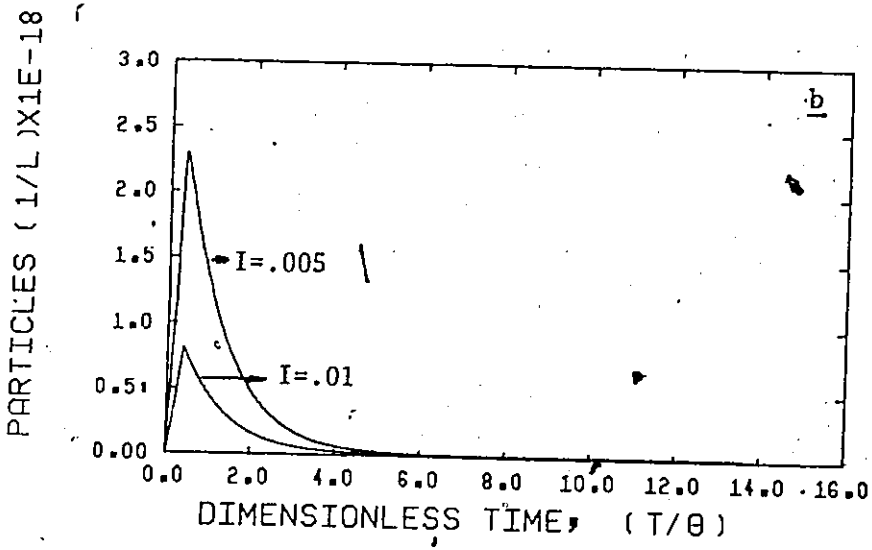

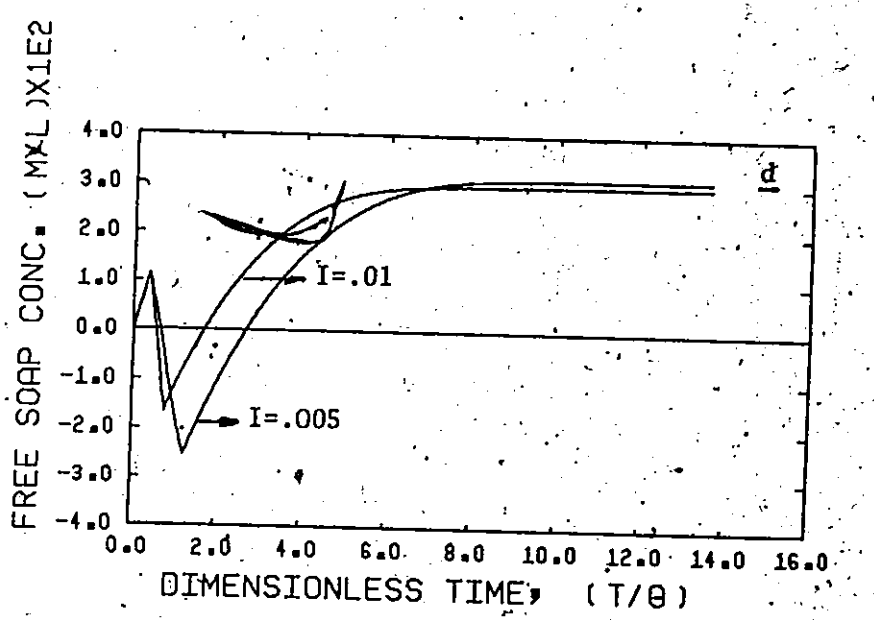

Figure (5-4) Simulation Results ((S) = .06 mole/ℓ-H_2O, T = 50°C, M/W = 4/10, r.p.m. = 320)

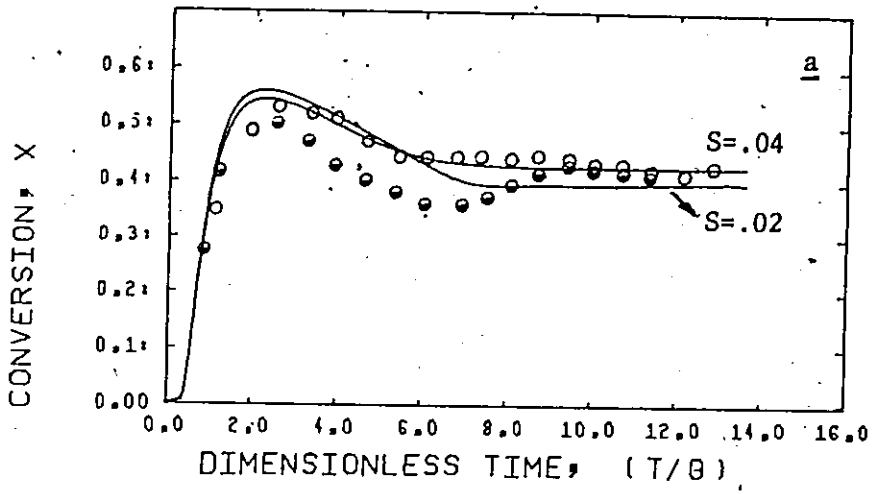

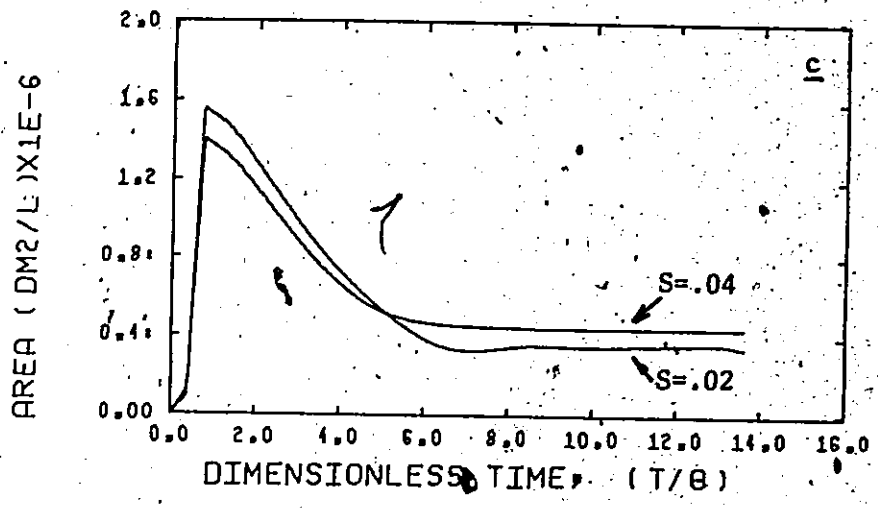

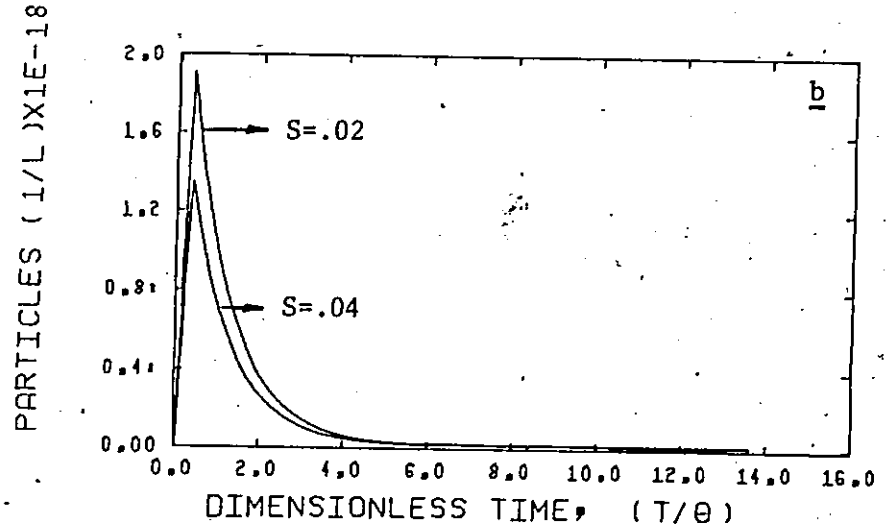

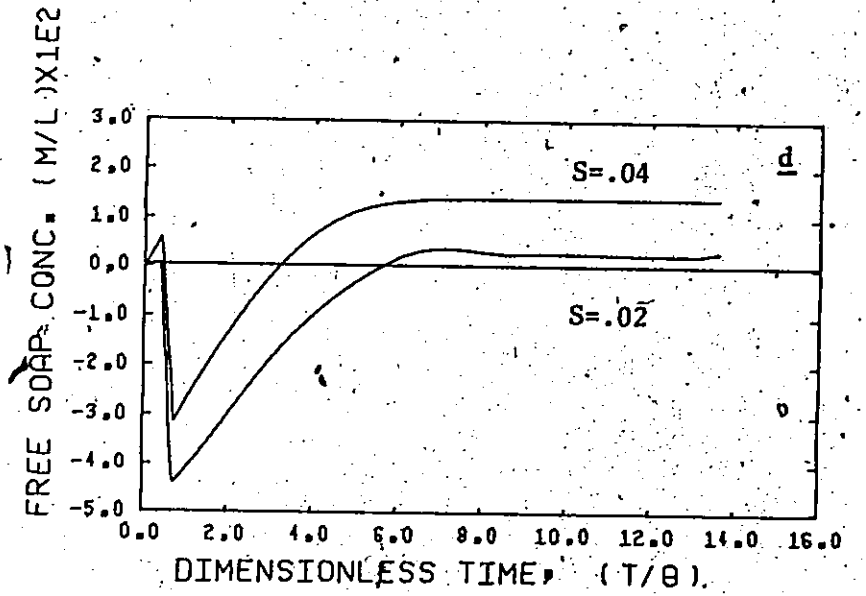

Figure (5-5) Simulation Results ((I) = .01 mole/ℓ-H_2O, T = 50°C, M/W = 4/10, r.p.m. = 320)

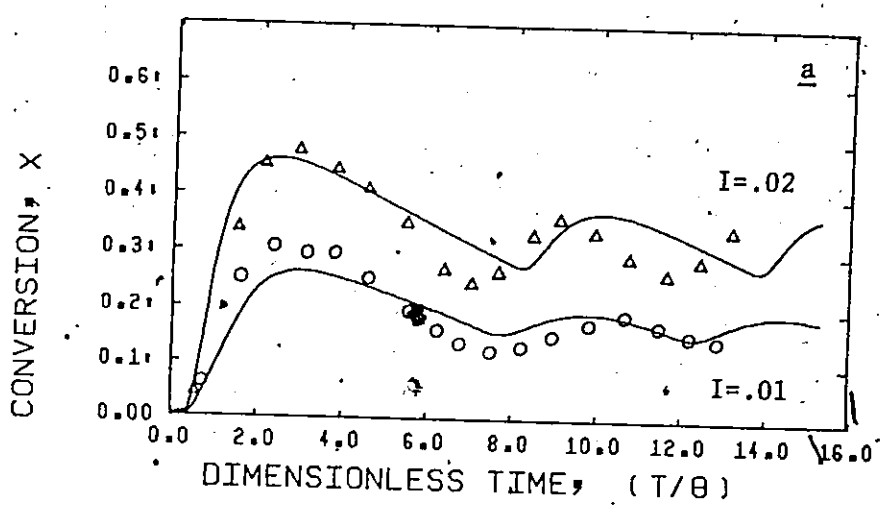

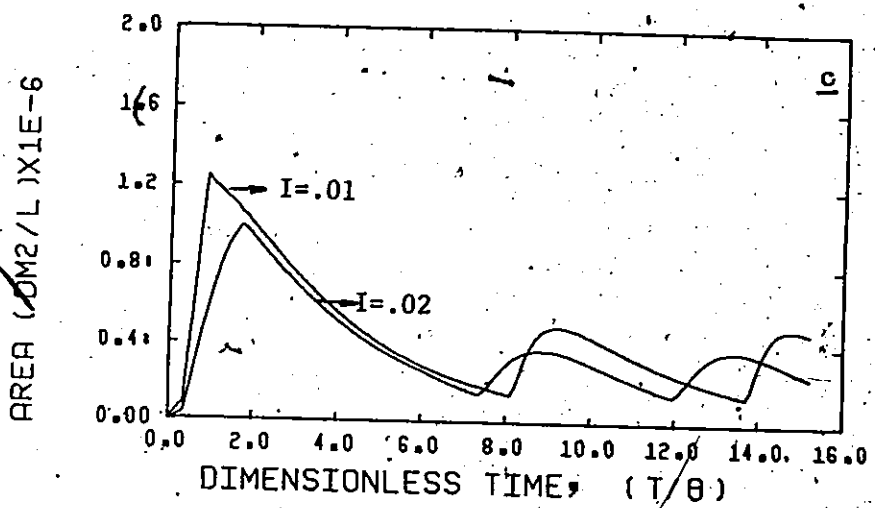

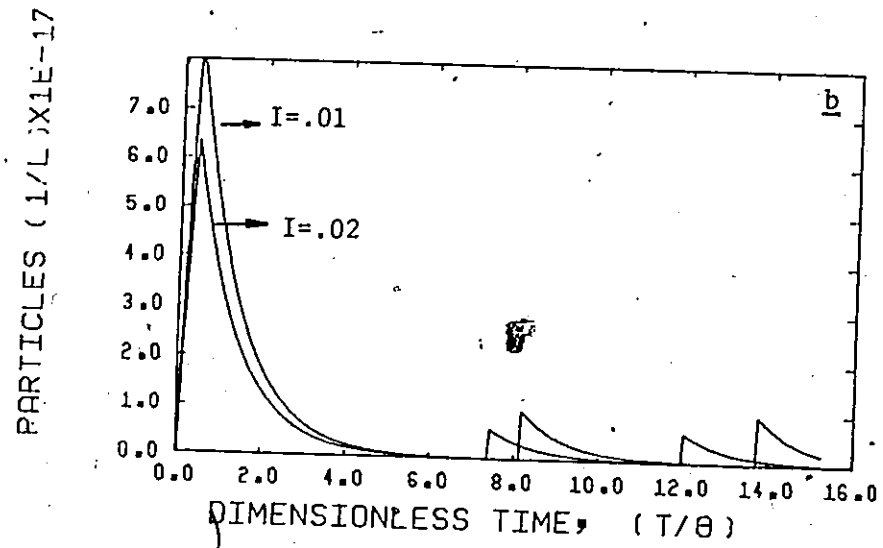

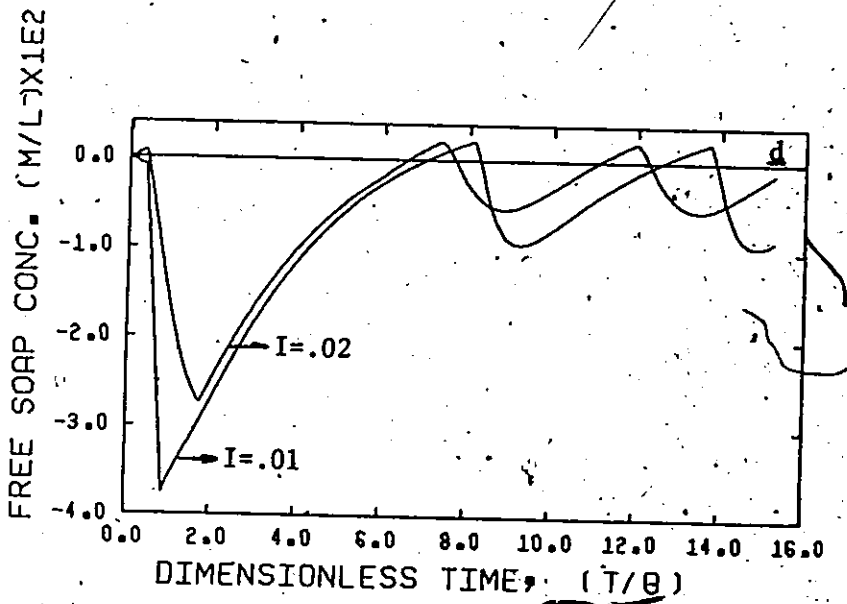

Figure (5-6) Simulation Results ((S) = .01 mole/ℓ-H_2O, T = 50°C, M/W = 4/10, r.p.m. = 320)

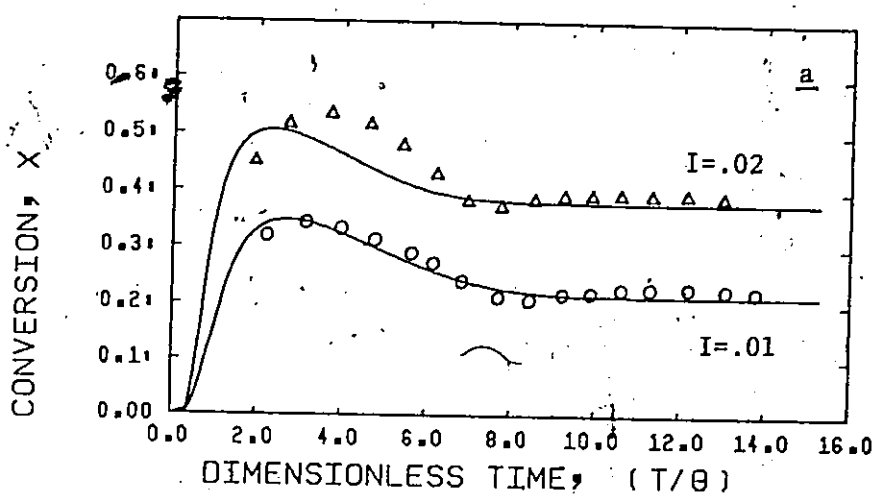

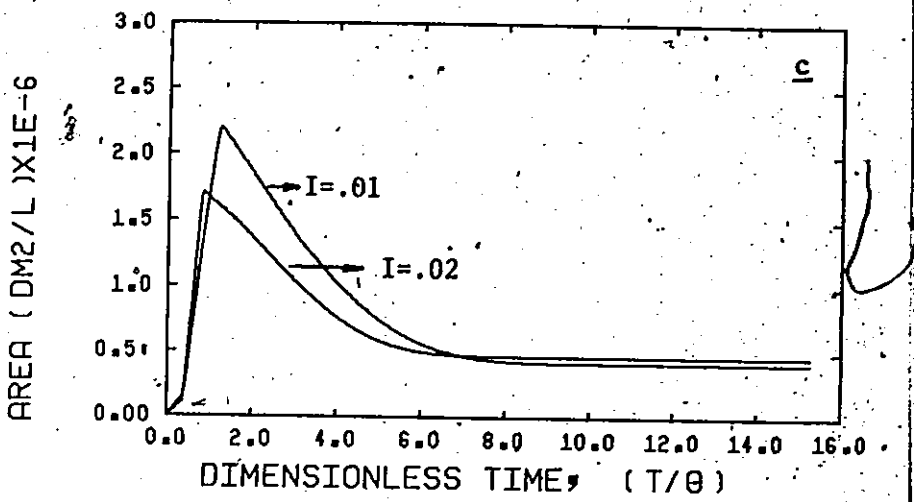

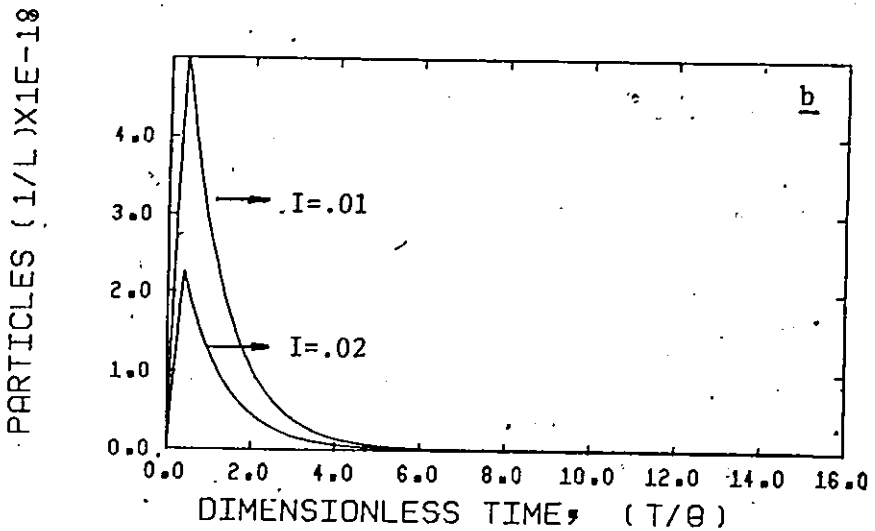

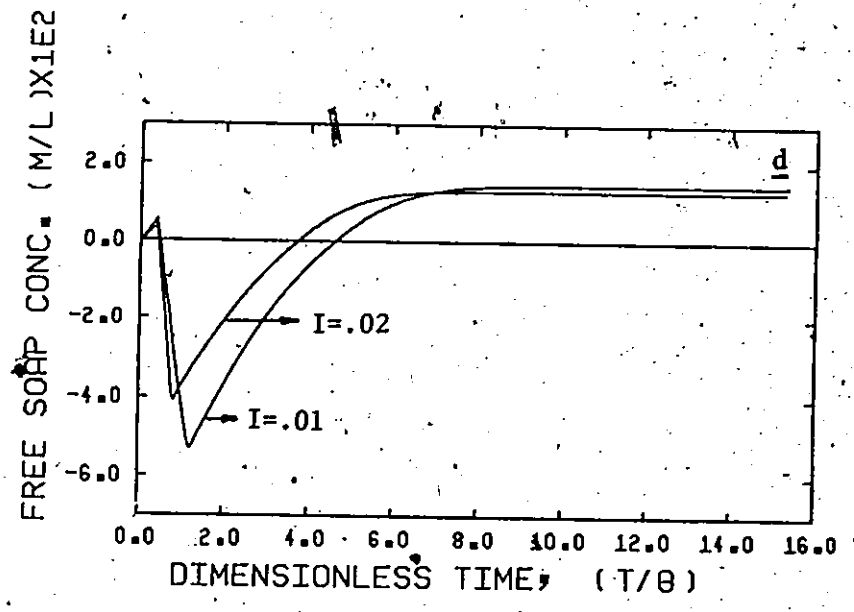

Figure (5-7) Simulation Results ((S) = .04 mole/ℓ-H_2O, T = 50°C, M/W = 4/10, r.p.m. = 320)

5.2.4. Fitting the Comprehensive Model

In a recent publication (Kiparissides et al. (1978)) we demonstrated the use of the comprehensive model by simulating successfully experimental results obtained by Greene et al. (1976).

However, the numerical solution of this model requires large computation time and effort. Specifically for a steady-state reactor operation where continuous particle nucleation takes place, the number of discrete classes of particles that should be accounted for in the solution increases considerably and hence so does the computation time and memory requirements. Of course, we may halt the numerical solution of the problem whenever a steady-state value has been achieved. However, under a dynamic environment where we need to know continuously the system responses to different changes in the manipulated variables, this model becomes computationally unattractive.

Nevertheless, the model can be used in simulation studies to reveal the different kinetic mechanisms governing the emulsion polymerization. For example, the diffusion or collision theory may be used to derive the different rates for radical entry into polymer particles or micelles. A particle coalescence rate may be included in the total population balances and so forth. However, any reasonable interpretation of simulation's results should be preferably followed by some kind of experimental evidence.

Figure 5-8 shows conversion-time histories for two different initiator concentrations. The dashed lines represent conversion values calculated using the present comprehensive model, equations (2.40-2.43).

The same numerical values (see Appendix IV) for the parameters of the model were used for both simulated runs. It is evident that there is a very good agreement between predicted and experimental results.

The number average diameter, D_n, and weight average diameter, D_w, of the PSD are plotted in Figures 5-9 and 5-10 against time. The polydispersity ratio D_w/D_n for the first particle generation is very close to one. However, after the appearance of a second particle generation, this ratio increases considerably since a lot of small particles are formed resulting in a large decrease of D_n. The polydispersity ratio starts decreasing again as the particle washout of the first generation continues and the particles of the newly formed generation grow. Gerren's (1974) reported similar experimental results with respect to the polydispersity ratio for the continuous emulsion polymerization of styrene under limit cycles conditions.

In Figure 5-11, the average number of radicals per particle, $\bar{q}$, is plotted with respect to time. It is interesting to note that $\bar{q}$ follows a similar limit cycle behaviour and can take values well above one. This is in qualitative agreement with Gerren's (1974) findings for styrene where he experimentally found that the average number of radicals per particle could take values of the order of 10^3.

Figure 5-12 compares the predicted conversion transient with experimental values for a run which achieves a steady state condition. In Figure 5-13, D_n and D_w are plotted against reaction time for this run. According to the present model, a rapid generation of particles occurs at the beginning of the reaction leading to the formation of a large surface

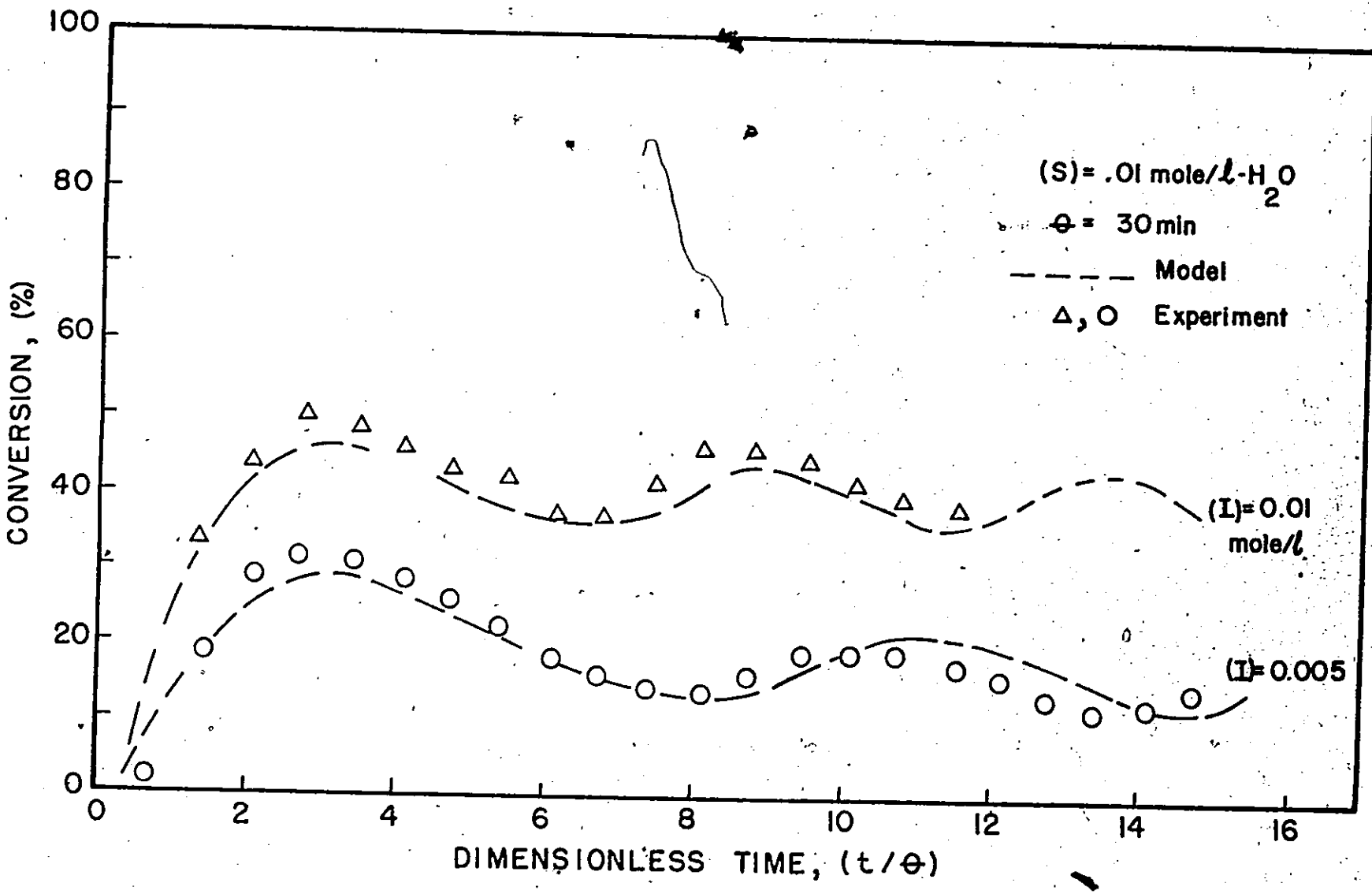

Figure (5-8) Comparison between Experimental and Predicted Results (Comprehensive Model, T = 50°C, M/W = 4/10, r.p.m. = 320)

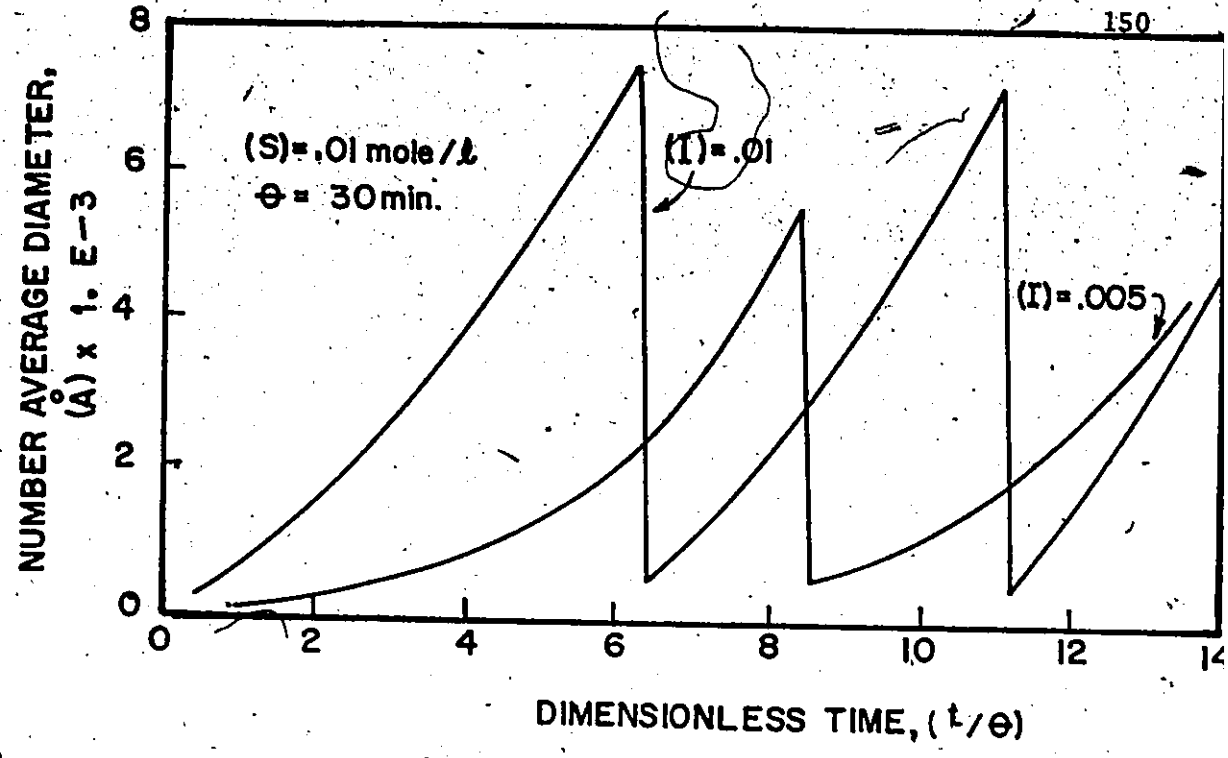

Figure (5-9) Number Average Diameter versus Dimensionless Time (Comprehensive Model)

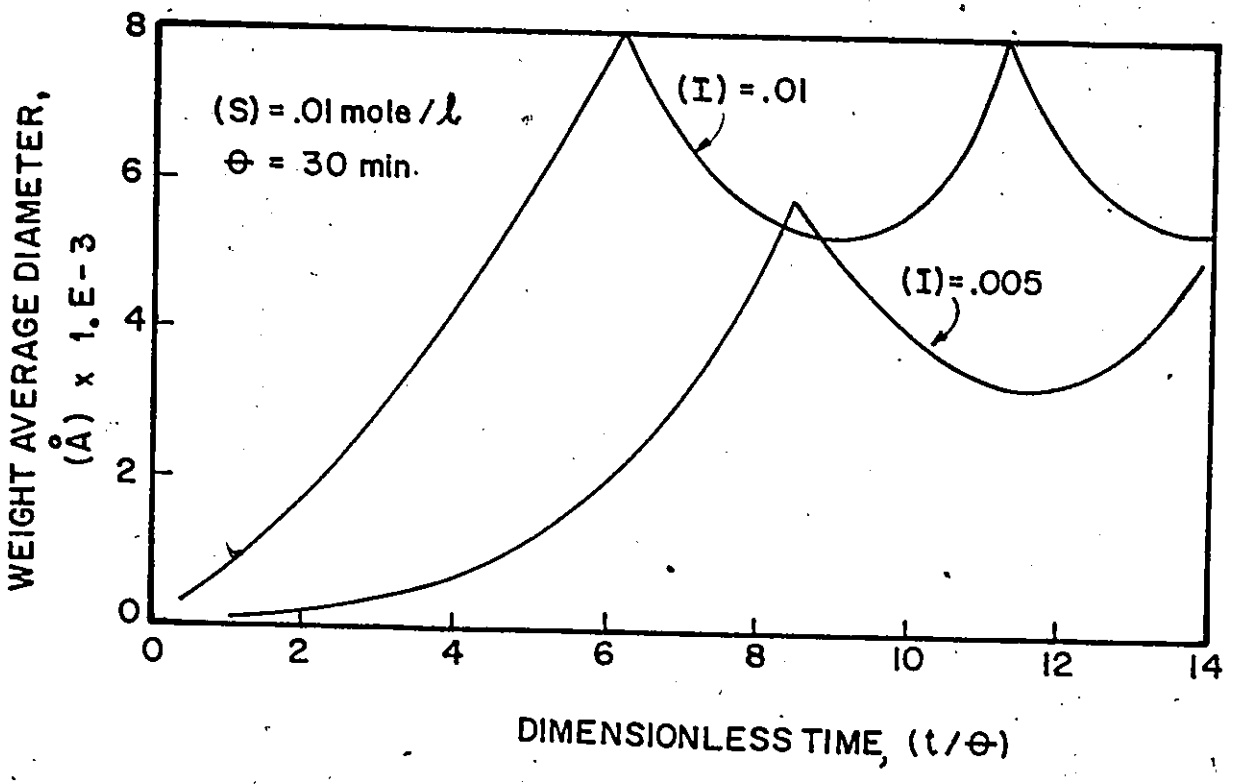

Figure (5-10) Weight Average Diameter versus Dimensionless Time (Comprehensive Model)

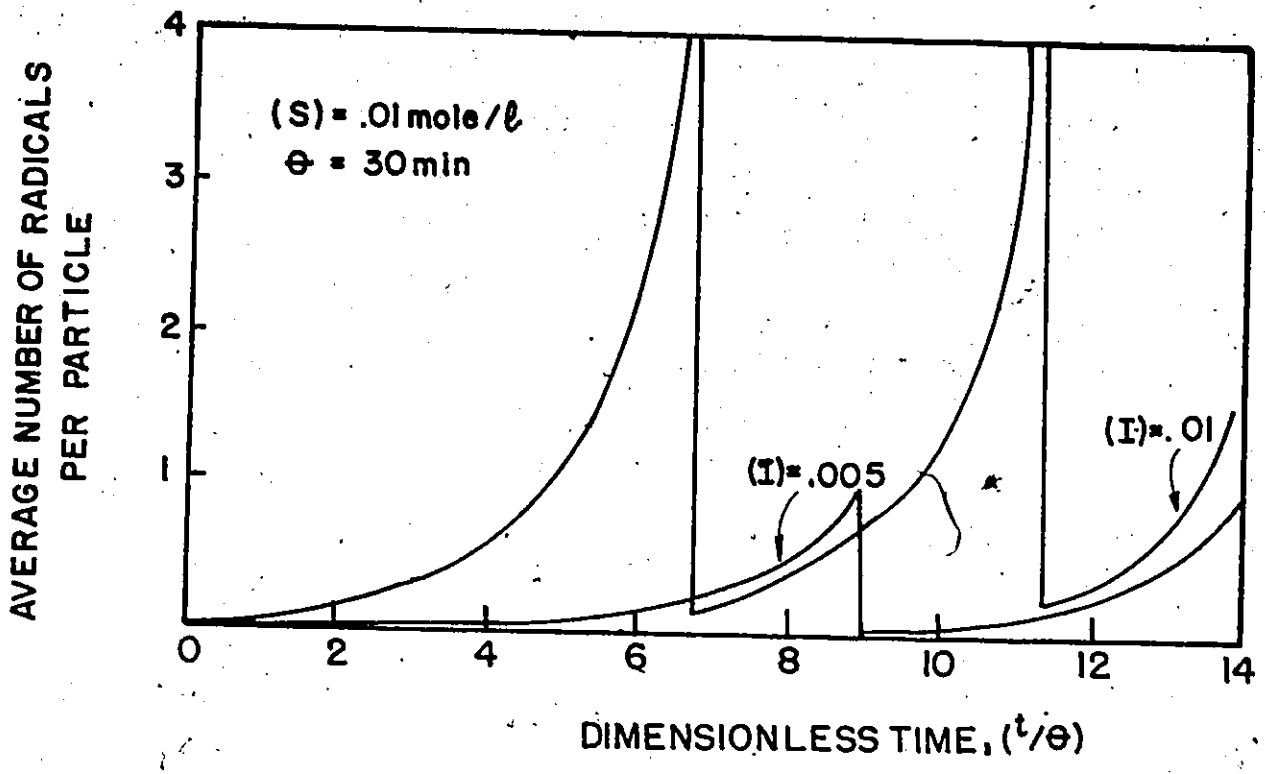

Figure (5-11) Average Number of Radicals per Particle versus Dimensionless Time (Comprehensive Model)

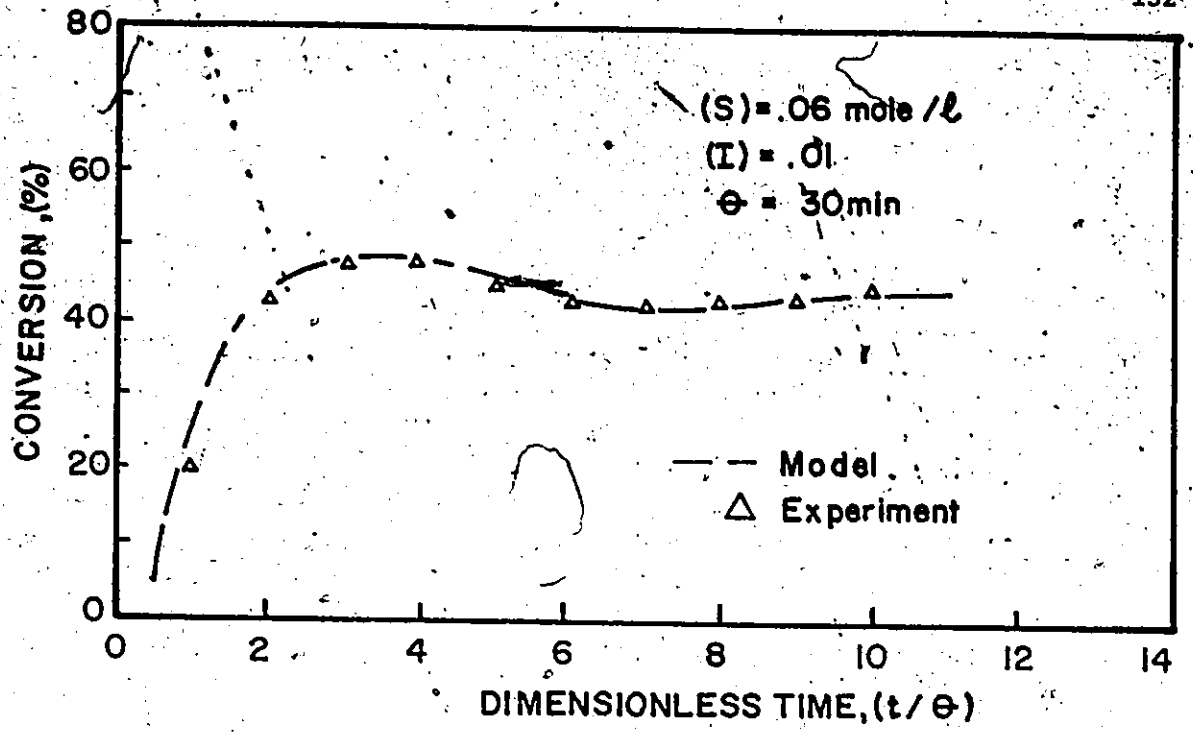

Figure (5-12) Conversion Transients - Comparison between Experimental and Predicted Results (Comprehensive Model, T = 50°C, M/W = 4/10, r.p.m. = 320)

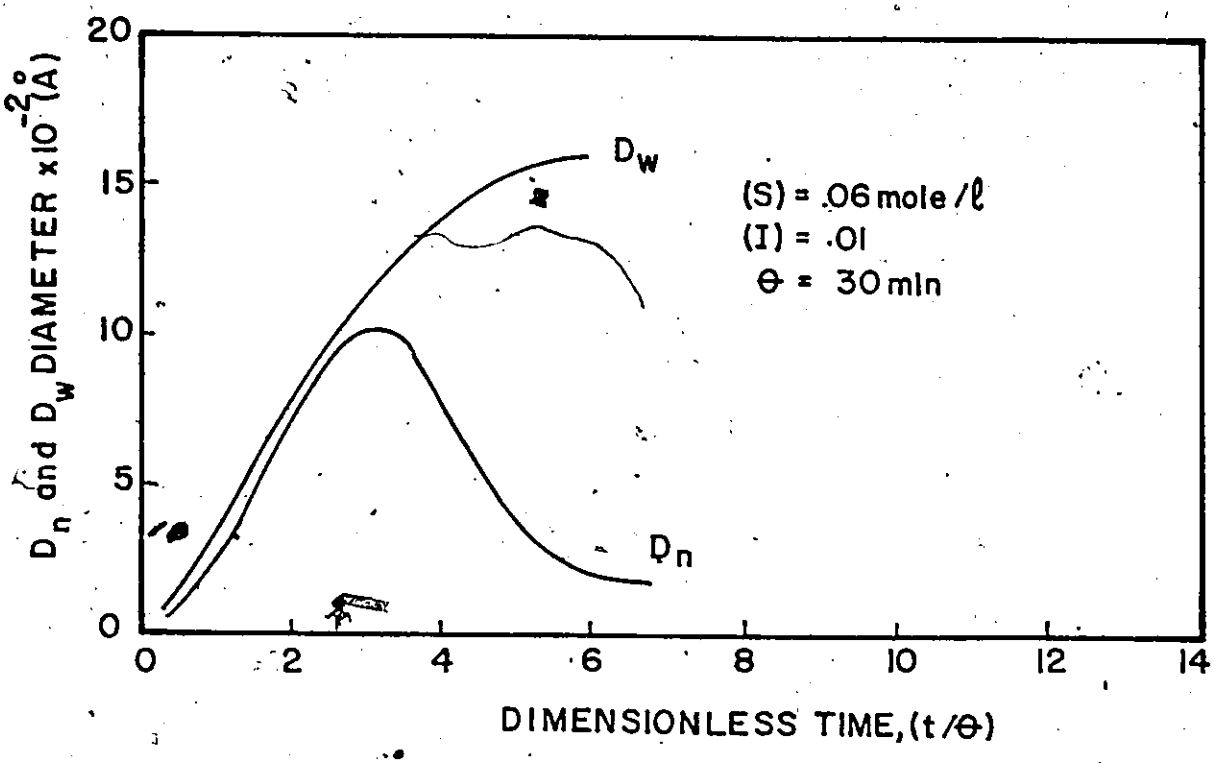

Figure (5-13) Number and Weight Average Diameters versus Dimensionless Time (Comprehensive Model)

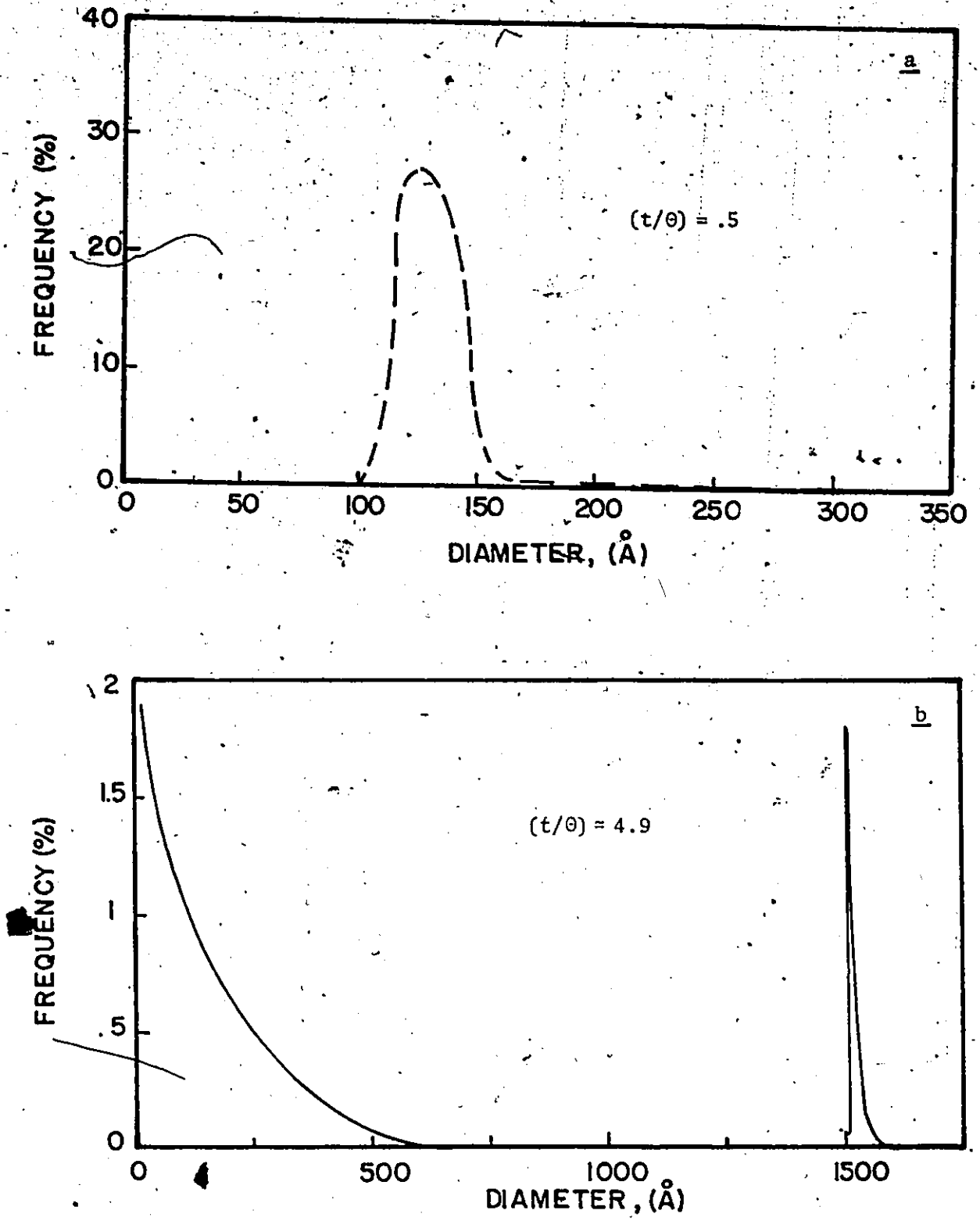

Figure (5-14) Particle Size Distribution at Two Different Reaction Times (Comprehensive Model)

area and a subsequent emulsifier deficit. However, after 2-3 mean residence times emulsifier concentration starts to build up in the reactor and a continuous particle nucleation begins. Figure 5-13 shows how the D_n and D_w change in this transient period.

Finally, Figure 5-14 shows the particle size distribution at two different reaction times. The single peak in the distribution in Figure 5-14a indicates that a large particle population formed early in the run and then particle nucleation stopped. At t = 140 min., Figure 5-14b, a new particle population has started and continuous particle generation is occurring resulting in a broad particle size distribution.

5.2.5 Further Observations and Model Difficulties

By now, the careful reader will have realized the model complexities and estimation difficulties involved. In Section 5.2.2, two important groups of parameters were identified. This assumed that all other kinetic parameters were "known" from the literature. It is common practice to perform kinetic studies on one reactor system and then use the kinetic estimates on another reactor system when dealing with the same reaction. However, it is true to say that the kinetic parameters estimated by studies on one reactor may not be valid for a new reactor. In fact, the parameters obtained should be treated as prior information and re-estimated along with the new parameters (Hoffman and Reilly (1977). In our problem unfortunately, the introduction of 15 or more kinetic parameters would make our estimation problem computationally infeasible. Therefore,

we have had to use these "known" numerical values for the parameters. In addition, it is possible that some of these parameters may well not be "constant" over the wide range of operating conditions we are employing.

Model assumptions and numerical approximations may yield another source of controversy. In deriving the differential equations for the simplified model, equations (2.69-2.72), the effect of particle size distribution has been neglected. To simplify the calculation of emulsifier concentration, the total particle area, A_p, has been approximated by an average expression instead of using the integral equation to calculate, A_p. Of course, this is an approximation and will hold better for narrow particle size distributions.

The way radicals are distributed among particles of different sizes (collision or diffusion theory) can affect the simulation results. In particular, different estimates for the unknown kinetic parameters of the reactor model were obtained depending upon the type of model considered to describe the radical entry rate of radicals into polymer particles (collision or diffusion model). Experimental conversion-time histories were fitted equally well by both models; however, these models resulted in different results for the number of polymer particles and average particle diameter. This clearly indicates that additional information is needed if we want to distinguish between the different radical entry mechanisms.

The discrete form of the particle nucleation rate and its large numerical value ($\sim 10^{15}$) can cause extra numerical problems in solving

the non-linear system of differential equations for the total system properties.

In conclusion, it should be noted that simulation results should be carefully examined especially in lack of any experimental evidence.

5.3 Stability Analysis-Limit Cycles

In a non-linear system, it is possible to have a self-sustained oscillation with the amplitude of oscillation being constant for a given constant input value. In the phase plane, where one dependent variable is plotted against another, this can be represented as an isolated closed trajectory. Such a free oscillation is called a limit cycle. Under some conditions constant input into a continuous stirred tank latex reactor (CSTR) can produce a limit cycle in the conversion and number of polymer particles. This oscillation can be large enough to make the product undesirable or even to cause an excessive agglomeration of the particles (see Figures 4-2, 4-4, 4-11 and 4-12). Furthermore, for monomer systems where long chain branching occurs, excursions to high polymer concentrations, due to the cycling behaviour of conversion, can result in polymers with excessive branching and poor processability. It is thus important, from both a theoretical and an applied point of view, to detect the presence of such limit cycles.

From the theoretical point of view, it is hard to formulate the necessary and sufficient conditions on the form of the differential equations to guarantee the existence of a limit cycle in a given region.

On the other hand, we have Bendixson's First Theorem (1901), which provides conditions under which limit cycles cannot exist in a given region.

Let us consider two autonomous differential equations in the form

$$\dot{x} = X(x,y), \quad \dot{y} = Y(x,y) \tag{5.10}$$

where X,Y are some functions of x and y and $X(0,0) = Y(0,0) = 0$. Equation (5.10) can be combined to give

$$\frac{dy}{dx} = \frac{Y(x,y)}{X(x,y)} \tag{5.11}$$

or $$X(x,y)dy - Y(x,y)dx = 0 \tag{5.12}$$

If there is a closed solution curve (that is, a limit cycle) we may integrate the left-hand side of equation (5.12) along this contour. The line integral can be expressed as a surface integral where the surface, Ω, is the part inside the closed curve (Green's theorem in the plane). We shall have

$$\int_{\gamma} (X(x,y)dy - Y(x,y)dx) = \iint_{\Omega} \left(\frac{\partial X}{\partial x} + \frac{\partial Y}{\partial y}\right) dxdy \tag{5.13}$$

However, since the left-hand side is zero everywhere,

$$\iint_{\Omega} \left(\frac{\partial X}{\partial x} + \frac{\partial Y}{\partial y}\right) dxdy = 0 \tag{5.14}$$

if there is a limit cycle. In order to satisfy equation (5.14), $(\frac{\partial X}{\partial x} + \frac{\partial Y}{\partial y})$ must be zero somewhere in the region. If $(\frac{\partial X}{\partial x} + \frac{\partial Y}{\partial y})$ is of fixed sign everywhere in the region, a limit cycle cannot lie completely in that region.

Existence of a limit cycle can be proved by the Theorem of Poincare-Bendixson-Poincare. According to this theorem if a closed bounded region Σ contains no equilibrium points of equations (5.10), and if a trajectory γ is in Σ for all $t \geq t_o$, then there is at least one limit cycle in Σ. In particular, this theorem proves the existence of a limit cycle in an annular region Σ, which contains no equilibrium points, if all trajectories cross the boundary of Σ in the same sense (Willems 1970).

An extension of the Bendixson theorem to the case of more than one trajectory is given by Daoud (1976). If two closed trajectories, one completely enclosing the other, are to exist in a domain Σ in the phase plane of the differential system (5.10) then the sum $(\frac{\partial Y}{\partial y} + \frac{\partial X}{\partial x})$ must change sign or be zero everywhere within the area enclosed between the two closed trajectories provided no singular point exists in that region.

Bendixons's First Theorem was applied to a latex CSTR to investigate conditions under which limit cycles might exist in a given region.

The equations which describe the number of polymer particles and the conversion in a latex reactor can be written as

$$\dot{N} = -\frac{N}{\theta} + f(t) \qquad (5.15)$$

$$\dot{x} = -\frac{x}{\theta} + \frac{k_p d_m}{N a M_T M_w} \Phi \bar{q} N \qquad (5.16)$$

where $\Phi = (1-x)/(1-x\,(1-\frac{d_m}{d_p}))$ (5.17)

$$\bar{q} = (R_I/2k_{de}N)^{\frac{1}{2}} \quad (5.18)$$

$$k_{de} = (\frac{12D_w\delta}{mD_{pp}^2})(\frac{k_{fm}}{k_p}) \quad (5.19)$$

$$D_{pp}^2 = (\frac{6}{\pi})^{2/3}(\frac{M_T M_W}{d_p})^{2/3}\ N^{-2/3}\ (\frac{x}{1-\phi})^{2/3} \quad (5.20)$$

$$f(t) = \frac{\rho}{1+\epsilon A_p/A_m} = \frac{(R_I + k_{de}N\bar{q})(S-A_p)}{S + A_p(\epsilon-1)} \quad (5.21)$$

$$A_m = S_T - S_{CMC} - A_p = S - A_p \quad (5.22)$$

$$A_p = (36\pi)^{1/3}\ (\frac{M_T M_W}{d_p})^{2/3}\ (\frac{x}{1-\Phi})^{2/3}\ N^{1/3} \quad (5.23)$$

The system consisting of equations (5.15) and (5.16) is an autonomous system of two non-linear differential equations of the form (5.10) and hence we can apply the theory of limit cycles on it.

By differentiating equations (5.15) and (5.16) we obtain the partial derivatives $\frac{\partial \dot{N}}{\partial N}$ and $\frac{\partial \dot{x}}{\partial x}$. On adding these derivatives an expression for SUM = $(\frac{\partial \dot{N}}{\partial N} + \frac{\partial \dot{x}}{\partial x})$ is obtained.

Then for different emulsifier concentrations a screening test in the (N,x) phase plane was performed to determine the sign pattern of the SUM in the region of interest. For low surfactant concentrations a sign change was always detected (from minus to plus), which suggested the

possible existence of a limit cycle. For example, for S = 0.01 mole/ℓ and I = 0.012 mole/ℓ the SUM changed sign from negative to positive for a value of $N = 6.10^{16}$ particles/ℓ-latex. It is interesting to note that a similar sign change of the SUM occurred even at higher surfactant concentrations but always for higher values of N($\sim 10^{18}$ particles/ℓ-latex).

However, a sign change of the SUM does not necessarily prove the existence of a stable limit cycle and further investigation is required.

To show that sustained oscillations always result in a closed trajectory in a phase-plane plot, some simulation results obtained in section 5.2.3 are plotted in the (x,A_m), (x,N) and (x,A_p) planes.

It should be noted that a low surfactant concentration (S = 0.01 mole/ℓ) always results in a closed trajectory (Figures 5-15, 5-16, 5-17, a,b,d). On the other hand, an open trajectory (Figures 5-15, 5-16, 5-17, c) is obtained in the phase plane for S = 0.04 mole/ℓ, that is, for a steady-state reactor performance.

5.4 Conclusions

Experimental conversion-time histories obtained under a variety of operating conditions were successfully simulated by both models (simplified and comprehensive), and the unknown kinetic parameters ϵ and δ' estimated by a non-linear regression routine. It was found that ϵ was a function of surfactant concentration and that a linear relationship could be written between the parameter δ' and initiator concentration. In section 5.3, Bendixson's theorem was used to prove the possible existence of limit cycles

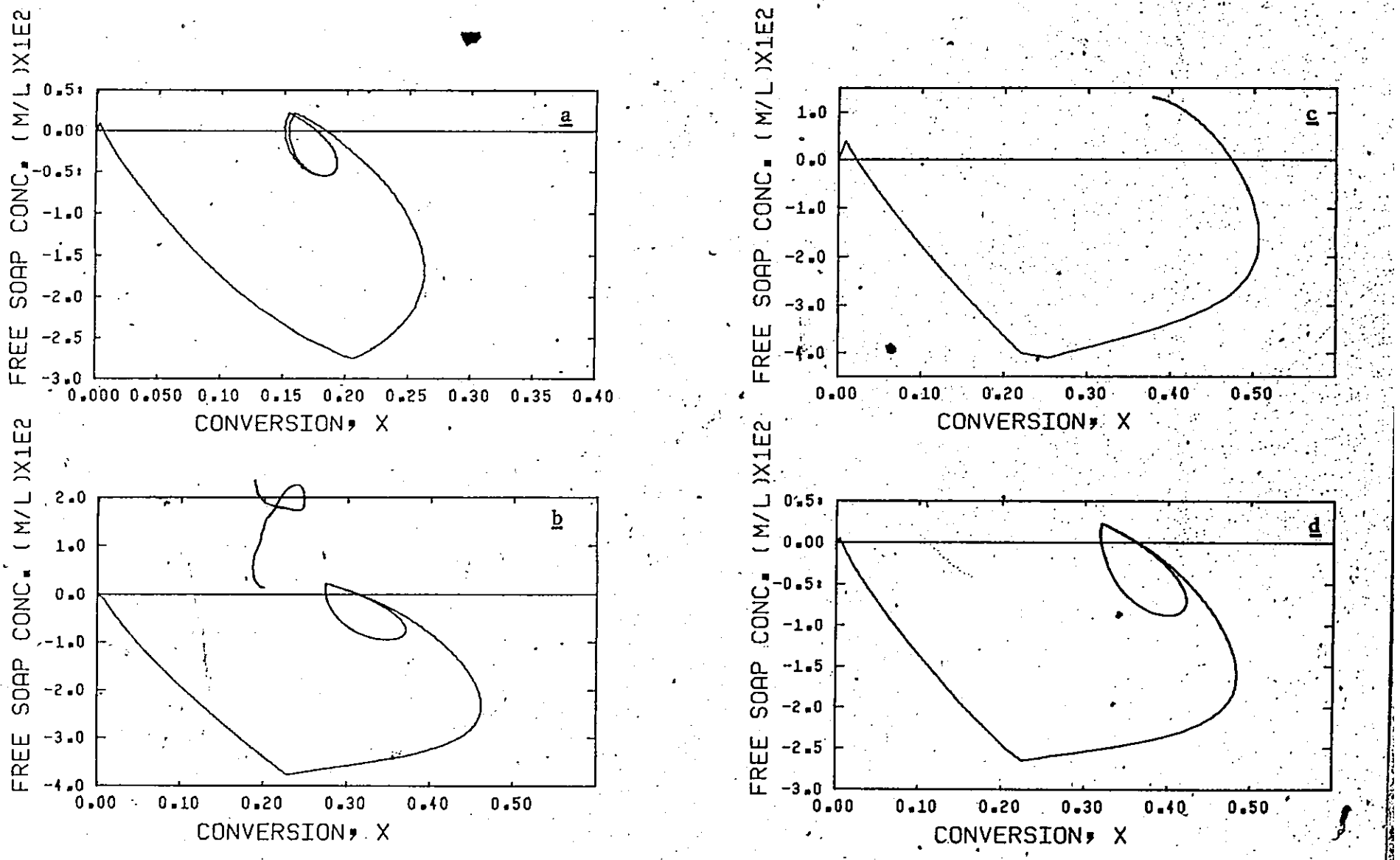

Figure (5-15) Phase Plane Plots for Conversion and Free Soap Concentration

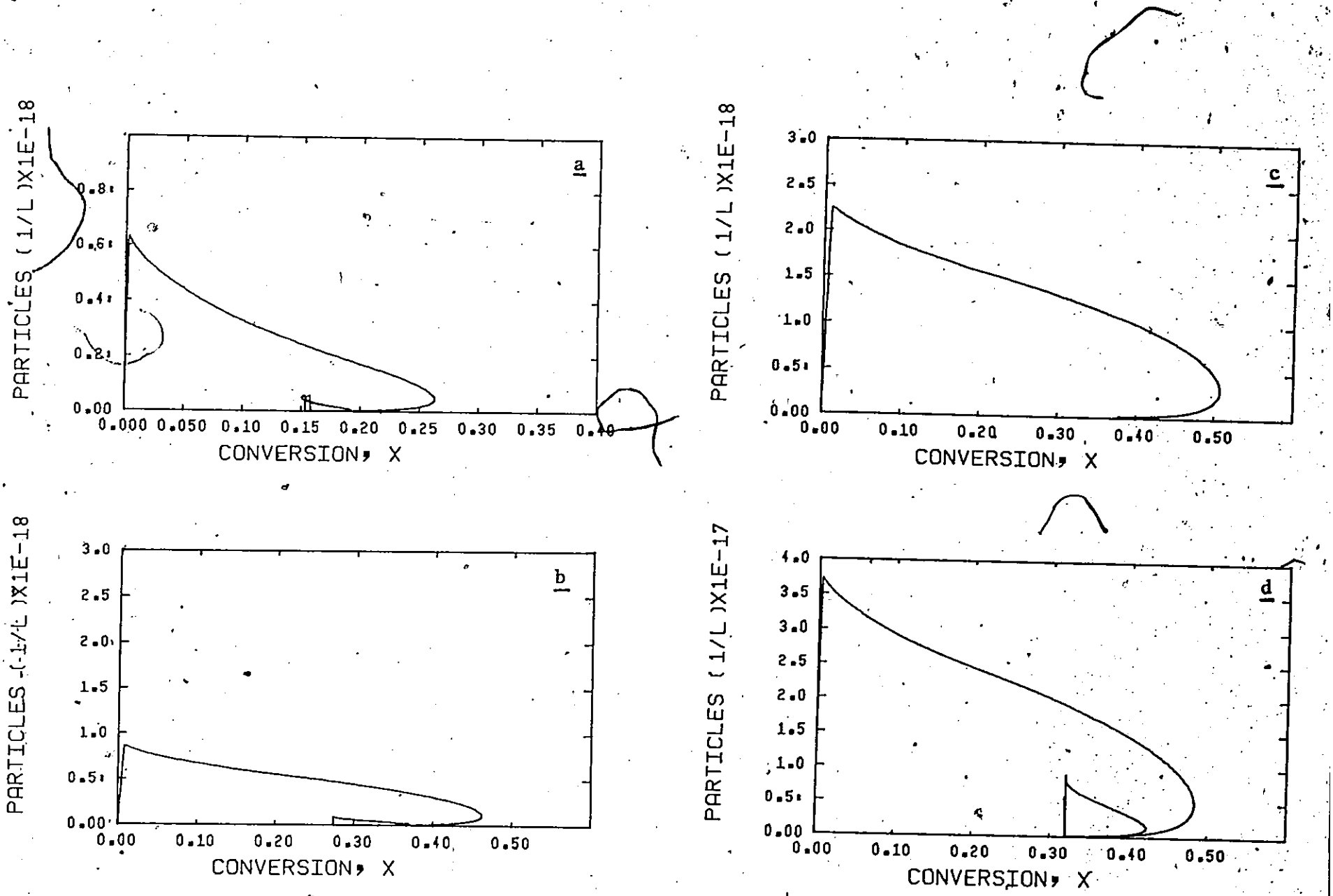

Figure (5-16) Phase Plane Plots for Conversion and Number of Polymer Particles

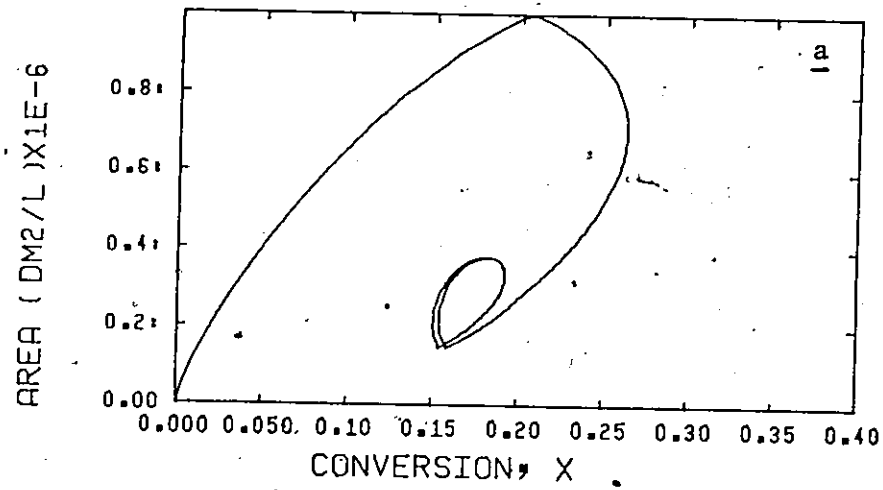

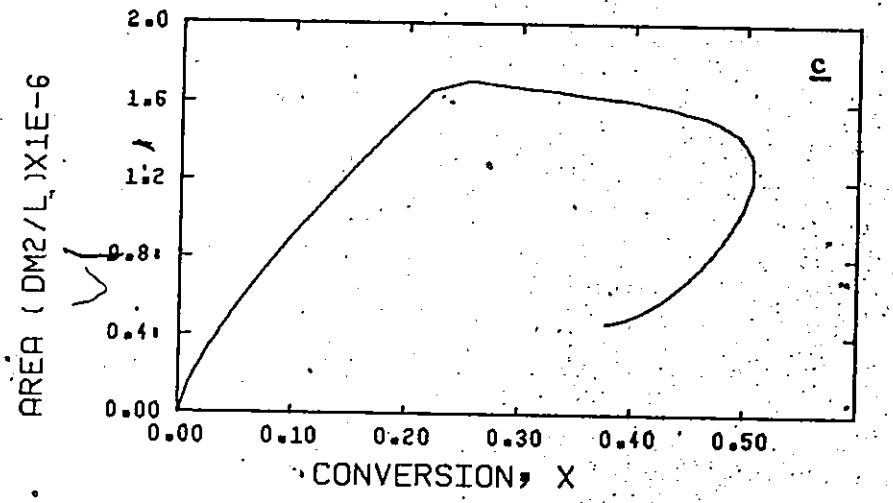

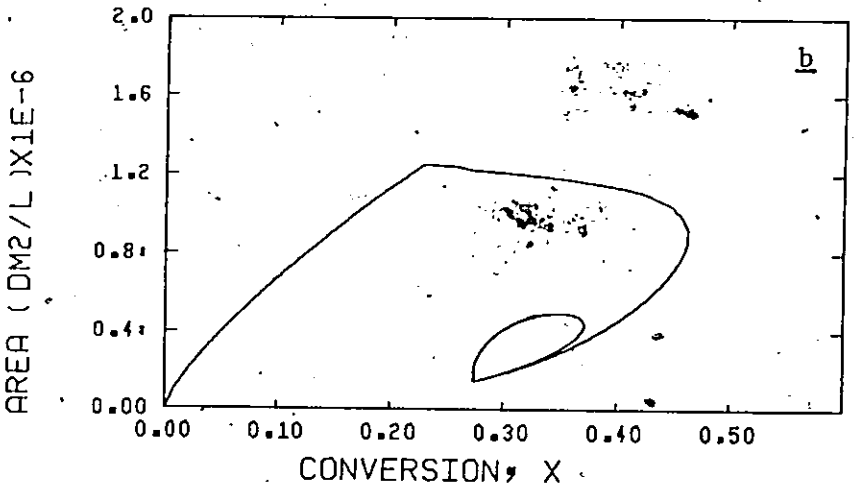

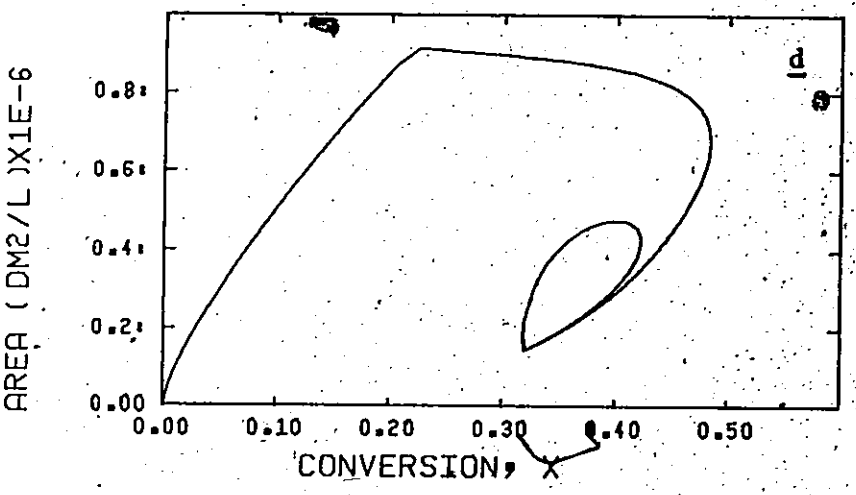

Figure (5-17) Phase Plane Plots for Conversion and Total Particle Area

in our emulsion polymerization system. Then, it was shown that sustained oscillations always resulted in a closed trajectory in the phase plane.

CHAPTER 6

TURBIDITY AND LEC RESULTS

6.1 Introduction

As stated in the Introduction (Chapter 1), one of the main objectives of the present work was the development of practical on-line techniques for measuring and following changes in the properties of the latex product. These measurements can be used to track the states of our system and finally control some properties of the latex to achieve a desired reactor performance and product quality.

From those techniques described in Chapter 3, turbidity spectra analysis and LEC appear to have some specific advantages. They are simple, fast and can be easily employed as on-line detectors.

6.2 Turbidity Measurements

A Beckman DU spectrophotometer was used for turbidity measurements. This model can provide a BCD output to be used with a Mini-computer. Turbidity data for most runs have been tabulated and are given in Appendix III.

In Figure 6-1, typical turbidity curves at different reaction times are shown. These curves correspond to run-27 (I= .02, S = 0.1 mole/ℓ, θ = 20 min) during which sustained oscillations appear. It should be noted

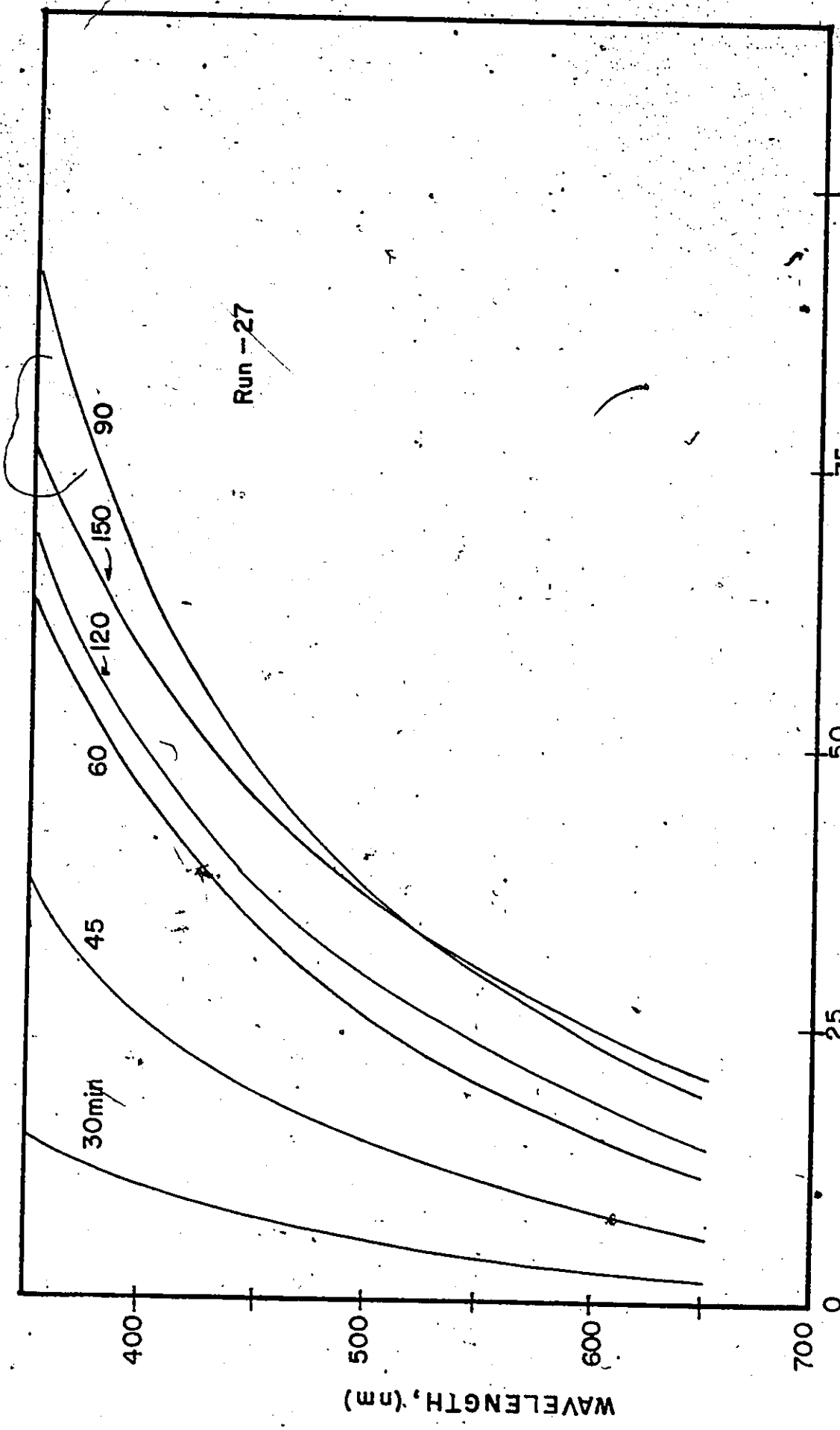

Figure (6-1) Turbidity Curves at Different Reaction Times

that changes in conversion and number of particles (Figure 4-4) result in corresponding rotational and/or translational changes of the turbidity curves (Figure 6-1).

In Figures 6-2 through 6-5, absorbance at W.L. = 3500Å is plotted against reaction time. It is very interesting to note that these absorbance measurements can follow reactor changes for both cases of sustained oscillation and steady-state reactor operation. Therefore, by monitoring continuously the absorbance at 3500Å we can know if the reactor is operating at steady state or under sustained oscillations. This important qualitative result shows that light transmission measurements can easily follow variations in the reactor performance due to changes in conversion and number of particles.

In Figures 6-6 through 6-8, the turbidity ratio (τ3500Å/τ6500Å) is plotted against time. This turbidity ratio has several rather important qualities. First, it is independent of both the concentration of sample and the number of particles within the sample, that is, it is a function only of the particle size distribution. The second important quality of the turbidity ratio is that several qualitative conclusions can be made about the numerical value of this turbidity ratio. To better demonstrate the qualities of the turbidity ratio we make use of the turbidity definition, equation (3.8)

$$\frac{\tau_{\lambda_1}}{\tau_{\lambda_2}} = \frac{\int_0^\infty K\left(\frac{D}{\lambda_1}, \frac{n}{n_m}\right) \frac{\pi D^2}{4} f(D)\,dD}{\int_0^\infty K\left(\frac{D}{\lambda_2}, \frac{n}{n_m}\right) \frac{\pi D^2}{4} f(D)\,dD} \qquad (6.1)$$

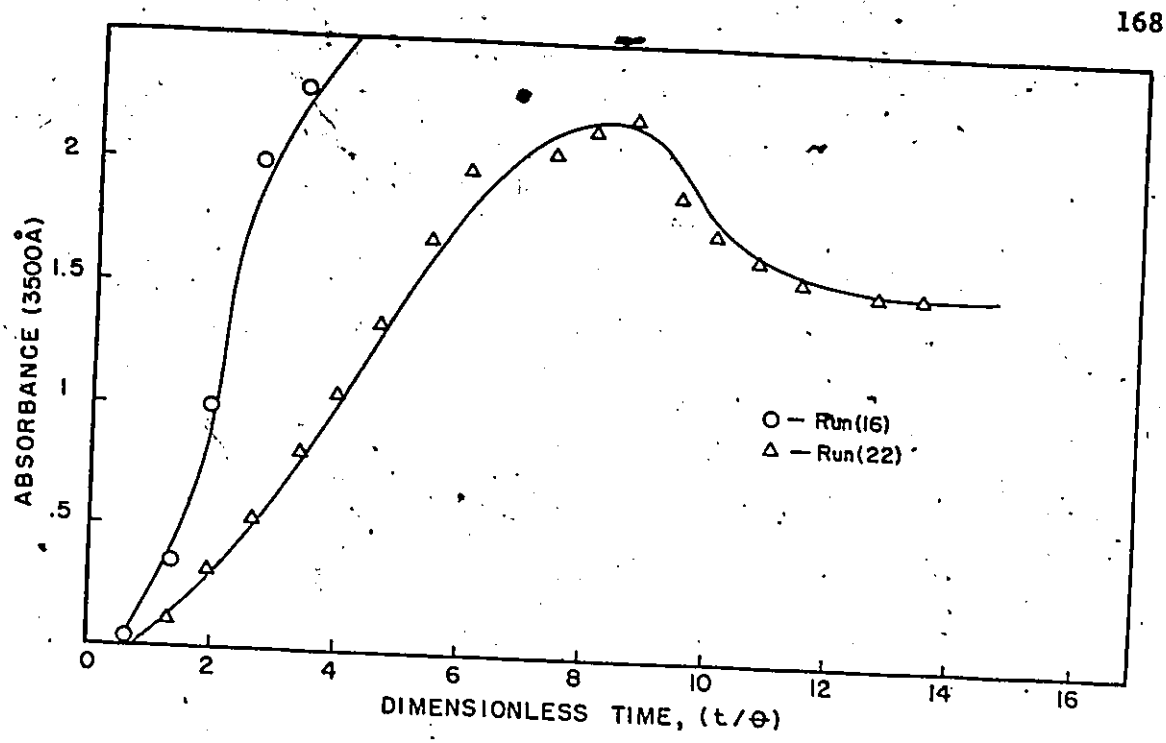

Figure (6-2) Absorbance at 3500Å as a Function of Reaction Time

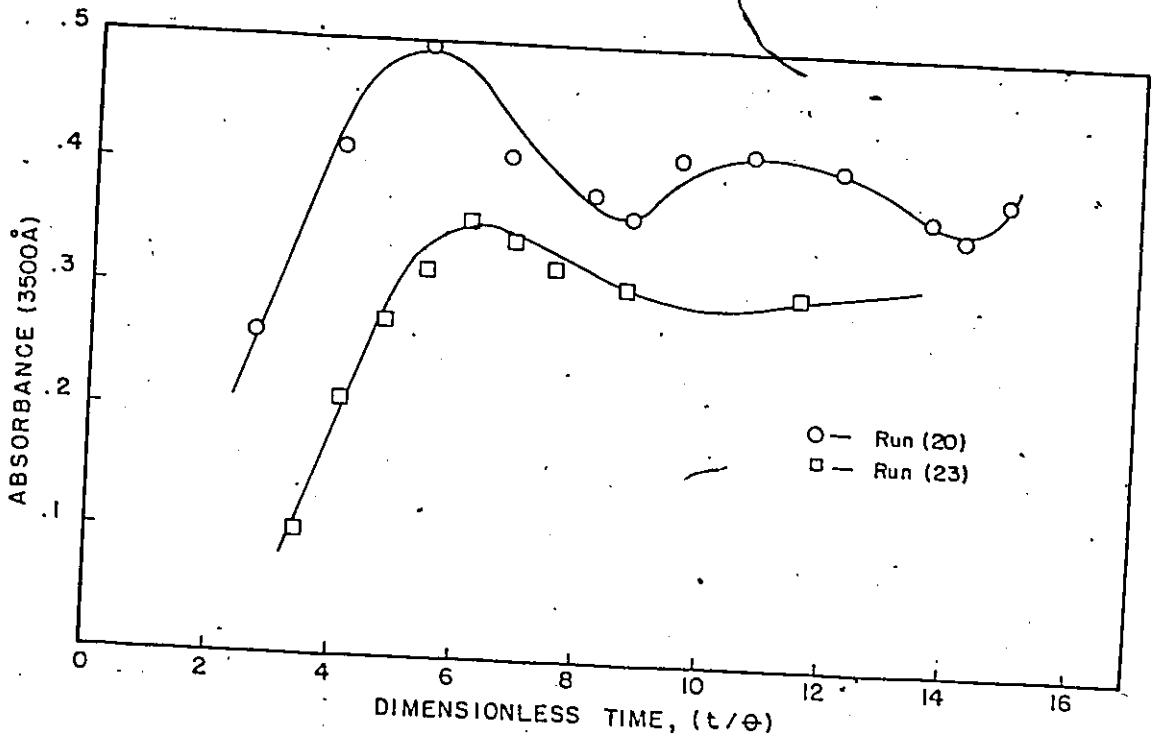

Figure (6-3) Absorbance at 3500Å as a Function of Reaction Time

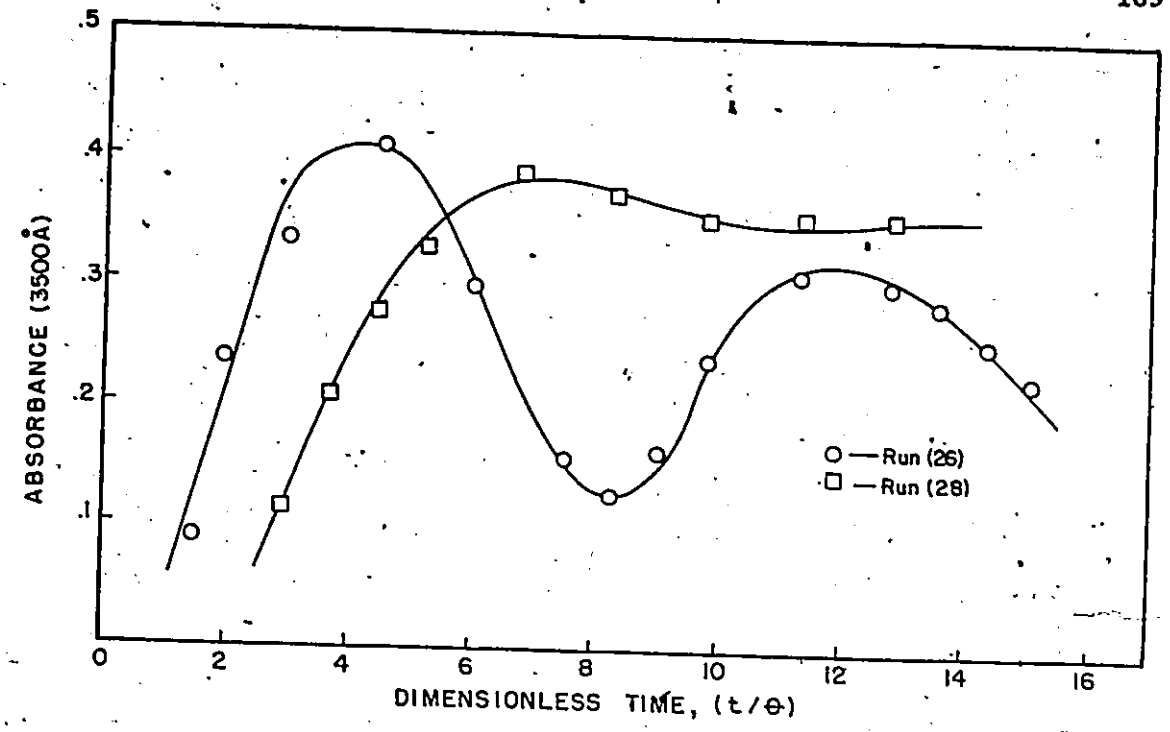

Figure (6-4) Absorbance at 3500Å as a Function of Reaction Time

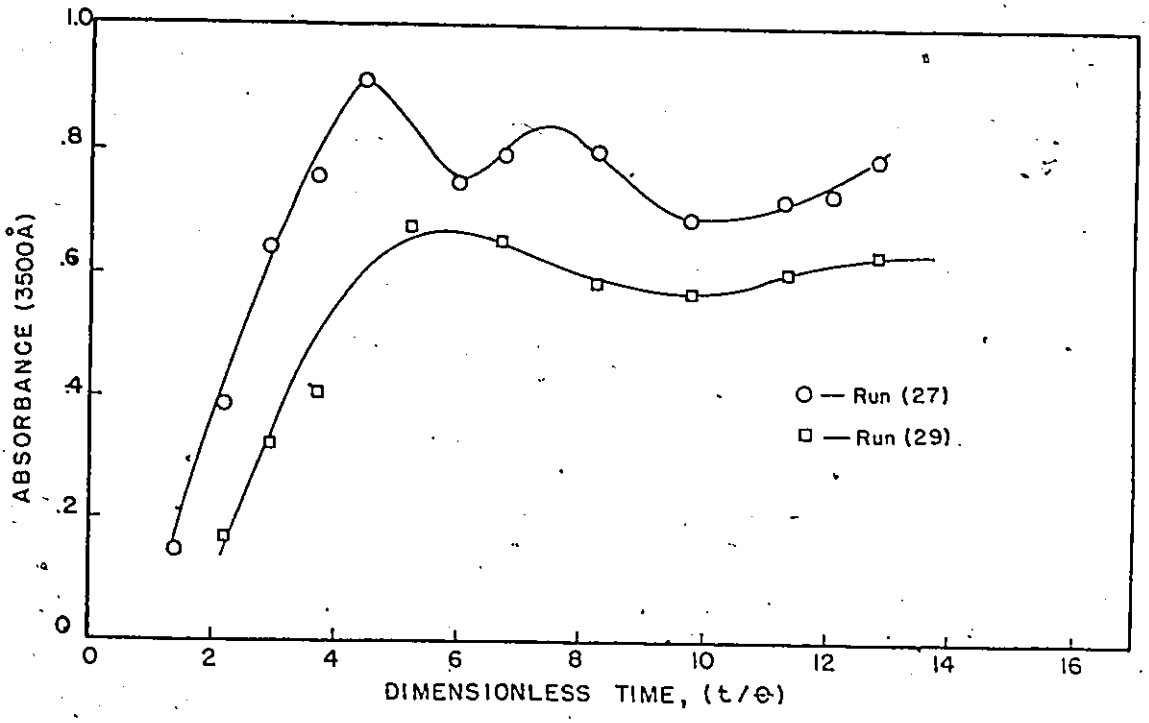

Figure (6-5) Absorbance at 3500Å as a Function of Reaction Time

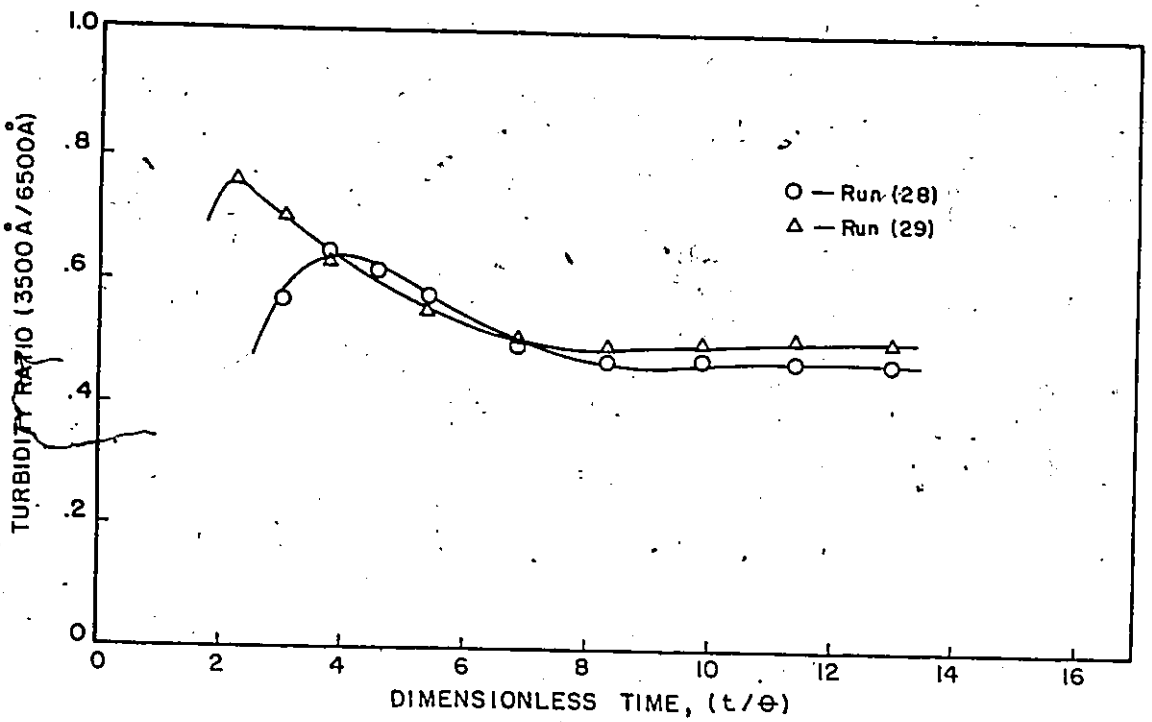

Figure (6-6) Turbidity Ratio (3500Å/6500Å) as a Function of Reaction Time

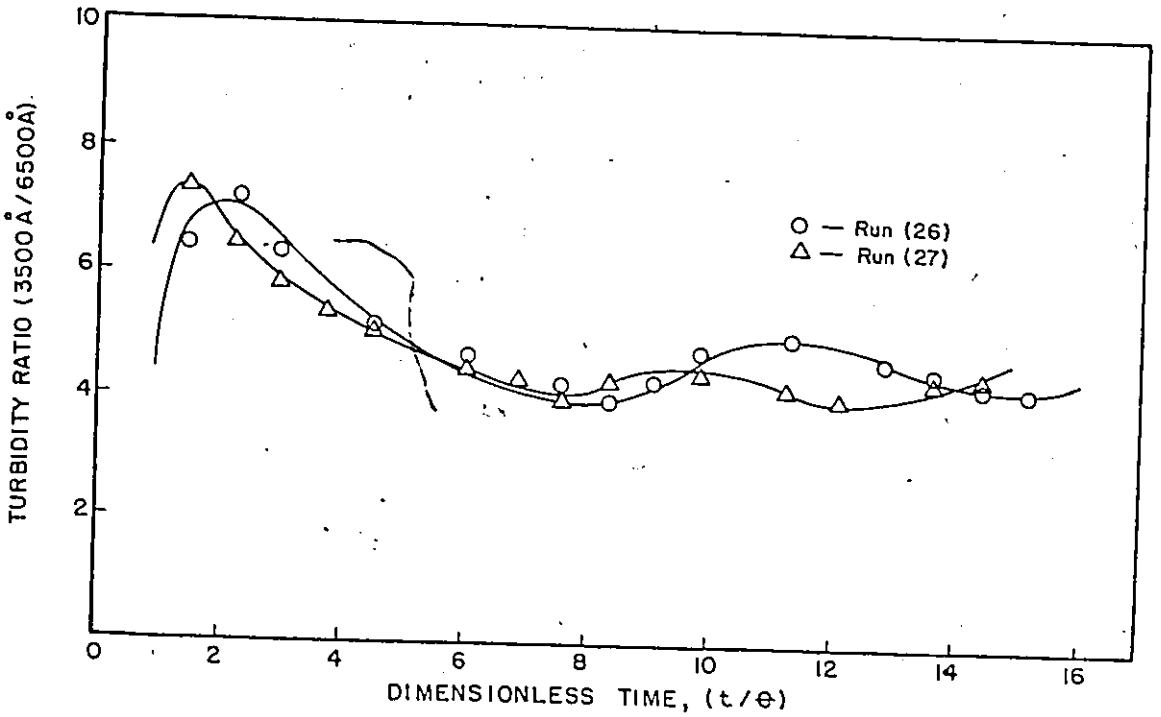

Figure (6-7) Turbidity Ratio (3500Å/6500Å) as a Function of Reaction Time

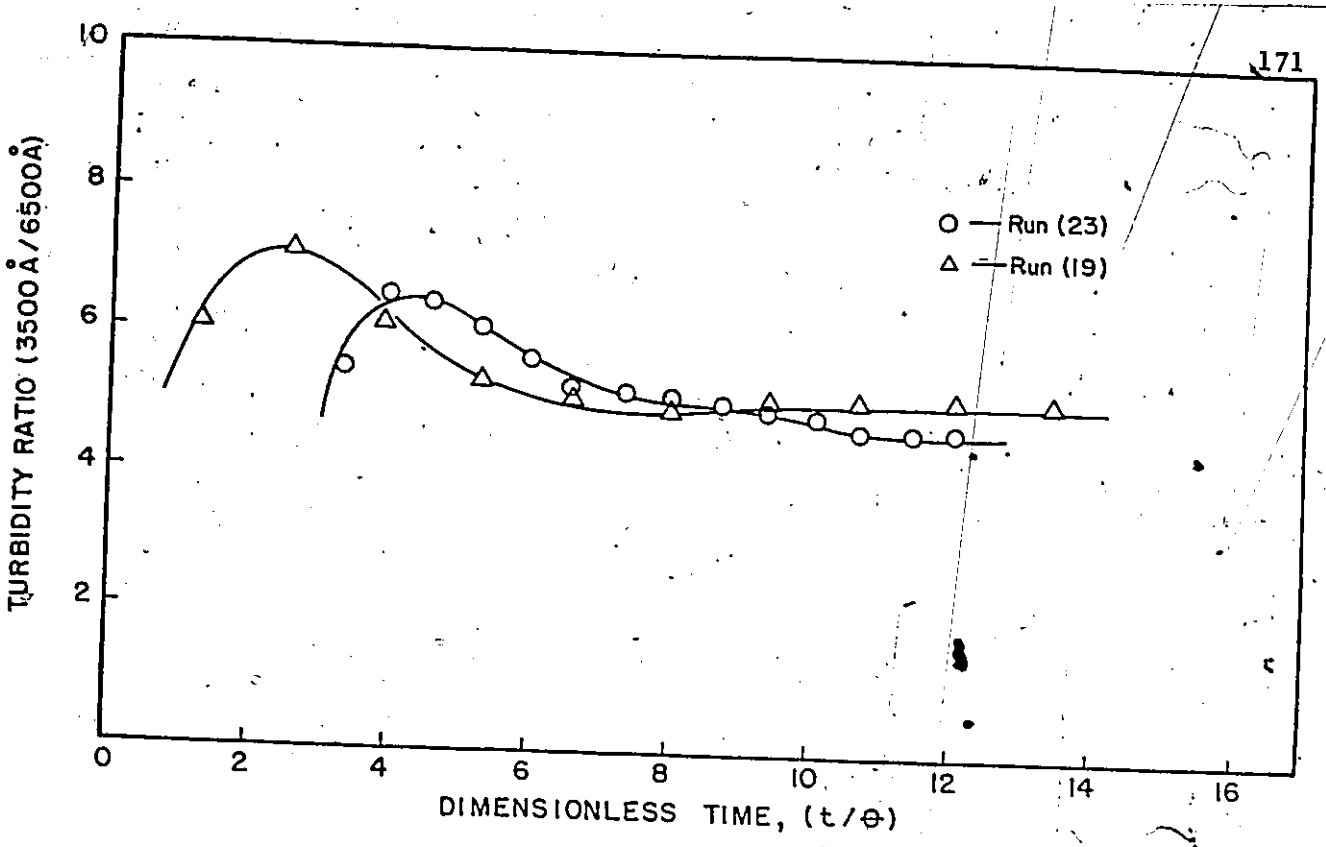

Figure (6-8) Turbidity Ratio (3500Å/6500Å) as a Function of Reaction Time

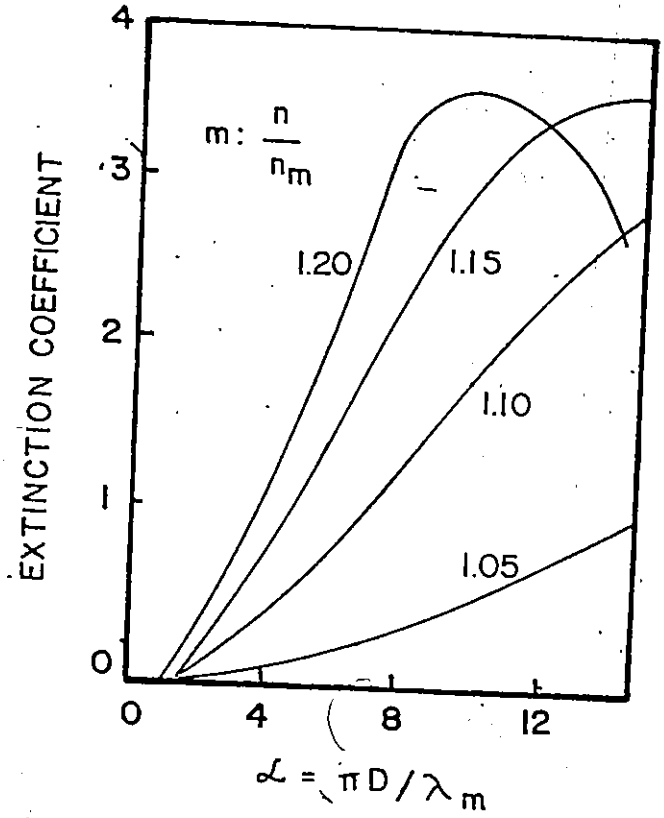

Figure (6-9) Relationship between the Extinction Coefficient and $\alpha = \pi D/\lambda_m$

where $\lambda_1 = 3500\text{Å}$ and $\lambda_2 = 6500\text{Å}$.

In Figure 6-9, the extinction coefficient, K, is plotted against $\alpha = \pi D/\lambda_m$ for different values of the parameter m ($=n/n_m$). If we combine equation (6.1) with the numerical values of the extinction coefficient for a certain value of m (Figure 6-9), some qualitative conclusions about the numerical value of turbidity ratio can be easily drawn.

Narrow particle size distributions cause lower values for the turbidity ratio, while the ratio increases as the distribution becomes broader. Note that near the start of the reaction the turbidity ratio is high (Figures 6-6 to 6-8). The probable reason is that early in the reaction a wider distribution of particles is obtained. As soon as a polymer particle is formed it grows very rapidly but new particles continue to form resulting in a wide distribution. However, the distribution becomes narrower as the smaller particles grow more rapidly because of their large surface. Thus the turbidity ratio decreases until the particle size distribution becomes established, which results in a constant value of the turbidity ratio, Figures 6-6 and 6-8. In case of sustained oscillations (Figure 6-7) particles are not generated continuously but only during short time periods which are 6-7 residence times apart. This results in a considerable decrease of the turbidity ratio because new particles are not longer formed; therefore, the initial particle size distribution becomes narrower and narrower. However, as we have already seen in Section 4.3.1, when the feed of emulsifier exceeds the consumption rate for surface coverage of the existing particles, emulsifier becomes again available for particle

nucleation. This new particle formation gives rise to a new broader particle size distribution resulting in a larger value for the turbidity ratio and so on. Similar changes for the polydispersity ratio D_w/D_n have been reported by Gerrens (1974) for the emulsion polymerization of styrene under limit cycle conditions, and in a recent publication by Kiparissides et al. (1978) (see Chapter 6).

An important problem encountered in section 4.3.4 for the continuous emulsion polymerization of vinyl acetate was to determine the start of reaction, in other words, the length of the induction period. The induction period can be determined accurately by monitoring the absorbance near the start of the reaction. A significant increase in absorbance can be seen at the start of the polymerization. This is demonstrated in Figures 6-2 through 6-5. The exact determination of the induction period is particularly important for the on-line control studies, since the end of this period marks the start time for the numerical solution of the model, equation (2.75), and application of the control strategy.

Another important feature of turbidity spectra analysis is the determination of the rate and extent of particle coagulation. The basis for this optical method can be found in Rayleigh's law which states that the Tyndall scattering is proportional to the square of the volume of the particles. Therefore, although the number of particles decreases during flocculation, the total scattering increases (Kruyt (1952)). Thus, a dramatic increase of the absorbance clearly indicates that particle flocculation has taken place. An abnormal increase of the absorbance was

observed for those experiments during which extensive agglomeration and fouling of the reactor occurred, Figure 4-12. In Figure 6-2 absorbance values are plotted for two different runs. Circles (O) indicate absorbance values measured at different reaction times for an experiment (I = 0.02 mole/ℓ, S = 0.01 mole/ℓ, θ = 30 min) during which very rapid and extensive agglomeration took place. Triangles (Δ) correspond to an experiment (I = 0.015 mole/ℓ, S = 0.06 mole/ℓ, θ = 30 min) in which some agglomeration observed initially before the system reached its final steady state value. Obviously, in the case of high emulsifier concentration the repulsive forces are strong enough to keep the particles apart. On the other hand, when the repulsion is absent (low emulsifier concentration) agglomerates are formed which increase the scattered light and result in a dramatic increase in absorbance values.

It is important that turbidity measurements be taken in the absence of multiple scattering, that is, from a dilute solution in which the particles are far removed from each other. To avoid multiple scattering the aqueous suspensions of latex were adjusted in concentrations to give absorbance values in a range 0.1-1.2 over the wavelength region 350-700 nm. Therefore, different dilution ratios (0.2/100-0.2/500) of latex volume over the dilution volume of water were used to ensure that absorbance values were in the above range.

6.2.1 Analysis of Turbidity Measurements

In Section 3.3.3 a new technique was developed to estimate the moments of the unknown particle size distribution from turbidity measurements. According to this method of moments, turbidity at a specific wavelength is

expressed in terms of the six first moments of the unknown PSD. To estimate the unknown moments, a system of six simultaneous algebraic equations (at six different wavelengths) has to be solved. The weight average particle diameter, D_w, is easily then calculated as the ratio J_4/J_3.

In Figures 6-10 through 6-13, an estimated D_w is plotted against time for different reaction conditions. It can be seen that the computed weight average diameter follows closely conversion changes for both cases of sustained oscillations and steady-state behaviour.

Other particle average diameters can be, of course, estimated as ratios of the computed moments. However, the number average particle diameter, D_n, does not show the same precision as the other higher moments. This is mainly due to the polynomial approximation of the term $K(\frac{D}{\lambda_m}, \frac{n}{n_m})\frac{\pi D^2}{4}$ in equation (3.14), especially at small values of $D(<500\text{Å})$ where the approximation becomes less accurate. Moreover, it should be remembered that turbidity measurements are far more sensitive to variations due to large particles than to small size ones. This is easily seen from Figure 6-9, where the extinction coefficient is plotted against α. In addition, it has been shown (Hamielec (1976)) that for particles which fall in the Rayleigh scattering region ($0 < \alpha < 1.0$) only a weight average diameter can be calculated from turbidity measurements.

6.2.2 Principal Component Analysis

In Figures 6-2 through 6-8, it was shown how absorbance measurements could follow reactor variations due to changes occurring in the number of

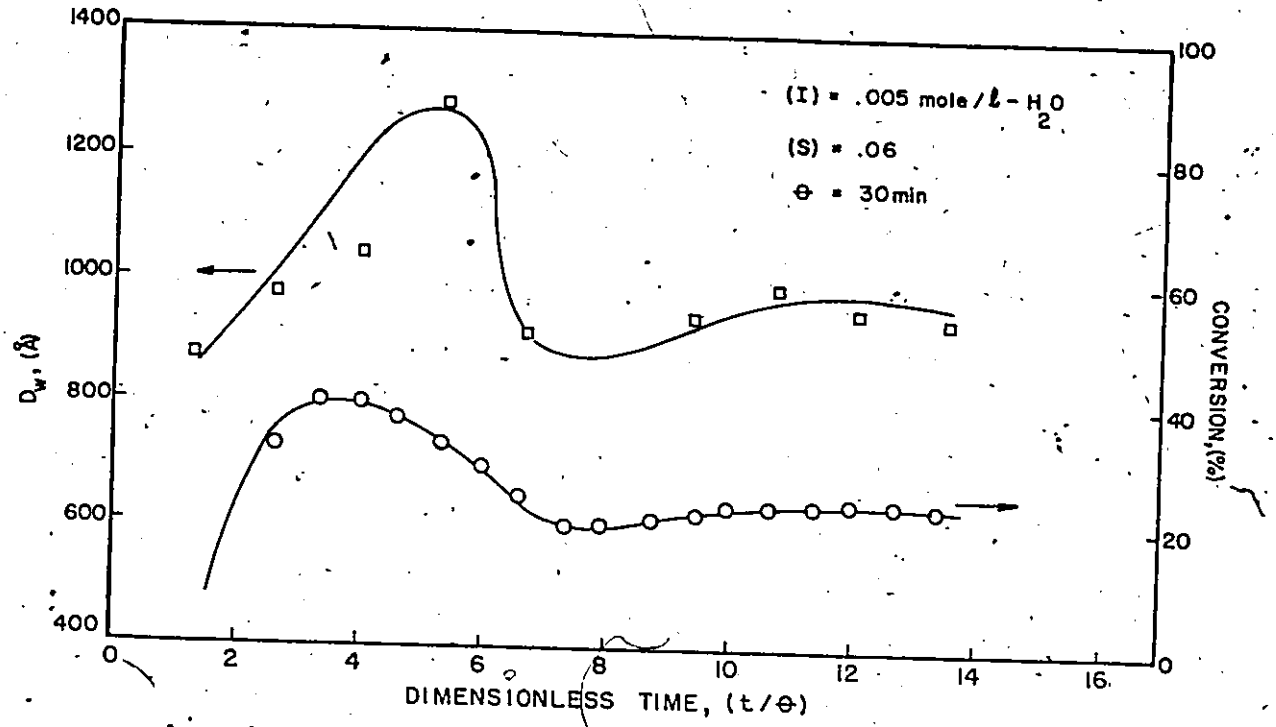

Figure (6-10) Predicted Weight Average Diameter and Experimental Conversion Values versus Dimensionless Time

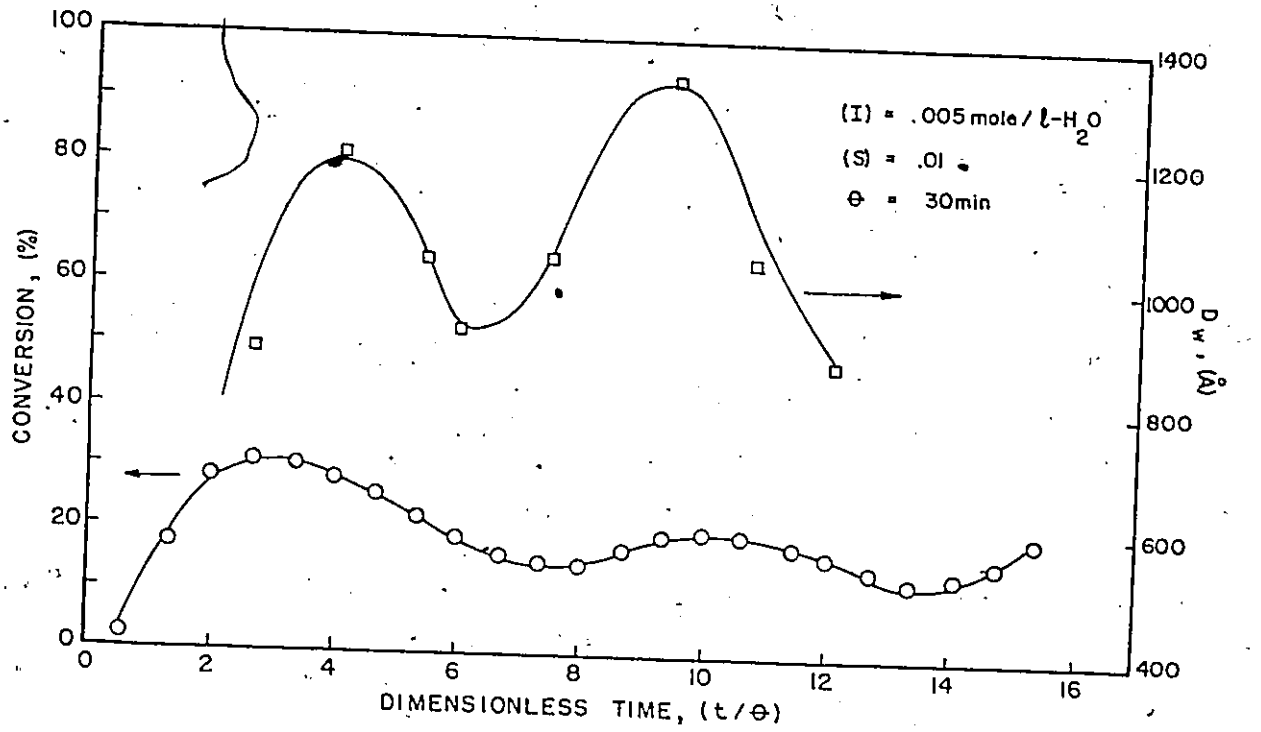

Figure (6-11) Predicted Weight Average Diameter and Experimental Conversion Values versus Dimensionless Time

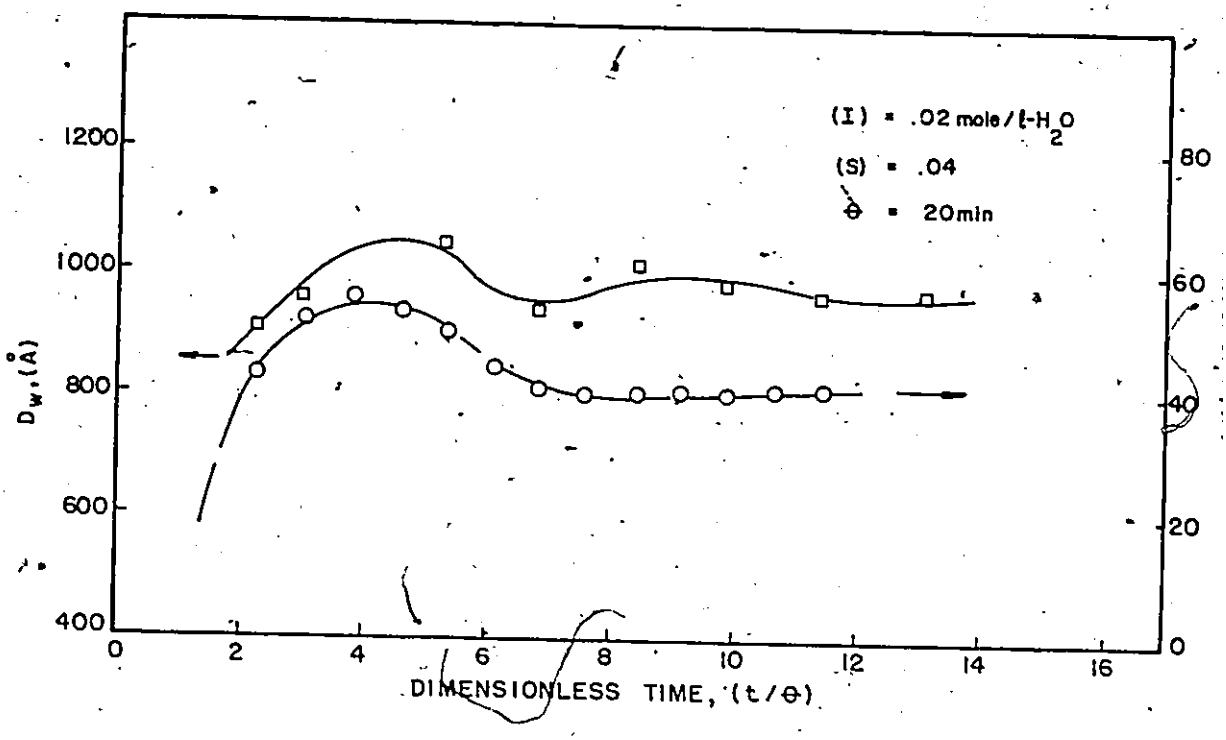

Figure (6-12) Predicted Weight Average Diameter and Experimental Conversion Values versus Dimensionless Time.

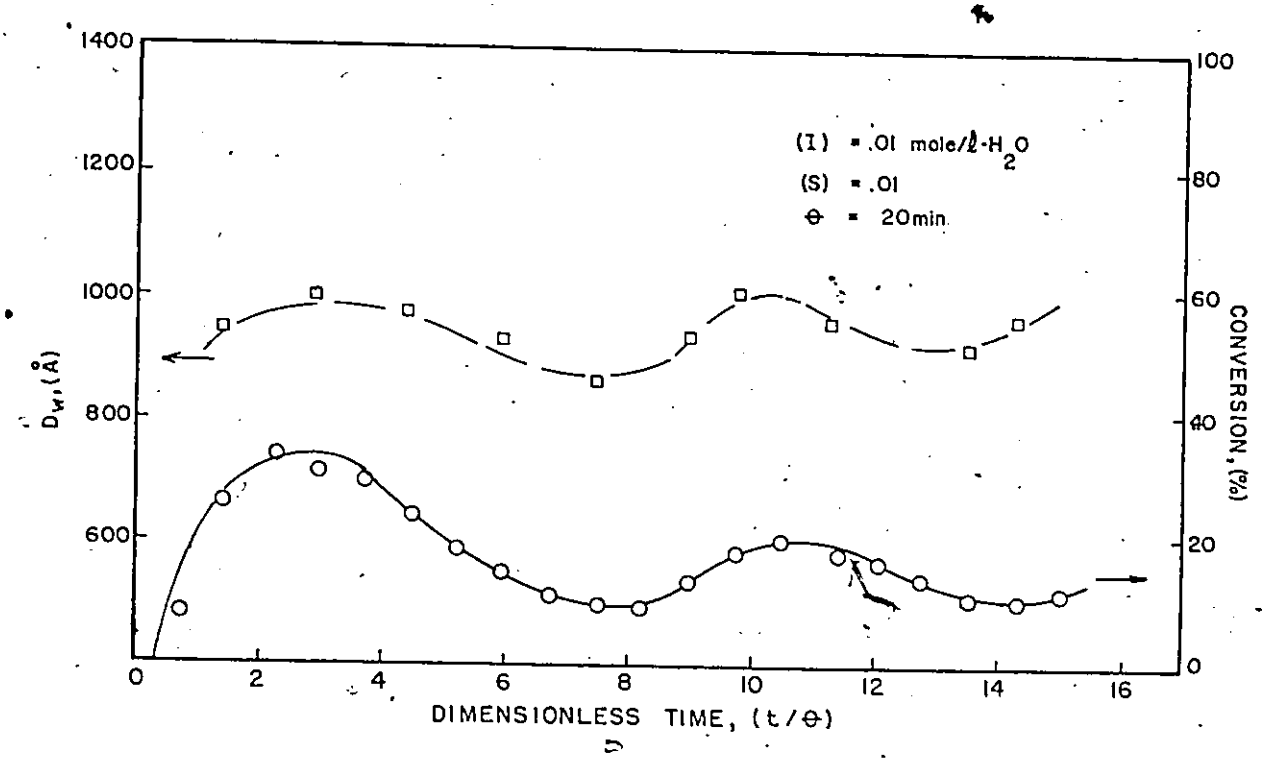

Figure (6-13) Predicted Weight Average Diameter and Experimental Conversion Values versus Dimensionless Time

polymer particles and polymer volume. On the other hand, in Section 3.3.4 a technique was described to resolve the additive mixtures of overlapping N and V_p by combining linear regression and the principal-component analysis.

As shown in Anderson (1958) the principal components are given by the eigenvectors of the covariance matrix $\Sigma = E(\underline{X}_i(\lambda)\underline{X}_i'(\lambda))$ where $\underline{X}_i(\lambda)$ denotes the observed turbidity values at different wavelengths. These eigenvectors which are linear combinations of seven absorbance values measured at the range of (6500-3500Å) provide us with a new set of linearly combined measurements that account for most of the observed variations in absorbance from one wavelength to another.

To find these principal components absorbance measurements from ten different runs (see Appendix III) covering a wide range of operating conditions were combined together. A total number of 672 absorbance measurements were used for the analysis (7 absorbance values measured at 96 different reaction conditions). Before carrying out the principal component analysis all absorbance values were adjusted to their equivalent value at a reference dilution ratio (1 ml latex/1000 ml H_2O).

Results of the principal component analysis are given in Table 6-1. It is interesting to note that the last two eigenvectors can account for most of the observed total variation of absorbance at different reaction times.

Subsequently linear regression models were sought for conversion, x, polymer volume, V_p and number of particles, N, in terms of the principal components,

Table 6-1

Principal Component Analysis

Covariance Matrix ($\Sigma = e(XX')$)

.00262						
.00319	.00599					
.00389	.00739	.01190				
.00392	.00927	.01530	.01567			
.00479	.00628	.00823	.02017	.01369		
.00591	.00768	.01008	.02666	.01697	.02756	
.00490	.00948	.01247	.01117	.02136	.03651	.05017

Eigenvalues

.00000	.00000	.00000	.00000	.00000	.00047	.11332

Eigenvectors - Principal Components

ℓ_1	ℓ_2	ℓ_3	ℓ_4	ℓ_5	ℓ_6	ℓ_7
-.06151	.41495	.46595	-.65030	.09896	.38961	-.14984
.27687	-.70562	-.28107	-.38511	.08227	.39713	-.18343
.09113	-.00188	.17180	.26773	-.083252	.38200	-.22689
-.77723	.07100	-.40112	.12274	.10923	.34886	-.28508
.55121	.47433	-.35354	.26956	.28379	.24135	-.36707
-.05056	-.31371	.60274	.39928	.37548	-.01016	-.48500
-.02782	.03836	-.15874	-.33161	-.23854	-.60375	-.66422

Percentage (%) of the Total Variation

.00024	.00029	.00083	.00277	.00355	.41313	99.57919

$$y_j = b_{jo} + \sum_{i=1}^{7} b_{ji} \underset{\sim}{\ell}_i' \underset{\sim}{a} + \underset{\sim}{e} \qquad (6.2)$$

where $\underset{\sim}{\ell}_i'$ denotes the i^{th} eigenvector in table 6-1, $\underset{\sim}{a}$ is a vector of seven absorbance values measured at time t, $\underset{\sim}{y}$ is a vector of $(x, V_p, N)'$ measurements, and $\underset{\sim}{e}$ is the error vector.

To select the regression model and estimate the b_{ij}'s coefficients a forward stepwise algorithm (RLSEP) was used. This routine computes entries for the standard analysis of variance table and other summary statistics. Optionally, selected variables, $\underset{\sim}{\ell}_i' \underset{\sim}{a}$, may be forced into the model, a lack of fit test may be applied, and/or a partial F-test for each selected model term may be performed. The stepwise selection algorithm is described in Efroymson (1960) and Draper and Smith (1966).

The seven independent variables used for the regression analysis were linear combinations of the absorbance values, $\underset{\sim}{\ell}_i' \underset{\sim}{a}$. The corresponding $\underset{\sim}{y}$ responses were obtained from experimental measurements (conversion, x, and polymer volume, V_p) and simulation results (number of polymer particles, N).

The significance level, for entering or deleting an independent variable was chosen to be .25. The selected regression models had as follows:

$$x = .0761 - (17.7716\underset{\sim}{\ell}_1' + 4.9973\underset{\sim}{\ell}_5' + 3.8029\underset{\sim}{\ell}_6' - .0761\underset{\sim}{\ell}_7')\ \underset{\sim}{a} \qquad (6.3)$$

$$V_p = .0160 - (4.0625\underset{\sim}{\ell}_1' + .9860\underset{\sim}{\ell}_5' + .8196\underset{\sim}{\ell}_6' + .0564\underset{\sim}{\ell}_7')\ \underset{\sim}{a} \qquad (6.4)$$

$$N = .1016\times10^{18} + (.1558\times10^{20}\underset{\sim}{\ell}_3' - .8064\times10^{19}\underset{\sim}{\ell}_5' + .1016\times10^{17}\underset{\sim}{\ell}_7')\ \underset{\sim}{a} \qquad (6.5)$$

The above regression models constitute actually the measurement equations as they will be used for the on-line control studies. However, it should be noted that when the significance level for entering an independent variable into the regression models is chosen to be 0.05, the $\underset{\sim}{\ell}_1$, $\underset{\sim}{\ell}_3$ and $\underset{\sim}{\ell}_5$ eigenvectors do not appeared in equations (6.3) to (6.5). This changes only slightly the predicted values.

Equations (6.3) to (6.5) can be recast into a state model as

$$\underset{\sim}{y} = H\underset{\sim}{L} + \underset{\sim}{e} \qquad (6.6)$$

where H is a (3x8) constant matrix, $\underset{\sim}{L}' = (1, \underset{\sim}{\ell}_1'\underset{\sim}{a},\ldots,\underset{\sim}{\ell}_7'\underset{\sim}{a})$ is a (8x1) vector and $\underset{\sim}{e}$ is a (3x1) error vector for the measurements.

The standard deviations of the residuals, the conversion and polymer volume models are .054 and .012 respectively, while the predicted values for the number of particles are less accurate. Experimental and predicted values are shown in Table 6-2 for some sample runs.

Predicted values seem to agree reasonably well with experimental results and follow adequately reactor variations. However, predictions for the number of polymer particles do not agree well with simulation results. This is due to two reasons. First, experimental values for N are not available and the simulated values might involve a large error. Second, the number of particles-time relationship is highly non-linear and a linear regression model is not likely to be adequate.

A quadratic model of the following form

$$x = b_0 + b_1L_1 + b_2L_2 + b_3L_1^2 + b_4L_2^2 + b_5L_1L_2 \qquad (6.7)$$

Table 6-2

Experimental Versus Predicted Values

	Experimental		Predicted	
Run	V_p	x	V_p	x
19	.1096	.4834	.0932	.4176
	.1035	.4518	.1000	.4426
	.0966	.4204	.0862	.3809
	.0989	.4298	.0872	.3836
	.1010	.4391	.0843	.3710
	.1015	.4414	.0915	.4021
27	.0961	.4637	.0848	.3814
	.1069	.4852	.1248	.5575
	.1042	.4601	.1220	.5400
	.0959	.4181	.0849	.3660
	.0558	.2407	.755	.3197
	.0656	.2829	.0513	.2067
	.0800	.3450	.0751	.3181
	.0737	.3175	.0670	.2857
	.0550	.2372	.0619	.2606
	.0639	.2755	.0626	.2622
	.0776	.3343	.0731	.3092
	.0789	.3402	.0760	.3221
28	.0237	.1148	.0149	.0708
	.0770	.3414	.0569	.2581
	.0775	.3393	.0649	.2936
	.0712	.3098	.0708	.3182
	.0587	.2543	.0663	.2950
	.0507	.2194	.0582	.2578
	.0522	.2258	.0586	.2591
	.0579	.2504	.0558	.2476

where $L_1 = \underset{\sim}{\ell}_7'\underset{\sim}{a}$ and $L_2 = \underset{\sim}{\ell}_6'\underset{\sim}{a}$ improved only slightly the predicted values.

It should be noted that the present analysis does not account for changes in absorbance values due to the particle size distribution, but it considers that the observed variations in absorbance are due only to changes in conversion, polymer volume and number of polymer particles. This, in fact, is not true and can explain some of the observed error between experimental and predicted values. However, it is intended that these equations be used for predictions only in the range of conversion, covered by the experimental data to which they fitted.

6.3 LEC Results

To monitor the latex particle growth and find the distributional form of the latex particle size distribution in the continuous emulsion polymerization of vinyl acetate, the LEC technique was employed. A description of the LEC system can be found in Singh's thesis (1977).

Typical LEC-chromatographs are shown in Figure 6-14. It should be noted that the unimodal chromatograph corresponds to a steady state conversion-time history in which there has been a continuous generation of particles, while the bimodal chromatograph indicates that two particle populations exist. The latter is consistent with the operation of the reactor under sustained oscillations. These conclusions are in agreement with electron microscopy results and predictions of the comprehensive model (Chapter 5).

The size of the polymer particles in emulsion polymerization at any time is calculated from the particle diameter-retention volume calibration

curve shown in Figure 6-15, in which the particle diameter versus the retention volume at which the peak of the chromatograph appears are plotted. This curve was obtained by injecting monodisperse latices with known diameters under similar operating conditions. Figure 6-16 shows the growth of the polyvinyl acetate particles measured by LEC. The corresponding conversion-time histories (Run-26(O), Run-27(Δ)) are shown in Figure 4-4. The observed decrease in the average particle diameter is due to the appearance of another class of particles of smaller size. This results in an overall decrease of the average particle diameter because the number of particles of the new class is significantly larger than the number of particles of the old class. Figure 6-17 shows the growth of polymer particles for steady-state reactor operation. The corresponding conversion-time histories (Run-19(Δ), Run-22(□)) are shown in Figure 4-3.

In Figure 6-18, polymer particle diameter is plotted against time for run-34. An improved set of columns was used for the analysis of the samples of run-34. These new set of columns actually increased the particle separation through the columns so that a bimodal particle size distribution resulted in a bimodal chromatograph. A second peak in the chromatograph appeared about 7 residence times after the polymerization started and was due to the appearance of a second class of particles. This is in agreement with simulation results of Chapter 5 which have shown a similar behaviour for the particle size distribution (Figure 5-34b). Finally, in Figures 6-19 and 6-20 predicted particle average diameters, $(\frac{6}{\pi} \cdot \frac{V_p}{N})^{1/3}$, (simplified model) are compared with the experimental

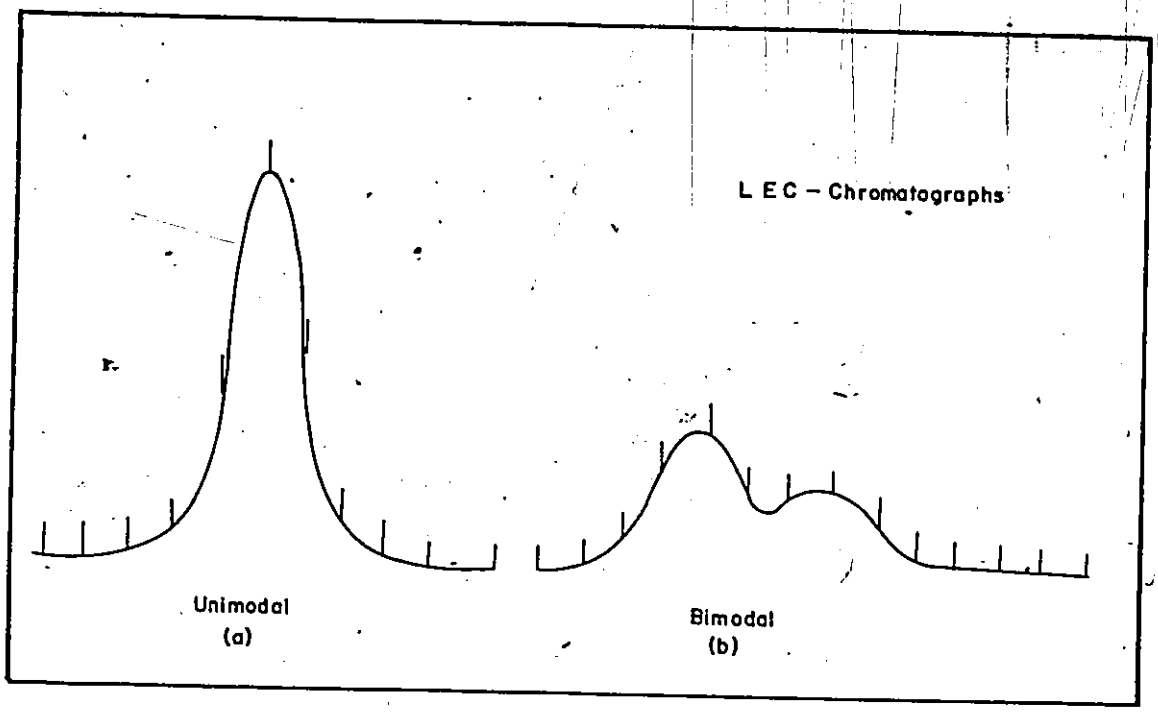

Figure (6-14) Typical LEC-chromatograms .

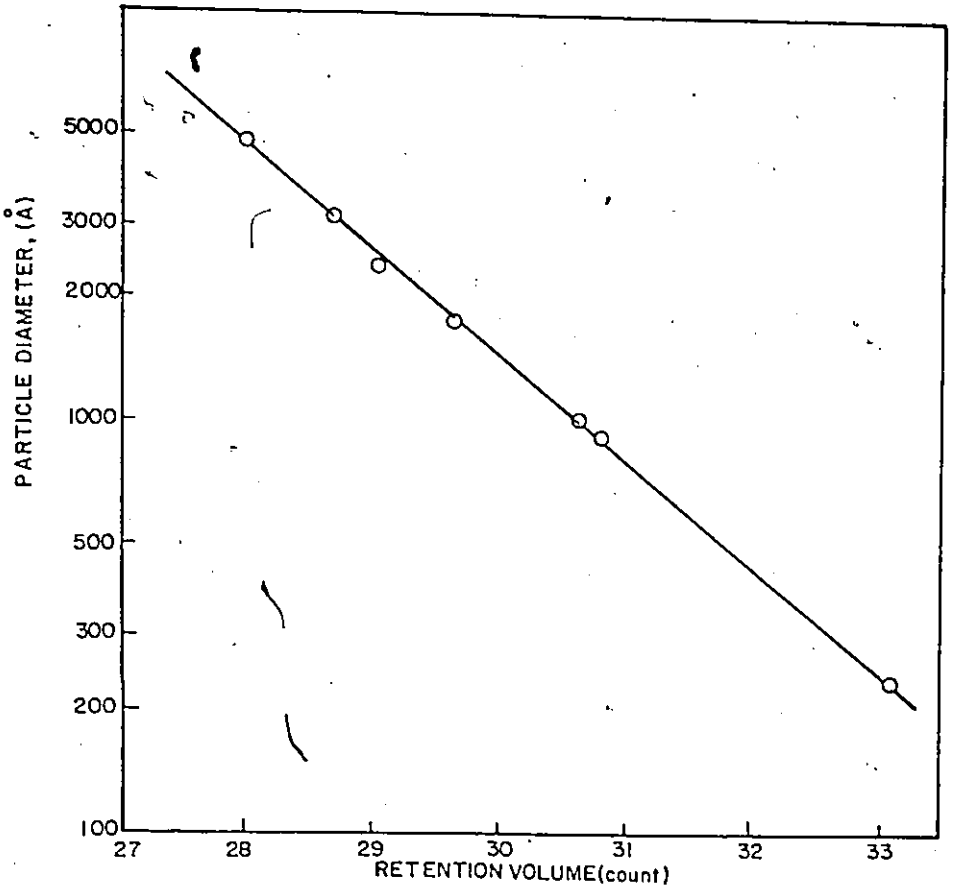

Figure (6-15) Particle Diameter-Retention Volume Calibration Curve

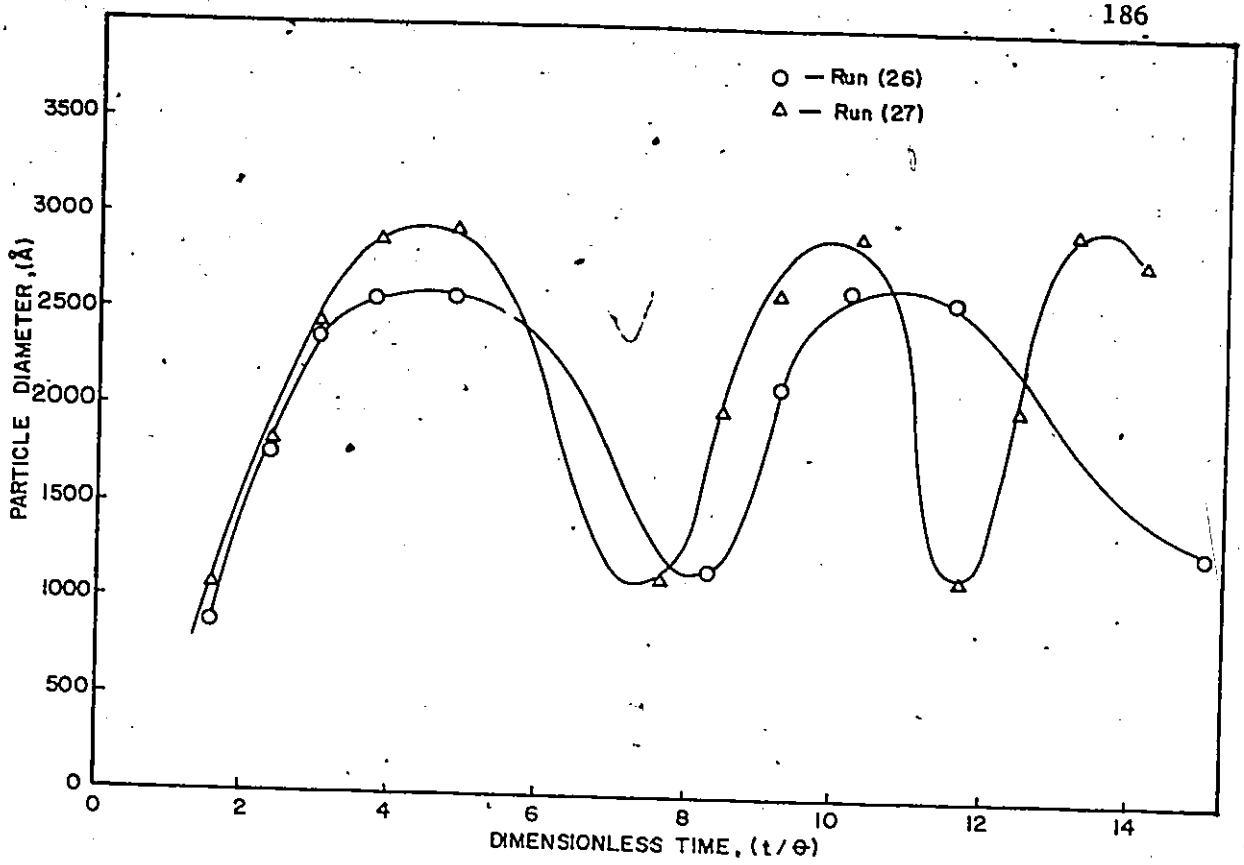

Figure (6-16) Measured Particle Diameter (LEC) versus Reaction Time (sustained oscillations

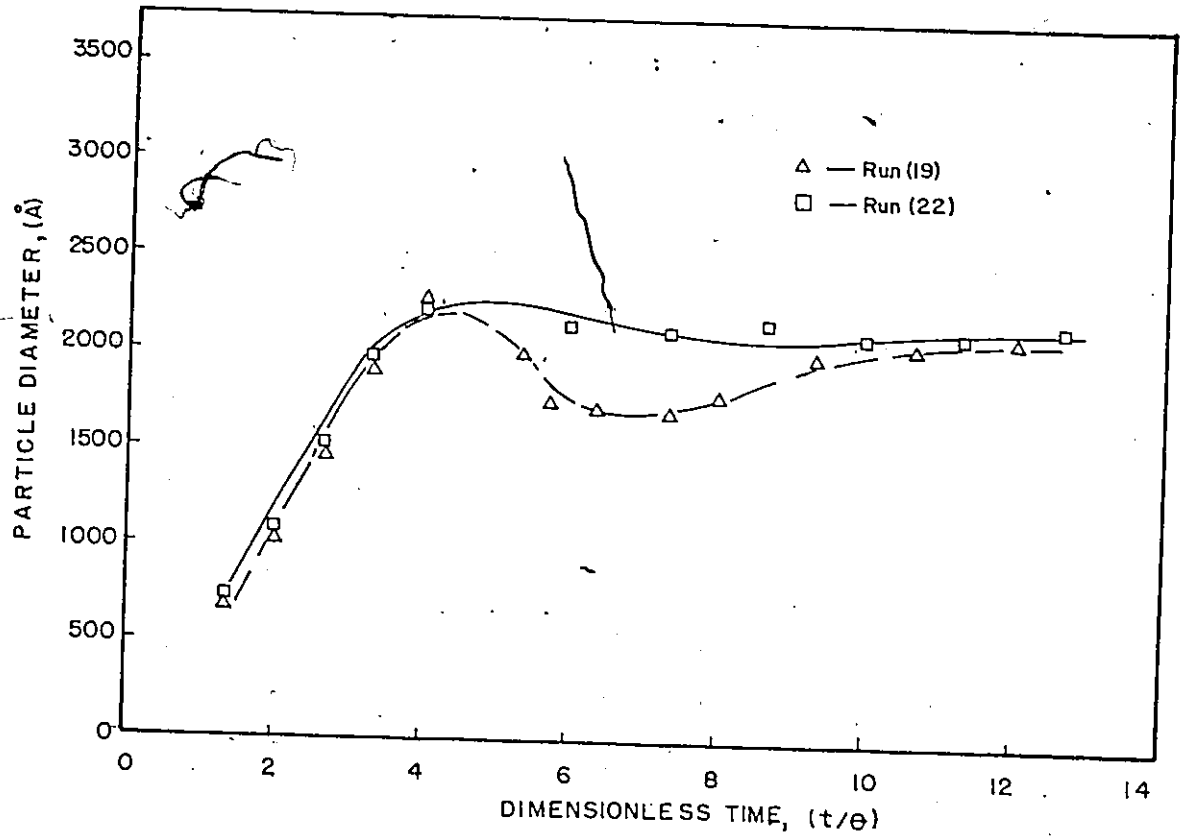

Figure (6-17) Measured Particle Diameter (LEC) versus Reaction Time (steady-state)

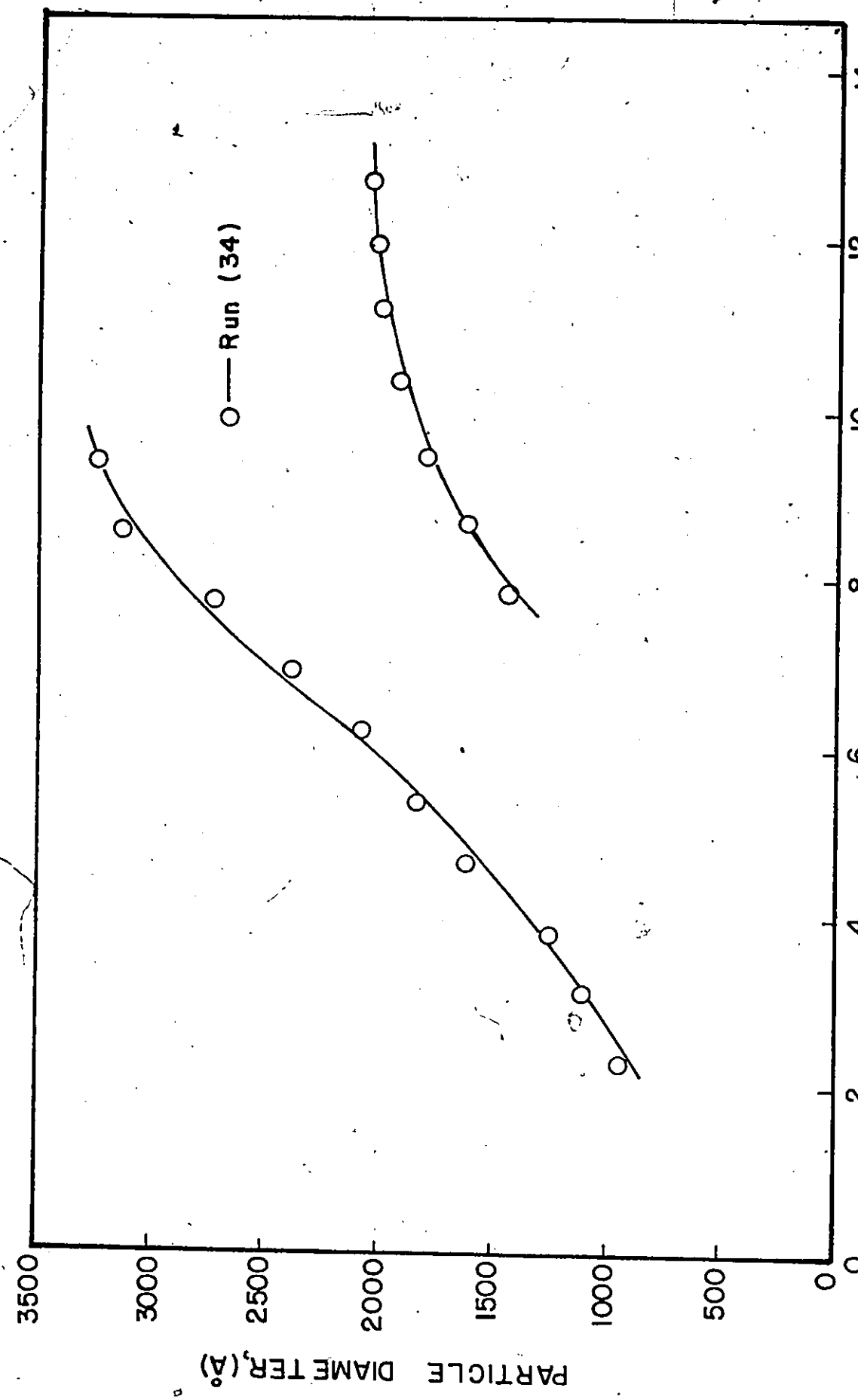

Figure (6-18) Measured Particle Diameter (LEC) versus Reaction Time (steady-state)

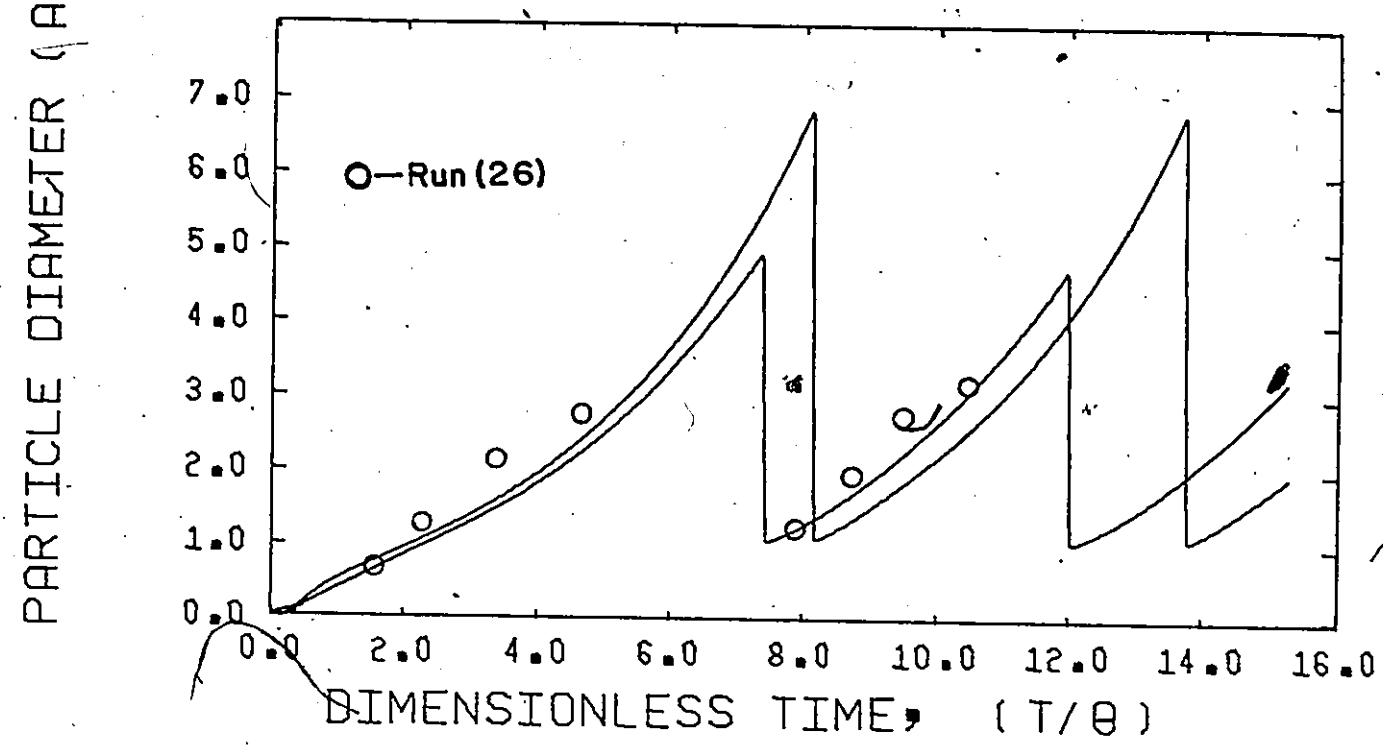

Figure (6-19) Predicted (simplified model) and Measured[4] (LEC) Particle Diameter versus Time

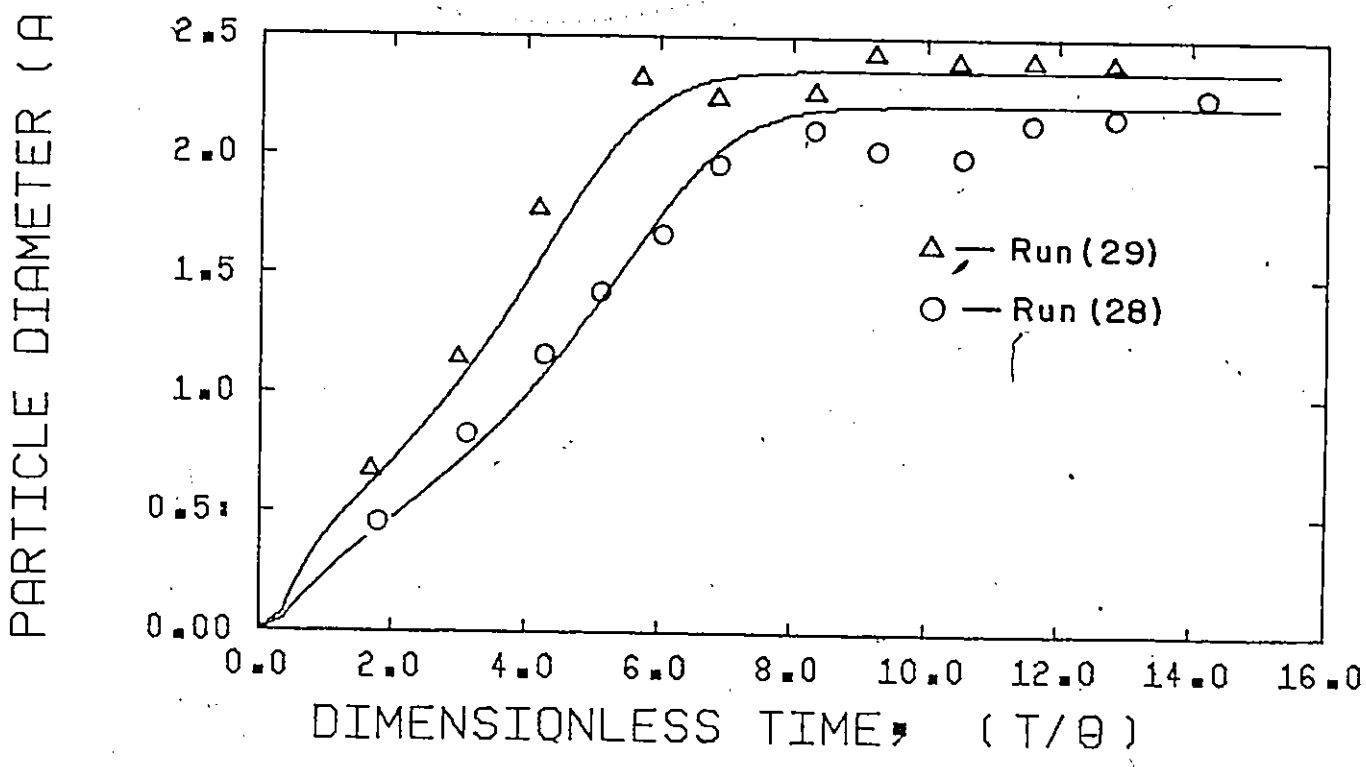

Figure (6-20) Predicted (Simplified Model) and Measured (LEC) Particle Diameter versus Time

measured diameters by LEC (peak position of chromatograph).

The point to note here is that no difficulty was experienced in analyzing the polyvinyl acetate latices which are rather soft compared to polystyrene latices. Moreover, the fine qualitative agreement of conversion-time and diameter-time histories demonstrates the usefulness of the LEC method and its great potential as an on-line technique.

6.4 Conclusions

Turbidity and LEC results were presented in this chapter. It was shown that both techniques can qualitatively follow reactor variations, and determine the induction time and extent of particle flocculation. Operation of reactor under sustained oscillations can produce bimodal particle size distributions which are easily detected by the LEC.

Turbidity measurements were also analysed by the methods of moments and principal components. Both techniques appear to give satisfactory results and they are able to follow quantitatively changes in weight average particle diameter, conversion, polymer volume and number of particles.

In chapter 7, the reactor model developed in section 2.5.2 and the measurement equations derived in this chapter are employed to study the dynamics and control of a continuous latex reactor for vinyl acetate.

CHAPTER 7

CONTROL STUDIES

7.1 Introduction

Many workers in the area of process control readily acknowledge that there is a wide gap between the theory of process control and its application to the chemical industry. Some contend that the theoreticians are far ahead of those who apply the theories and it is simply a question of catching up. A critical discussion on the state of modern control theory has been given by Jutan (1976).

Foss (1973) in his paper "Critique of Chemical Process Control Theory" presents a strong case against modern control theory and emphasizes the complex non-linear interactions present in a typical reaction system. Moreover, he points out that often it is not possible or economical to measure all the relevant variables of the system. Foss concludes by enumerating some central problems to be solved in applying modern control theory.

(1) A practical way of formulating low order models of large multivariable systems.

(2) What and how many variables should be measured, with how much accuracy, and how fast.

(3) What inputs should be manipulated.

(4) Parameter estimation in control studies and development of adaptive strategies to account for changing process variables.

(5) Formulation of meaningful control objective functions.

(6) Problems associated with applying present day multivariable control theory (which applies mainly to systems described by sets of ordinary differential equations) to systems described by partial differential or integro-differential equations.

These problems are discussed in the following sections in relation with the control of a continuous stirred tank latex reactor for vinyl acetate.

7.2 Control of Polymerization Reactors

Compared to optimal control of chemically simpler systems, there are few successful attempts at the control of polymer reactors. Two factors account for this.

(1) Polymer reactions are highly complex; therefore, it is difficult to formulate an adequate dynamic model of low order.

(2) The formulation of an adequate objective function for polymer reactor systems may not be easy, since it is difficult to measure on-line desired physical, chemical and mechanical properties of polymers. Therefore, there is a growing need for fast and accurate on-line measurements.

Fortunately, it is sometimes sufficient to characterize a polymer product by one or more of monomer conversion, number average and weight average molecular weight, or polydispersity, in which case only relatively

few equations and measurements need be considered.

In the past most attention has been given to the optimization of homogeneous polymer reaction systems in both batch and continuous reactors where a variety of objective functions have been utilized.

Rhee et al. (1968) investigated the start-up of a continuous reactor so as to maintain the same number average molecular weight and polydispersity as during steady state operation; whereas, Ray (1967), Hicks et al. (1969) and Osakada and Fan (1970) minimized weighted sums of squared deviations of conversion, number average molecular weight, and polydispersity from their respective specified terminal values. Yoshimoto et al. (1968) minimized the batch time to achieve a given monomer conversion. Nishimura and Yokoyama (1968) and Kwon et al. (1972) also minimized batch time to a given conversion, but subject to the added constraint of attaining a specified number average molecular weight. Similar optimal control strategies for semicontinuous reactors have also been studied by Beste and Hall (1966), Hoffman et al. (1964) and Shirotsuka and Terauchi (1972). In all cases the control variables considered were temperature, and initiator or monomer addition rate, or some combination of these.

Keyes and Kennedy (1974) applied an adaptive control technique for the control of suspension PVC production. First, they developed a non-linear process model and secondly derived a regulator from the model utilizing variational techniques and allowing for state dependent or time dependent values of the system coefficients. Recently, Jo and Bankoff (1976) both experimentally and by simulation studied the solution

polymerization of vinyl acetate in a CSTR. They used the Kalman filter in a variety of forms and a semi-empirical model for the measurement variables to obtain estimates of conversion and weight average molecular weight, which were then compared with results obtained through sample analysis. They concluded that simulation studies of Kalman filtering on complex systems with detailed descriptive equations may easily lead to overoptimistic conclusions. The Kalman filter used in the estimation of such processes was best justified when the model errors, by batch processing of experimental data, had been made comparable to the measurement errors. Hynn and Bankoff (1976) used a semi-empirical model for the kinetics of a vinyl polymerization reactor to obtain estimates of the performance of a linearized Kalman filter in early detection of on-line process drifts.

In a recent paper Amrehn (1977) reviews the present state of computer control in the polymerization industry and points out that marked process improvements are possible by application of advanced control concepts such as multivariable control, adaptive control and dynamic optimization.

7.2.1 Control of an Emulsion Polymerization Reactor

Normally, in the start-up of a single CSTR one observes an initial conversion overshoot followed by a long period of damped oscillations. Furthermore, in commercial reactor chains, oscillatory behaviour and excursions into very high conversion regions are usually unacceptable, and thus control and start-up policies require investigation. There are few publications in the area of continuous emulsion polymerization control.

Omi et al. (1969), Nomura et al. (1971), and Sautin and co-workers (1971) presented design equations which optimize reactor train efficiency by maximizing, with respect to reactor mean residence time, the number of particles produced at steady state in the first reactor.

Regulator control, to minimize the effects of process disturbances, has also been considered by some authors. Roquemore and Eddey (1961) developed a discrete deterministic model and implemented a feedback control scheme to regulate terminal conversion in a series of 9 to 12 continuous SBR emulsion polymerization reactors by changes in temperature and the number of reactors in the chain. Their control scheme resulted in a more uniform product and a significant increase in plant productivity. A similar feed-forward scheme for control of final product conversion in a train of continuous SBR reactors has been developed by Wismer (1965). The control is achieved by temperature manipulation in the latter reactors and utilizes a continuous conversion measurement within the train. The control scheme was developed in terms of difference equations which were suitable for implementation on a digital control computer and evaluated by a digital computer simulation. Fellows (1969) studied theoretically the regulator control of five, non-isothermal continuous SBR reactors in series where the feedstock was subject to random disturbances. He used a linearized form of Katz and Saidel's (1969) constant particle number model to minimize deviations of conversion and molecular weight from specified values using as manipulated variables the coolant flow, as well as initiator, modifier, and soap feed concentrations.

The optimal start-up control problem of emulsion polymerization reactor chains was theoretically investigated by Dickinson (1976) for styrene monomer. He developed numerical algorithms and applied them to the problem of achieving steady state conversion in the shortest possible time (i.e., the minimum time problem). Simulation results showed that a considerable reduction in start-up time to low steady state conversions without extended transient oscillatory behaviour or excessively large steady state conversion overshoots can be attained by application of an optimal soap start-up program which allowed particle generation at specific times only, in the first reactor of a chain. Minimum time solutions were found by solving a succession of minimum norm problems at specified final times by using techniques of functional analysis to reduce the dimensions of the problem.

Ahlberg and Cheyne (1977) implemented a computer control scheme on a full scale continuous solution polymerization process for the production of rubber. Some of the process model parameters were updated by an extended Kalman filter and control action was based on solution of the Ricatti equation. They emphasized the numerous practical problems that had to be overcome to produce a rugged system suited to the plant environment.

As in homogeneous polymerization reactions, reactor temperature, mean residence time, monomer concentration, modifier concentration, initiator and emulsifier concentrations, can be utilized as control variables.

Open-loop simulation studies were used to determine the effects

of initiator and emulsifier concentrations on the dynamic behaviour of our latex reactor. It was found that initiator concentration could be effectively used to change the steady-state conversion level, Figure 7-1. On the other hand, emulsifier concentration could affect the reactor operation (steady-state or oscillatory behaviour), Figure 7-2. These results indicate that initiator and emulsifier concentrations can be effectively utilized as manipulated variables to control the reactor performance. This is discussed next.

7.3 Suboptimal Stochastic Control of a Continuous Latex Reactor

With the availability of modern process control computers, the practical implementation of advanced control theory in the process industries is certainly a reasonable possibility. However, before an advanced control strategy can be developed, a mathematical model of the process is required which can accurately predict the response of the system to various control actions and can be solved in real time by a process control computer. Such a mathematical model has been derived in section 2.5 and tested extensively in Chapter 5. Moreover, in Chapter 6 measurement equations have been developed which can provide information about the model states from turbidity measurements. However, in a real application uncertainties arise because of imprecise knowledge of physical parameters such as ε, δ', k_p, k_d, D_w (see section 5.2.2), and by the presence of experimental measurement errors and other stochastic disturbances. Such a dynamic system which also contains elements of a

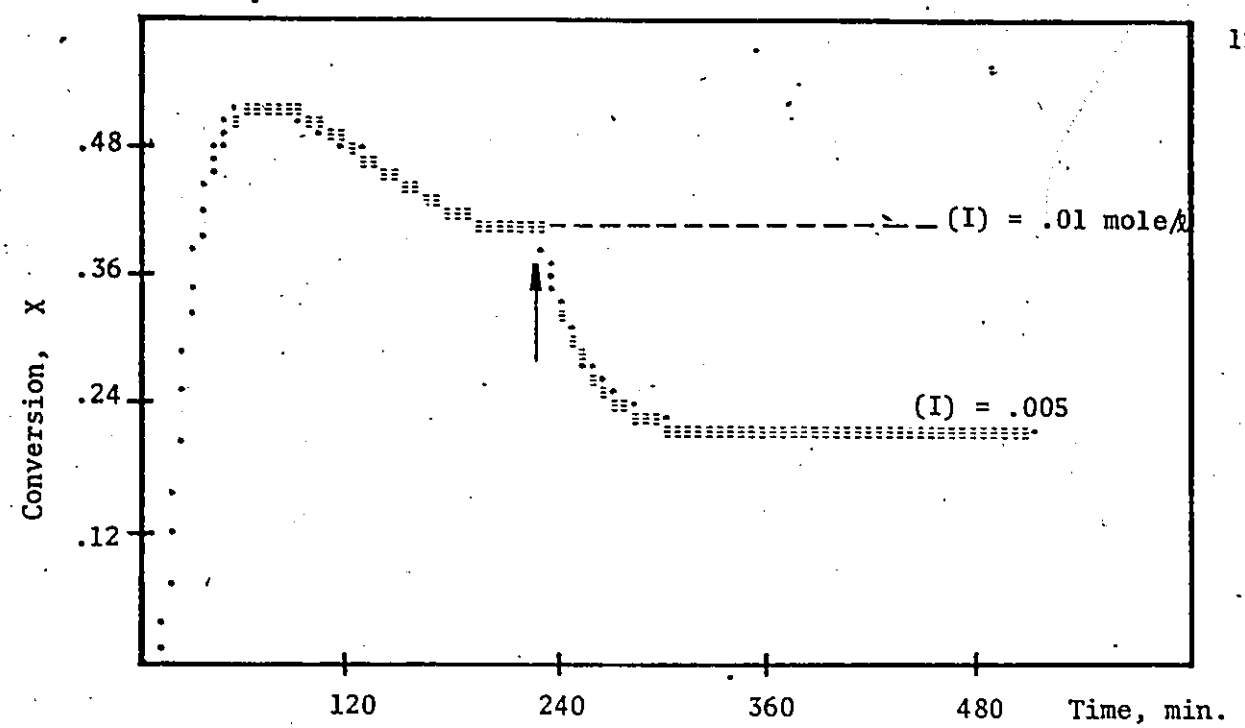

Figure (7-1) The Effect of Initiator Concentration on the Steady-State Conversion Level ((S) = .06 mole/ℓ-H_2O, T = 50°C, M/W = 4/10)

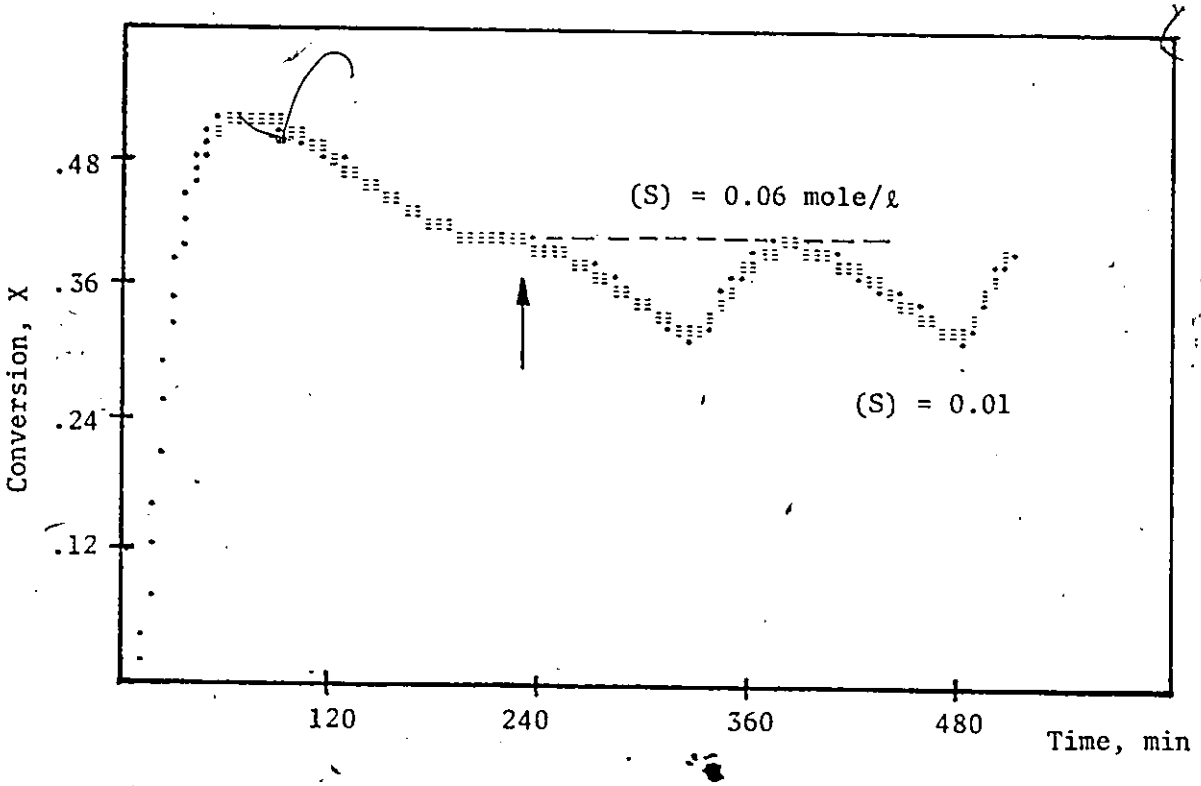

Figure (7-2) The Effect of Emulsifier Concentration on the Reactor Performance ((I) = .01 mole/ℓ-H_2O, T = 50°C, M/W = 4/10)

random or statistical nature is termed a stochastic system.

The optimal non-linear stochastic control problem has been formulated by Kushner (1964), (1965), but the resulting partial differential equations cannot be solved in general. The objective of this study is to consider practical on-line techniques for the approximate optimal control of the latex reactor subject to deterministic and stochastic disturbances to achieve one or more of the following process objectives:

(1) Optimal start-up control of a continuous emulsion polymerization reactor for vinyl acetate.

(2) Optimal change of operating production levels.

(3) Regulator control of conversion, to minimize the effects of process disturbances and of possible sustained oscillations.

Commercial production of poly-vinyl acetate in a CSTR is closely linked with solving the above control problems.

The optimal non-linear stochastic control can be formulated as follows.

System	$\dot{\underline{x}} = \underline{f}(\underline{x},\underline{u},\underline{k},t) + \underline{w}$	(7.1)
Observation	$\underline{y} = \underline{h}(\underline{x},t) + \underline{v}$	(7.2)
Performance index	$J = E\{\int_0^{t_f} F(\underline{x},\underline{u},t)dt\}$	(7.3)

where $\underline{x}$ is a (nx1) vector of state variables, $\underline{y}$ is a (mx1) vector of measureable output variables, $\underline{k}$ is a vector of system parameters and $\underline{w}$, $\underline{v}$ are the process and measurement noise vectors of (nx1) and (mx1) dimensions respectively. It is desired to choose the control variables $\underline{u}(t)$ (an (rx1) vector) to minimize J, where $E\{\cdot\}$ represents the expectation

operation. In the control of a deterministic system, it is possible to have $\underset{\sim}{u}(t)$ depend only on the initial state of the system and time, that is, open-loop control, or to have $\underset{\sim}{u}(t)$ depend on the correct state of the system, that is, feedback control. Only feedback control is possible in a stochastic system.

The solution of even the deterministic non-linear optimal control problem in terms of a feedback control law is not possible in general. Thus, it is necessary to consider approximate methods to determine a feedback control law. In section 7.3.1, a linearization technique is applied to the state model equations to obtain a linearized state space model, which is subsequently discretized to give an equivalent discrete system of equations. The Kalman filter theory (section 7.3.2) is then used to obtain state estimates for the system. Then, discrete linear quadratic control theory is used to formulate the control action at each time interval (section 7.3.3). After identifying the covariance matrices for the noise terms $\underset{\sim}{w}$ and $\underset{\sim}{v}$ in equations (7.1) and (7.2) the control algorithm is developed and tested in a series of sumulated control runs.

7.3.1 The Linearized-Discrete State Model

As developed in section (2.5), the state equations describing the ith generation of particles in a CSTR for the number of particles, N_i, the volume of particles, V_{pi}, and the conversion of particles, x_i are

$$\frac{dN_i(t)}{dt} = -\frac{N_i(t)}{\theta} + f(t) \qquad (7.4)$$

$$\frac{dV_{pi}(t)}{dt} = -\frac{V_{pi}(t)}{\Theta} + \frac{k_p d_m}{Nad_p}\Phi(t)\bar{q}_i(t)N_i(t) \qquad (7.5)$$

$$\frac{dx_i(t)}{dt} = -\frac{x_i(t)}{\Theta} + \frac{k_p d_m}{M_T M_W}\Phi(t)\bar{q}_i(t)N_i(t) \qquad (7.6)$$

When two or more particle generations have appeared in the reactor the total properties of the latex product at the exit of the reactor will be given by

$$x(t) = \sum_{i=1}^{q_t} x_i(t), \quad V_p(t) = \sum_{i=1}^{q_t} V_{pi}(t), \quad N(t) = \sum_{i=1}^{q_t} N_i(t) \qquad (7.7)$$

where q_t denotes the number of discrete particle generations which have appeared in the reactor and is taken to be equal to one for steady state reactor operation (i.e. continuous generation of particles). Equations (7.4) to (7.7) are highly coupled with the mass balance equations for initiator, emulsifier and monomer concentrations,

$$\frac{d[I]_w}{dt} = \frac{1}{\Theta}([I]_{feed} - [I]_w) - k_d[I]_w \qquad (7.8)$$

$$\frac{d[S]_T}{dt} = \frac{1}{\Theta}(S_F - S_T) \qquad (7.9)$$

$$\frac{dM_T}{dt} = \frac{1}{\Theta}(M_F - M_T) \qquad (7.10)$$

as well as with equations for the total rate of particle generation, $f(t)$, average number of radicals per particle, $\bar{q}$, monomer volume fraction, $\Phi(t)$, and total radical concentration in the water phase $[R]_w$.

It is clear that the normal variational approach in which a non-linear system of the form (7.1) is converted via Taylor Series to

$$\delta\dot{\underset{\sim}{x}} = \underset{\sim}{f}_x \, \delta\underset{\sim}{x} + \underset{\sim}{f}_u \delta\underset{\sim}{u} \tag{7.11}$$

or $$\delta\dot{\underset{\sim}{x}} = A(t)\delta\underset{\sim}{x} + B(t)\delta\underset{\sim}{u} \tag{7.12}$$

can not be easily employed for the linearization of the system of equations (7.4) to (7.7). Moreover, under a limit-cycle behaviour it is difficult to choose an operational steady state profile about which the model equations can be linearized. Therefore, instead of using the variational approach for linearization, we prefer to use a method proposed by Pearson (1962) and used successfully by Weber and Lapidus (1971) and McGreavy and Vago (1975).

The basis of this approach is the adoption of an instantaneously linearized time and state dependent model of the general form:

$$\begin{cases} \dot{\underset{\sim}{x}} = A(\underset{\sim}{x},\underset{\sim}{u},t)\underset{\sim}{x} + B(\underset{\sim}{x},\underset{\sim}{u},t)\underset{\sim}{u} \\ \underset{\sim}{x}(t_o) = \underset{\sim}{c} \end{cases} \tag{7.13}$$

$\underset{\sim}{x}$ and $\underset{\sim}{u}$ are the state and control vectors. A and B are general (nxm) and (nxr) system matrices found by estimation or mathematical linearization at a certain time. The selection of the coefficient matrices A and B is not unique and the following example briefly illustrates this method.

Equation (7.1) may be written for i = 1,2 and a single control u as

$$\dot{x}_i(t) = g_i(\underset{\sim}{x},u,t) + h_i(\underset{\sim}{x},u,t) + p_i(\underset{\sim}{x},u,t) \qquad (7.14)$$

with at least one term not zero. We now write equation (7.14) as

$$\dot{x}_i(t) = (\frac{g_i}{x_1})x_1 + (\frac{h_i}{x_2})x_2 + (\frac{p_i}{u})u \qquad (7.15)$$

where

$$\lim_{x_1 \to 0} |\frac{g_i}{x_1}| < \infty, \quad \lim_{x_2 \to 0} |\frac{h_i}{x_2}| < \infty, \text{ and } \lim_{u \to 0} |\frac{p_i}{u}| < \infty \quad (i=1,2) \qquad (7.16)$$

The coefficient matrices of the linearized system (7.13) would be

$$A = \begin{bmatrix} g_1/x_1 & h_1/x_2 \\ g_2/x_1 & h_2/x_2 \end{bmatrix} \quad \text{and} \quad B = \begin{bmatrix} p_1/u \\ p_2/u \end{bmatrix} \qquad (7.17)$$

By providing instantaneous state and control values, the dependence of A and B on $\underset{\sim}{x}$ and $\underset{\sim}{u}$ can be eliminated to yield A(t) and B(t). Note that this form of system rearrangement merely transforms the equations so that if $\underset{\sim}{x}$ and $\underset{\sim}{u}$ are specified the equations appear to be linear. Thus we refer to it as an apparent linearization.

Since the reactor is to be controlled directly by a digital computer, it will be more convenient to have a corresponding discrete state space model. Thus, if the structure of A and B can be established

by effectively factoring out $\underset{\sim}{x}$ and $\underset{\sim}{u}$ from the non-linear system of equations (7.4) to (7.7). A discrete system of equations can be obtained directly from the linearized continuous system (7.13). By treating equation (7.13) as a piecewise constant coefficient equation, that is by approximating $A(\underset{\sim}{x},\underset{\sim}{u},t)$ and $B(\underset{\sim}{x},\underset{\sim}{u},t)$ with $A(\underset{\sim}{x}(k+1), \underset{\sim}{u}(k), kT)$ and $B(\underset{\sim}{x}(k+1), \underset{\sim}{u}(k), kT)$, it may be solved directly to give (Noton (1972)),

$$\underset{\sim}{x}(k+1) = \Phi(k+1,k)\underset{\sim}{x}(k) + \Delta(k+1,k)\underset{\sim}{u}(k) \qquad (7.18)$$

where

$$\Phi(k+1,k) = \exp[A(\underset{\sim}{x}(k+1),\underset{\sim}{u}(k),k)T] \qquad (7.19)$$

and

$$\Delta(k+1,k) = B(k+1,k)\left[\int_0^T \exp(A[(k+1)T-t])dt\right] \qquad (7.20)$$

where T is the discrete time interval.

As expected, the method described is a function of the non-linearity encountered but generally gives remarkable correspondence. The linearization adopted has the advantage that a Lyapounov stability analysis can almost immediately be performed (Pearson (1962)).

The linearization and discretization methods described above can be applied to the reactor equations (7.4) to (7.7). First an instantaneously linear system is constructed in terms of the total properties (7.7). Then a discrete model is derived by estimating $\Phi(k+1,k)$ and $\Delta(k+1,k)$ matrices in terms of the A and B matrices.

The control variables, u, chosen for this study are the initiator and emulsifier concentrations in the reactor. Earlier simulation studies showed (Figures 7-1, 7-2) that these variables could change the production level and reactor performance (oscillatory or steady state). They can in turn be changed by proper manipulation of the corresponding feed rates. A more detailed discussion on this subject is given later in section 7.3.5. Thus, the system of equations (7.4) to (7.7) can be written

$$\begin{bmatrix} \dot{N} \\ \dot{V}_p \\ \dot{x} \end{bmatrix} = \begin{bmatrix} -1/\Theta & 0 & 0 \\ 0 & -1/\Theta & 0 \\ 0 & 0 & -1/\Theta \end{bmatrix} \begin{bmatrix} N \\ V_p \\ x \end{bmatrix} + \begin{bmatrix} B_{11} & B_{12} \\ B_{21} & B_{22} \\ B_{31} & B_{32} \end{bmatrix} \begin{bmatrix} I \\ S \end{bmatrix} \quad (7.21)$$

where
$$B_{11} = f(t)/2I, \quad B_{12} = f(t)/2S$$
$$B_{21} = K_1\bar{q}N/2I, \quad B_{22} = K_1\bar{q}N/2S \quad (7.22)$$
$$B_{31} = K_2\bar{q}N/2I, \quad B_{32} = K_2\bar{q}N/2S$$

$$K_1 = \frac{k_p d_m \Phi}{N a d_p}, \quad K_2 = \frac{k_p d_m \Phi}{M_T M_W}$$

N, V_p, x, $\bar{q}$ are standing for the overall number of particles, polymer volume, conversion, and average number of radicals respectively and calculated by equation (7.7). The corresponding constant matrices of the discrete system are

$$\Phi(k+1,k) = [I_3]\, e^{-T/\Theta} \quad (7.23)$$

$$\Delta(k+1,k) = B \int_0^T e^{-(T-t)/\theta} dt = B\,\theta(1-e^{-T/\theta}) \qquad (7.24)$$

Therefore, the original non-linear system can be recast into an equivalent discrete system of which Φ and Δ matrices are given by equations (7.23) and (7.24) at each sampling interval.

Equation (7.21) satisfies the conditions (7.16) since the total initiator and emulsifier concentrations in the reactor can not be zero. Moreover, the established structure for A and B considerably facilitates the analytical solution of the discrete matrices Φ and Δ (see equations (7.23) and (7.24)).

Simulation results obtained by an apparent linearization and subsequent discretization based on a 5 minute interval (equations (7.23) and (7.24)) are in very good agreement with results obtained by solving the continuous non-linear equations (7.4) to (7.7), which indicates that the approach followed is reliable.

7.3.2 The Kalman Filter

The discrete Kalman filter has been derived in several ways (Sage and Melsa (1971), Jazwinski (1970)) and only the final equations will be given here.

The Kalman filter is an optimal estimator of the state vector $\underline{x}$ (in a Bayesian or a minimum mean squared error sense) based on the information available at the current time y_t. If observability conditions are satisfied, it is possible to obtain optimal estimates of unmeasured

state variables. In the Kalman filter the estimate of the state at any instant is a weighted sum of the extrapolated past estimate and the information from the new observations.

Consider the general dynamic-stochastic model

$$\underset{\sim}{x}(k+1) = \Phi(k+1,k)\underset{\sim}{x}(k) + \Delta(k+1,k)\underset{\sim}{u}(k) + \underset{\sim}{w}(k) \qquad (7.25)$$

$$\underset{\sim}{y}(k) = H(k)\underset{\sim}{x}(k) + \underset{\sim}{v}(k) \qquad (7.26)$$

where as before, $\underset{\sim}{x}(k)$ is an (nxl) state vector, $\underset{\sim}{y}(k)$ is an (mxl) vector of observed outputs and $\underset{\sim}{u}(k)$ is an (rxl) vector of input variables. $\underset{\sim}{w}(k)$ and $\underset{\sim}{v}(k)$ are white Gausian noise vectors with zero mean and covariances,

$$E[\underset{\sim}{w}(k)\underset{\sim}{w}(k)'] = R_W$$

$$E[\underset{\sim}{w}(k)\underset{\sim}{v}'(j)] = 0 \text{ for all } j$$

$$E[\underset{\sim}{v}(k)\underset{\sim}{v}'(k)] = R_V$$

For this model the conditional simultaneous and delayed state estimates are given by

$$\hat{\underset{\sim}{x}}(k+1/k+1) = \hat{\underset{\sim}{x}}(k+1/k) + K(k+1)\,[\underset{\sim}{y}(k+1) - H(k+1)\hat{\underset{\sim}{x}}(k+1/k)] \qquad (7.27)$$

$$\hat{\underset{\sim}{x}}(k+1/k) = \Phi(k+1,k)\hat{\underset{\sim}{x}}(k/k) + \Delta(k+1,k)\underset{\sim}{u}(k) \qquad (7.28)$$

The covariance matrices of the state estimates are given respectively by

$$P(k+1/k+1) = P(k+1/k) - K(k+1)H(k+1)P(k+1/k) \tag{7.29}$$

$$P(k+1/k) = \Phi(k+1,k)P(k/k)\Phi'(k+1,k) + R_w \tag{7.30}$$

The Kalman gain matrix K(k+1) which makes these estimates optimal (in the Bayesian or MMSE sense) is

$$K(k+1) = P(k+1/k)H'(k+1)[H(k+1)P(k+1/k)H'(k+1)+R_v]^{-1} \tag{7.31}$$

The steps involved in the practical implementation of the filter may be summarized as follows:

1. For k=0, the matrices A and B are evaluated with $\underset{\sim}{u}(t) = \underset{\sim}{u}(0)$, i.e., $A(\underset{\sim}{x}(1),\underset{\sim}{u}(0),0)$, $B(\underset{\sim}{x}(1),\underset{\sim}{u}(0),0)$. With these values of A and B, the dynamical equations can be put into the discrete-time form (7.25) by the method of equations (7.23) and (7.24). This may be looked upon as using the assumed control trajectory $\underset{\sim}{u}(0) = \underset{\sim}{u}(t)$ and then integrating the non-linear system of equations (7.4) to (7.10) over t=0 to t=T and then computing the value of $\underset{\sim}{x}(1) = \underset{\sim}{x}(T)$. Note that this procedure uses the apparent linearization to freeze the coefficient matrices in the dynamical equations over the sampling interval.

2. Calculate $\hat{\underset{\sim}{x}}(k+1/k)$ and P(k+1/k) from equations (7.28) and (7.30). These are the a priori estimates of $\underset{\sim}{x}(k+1)$ and P(k+1) at t_k.

3. Calculate the Kalman gain matrix K(k+1) from equation (7.31), where the matrices H and R_v come from the measurement equations and their

noise properties (in our case, H is equal to identity matrix and R_v is a diagonal constant matrix).

4. Once the measurement $\underset{\sim}{y}(k+1)$ is available at time $t = t_{k+1}$, calculate a posteriori estimates $\hat{\underset{\sim}{x}}(k+1/k+1)$ and $P(k+1/k+1)$ from equations (7.27) and (7.29).

5. Increment k by 1, go back to step 1 and repeat.

7.3.3 Linear-Quadratic Stochastic Feedback Control

The design of constrained feedback controllers for linear, discrete, state space systems with constant coefficient matrices Φ, Δ; is well known (Noton (1972), MacGregor (1973), Lapidus and Luus (1967), Aström (1970)). Analytical solutions to the general problem are available for systems which can be formulated with a quadratic performance criterion or objective function.

Consider the linear discrete state space equations

$$\underset{\sim}{x}(k+1) = \Phi\, \underset{\sim}{x}(k) + \Delta \underset{\sim}{u}(k) + \underset{\sim}{w}(k) \qquad (7.32)$$

The linear-quadratic discrete control problem is defined as that sequence of discrete control policies $\underset{\sim}{u}(k)$, k = 0,1,2...N-1 which minimizes the performance index

$$J = E\left[\sum_{k=1}^{N} \{\underset{\sim}{x}'(k)Q\underset{\sim}{x}(k) + \underset{\sim}{u}'(k-1)R\underset{\sim}{u}(k-1)\}\right] \qquad (7.33)$$

where Q and R are (nxn) and (rxr) weighting matrices required to be symmetric and positive semidefinite. However, these results are based

on two simplifying assumptions.

(i) Φ and Δ are constant matrices

(ii) The state and control vectors can be expressed in deviation form, that is,

$$\delta\underset{\sim}{x}(t) = \underset{\sim}{x}(t)-\underset{\sim}{x}^{d}, \quad \delta\underset{\sim}{u}(t) = \underset{\sim}{u}(t)-\underset{\sim}{u}^{d} \tag{7:34}$$

where superscript d denotes the desired state of the system and in equation (7.33) has been implied that $\underset{\sim}{x}^{d} = 0$ and $\underset{\sim}{u}^{d} = 0$.

These assumptions are insufficient for our problem. In fact, we need to consider Φ and Δ matrices as functions of time. Furthermore, we cannot conveniently define the deviation state, $\delta\underset{\sim}{x}(t)$, and control, $\delta\underset{\sim}{u}(t)$, vectors for two reasons. Firstly, Φ and Δ are time dependent and secondly, it is difficult to define $\underset{\sim}{x}^{d}$ and $\underset{\sim}{u}^{d}$ trajectories for limit-cycle behaviour. In such cases, as Lapidus and Luus (1967) have noted, there is no work available regarding the linearized behaviour of a non-linear system with such peculiar but not unusual behaviour.

However, Weber (1969) has shown by an argument of mathematical induction that even when Φ and Δ are time varying the same recurrence equations, as for a constant case, can be applied to estimate the feedback control matrix, $L(t)$.

To account for the desired levels of the state and control vectors we define a new augmented state vector, $\underset{\sim}{z}$, in terms of state vector $\underset{\sim}{x}$ and the desired final values $\underset{\sim}{x}^{d}$ and $\underset{\sim}{u}^{d}$.

Therefore, for the case of time varying Φ, Δ, matrices and $\underset{\sim}{x}^d \neq \underset{\sim}{0}$, $\underset{\sim}{u}^d \neq \underset{\sim}{0}$, the linear-quadratic performance index corresponding to equation (7.33) becomes

$$J = E\left[\sum_{k=1}^{N} \{(\underset{\sim}{x}(k)-\underset{\sim}{x}^d)'Q(\underset{\sim}{x}(k)-\underset{\sim}{x}^d) + (\underset{\sim}{u}(k-1)-\underset{\sim}{u}^d)'R(\underset{\sim}{u}(k-1)-\underset{\sim}{u}^d)\}\right] \tag{7.35}$$

Considering an augmented vector, $\underset{\sim}{z}$,

$$\underset{\sim}{z}(k) = (\underset{\sim}{x}(k), \underset{\sim}{x}^d, \underset{\sim}{u}^d)' \tag{7.36}$$

the state space equations (7.25) can be written in terms of the new vector $\underset{\sim}{z}$ as

$$\underset{\sim}{z}(k+1) = \begin{bmatrix} \Phi(k+1,k) & 0 & 0 \\ 0 & I_3 & 0 \\ 0 & 0 & I_2 \end{bmatrix} \underset{\sim}{z}(k) + \begin{bmatrix} \Delta(k+1,k) \\ 0_3 \\ 0_2 \end{bmatrix} \underset{\sim}{u}(k) + \begin{bmatrix} I \\ 0_3 \\ 0_2 \end{bmatrix} \underset{\sim}{w}(k) \tag{7.37}$$

where $\underset{\sim}{x}^d(k+1) = \underset{\sim}{x}^d(k)$; $\underset{\sim}{u}^d(k+1) = \underset{\sim}{u}^d(k)$ and I_3, I_2 are identity matrices. The performance index (7.35) can then be written

$$J = E\left[\sum\{\underset{\sim}{z}'(k)Q_1\underset{\sim}{z}(k) + \underset{\sim}{u}'(k-1)Q_2\underset{\sim}{u}(k-1) + \underset{\sim}{z}'(k)V'\underset{\sim}{u}(k-1) + \underset{\sim}{u}'(k-1)V\underset{\sim}{z}'(k)\}\right] \tag{7.38}$$

where Q_1 and Q_2 are symmetric positive semi-definite matrices given as

$$Q_1 = [I_3,-I_3,O_2]'\, Q[I_3,-I_3,O] + [O_3,O_3,I_2]'R[O_3,O_3,I_2]$$

$$Q_2 = R \qquad V = R[O_3,O_3,-I_2] \tag{7.39}$$

This quadratic performance criterion is quite general and the solution to this problem is given by the recursive set of matrix equations (Astrom (1970)),

$$L(k) = [Q_2 + \Delta^{*\prime}(k,k-1)S(k+1)\Delta^*(k,k-1)]^{-1}\,[V+\Delta^{*\prime}(k,k-1) S(k+1)\Phi^*(k,k-1)] \tag{7.40}$$

$$S(k) = \Phi^{*\prime}(k,k-1)S(k+1)[\Phi^{*\prime}(k,k-1)-\Delta^*(k,k-1)L(k)] - V'L(k) + Q_1 \tag{7.41}$$

with initial $S(N) = Q_1$ and $k = N-1,\ldots,1$. In these equations $N = t_f/T$ where t_f is the final control time.

The optimal feedback solution to this problem is given by

$$\underline{u}(k) = -L(k)\hat{\underline{z}}(k/\tau) \tag{7.42}$$

where $\underline{u}(k)$ is the optimal control setting to be applied at time t_k, and $\hat{\underline{z}}(t/\tau)$ is the conditional expectation of the state vector

$$E[\underline{x}(k)/\underline{y}(\tau)] \quad \text{where } \underline{Y}'(\tau) = (\underline{y}(\tau),\underline{y}(\tau-1), \ldots, y(0))$$

represents the data available for determining the control action. L(k) is a constant feedback control matrix given by the solution of recursive equations (7.40) and (7.41). The state estimator $\underset{\sim}{z}(k/\tau)$ can be obtained from the appropriate Kalman filter given previously.

This result implies that the optimal strategy can be separated into two parts: a state estimator for obtaining the best estimate of the state variables, and a linear feedback law which operates on the estimated state, both of which may be calculated independently of the other. This important result is referred to as the separation theorem or certainty equivalence principle, and results because we have assumed a linear system with Gaussian inputs and have minimized a quadratic cost function.

One special case is also of interest. When N becomes large and Q_1 and Q_2 have the properties mentioned above, it is possible to show that $\lim_{N\to\infty} L(k) = L_\infty$, a constant matrix. In this case the optimal feedback equation becomes merely

$$\underset{\sim}{u}^o(k) = -L_\infty \underset{\sim}{\hat{z}}(k/T) \qquad (7.43)$$

The arrangement of such a controller and estimator is represented in Figure 7-3. In deriving equations (7.36) to (7.39) in terms of the augmented vector $\underset{\sim}{z}$ it was considered that our objective was to control the reactor, so that a desired number of particles, polymer volume and

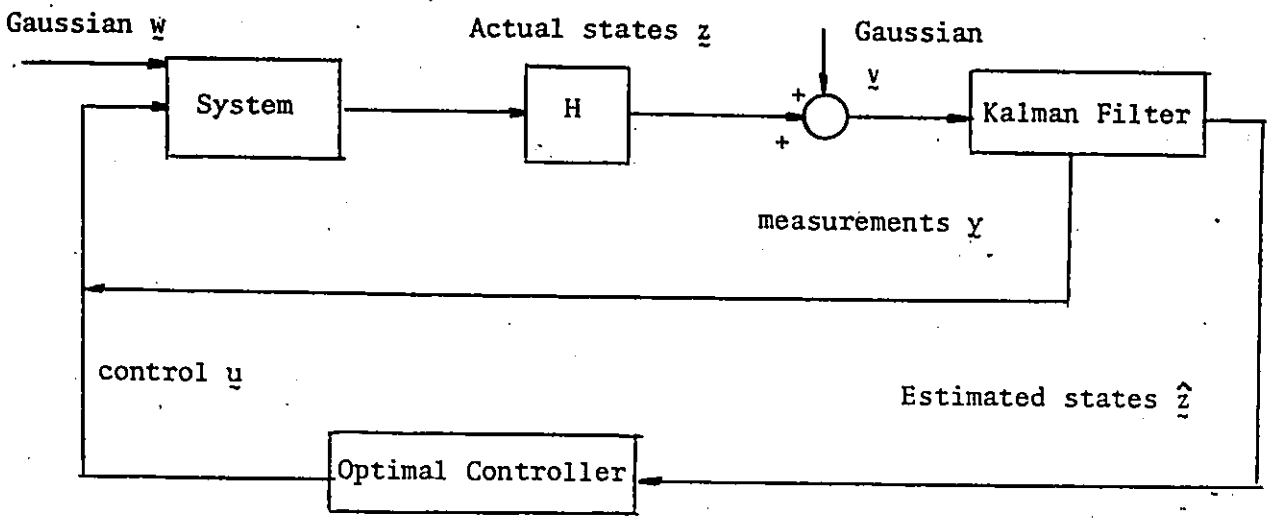

Figure 7-3 Stochastic Feedback Control by Means of the Separation Theorem.

conversion could be obtained. However, as discussed in section 6.2.2, it is more difficult to estimate the number of polymer particles at the present state of our modelling and our on-line measurements. Therefore, we will study the problem of controlling the reactor to a certain desired conversion for given desired initiator and emulsifier concentrations. Thus, the augmented vector

$$\underset{\sim}{z}'(k) = (\underset{\sim}{x}(k),\ x^d, I^d, S^d)$$

and the Q_1, Q_2, V matrices will be given as

$$Q_1 = \begin{bmatrix} q & 0 & 0 & -q & 0 & 0 \\ 0 & 0 & 0 & 0 & 0 & 0 \\ 0 & 0 & 0 & 0 & 0 & 0 \\ -q & 0 & 0 & q & 0 & 0 \\ 0 & 0 & 0 & 0 & r_1 & 0 \\ 0 & 0 & 0 & 0 & 0 & r_2 \end{bmatrix}, \quad V' = \begin{bmatrix} 0 & 0 \\ 0 & 0 \\ 0 & 0 \\ 0 & 0 \\ -r_1 & 0 \\ 0 & -r_2 \end{bmatrix} \quad Q_2 = \begin{bmatrix} r_1 & 0 \\ 0 & r_2 \end{bmatrix} \qquad (7.44)$$

It is clear that before any further control analysis, the covariance matrices R_v and R_w as well as suitable values for the matrices Q and R should be determined. This is done next.

7.3.4 Determination of R_v, R_w, Q, and R Matrices

In section 6.2.2 we discussed how seven measured turbidity values were used to provide measurements of the three model states. The measurement error $\underline{v}(k)$ in equation (7.26) can be approximated by the error, $\underline{e}$, resulting in equation (6.6) in fitting the model states as a function of turbidity measurements and choosing the covariance matrix R_v to be

$$R_v = \begin{bmatrix} \sigma_N^2 & 0 & 0 \\ 0 & \sigma_v^2 & 0 \\ 0 & 0 & \sigma_x^2 \end{bmatrix} \qquad (7.45)$$

To determine the filter gain matrix K from equations (7.27) to (7.31) both R_v and R_w are required. $\underline{w}(k)$ is often referred to as the "generation" noise and is difficult to interpret. For simplicity then (Jutan (1976)), it is assumed that $\underline{w}(k)$ can be approximated by specifying a covariance matrix R_w as a diagonal matrix

$$R_w = \beta R_v \qquad (7.46)$$

where β is a single parameter to be chosen. A similar idea was proposed by Hamilton et al. (1973) where the ratio between the diagonals of R_v and R_w determines the relative weight applied to the model against that applied

to the measurements in the state estimation. A large ratio of R_v to R_w caused the model's contribution to be emphasised in the state estimate while a small ratio caused the data to be emphasised.

Another way to identify and fit a noise model for a state space model from input-output data is to treat the residual vector $\underline{n}(k) = \underline{y}(k)_{\text{observed}} - \underline{y}(k)_{\text{predicted}}$ as the stochastic noise sequence and write the dynamic-stochastic model as

$$\underline{x}(k+1) = \Phi\underline{x}(k) + \Delta\underline{u}(k) \tag{7.47}$$

$$\underline{y}(k) = H\underline{x}(k) + \underline{n}(k) \tag{7.48}$$

In general, $\underline{n}(k)$ can be modelled by a multivariable linear autoregressive integrated-moving average (ARIMA) time series model (Box and Jenkins (1970), MacGregor (1973)) of the form

$$\phi(B)\nabla^d\underline{n}(k) = \theta(B)\underline{a}(k) \tag{7.49}$$

where $\phi(B)$ is a matrix autoregressive polynomial of back shift operator B, $\Theta(B)$ is a matrix moving average polynomial in B and $\underline{a}(k)$ is a white noise vector sequence with covariance matrix Σ.

However, many common stochastic disturbances are well approximated by an autoregressive process of finite order. For simplicity, we can consider a first order single variable noise model AR(1) to be identified from conversion measurements

$$n(k+1) = \phi n(k) + a(k+1) \tag{7.50}$$

where the estimate of ϕ is given by

$$\hat{\phi} = \frac{\Sigma e(k)e(k+1)}{\Sigma e^2(k)} \quad ; \qquad e(k) = x_{obs.} - x_{pred.} \tag{7.51}$$

and the variance of the white noise sequence a(k) is estimated by

$$\sigma_a^2 = \hat{\sigma}_x^2(1-\hat{\phi}^2); \quad \hat{\sigma}_x^2 = \frac{1}{N}\Sigma e^2(k) \tag{7.52}$$

If we define a new augmented vector $\underset{\sim}{x}^{*\prime}(k) = (\underset{\sim}{x}(k), n(k))$ then the system of equations (7.47) and (7.48) can also be represented in the form (7.25) and (7.26) as,

$$\underset{\sim}{x}^*(k+1) = \Phi^*\underset{\sim}{x}^*(k) + \Delta^*\underset{\sim}{u}(k) + \underset{\sim}{w}^*(k) \tag{7.53}$$

$$\underset{\sim}{y}(k) = H^*\underset{\sim}{x}^*(k) + \underset{\sim}{v}^*(k) \tag{7.54}$$

where

$$\Phi^* = \begin{bmatrix} \Phi & 0 \\ \hline 0 & \hat{\phi} \end{bmatrix}, \quad \Delta^* = \begin{bmatrix} \Delta \\ \hline 0 \end{bmatrix}, \quad H^* = [\,H \;\; 1\,] \tag{7.55}$$

$$\underset{\sim}{w}^*(k) = \begin{bmatrix} 0 \\ \hline 1 \end{bmatrix} a(k), \quad R_w = \begin{bmatrix} 0 & 0 \\ \hline 0 & \sigma_a^2 \end{bmatrix}, \quad \underset{\sim}{v}^*(k)=0, \quad R_{v^*}=0$$

For a multivariable noise model a least squares routine should be used to estimate the parameters of the equation (7.49). This problem is discussed extensively by Wilson (1970), Jutan, MacGregor and Wright (1977a,b).

The quadratic performance criterion (7.38) is quite general and includes the case of minimum mean square error control, that is Q = Identity matrix, subject to a constrain matrix R, on the variance of the manipulated variables. Therefore, in equation (7.44) q will be equal to one.

A satisfactory constraint matrix R may be chosen by calculating the variances of the outputs $\underline{y}$ and inputs $\underline{u}$ either analytically or by computer simulation. These variances should be jointly acceptable for a given R. For simplicity, R is chosen to be

$$R = \begin{bmatrix} r_1 & 0 \\ 0 & r_2 \end{bmatrix}$$

and the parameters r_1, r_2 are varied until a satisfactory combination of input-output variances is obtained.

7.3.5 Computer Control of a Latex Reactor (Flow Sheet)

A computer algorithm has been developed to study the regulator control problem of a continuous latex reactor. This includes a routine which solves the non-linear model, a routine for linearization and discretization, a Kalman filter and a routine which computes the optimal initiator and emulsifier concentrations.

A schematic diagram of the proposed control system is shown in Figure 7-4. Two separate feeds are fed into the reactor at constant rate by an MPL-micro duplex pump. One feed stream contains the total amount

of monomer, part of the recipe's total water and part of the emulsifier at a concentration, S_1. The other feed contains an initiator solution of concentration, I_1. However, these constant flowrate streams represent only a small amount of the total soap and initiator concentrations. The rest of the recipe's soap and initiator together with additional water are pumped through a set of two variable speed pumps. The flowrates of these two streams are actually the two control variables. By varying the r.p.m. of these two pumps the total initiator or emulsifier concentration in the reactor feed can be changed. However, because the concentrations of these two streams are very high (i.e. $I_2 = 5I_1$, $S_2 = 10S_1$), small changes in the flowrates around their steady-state values can easily change the total initiator and emulsifier concentrations in the feed without unduly upsetting the mean residence time of the reactor. This is necessary, since small changes of the mean residence time can drive the reactor far from the desired performance level. To see this consider the situation where one would like to increase the conversion in the reactor. An increase of the initiator flowrate may not accomplish the desired result if it were to simultaneously decrease the mean residence time of the reactor by too great an extent. Of course, the effect of residence time on the reactor performance could be eliminated or favourably exploited by adding a variable speed pump on the system to regulate the flowrate of the exit stream. This could definitely improve the ease with which the system could be controlled. Another alternative would be to choose the reaction temperature as our manipulated variable. Thus, by varying the temperature in the reactor we

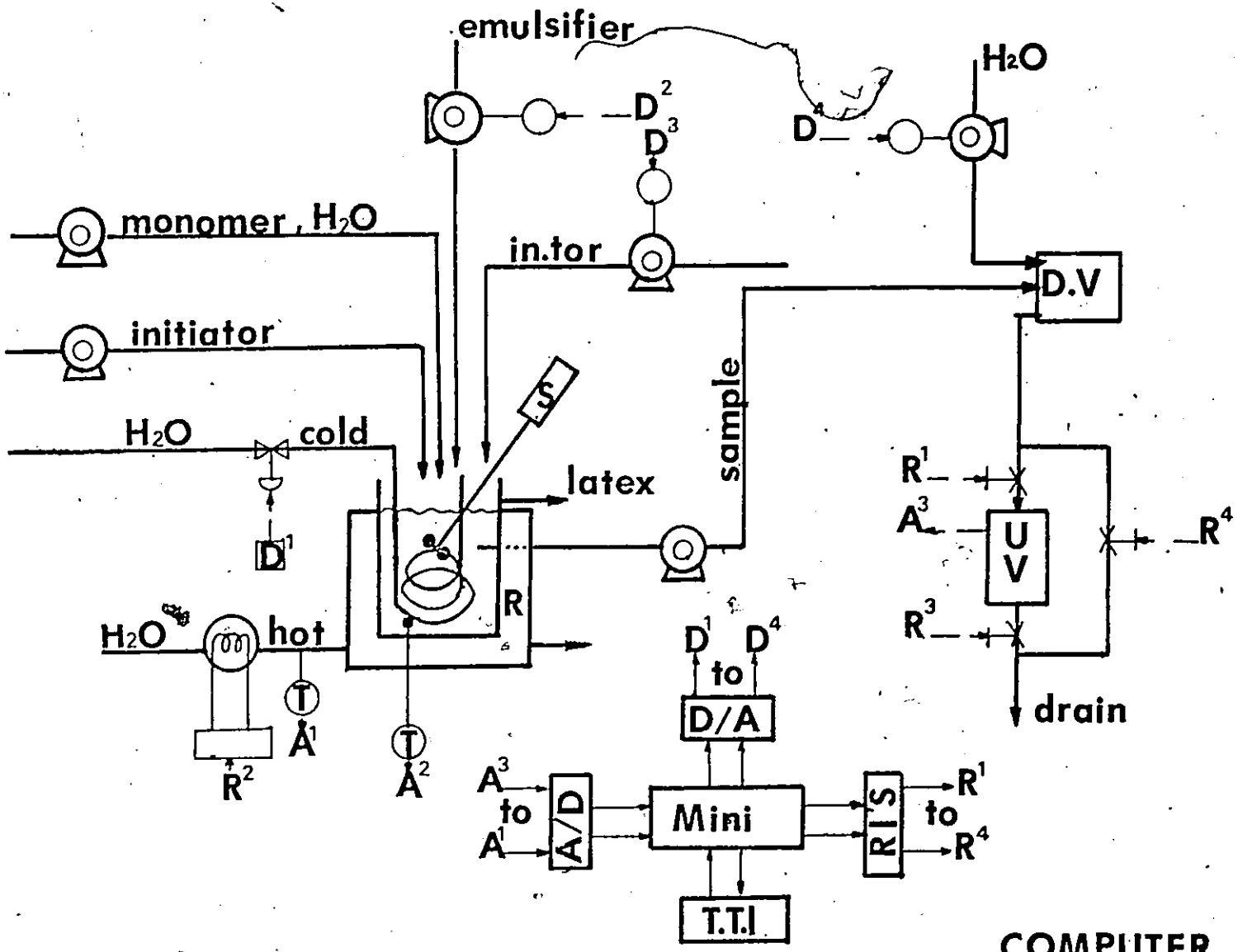

Figure (7-4) Schematic Diagram of the Proposed Control System

COMPUTER CONTROL OF A LATEX REACTOR

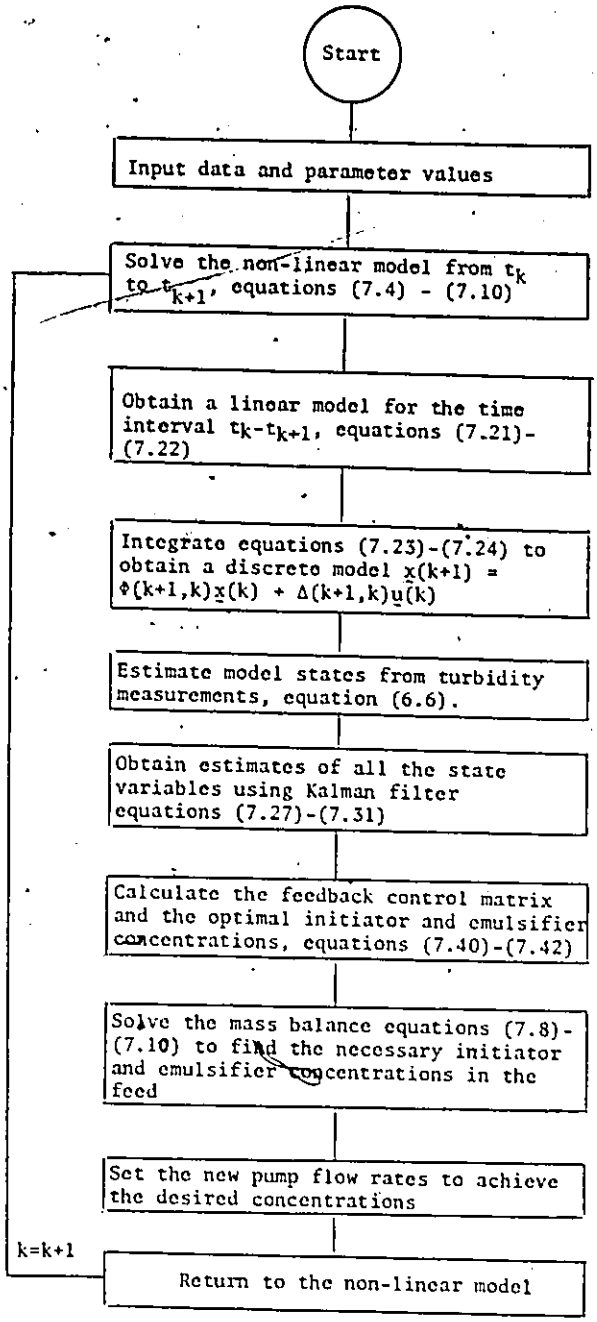

Figure 7-5 Suboptimal Stochastic Feedback Control of a Latex Reactor - Flow Chart.

could change the conversion without upsetting the mean residence time of the reactor. A flow sheet of the computer algorithm is presented in Figure 7-5.

7.4 Optimal Start-up Control of the Latex Reactor

Excursions into very high conversion regions and oscillatory behaviour are usually unacceptable in commercial reactors, and thus optimal start-up control of a latex reactor is highly desirable. The numerical algorithm developed in the previous sections is applied to the problem of achieving steady state conversion in such a way as to minimize the performance index (7.38). Simulation results are shown in Figures 7-6, 7-7 and 7-8. In Figure 7-6 deterministic and filtered conversion responses are plotted against time for different values of constraint parameter r. The desired steady state conversion value, x^d, was set equal to 42% and the desired emulsifier and initiator concentrations were $S^d = 0.06$ mole/ℓ-H_2O and $I^d = 0.01$ mole/ℓ-H_2O respectively. The constraint matrix R, in equation (7.35), was chosen to be

$$R = \begin{bmatrix} r & 0 \\ 0 & r \end{bmatrix} = rI_2 \qquad (7.56)$$

A satisfactory constraint, r is chosen by calculating the residual sum of sqaures for the conversion output $\sum_{i=1}^{N}(x_i - x^d)^2$, and emulsifier and initiator inputs, u,

$$\sum_{i=1}^{N}(S-S^d)^2, \quad \sum_{i=1}^{N}(I-I^d)^2$$

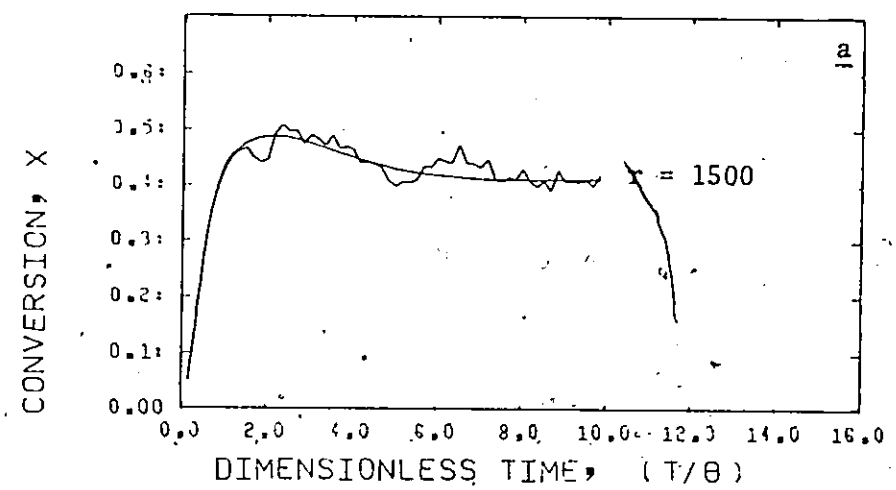

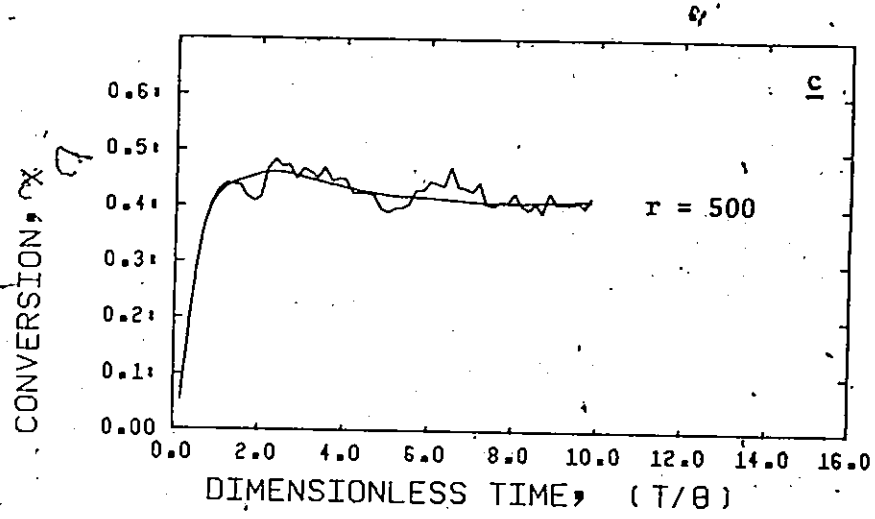

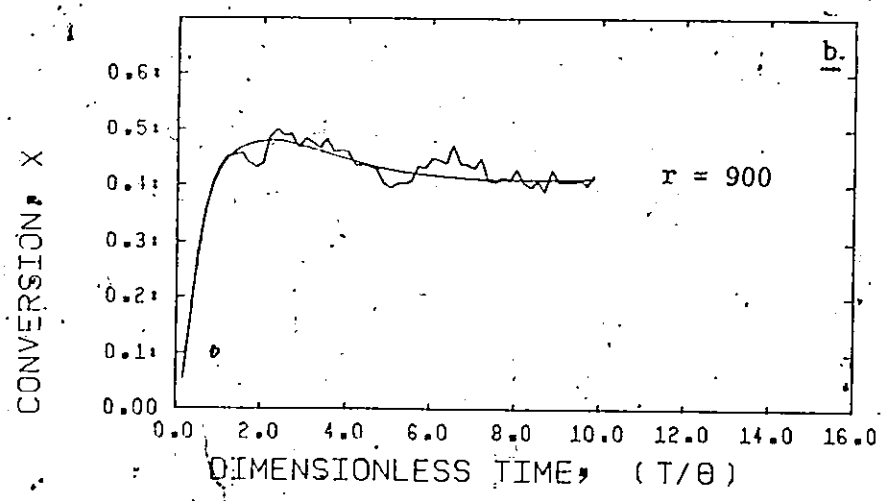

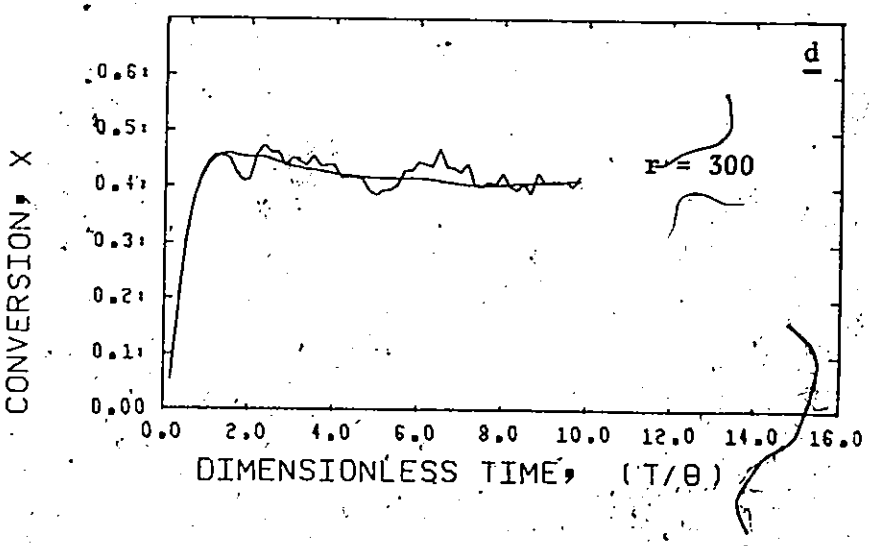

Figure (7-6) Start-up Control. Deterministic and Filtered Conversion Responses for Different Values of Parameter r.

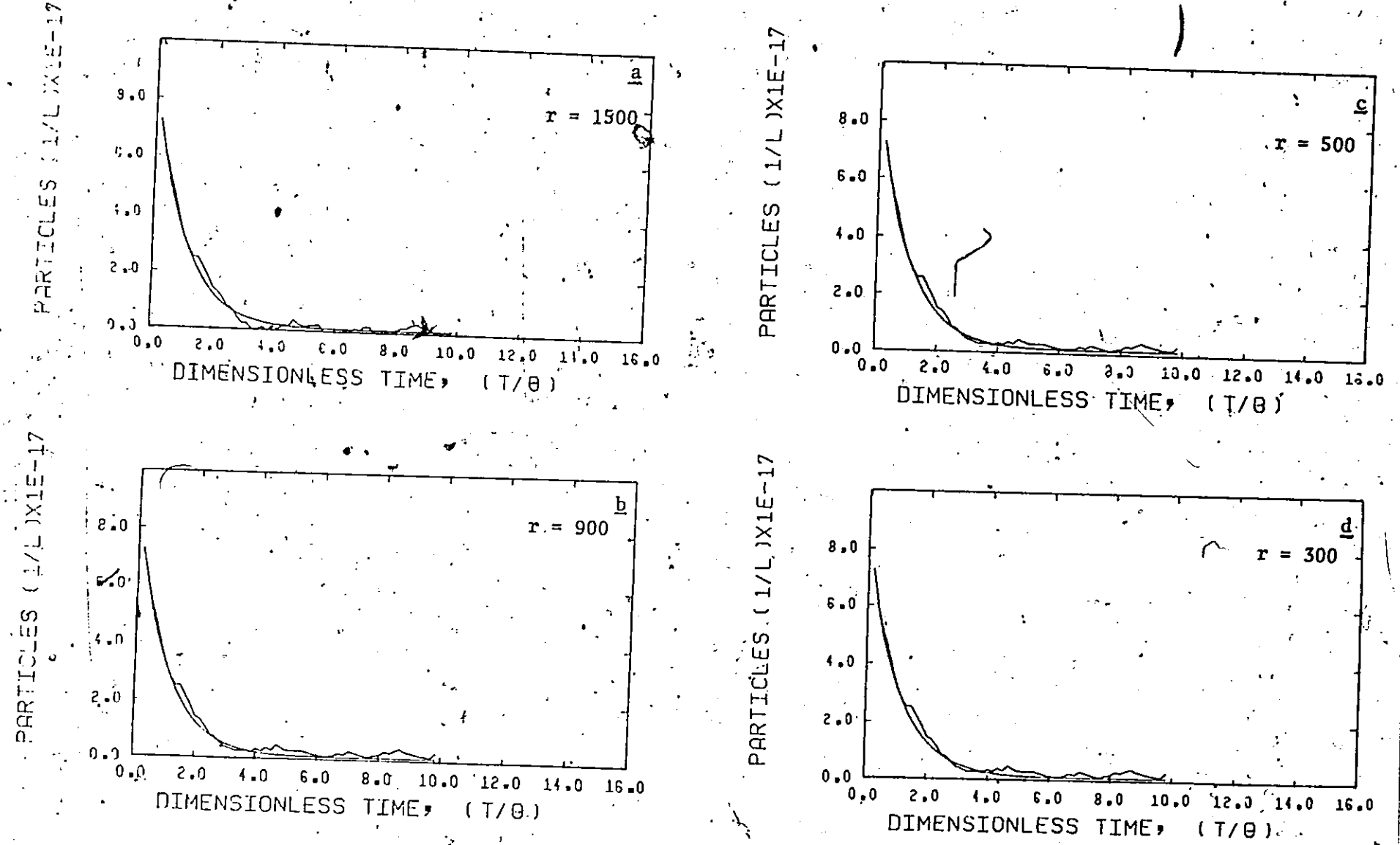

Figure (7-7) Start-up Control. Deterministic and Filtered Responses for the Number of Particles for Different Values of Parameter r.

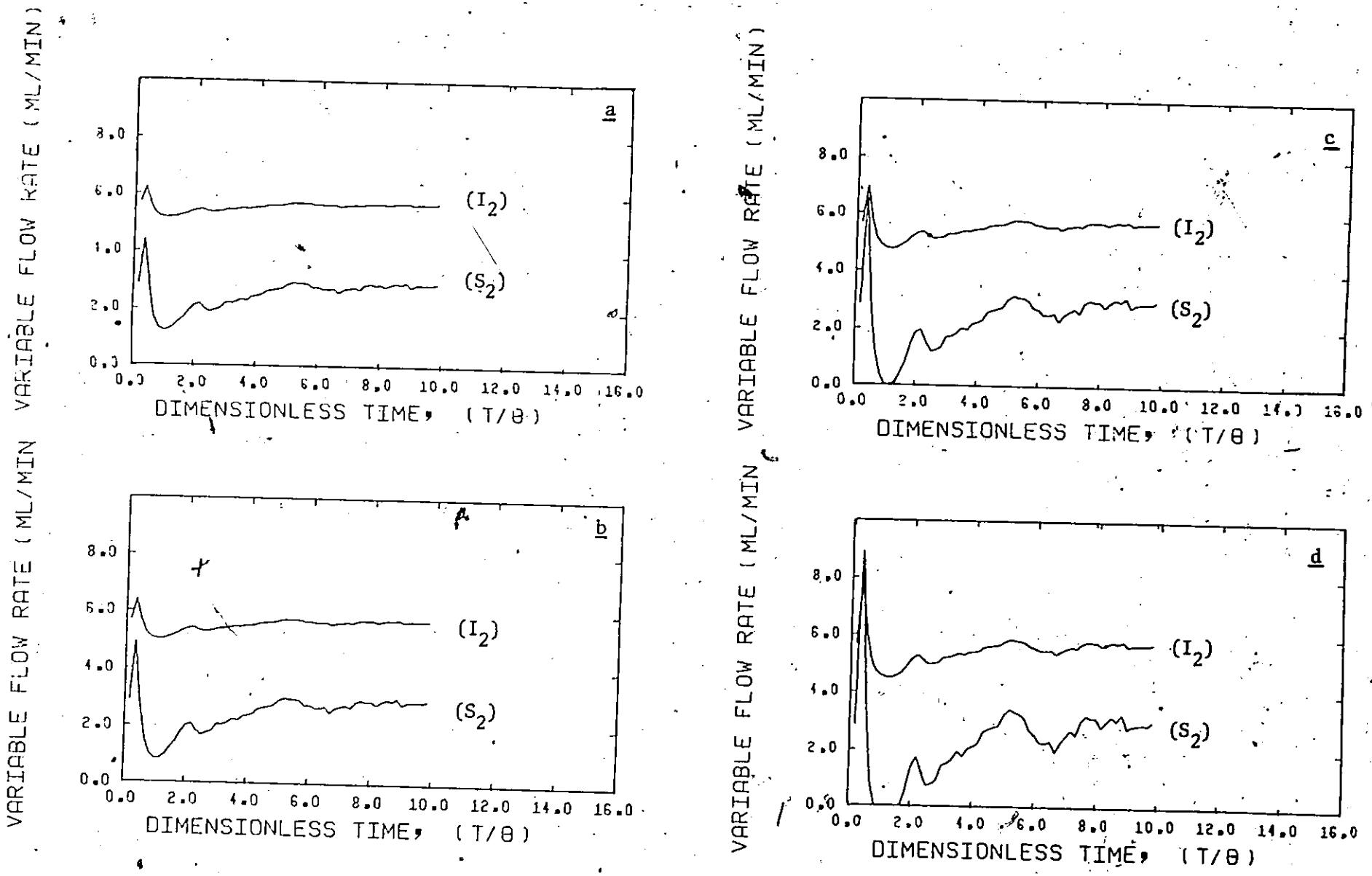

Figure (7-8) Start-up Control. Control Variables versus Time for Different Values of Parameter r (I_1 = 0 mole/ℓ-H_2O, I_2 = .05 mole/ℓ-H_2O, S_1 = .018 mole/ℓ-H_2O, S_2 = .18 mole/ℓ-H_2O)

It is interesting to note that as the value of parameter r is decreased (Figure 7-6) a faster output response is obtained. Thus, for r = 300 the steady-state conversion value is achieved in the shortest time with very small overshoot (Figure 7-6d). By comparing the results of Figure 7-6d with those of Figure 4-3 (uncontrolled) it can be seen that a considerable reduction in start-up time and conversion overshoot has been achieved. Corresponding deterministic and filtered responses of the total number of polymer particles are plotted in Figure 7-7 for different values of constraint r. In Figure 7-8 the control variables (emulsifier and initiator flowrates) are plotted against time. It can be seen that the control variables deviate more from their corresponding steady state values as the constraint r decreases, which is expected since the constraints on the manipulated variables are relaxed. Large changes in the manipulated variables occur at the start of the polymerization and they are due to the initially large nucleation rates. It is clear from the results presented in this section that reactor overshoots and long reactor transients can be easily regulated by applying our suboptimal control algorithm on the reactor.

7.5 Control of Reactor Sustained Oscillations

In this area there does not appear to be any publication in the open literature. This can be attributed to the following reasons.

(i) The lack of adequate dynamic models which can equally well predict the oscillatory and the steady-state behaviour of the latex reactor.

(ii) The lack of a linearization technique which will allow us to obtain a linear form of the non-linear model especially in the case in which the reactor operates under sustained oscillations.

However, as has been already shown, a satisfactory solution to these problems has been given in Section 7.3.1. For the regulatory control of latex reactors, it would be desirable to attain specified steady state values of conversion, to change in an optimal way the production level and to control or eliminate oscillations in the production rate. A successful solution to these problems can largely improve the quality of the commercially produced latices with obvious economical advantages. In what follows simulation results are presented which demonstrate the ability of our control algorithm to cope with the pathological behaviour (sustained oscillations) often occurring in continuous emulsion reactors.

In Figures 7-9, 7-10, and 7-11, simulation results are presented for conversion, number of polymer particles, and control variables. Under constant feed rate conditions, the reactor exhibits sustained oscillation up to the time (9 mean residence times) when regulatory control is applied and a steady-state reactor behaviour is obtained. However, the conversion does not attain its final steady-state value $x^d = .35$, since the new increased emulsifier flow rate results in an actual decrease of the mean residence and in a subsequent decrease of conversion according to Figure 4-6. It is believed that the reactor performance can be improved more if the mean residence time could be employed as a control variable.

Figures 7-12, 7-13 and 7-14 show the effect of the constraint

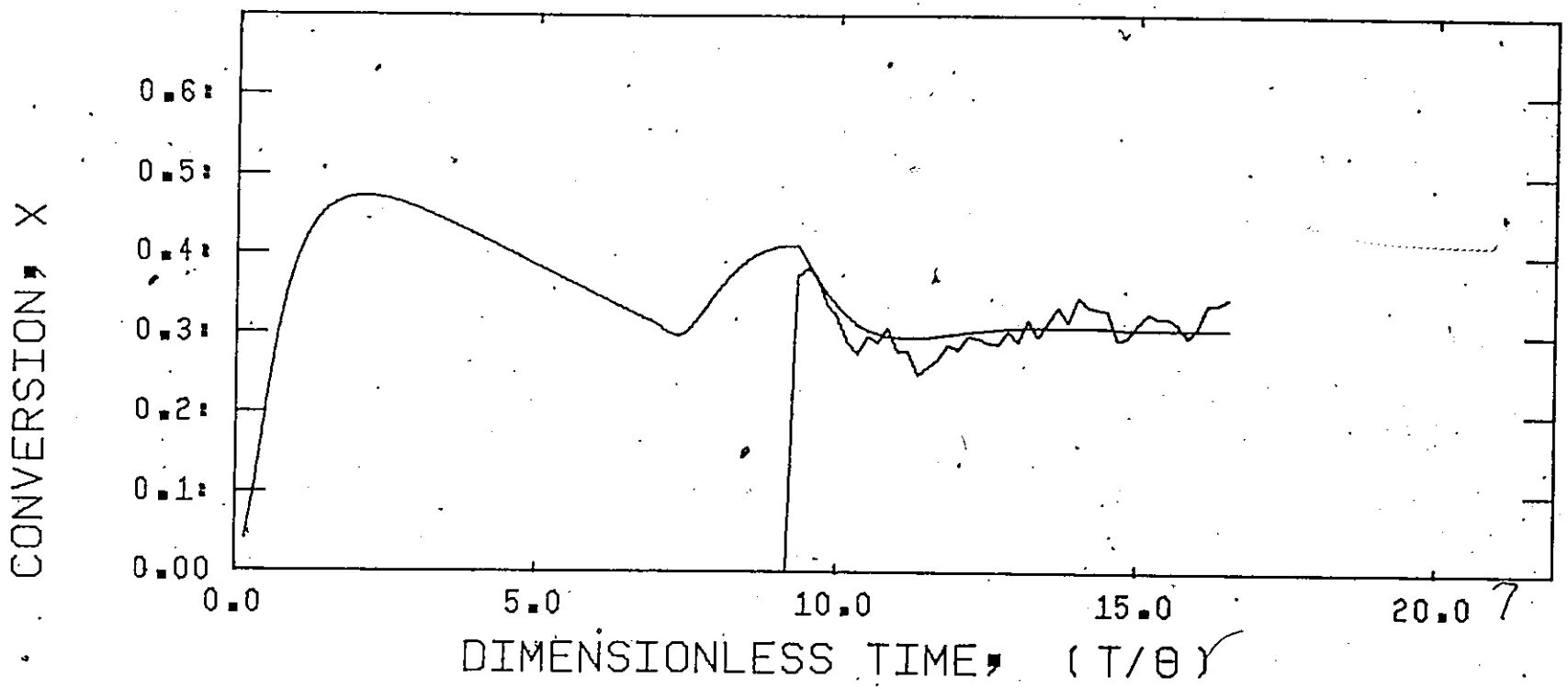

Figure (7-9) Control of Sustained Oscillations. Conversion-Time Histories.
(I^d = 0.01 mole/ℓ-H_2O; S^d = 0.03 mole/ℓ-H_2O)

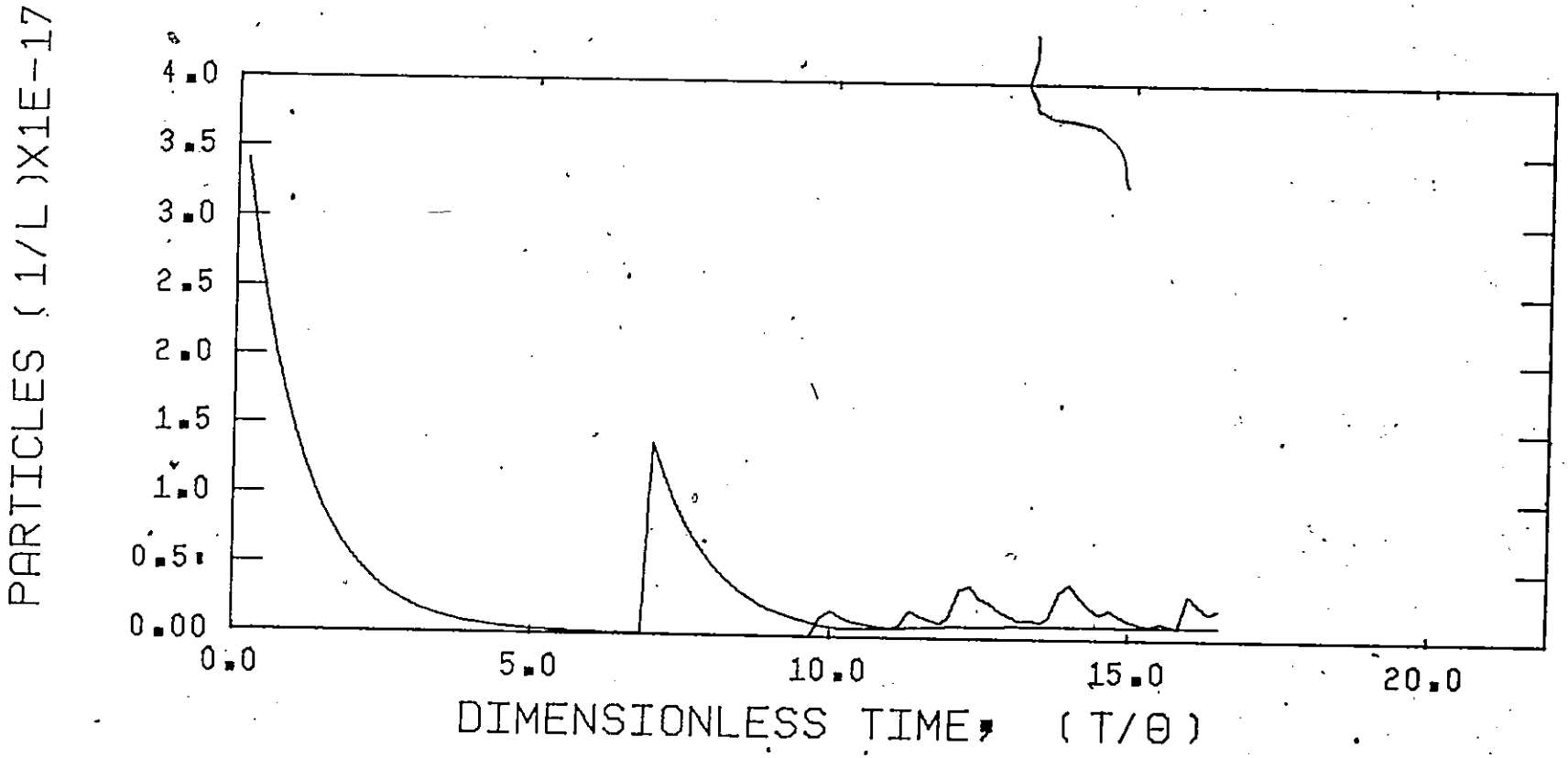

Figure (7-10) Control of Sustained Oscillations. Number of Particles versus Time (I^d = .01 mole/ℓ-H_2O, S^d = 0.03 mole/ℓ-H_2O)

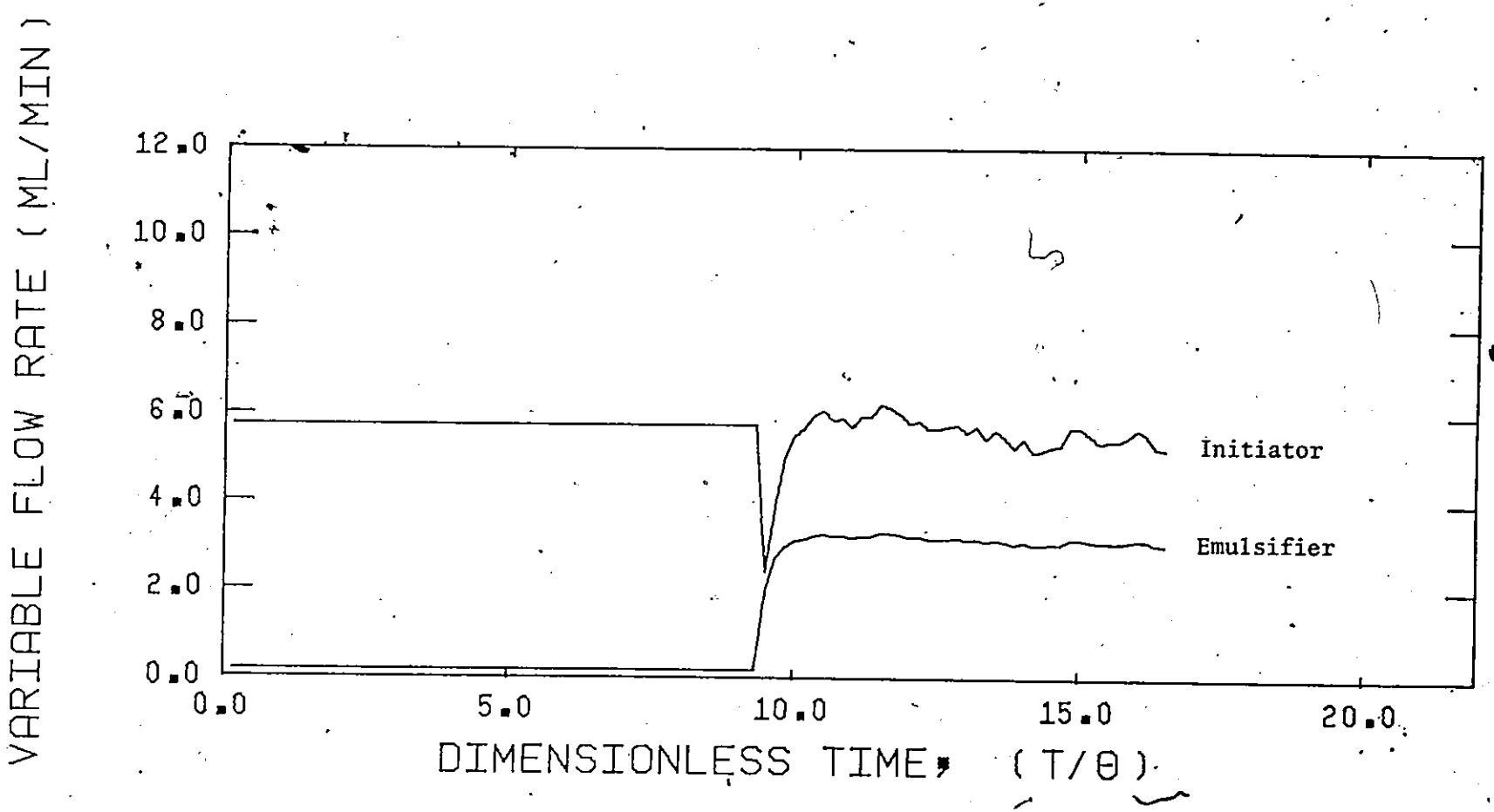

Figure (7-11) Emulsifier and Initiator Variable Flow Rates Versus Time (I_1 = 0, I_2 = .05 mole/ℓ-H_2O, S_1 = .018, S_2 = .18 mole/ℓ-H_2O)

matrix R on the reactor performance. Regulatory control is applied for both cases from the start of the reaction. The steady-state emulsifier concentration is equal to 0.01 mole/ℓ-H_2O and the corresponding initiator concentration is 0.01 mole/ℓ-H_2O. The steady-state mean residence time is 30 min. Figure 4-2 shows that under these constant input conditions sustained oscillations will appear. To control this pathological behaviour our suboptimal control algorithm is applied for different values of the constraint matrix R. It can be seen that for a constraint matrix

$$R = \begin{bmatrix} r_1 & 0 \\ 0 & r_2 \end{bmatrix} = \begin{bmatrix} 300 & 0 \\ 0 & 50 \end{bmatrix}$$

sustained oscillations still appear, Figure 7-12a. However, particles are now formed during longer time periods (about 30 min), Figure 7-13a, compared with the nucleation periods of 5-10 min for the uncontrolled process (Figure 5-3b). It is interesting to note in Figure 7-14a that both manipulated variables follow a similar behaviour. This can be explained as follows. When particle nucleation begins a large particle surface area is formed resulting in a large emulsifier deficit and a subsequent decrease in the nucleation rate. Moreover, the total growth rate of the newly generated particles is not enough to drive the conversion back to its desired level. Thus, an increase in the flowrate of both variables results in an attempt of the system to prolong the particle generation and simultaneously increase the total particle growth rate. However, because of the input constraints (matrix R) the feed rates are moving back

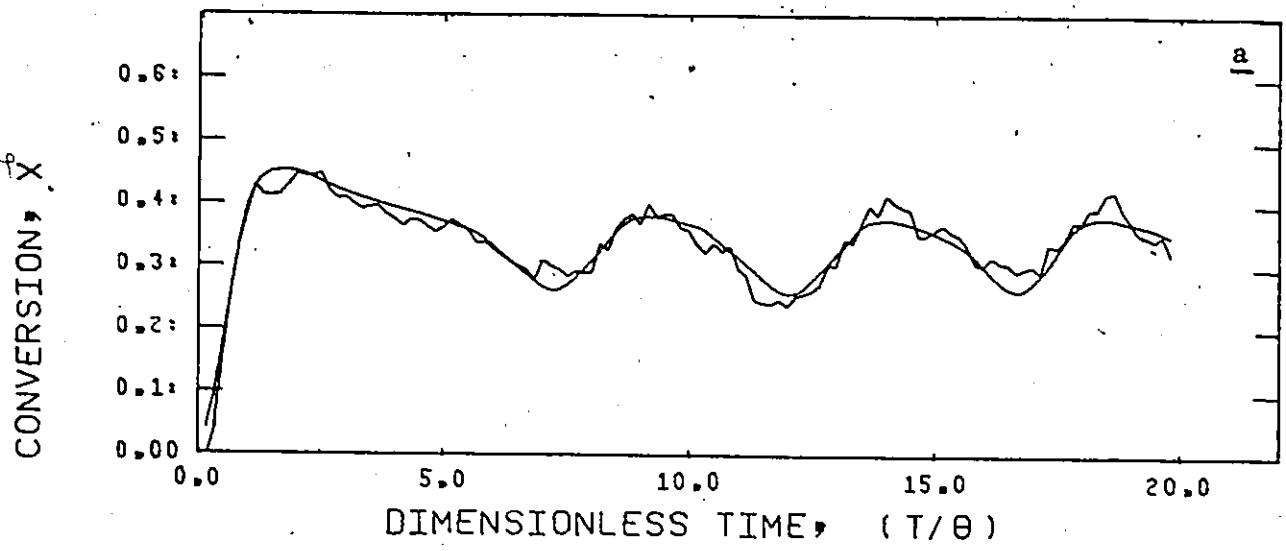

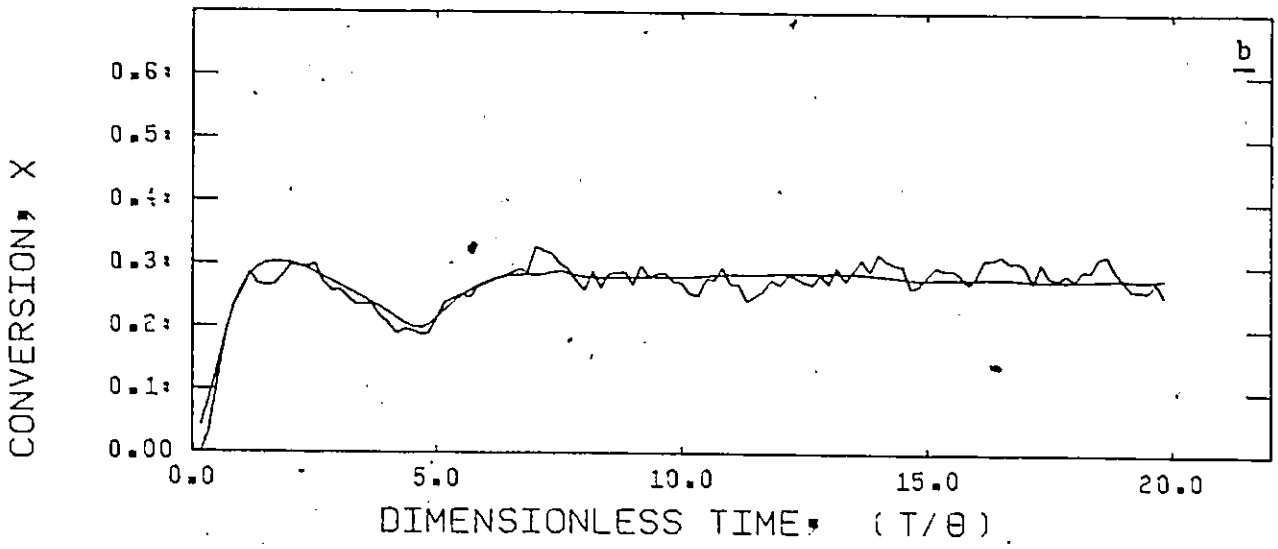

Figure (7-12) Control of Sustained Oscillations. Conversion-Time Histories (I^d = 0.01 mole/ℓ-H_2O, S^d = 0.01 mole/ℓ-H_2O)

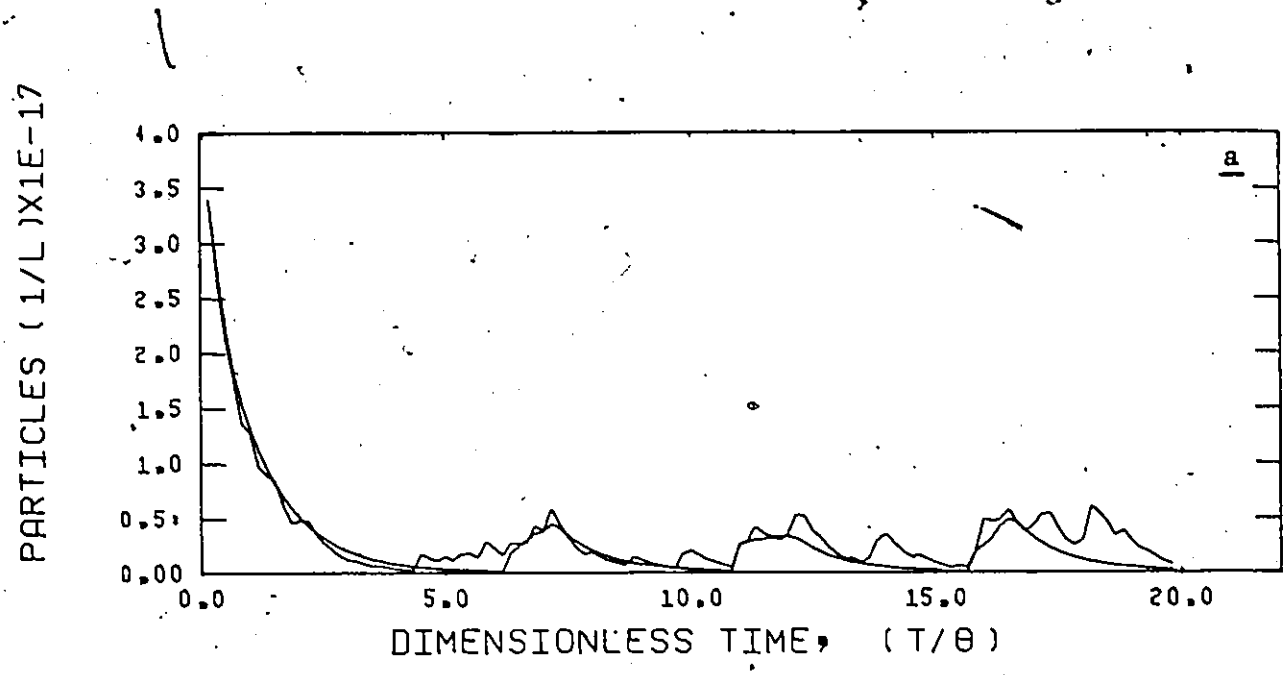

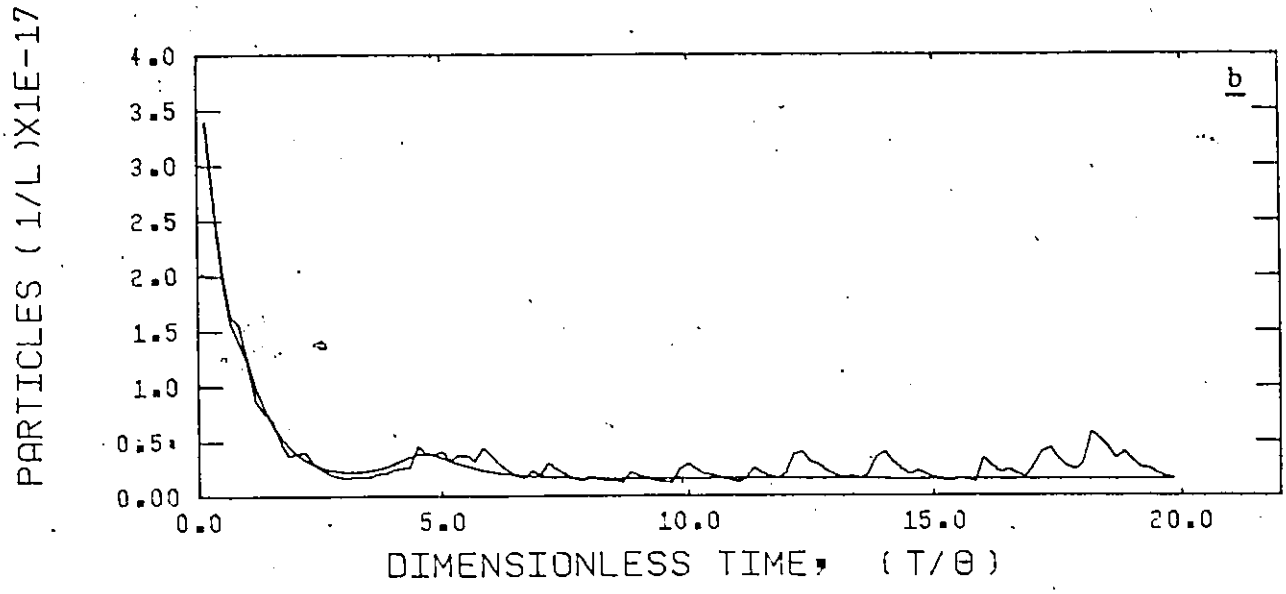

Figure (7-13) Control of Sustained Oscillations. Number of Particles versus Time (I^d = 0.01 mole/ℓ-H_2O, S^d = 0.01 mole/ℓ-H_2O)

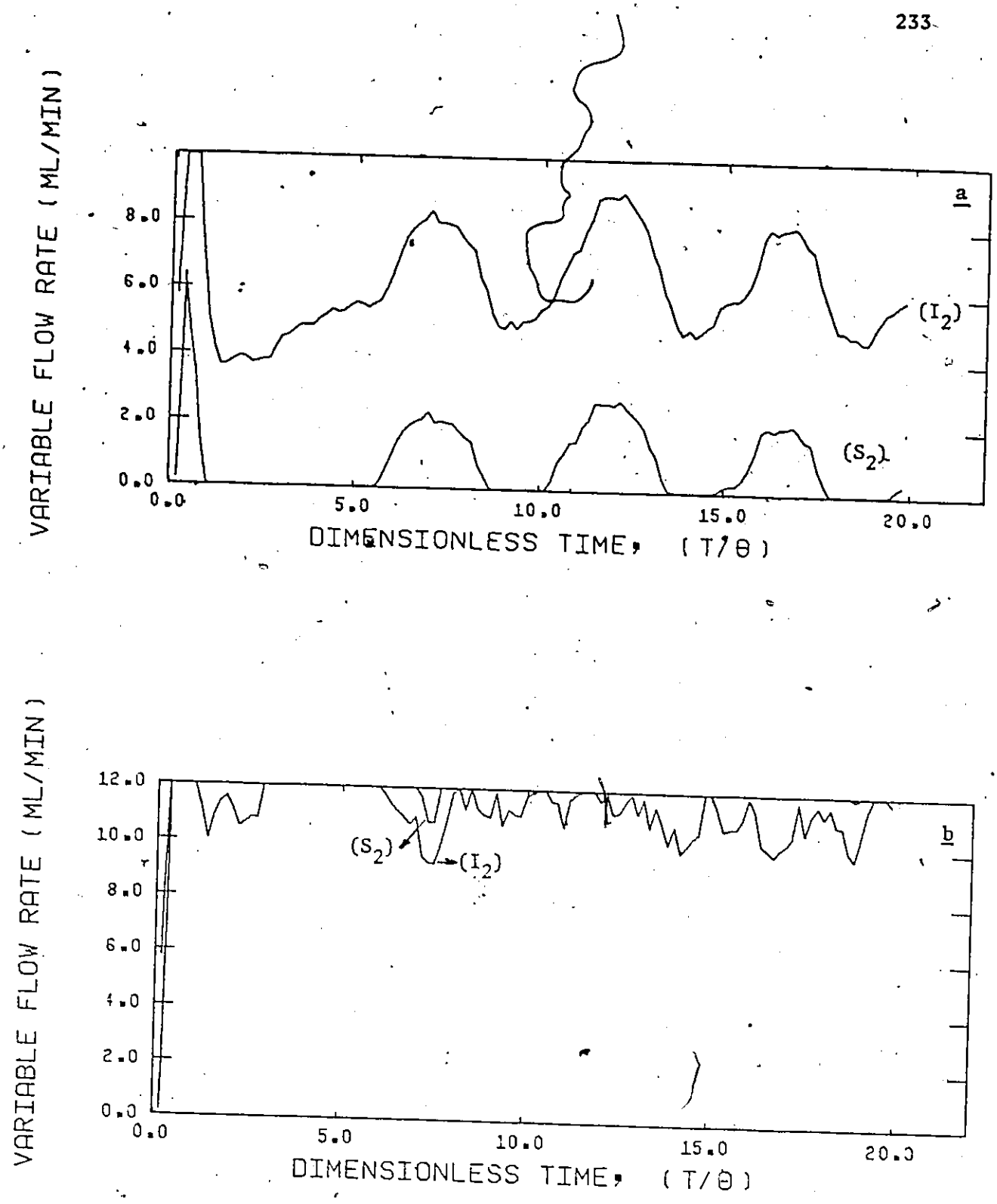

Figure (7-14) Emulsifier and Initiator Variable Flow Rates Versus Time ($I_1 = 0$, $I_2 = .05$ mole/ℓ-H_2O, $S_1 = .018$, $S_2 = 0.18$ mole/ℓ-H_2O)

to their steady state levels as conversion begins to move to its desired level. Thus, a cycling behaviour for the variable emulsifier and initiator flowrates is observed.

On the other hand, with a constraint matrix

$$R = \begin{bmatrix} 700 & 0 \\ 0 & 3 \end{bmatrix}$$

we were able to control the oscillations and achieve a steady state reactor performance, Figures 7-12b and 7-13b. However, large deviations in the manipulated variables (Figure 7-14b) did not allow us to achieve the desired conversion level (35%). Instead, a 30% steady-state conversion value was obtained. The offset in conversion is then simply due to not having I^d set correctly. Integral action in the controller could eliminate this. It is interesting to note that oscillations can be eliminated by reducing the constraints on the emulsifier flowrate and thereby allowing it to go to a much higher level. However, a high emulsifier flowrate will decrease the mean residence time resulting, thus, in an actual decrease in the polymer volume, V_p, produced. To eliminate this undesirable result a new augmented vector, z, can be defined in terms of the state vector x and the desired final values x^d, V_p^d, I^d, S^d, as $z = (x, x^d, V_p^d, I^d, S^d)'$. This will result in large deviations in the polymer volume not being acceptable since the performance index (7.38) will include the term $(V_p - V_p^d)^2$ to account for these deviations.

It is well known from simulation studies (Chapter 5) that the free

soap concentration shows an oscillatory behaviour when the reactor operates under sustained oscillations (Figures 5-3, 5-6). Thus, particle nucleation stops whenever there is an emulsifier deficit in the reactor. This might suggest that a single Proportional-Integral controller acting on a measured (via conductivity etc.) or estimated from a Kalman filter free soap concentration could eliminate sustained oscillations. This practical PI control scheme is simple and might be easily implemented on large industrial latex reactors.

7.6 Conclusions

In this Chapter, we have successfully shown by applying a multivariable stochastic control algorithm that latex reactors can be controlled to achieve a desired reactor performance. In particular, optimal start-up control policies greatly reduced the conversion overshoot and largely minimized the time required to achieve a steady-state value. The ability of the algorithm to achieve control under such severe reactor behaviour as sustained oscillations has encouraged us to begin preparations to apply this control policy to the real pilot plant reactor system. Currently, a new reactor system is being constructed (Figure 7-4) by Mark Pollock to test the proposed control policies. The experimental evaluation of the simulation results described here will be the primary follow-up of control analysis described in this Chapter.

CHAPTER 8

CONCLUSIONS AND FUTURE WORK

In an attempt to model and explain physical and chemical phenomena occurring in continuous emulsion polymerization, and to apply the concepts of multivariable stochastic control theory to such a complex process a number of difficult theoretical and practical problems were encountered. The continuous emulsion polymerization represents a challenge from the modelling, the parameter estimation, the on-line measurements and the control point of view. This study is one on the application of multivariable stochastic control to an emulsion system operating under sustained oscillations. It should provide a sound basis for any future studies on the computer control of latex reactors.

In particular, this thesis has examined the problems of formulating dynamic models for an emulsion system based on population balance principles. In Section 2.5, two levels of models were developed: a comprehensive one, which uses the age distribution function and a simplified model suitable for use in control studies. The ability of both models to simulate the reactor behaviour has been demonstrated in Chapter 5. This is the first attempt to model sustained oscillations occurring in continuous

latex reactors for PVAc and it is believed that this work has largely contributed to the modelling of these systems.

In Chapter 3 it is shown that turbidity spectra analysis and liquid exclusion chromatography have some specific advantages over other available techniques. They are simple, rapid and can be used as on-line monitors. A method for calculating the leading moments of the unknown particle size distribution from turbidity measurements has been developed. A statistical technique is also described which can be used to predict directly the states of the model from turbidity measurements.

Experimental results obtained under a variety of operating conditions are given in Chapter 4. Along with Greene's work (1976), this is the only extensive study on continuous PVAc emulsion polymerization. It was found that the rate of polymerization is proportional to the initiator concentration. On the other hand, emulsifier concentration has a negligible effect on the production rate. These results agree with those reported in the literature. The effects of the agitation rate and the presence of impurities on the rate of polymerization were also studied. Stirring can significantly affect the course of polymerization in the presence of dissolved impurities and imperfectly purified nitrogen atmosphere. Reactor fouling and stability of the latex were examined in relation with the DLVO theory. A high ionic concentration with simultaneous presence of small and large particles can dramatically increase the coagulation rate. This was experimentally confirmed. Finally, turbidity and LEC results showed that both techniques could

follow variations in conversion and number of polymer particles, determine the induction period and the extent of particle flocculation. It is believed that the experimental results presented here have greatly improved our understanding of the emulsion polymerization process.

Experimental conversion-time histories were successfully simulated by both simplified and comprehensive models. The unknown kinetic model parameters were estimated using a non-linear regression routine. To prove theoretically the existence of limit cycles Bendixson's theorem was used. It was shown that sustained oscillations always resulted in a closed trajectory on the phase plane.

Turbidity measurements were analyzed by the method of moments and principal components. Both methods appeared to give satisfactory results and adequately follow changes in the reactor.

In Chapter 7 a modern multivariable stochastic control theory was applied to simulate the control of the latex reactor. A new reactor design is proposed which utilizes two additional streams of initiator and emulsifier as the control variables. An instantaneous linearization technique is employed to obtain a locally linear model which is subsequently integrated to give an equivalent discrete model suitable for computer control. Noise models for the process and measurements are identified and a linear-quadratic objective function is employed to derive the optimal feedback control law. The successful application of this control algorithm to the simulated continuous latex reactor should provide a good criterion of its value on the real process since

the simulation was previously shown to represent the behaviour of the actual reactor very well.

An abundance of ideas and projects for future work arise from this thesis. Of course, the primary follow-up will be the experimental evaluation of the derived control algorithm. The use of the mean residence time as an additional control variable should be considered. Moreover, inhibitor concentration and reactor temperature can be employed as control variables. A PI controller acting on a measured or estimated soap concentration can be employed to eliminate sustained oscillations. Control of PSD and MWD are problems which may follow the present work. The extension of this mathematical and experimental investigation to two or more CSTR's in series would be of great importance since it would parallel more closely the industrial situation. Batch reactor results (in Appendix II) have shown that our model can be satisfactorily used for simulation and control studies for batch and semi-batch reactors. A correct interpretation of LEC-chromatograms may yield more information about the shape of the unknown PSD which then can be used with some turbidity measurements to calculate the PSD or some important moments of it.

The list of future projects and ideas can go on. However, at this point I think it is appropriate to close my thesis believing that the above ideas will soon find their justification.

REFERENCES

Adamson, A.W., "Physical Chemistry of Surfaces", 2nd ed., Interscience, N.Y. (1967)

Ahlberg, D.T. and Cheyne, I., AIChE Symposium Series in Chemical Process Control, No. 159, Vol. 72 (1977).

Alexander, A.E. and Napper, D.H., Progr. Polym. Sci., 3, 145 (1971).

Amrehn, H., Autom., 13, 533 (1977).

Anderson, T.W., "An Introduction to Multivariate Statistical Analysis", John Wiley (1958).

Argyriou, D.T., List, H.L. and Shinnar, R., AIChE, 17, 122 (1971).

Aström, K.J., "Introduction to Stochastic Control Theory", Acad. Press, N.Y. (1970).

Bendixson, Ivar, Acta Mathematica, 24, 1 (1901).

Beste, L.F. and Hall, H.K., J. Macromol. Chem., 1, 121 (1966).

Bierman, A., J. Coll. Interf. Sci., 10, 231 (1955).

Bird, R.B., Stewart, W.E. and Lightfoot, E.N., "Transport Phenomena", John Wiley (1960).

Box, G.E.P. and Draper, N.R., Biometrica, 52, 355 (1965).

Box, G.E.P. and Jenkins, G.H., "Time Series Analysis Forecasting and Control", Holden Day, San Francisco (1970).

Brooks, B.W., Br. Polym. J., 5, 199 (1973).

Coll, H., Fague, G.R. and Robillard, K.A., private communication, Eastman Kodak, Rochester, N.Y. (1975).

Collins, E.A., Davidson, J.A. and Daniels, C.A., "Review of Common Methods of Particle Size Measurement", chapter in "Advances in Emulsion Polymerization and Latex Technology" by G. Poehlein, Lehigh University, Bethlehem, Pa. (1975).

Daqud, A.T., Chem. Eng. Sci., 31, 510 (1976).

Dave, J.V., IBM Report No. 320-3237, Palo Alto, California (1968).

DeGraff, A.W. and Poehlein, G.W., J. Polym. Sci., A-2, 9, 1955 (1971).

Dickinson, R.F. and Gall, C.E., paper presented in 59th CIC Conference, London, Ontario, June (1976).

Dickinson, R.F., "Dynamic Behaviour and Minimum Norm Control of Continuous Emulsion Polymerization Chains", Ph.D. Thesis, University of Waterloo, Waterloo, Ontario (1976).

DiMarzio, E.A. and Guttman, C.M., J. Polym. Sci., Part B, 7, 267 (1969).

Draper, N.R. and Smith, H., "Applied Regression Analysis", John Wiley, N.Y. (1966).

Dunn, A.S. and Chong, L.C.-H., Br. Polym. J., 2, 49 (1970).

Evans, C.P., Hay, P.M., Marker, L., Murray, R.W., and Sweeting, O.J., J. Appl. Polym. Sci., 5, 39 (1961).

Efroymson, M.A., "Multiple Regression Analysis" in Mathematical Methods for Digital Computers, John Wiley, N.Y. (1960).

Fellows, D.M., Ph.D. Thesis, Department of Electrical Engineering, University of Waterloo, Waterloo, Ontario (1969).

Finlayson, B.A. and Scriven, L.E., Appl. Mech. Rev., 19, 735 (1966).

Fitch, R.M. and Tsai, C.H., in "Polymer Colloids", Plenum Press, N.Y. (1971).

Fitch, R.M. and Shih L.-bin, Progr. Colloid Polym. Sci., 56, 1 (1975).

Friis, N., Ph.D. Thesis, Danish Atomic Energy Commission Research Establishment, Riso, 4000, Roskilde, Denmark (1973).

Friis, N. and Hamielec, A.E., J. Polym. Sci., 11, 3341 (1973).

Friis, N. and Nyhagen, L., J. Appl. Polym. Sci., 17, 2311 (1973).

Foss, A.S., AIChE, 19(2), 209 (1973).

Fuchs, O.Z., Phys., 89, 736 (1934).

Gardon, J.L., J. Polym. Sci., A-1, 6, 665 (1968a).

Gardon, J.L., J. Polym. Sci., A-1, 6, 623 (1968b).

Gatta, G., Benetta, G., Talamini, G., and Vianello, G., Advances in Chemistry Series , No. 91, Amer. Chem.Soc., Washington, D.C., pp. 158ff (1969).

Gaylor, V.F. and James, H.L., Preprints - Pittsburg Conference on Analytical Chemistry, Cleveland, Ohio, March (1975).

Gerrens, H., J. Polym. Sci., C, 27, 77 (1969).

Gerrens, H., Kuchner, K., and Ley, G., Chemie Ing. Tech., 43, 12, 693 (1971).

Gerrens, H. and Ley, G., private communication (1974).

Gershberg, D.B. and Longfield, J.E., 45th American Institute of Chemical Engineers Meeting, New York, Preprint No. 10 (1961).

Gledhill, R.J., J. Phys. Chem., 66, 458 (1961).

Gorber, D.M., "The Dynamics of Continuous Emulsion Polymerization Reactors", Ph.D. Thesis, University of Waterloo, Waterloo, Ontario (1973).

Goryushko, V.E. and Vilesov, N.G., Int. Chem. Eng., 11, 57 (1971).

Greene, R.K., Conzalez, R.A., and Poehlein, G.W., paper in "Emulsion Polymerization", editors Irja Piirma and J.L. Gardon, ACS Symposium Series 24, Washington, D.C. (1976).

Hamielec, A.E. and Ray, W.H., J. Appl. Polym. Sci., 13, 1319 (1969).

Hamielec, A.E., course notes in Polymer Reactor Engineering, McMaster University, Ontario (1976).

Hamilton, J.C., Seborg, D.E., and Fisher, D.G., AIChE J., 19,901 (1973).

Hansen, F.K. and Ugelstad, J., private communication (1978).

Harkins, W.D., J. Am. Chem. Soc., 69, 1428 (1947).

Heller, W. and Pangonis, W.J., J. Chem. Phys., 26, 3, 498 (1957).

Heller, W. and Peters, J., J. Coll. Interf. Sci., 32, 4, 592 (1970).

Hicks, J., Mohan, A., and Ray, W.H., Can. J. Chem. Eng., 47, 590 (1969).

Hoffman, T.W. and Reilly, P.M., to appear in Can. J. Chem. Eng.

Hoffman, R.F., Schreiber, S., and Rosen, G., Indust. Eng. Chem., 56, 5, 51 (1964).

Hogg, R., Healy, T.W., and Fuerstenau, D.W., Trans. Faraday Soc., 62, 1638 (1966).

Hulburt, H.M. and Katz, S.L., Chem. Eng. Sci., 19, 555 (1964).

Hyun, J.C. and Bankoff, S.G., Chem. Eng. Sci., 31, 953 (1976).

Jazwinski, A.H., "Stochastic Processes and Filtering Theory", Acad. Press, N.Y. (1970).

Jaisinghani, R. and Ray, W.H., Chem. Eng. Sci., 32, 8, 811 (1977).

Jo, J.H. and Bankoff, S.G., AIChE J., 22, 2, 361 (1976).

Jutan, A., "State Space Modelling and Multivariable Stochastic Control of a Pilot Plant Packed-Bed Reactor", Ph.D. Thesis, McMaster University, Hamilton, Ontario (1976).

Jutan, A., MacGregor, J.F., and Wright, J.D., AIChE J., 23, 5, 742 (1977a).

Jutan, A., MacGregor, J.F., and Wright, J.D., AIChE J., 23, 5, 751 (1977b).

Katz, S. and Saidel, G., J. Polym. Sci., C, 27, 149 (1969).

Katz, S., Saidel, G., and Shinnar, R., "Advances in Chemistry", 91 (1968).

Keung, C.K.J., "Emulsion Polymerization of Vinyl Acetate: Particle Size and Molecular Weight Distributions"; M.Eng. Thesis, McMaster University, Hamilton, Ontario (1974).

Keyes, M.A. and Kennedy, J.P., Proceedings 2nd Purdue Conference on Process Control; Adaptive Control (1974).

Kiparissides, C., MacGregor, J.F., and Hamielec, A.E., J. Appl. Polym. Sci. (to appear in 1978).

Krebs, K.F. and Wunderlich, W., Angew Makrom. Chem., 20, 203 (1971).

Kruyt, H.R., "Colloid Science", Elsevier Publishing Company, New York (1952).

Kushner, H.J., S.I.A.M. J. Control, 2, 1, 106 (1964).

Kushner, H.J., Math. Analysis Applic., 11, 78 (1965).

Kwon, Y.D., Lawrence, B.E., and Noble, J.J., "Advances in Chemistry", 109, 98 (1972).

Lapidus, L. and Luus, R., "Optimal Control of Engineering Processes", Blaisdell Publishing Co., N.Y. (1967).

Litt, M., Patsiga, R., and Stannett, V., J. Polym. Sci., A-1, 8, 3607 (1970).

MacGregor, J.F., Can. J. Chem. Eng., 51, 468 (1973).

Maron, S.H., Pierce, P.E., and Ulevitch, I.N., J. Coll. Sci., 18, 470 (1963).

Marquardt, D.L., J. Soc. Ind. Appl. Math., 2, 431 (1963).

Matthews, B.A. and Rhodes, C.T., J. Coll. Interf. Sci., 32, 2, 339 (1970).

Maxim, L.D., Klein, A., Meyer, M.E., and Kuist, C.H., J. Polym. Sci., Part C, 27, 195 (1969).

McGreavey, C. and Vago, A., "Application of Non-Linear Filtering Techniques to Adaptive Optimal Control", private communication (1975).

Matsura, T. and Kato, M., Chem. Eng. Sci., 22, 171 (1967).

McHugh, A.J., "Hydrodynamic Chromatography for Latex Particle Size Distribution", private communication (1977).

Min, K.W., "The Modelling and Simulation of Emulsion Polymerization Reactors", Ph.D. Thesis, State University of New York at Buffalo, Buffalo, New York (1976).

Min, K.W. and Ray, W.H., J. Macromol. Sci., Rev. Macromol. Chem., C11, 177 (1974).

Mori, S., Porter, R.S., and Johnson, J.F., Analyt. Chem., 46, 11, 1599 (1974).

Nishimura, H. and Yokoyama, F., Kogaku Kogaku, 32, 601 (1968).

Nomura, M., Harada, M., Eguchi, W., and Nagata, S., J. Appl. Polym. Sci. 16, 835 (1972).

Nomura, M., Harada, M., Eguchi, W., and Nagata, S., paper in "Emulsion Polymerization", editors Irja Piirma and J.L. Gardon, ACS Symposium Series 24, Washington, D.C. (1976).

Nomura, M., Kojima, H., Harada, M., Eguchi, W., and Nagata, S., J. Appl. Polym. Sci., 15, 675 (1971).

Noton, M., "Modern Control Theory", Pergamon Press Inc., New York (1972).

Omi, S., Shiraishi, Y., Sato, H., and Kubota, H., J. Chem. Eng. Japan, 2, 64 (1969).

Omi, S., Ueda, T., and Kubota, H., J. Chem. Eng. Japan, 2, 193 (1969).

Osakada, K. and Fan, L.T., J. Appl. Polym. Sci., 14, 3065 (1970).

O'Toole, J.T., J. Appl. Polym. Sci., 9, 1291 (1965).

Overbeek, J.T.G., "Kinetics of Flocculation" in "Colloid Science", ed. by Kruyt, H.R., Elsevier, Amsterdam (1949).

Pearson, J.D., J. Electron. Control, 13, 453 (1962).

Peterlin, A., Yasuda, H., and Lamaze, C.E., J. Polym. Sci., A-2, 9, 1117 (1971).

Peters, J. and Heller, W., J. Coll. Interf. Sci., 33, 4, 578 (1970).

Pis'men, L.M. and Kuchanov, S.I., Vysokom.soyed. A13, No. 5, 1055 (1971).

Poehlein, G.W. and Dougherty, D.J., Rubber Chem. and Techn., 50, 601 (1977).

Ramkrishna, D., Chem. Eng. Sci., 26, 1134 (1971).

Ray, W.H., Can. J. Chem. Eng., 45, 356 (1967).

Rhee, S., Nozue, J., and Imoto, T., Kagaku Kogaku, 32(6), 614 (1968).

Roe, C.P., Ind. Eng. Chem., 60, 20 (1968).

Roquemore, K.G. and Eddey, E.E., Chem. Eng. Prog., 57(9), 35 (1961).

Sage, A.P. and Melsa, J.L., "Estimation Theory with Applications to Communications and Control", McGraw-Hill (1971).

Sautin, S.N., Kulle, P.A., and Smirnov, N.I., 2H PRIK KH, 44, 2503 (1971).

Schoot, C.J., Baker, J., and Klassens, K.H., J. Polym. Sci., 7, 657 (1951).

Shah, B.H., J.D. Borwanker and Ramkrisha, D., Math. Biosci., 31, 1 (1976).

Shirotsuka, T. and Terauchi, Y., Kagaku Kogaku, 36, 668 (1972).

Shunmukham, S.R., Hallenbeck, V.L., and Guile, R.L., J. Polym. Sci., 6, 691 (1951).

Singh, S., "Measurement of Particle Size in the Submicron Range-Evaluation of Liquid Exclusion Chromatography (LEC)", McMaster University, Hamilton, Ontario (1977).

Singh, S. and Hamielec, A.E., J. Appl. Polym. Sci., 22, 2, 577 (1978).

Singh, P.N. and Ramkrishna, D., Comp. Chem. Eng. 1, 23 (1977).

Small, H., J. Coll. Interf. Sci., 48, 1, 147 (1974).

Small, H., Saunders, F.L., and Solc J., Adv. Coll. Interf. Sci., 6, 237 (1976).

Smith, W.V. and Ewart, R.H., J. Chem. Phys., 16, 152 (1948).

Stevens, J.D. and Funderburk, J.O., Ind. Eng. Chem. Proc. Des. Dev., 11, 360 (1972).

Stevenson, A.F., Heller, W. and Wallach, M.L., J. Chem. Phys., 34, 5, 1789 (1961).

Stockmayer, W.H., J. Polym. Sci., 24, 314 (1957).

Subramanian, G. and Ramkrishna, D., Math. Biosci., 10, 1 (1971).

Sylvestre, E.A., Lawton, W.H., and Maggio, M.S., Technometrics, 16, 3, 353 (1974).

Thompson, R.W. and Stevens, J.D., Chem. Eng. Sci., 32(3), 311 (1977).

Ueda, T., Omi, S., and Kubota, H., J. Chem. Eng. Japan, 4, 50 (1971).

Ugelstad, J. and Hansen, F.K., Rubber Chem. and Techn., 49, 536 (1976).

Ugelstad, J., Mörk, P.C. and Aasen, J.O., J. Polym. Sci., A-1, 5, 2281 (1967).

Verwey, E.J.W. and Overbeek, J.T.G., "Theory of Stability of Lyophobic Colloids" in "Colloid Science", ed. by Kruyt, H.R., Elsevier, Amsterdam (1949).

Wallach, M.L. and Heller, W., J. Chem. Phys., 34, 5, 1796 (1961).

Weber, A.P.J. and Lapidus, L., AIChE J., 17, 3, 641 (1971).

Wessling, R.A., J. Polym. Sci., 12, 309 (1968).

Willems, J.L., "Stability Theory of Dynamical Systems", John Wiley Inc., New York (1970).

Wilson, G.T., "Modelling Linear Systems for Multivariable Control", Ph.D. Thesis, University of Lancester (1970).

Wismer, D.A., IEEE Trans. Auto Control, 10(4), 455 (1965).

Yamazaki, H. and Ichikawa, A., J. Chem. Eng. Japan, 2, 1, 100 (1969).

Yoshimoto, Y., Yanagaw, H., Suzuki, T., Inaba, Y., Araki, T., Kagaku Kogaku, 32 (6),595 (1968).

APPENDIX I

Calculation of the Average Number of Radicals per Particle, $\bar{q}$, for Polydisperse Systems

The basic problem in emulsion polymerization is the determination of the average number of radicals per particle. Smith-Ewart recursion formula (2.4) was derived for a monodisperse system. Moreover, they considered that the rate of absorption of radicals in a particle should, in general, be proportional to the surface area of the particle. However, both assumptions may not be true for the usual case of polydisperse systems. That is, different rate of absorption and desorption of radicals will exist for different sizes of particles. In this section, an expression for the average number of radicals per particle is derived for a polydisperse system which follows the case I kinetics ($\bar{q} << .5$). Under this condition $N_{0i} >> N_{1i} >> N_{qi}$ and accordingly one has only to consider the first of the relation of equation (2.4). Therefore, for the "i" class of particles we can write

$$N_{1i}k_{dei} = \rho_{Ai}N_{0i}/N_i \qquad \text{(I-1)}$$

where N_i is the total number of particles of ith class and N_{0i} denotes the number of particles with 0 radicals for the same class. If it is assumed

$N_i \simeq N_{Oi}$ ($\bar{q} \ll 0.5$) then equation (I-1) becomes,

$$N_{1i} = \frac{\rho_{Ai}}{k_{dei}} \qquad \text{(I-2)}$$

where k_{dei} is the rate "constant" for desorption of radicals from particles and ρ_{Ai} is the total rate of radical arrival in the particles of the ith class. The average number of radicals per particle of ith class will be given as

$$\bar{q}_i = \frac{N_{1i}}{N_i} = \frac{\rho_{Ai}}{k_{dei} N_i} \quad \text{(for convenience } \frac{\rho_i}{k_i N_i}\text{)} \qquad \text{(I-3)}$$

The rate of radical arrival ρ_{Ai} (or ρ_i) can be written as

$$\rho_i = \rho_A \left(\frac{A_i}{\bar{A}}\right)^r \qquad \text{(I-4)}$$

where ρ_A is the total rate of radical absorption in the particles of all classes. A_i denotes the particle area of the ith class of particles and $\bar{A}$ is an average particle area. The numerical value of the exponent r will be dependent upon the particular theory according to which radicals may be captured by particles. Therefore, for r = 1/2 the diffusion model will hold while for r = 1 the collision model will be true. The total rate of radical absorption may be written as

$$\rho_A = R_I + \sum_{i=1}^{q_t} k_i N_i \bar{q}_i \qquad \text{(I-5)}$$

where R_I is the total radical production in the water phase. Therefore, equation (I-3) can be written in terms of ρ_A as

$$\bar{q}_i = \frac{\rho_i}{k_i N_i} = \left(\frac{A_i}{\bar{A}}\right)^r \left(R_I + \sum_{i=1}^{q_t} k_i N_i \bar{q}_i\right) \frac{1}{N_i k_i} \qquad \text{(I-6)}$$

or

$$-1 = \frac{k_i N_i}{R_I} \left(1-\left(\frac{A_i}{\bar{A}}\right)^{-r}\right) \bar{q}_i + \sum_{\substack{j=1 \\ j\neq i}}^{q_t} k_j N_j \bar{q}_j / R_I \qquad \text{(I-7)}$$

To determine the average number of radicals $\bar{q}_i$ per class of particles, a system of q_t simultaneous algebraic equations should be solved (q_t denotes the total number of particle classes). An analytical solution to equation (I-7) can be easily obtained by applying Cramer's rule to estimate the unknown $\bar{q}_i$

$$\bar{q}_i = \left(\frac{R_I}{k_i N_i}\right)\left(\frac{A_i}{\bar{A}}\right)^r \frac{1}{1-\left(\sum_{i=1}^{q_t} (A_i/\bar{A})^r\right)} \qquad \text{(I-8)}$$

Equation (I-8) gives the average number of radicals per particle of the ith class. A collision or diffusion model for radical capture can be easily applied to equation (I-8) simply by changing the numerical value of the parameter r. Moreover, equation (I-8) allows the redistribution of radicals among particles of different classes.

If termination takes place exclusively in polymer particles and occurs instantaneously upon radical entry into a particle containing one

radical then the rate of generation of radicals by initiator decomposition, R_I, is equal to twice the rate of radical entry into particles containing one radical, in other words,

$$R_I = \sum_{i=1}^{q_t} 2\left(\frac{\rho_i}{N_i}\right) N_{1i} = \sum_{i=1}^{q_t} 2\left(\frac{\rho_A}{N_i}\right) N_{1i} \left(\frac{A_i}{\bar{A}}\right)^r \qquad \text{(I-9)}$$

or

$$\bar{A}^r = \frac{2\rho_A}{R_I} \sum_{i=1}^{q_t} A_i^r \bar{q}_i \qquad \text{(I-10)}$$

Equation (I-10) can be used to determine $\bar{A}$ which can be then substituted into equation (I-8) to calculate $\bar{q}_i$.

APPENDIX II

Simulation Studies for a Batch Latex Reactor

To find the particle size distribution in a batch emulsion reactor the concept of discrete particle nucleation developed in Section (2.5) can be employed. Particles in a batch emulsion reactor are mainly formed during the first 5-10 minutes of the reaction. At the end of stage 1 (see Chapter 2) particle nucleation ceases since there is no free soap left to stabilize new particles. Therefore, the total number of particles after nucleation has stopped remains practically constant. This has been shown in numerous experimental studies (Friis (1971), Keung (1974), Nomura (1976)).

If it is assumed that there is negligible particle agglomeration (there is sufficient soap to stabilize the particles) then the dynamic equations describing the development of each particle generation "i" during stage 1 where particles are formed can be written

$$\frac{dN_i(t)}{dt} = f(t)\delta(t-t_i) \qquad \text{(II-1)}$$

$$\frac{dx_i(t)}{dt} = \frac{k_p d_m}{M_F M_W} \Phi(t) \bar{q}_i(t) N_i(t) \qquad \text{(II-2)}$$

$$A_{pi}(t) = (36\Pi)^{1/3} (V_{pi})^{2/3} N_i^{1/3} \qquad \text{(II-3)}$$

When two or more particle generations have been formed in the reactor the total properties of the latex product in the reactor will be given by

$$x(t) = \sum_{i=1}^{q_t} x_i(t),\quad N(t) = \sum_{i=1}^{q_t} N_i(t),\quad A_p(t) = \sum_{i=1}^{q_t} A_{pi}(t) \qquad \text{(II-4)}$$

The system of equations (II-1) to (II-4) together with all other related balances for initiator, radicals, emulsifier etc. was numerically solved using the Runge-Kutta and Predictor-Corrector routines. It is clear that the method followed to predict the PSD often involved arbitrarily discretizing the time interval. Thus, a test for the adequacy of the fineness of discretization would be necessary in such a simulation procedure. However, a recent method by Shah et al. (1976), handles the artificial evolution of the system in an elegant manner by generating random numbers representing "intervals of quiescence". Each intervals of quiescence is a period, in which every member of population retains its identity, and has an exactly calculable probability distribution. Experimental results for a batch reactor obtained by Friis (1973) and Keung (1974) were successfully simulated and the simulation are shown in Figures II-1 to II-4. Solid lines in Figure II-1 represent the calculated conversion values. Experimental data for different reactor conditions are marked in the Figure II-1 as (O, □ , Δ,). It is interesting to note that there is a very good agreement between experimental and calculated results practically over the whole range of conversion.

Figure II-2 shows how the number of particles changes with conversion for different initiator levels. The predicted values are again in fine agreement with the experimental results.

Figure II-3 shows how the average number of radicals per particle, $\bar{q}$, changes with conversion for two different initiator levels. $\bar{q}$ was found to take small values throughout the whole conversion range (in agreement with case 1 kinetics) though it increased rapidly above 90% of conversion.

Finally, in Figure II-4, the predicted number average diameter, D_n, is compared with the particle diameter obtained by Keung (1974) from an electron microscopic analysis.

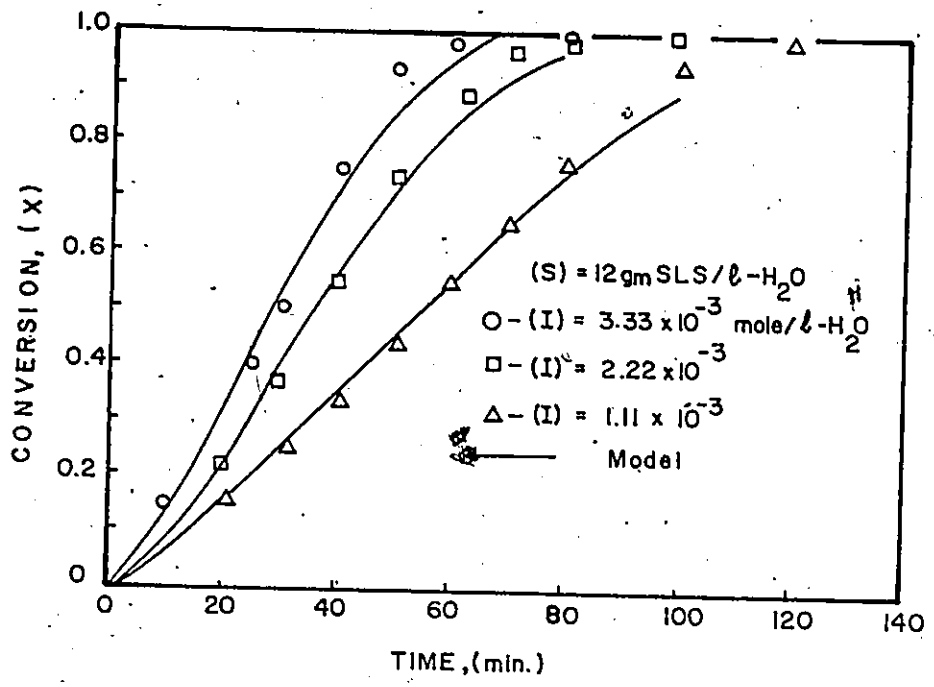

Figure (II-1) Simulation Results. Conversion-Time Histories

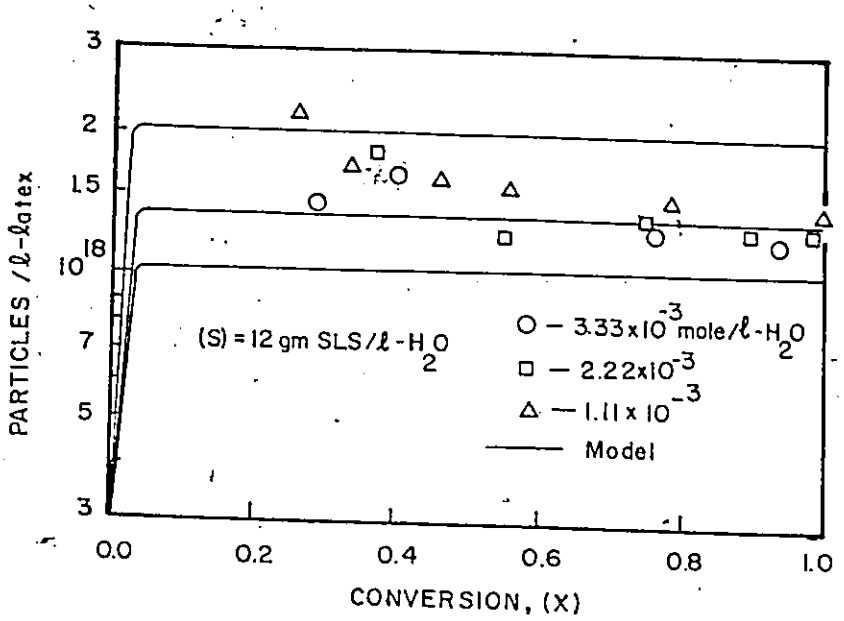

Figure (II-2) Simulation Results. Conversion-Time Histories

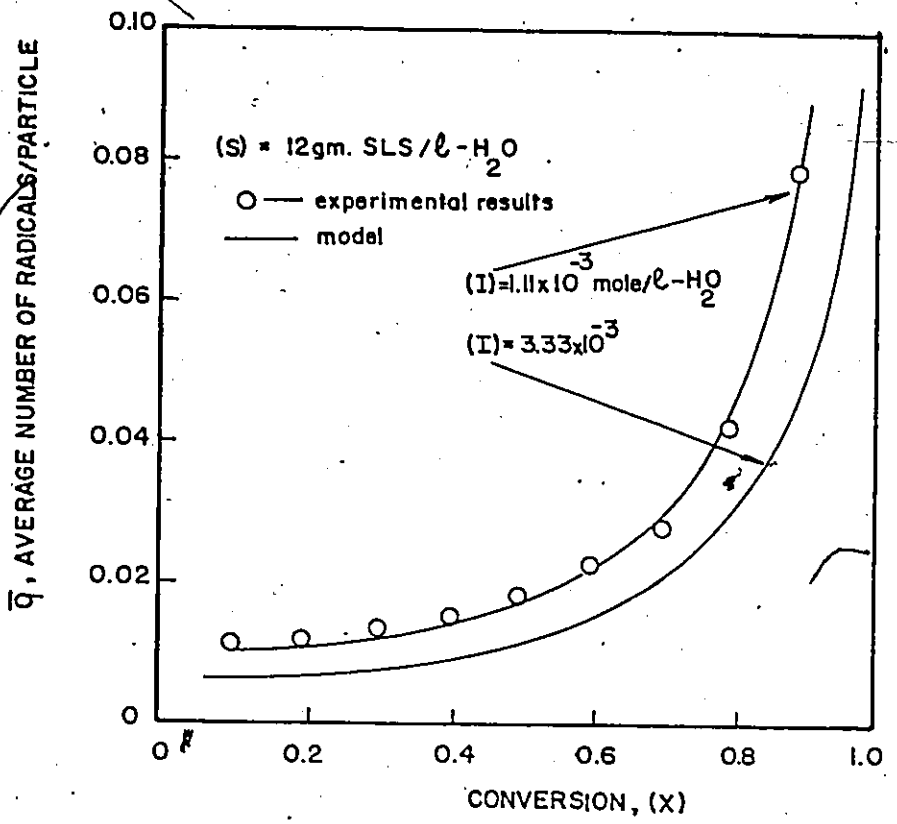

Figure (II-3) Simulation Results. Average Number of Radicals per Particle versus Conversion.

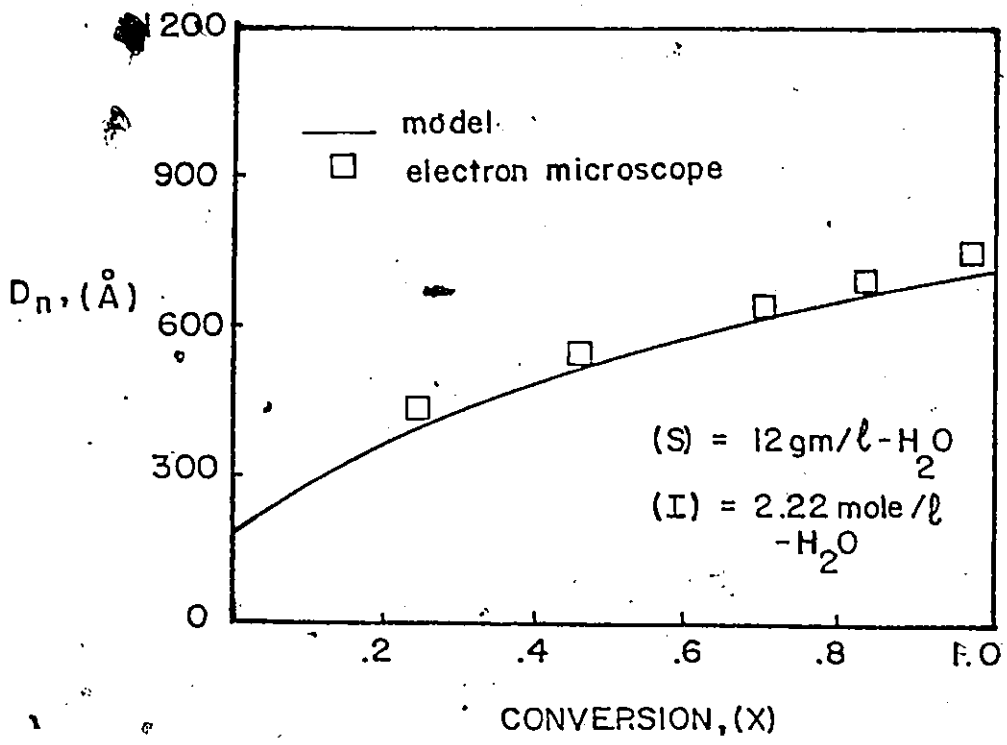

Figure (II-4) Simulation Results. Number Average Diameter, versus Conversion

APPENDIX III

Experimental Results

A total of 37 experimental runs were completed during the course of this study. The effects of initiator, emulsifier concentration, residence time, stirring rate and the presence of impurities on the conversion were studied and the results are shown in Table III-1. Initiator and emulsifier concentrations are given in mole/ℓ-H_2O. The reaction temperature was always kept at 50°C and the monomer to water ratio was 4/10. The agitation rate was usually 320 r.p.m. In Table III-1 the most successful runs are reported.

Absorbance measurements for different runs are given in Table III-2. For each sample absorbance was measured at seven different wavelengths in the visible range. Different dilution ratios were used to avoid multi-scattering effects on the absorbance measurements. The turbitity values can be easily found from

$$\tau = 2.303\ A/\ell$$

where A is the absorbance and ℓ is the path length of the transmission cell (1 cm).

Table III-1

RUN = 3

INITIATOR = .015M/L EMULSIFIER = .060M/L MONOMER/WATER = 4/10
TEMPERATURE = 50 C RESIDENCE TIME = 30.00MIN

NO	TIME	PLATE-1	PLATE-2	PLATE-3	CONVERS.	FCL.VOLUME
1	30.00	16.5790	17.6430	16.9310	82.98	.2382
2	45.00	13.7835	14.8675	13.9730	63.59	.1825
3	60.00	15.1960	16.1480	15.3595	58.59	.1682
4	75.00	14.9815	15.9525	15.1555	61.39	.1762
5	90.00	10.3400	11.3130	10.5220	64.33	.1847
6	105.00	13.7385	14.6715	13.9200	67.13	.1927
7	120.00	11.6530	12.6420	11.8506	69.10	.1984

RUN = 4

INITIATOR = .015M/L EMULSIFIER = .060M/L MONOMER/WATER = 4/10
TEMPERATURE = 50 C RESIDENCE TIME = 30.00MIN

NO	TIME	PLATE-1	PLATE-2	PLATE-3	CONVERS.	FCL.VOLUME
1	30.00	10.3400	11.2735	10.3990	31.78	.0576
2	40.00	13.0920	14.0325	13.1920	43.00	.0908
3	50.00	12.0660	13.0805	12.1795	45.97	.1070
4	60.00	10.5400	11.5245	10.6725	52.60	.1305
5	90.00	13.8330	14.8290	13.9965	58.99	.1609
6	105.00	13.6240	14.6325	13.8137	66.92	.1863
7	120.00	13.8680	14.8680	14.0660	69.82	.1967
8	135.00	12.2310	13.2660	12.4480	73.68	.2092
9	150.00	10.7040	11.7110	10.9250	77.03	.2196
10	165.00	16.5790	17.5805	16.8005	77.45	.2214
11	180.00	13.7835	14.7710	13.9980	75.83	.2171

RUN = 8

INITIATOR = .010M/L EMULSIFIER = .060M/L MONOMER/WATER = 4/10
TEMPERATURE = 50 C RESIDENCE TIME = 30.00MIN

NO	TIME	PLATE-1	PLATE-2	PLATE-3	CONVERS.	FCL.VOLUME
1	15.00	17.7220	18.6530	17.7335	6.42	.0072
2	30.00	15.4650	16.2850	15.4940	15.61	.0283
3	45.00	19.3360	20.1925	19.3805	19.69	.0439
4	60.00	18.7260	19.5530	18.7760	20.81	.0517
5	75.00	14.1190	15.1295	14.1865	21.87	.0577
6	90.00	19.1270	20.0830	19.1915	21.21	.0579
7	110.00	12.7845	13.4580	12.8310	21.15	.0592
8	130.00	16.5675	17.4295	16.6260	20.36	.0577
9	150.00	16.3190	17.1900	16.3785	20.37	.0581
10	170.00	16.0905	16.9820	16.1465	18.22	.0522
11	190.00	18.2000	19.2560	18.2635	17.17	.0493
12	210.00	19.4840	20.4530	19.5405	16.47	.0473
13	230.00	16.8040	17.8690	16.8650	16.07	.0462
14	250.00	17.5455	18.4010	17.5950	16.29	.0468
15	270.00	15.2310	16.4260	15.3015	16.71	.0480

RUN = 9

INITIATOR = .010M/L EMULSIFIER = .010M/L MONOMER/WATER = 4/10
TEMPERATURE = 50 C RESIDENCE TIME = 30.00MIN

NO	TIME	PLATE-1	PLATE-2	PLATE-3	CONVERS.	FCL.VOLUME
1	20.00	17.7215	18.7320	17.7315	6.09	.0085
2	40.00	15.4655	16.3150	15.4995	14.64	.0397
3	60.00	16.9325	17.5570	16.9745	27.37	.0686
4	80.00	18.7260	19.6120	18.7925	29.40	.0767
5	100.00	14.1195	15.0170	14.1835	25.90	.0725
6	120.00	19.1270	19.9520	19.1770	24.52	.0699
7	140.00	12.7940	13.6020	12.9340	21.35	.0614
8	160.00	16.5670	17.5270	16.6180	18.27	.0528
9	180.00	16.3205	17.1590	16.3580	15.10	.0437
10	200.00	16.0910	17.0395	16.1285	13.16	.0382

RUN = 10

INITIATOR = .010M/L EMULSIFIER = .010M/L MONOMER/WATER = 4/10

TEMPERATURE = 50 C RESICENCE TIME = 30.00MIN

NO	TIME	PLATE-1	PLATE-2	PLATE-3	CONVERS.	FCL.VOLUME
1	20.00	17.6510	18.7790	17.6570	2.58	.0036
2	40.00	19.4175	20.4480	19.4565	17.61	.0375
3	60.00	19.0555	20.0265	19.1200	27.01	.0677
4	80.00	17.8545	18.9550	17.9395	29.27	.0790
5	100.00	20.4910	21.4160	20.5700	31.32	.0876
6	120.00	11.6530	12.4075	11.7065	25.26	.0720
7	140.00	12.1335	13.0430	12.1970	20.49	.0585
8	160.00	13.8330	14.4880	13.8650	16.68	.0482
9	180.00	12.0645	12.9270	12.0975	12.70	.0368
10	200.00	10.7030	11.5950	10.7310	10.14	.0294
11	220.00	18.2005	19.2045	18.2325	10.31	.0299
12	240.00	19.4850	20.5740	19.5265	12.52	.0366
13	260.00	16.8045	17.5060	16.8390	16.72	.0485
14	280.00	17.5455	18.4585	17.5855	14.73	.0428
15	300.00	15.2315	16.2950	15.2740	13.30	.0386
16	320.00	18.3275	19.2080	18.3575	11.12	.0323
17	340.00	19.3365	20.2410	19.3555	6.28	.0182

RUN = 11

INITIATOR = .020M/L EMULSIFIER = .010M/L MONOMER/WATER = 4/10

TEMPERATURE = 50 C RESICENCE TIME = 30.00MIN

NO	TIME	PLATE-1	PLATE-2	PLATE-3	CONVERS.	FCL.VOLUME
1	30.00	17.7220	19.0220	17.7560	13.21	.0241
2	40.00	15.4655	16.5085	15.5190	23.72	.0504
3	60.00	16.9335	18.2410	17.0445	34.27	.0857
4	80.00	13.8330	14.7850	13.9140	31.74	.0855
5	100.00	14.1195	15.3515	14.2095	25.90	.0723
6	120.00	19.1275	20.2270	19.1995	19.09	.0543
7	140.00	12.7845	13.8550	12.9255	12.12	.0348
8	160.00	16.5675	17.7720	16.6000	7.83	.0226
9	180.00	16.3220	17.6350	16.3735	12.36	.0357
10	200.00	16.0905	17.1330	16.1590	22.19	.0642
11	220.00	12.2305	13.2170	12.2970	22.80	.0660
12	240.00	19.4850	20.4865	19.5415	18.71	.0542
13	260.00	16.8050	17.9585	16.8490	11.93	.0346
14	280.00	17.5460	18.7315	17.5760	7.16	.0208
15	300.00	15.2320	16.3230	15.2605	7.47	.0216
16	320.00	18.3280	19.4590	18.4000	21.40	.0620

RUN = 12

INITIATOR = .020M/L EMULSIFIER = .060M/L MONOMER/WATER = 4/10

TEMPERATURE = 50 C RESICENCE TIME = 30.00MIN

NO	TIME	PLATE-1	PLATE-2	PLATE-3	CONVERS.	FCL.VOLUME
1	20.00	17.7226	18.9430	17.7310	0.00	0.0000
2	40.00	15.4650	16.7035	15.5865	43.90	.0926
3	60.00	20.4985	21.4660	20.7135	62.11	.1539
4	80.00	18.7255	19.9525	18.9545	69.12	.1844
5	100.00	14.1180	15.3690	14.3715	72.70	.2010
6	120.00	19.1265	20.2940	19.3685	73.07	.2057
7	140.00	19.4170	20.6320	19.6765	74.74	.2123
8	160.00	16.9335	17.9995	17.1605	74.13	.2116
9	180.00	16.3205	17.5655	16.5850	73.75	.2110
10	200.00	16.0905	17.3770	16.3605	72.69	.2082
11	220.00	18.1990	19.2805	18.4330	75.08	.2152
12	240.00	19.4840	20.7695	19.7600	74.43	.2134
13	260.00	16.8030	17.9840	17.0645	76.65	.2198
14	280.00	17.5460	18.9030	17.8445	77.49	.2222
15	300.00	15.2320	16.4650	15.5020	76.00	.2180
16	320.00	18.3275	19.5360	18.5425	73.01	.2094
17	340.00	19.3370	20.4830	19.5460	75.36	.2161
18	360.00	16.7755	17.9170	17.0220	74.96	.2147

RUN = 13

INITIATOR = .015M/L EMULSIFIER = .060M/L MONOMER/WATER = 4/10
TEMPERATURE = 50 C RESICENCE TIME = 30.00MIN

NO	TIME	PLATE-1	PLATE-2	PLATE-3	CONVERS.	FCL.VOLUME
1	20.00	17.7215	18.7295	17.7410	9.19	.0128
2	40.00	15.4655	16.6240	15.6130	58.88	.1243
3	60.00	20.4985	21.7850	20.7245	70.41	.1747
4	80.00	18.7255	19.7110	18.9290	77.41	.2067
5	100.00	14.1185	15.3075	14.3745	77.91	.2156
6	120.00	19.1270	20.2105	19.3545	74.38	.2096
7	140.00	12.7830	13.9395	13.0165	70.61	.2008
8	160.00	19.0550	20.0575	19.2545	69.17	.1976
9	180.00	16.3200	17.2890	16.5165	70.41	.2016
10	200.00	16.0905	17.2085	16.3170	70.25	.2014
11	220.00	18.1995	19.2810	18.4130	68.26	.1958
12	240.00	19.4850	20.6055	19.7110	69.84	.2004

RUN = 15

INITIATOR = .010M/L EMULSIFIER = .010M/L MONOMER/WATER = 4/10
TEMPERATURE = 50 C RESICENCE TIME = 30.00MIN

NO	TIME	PLATE-1	PLATE-2	PLATE-3	CONVERS.	FCL.VOLUME
1	20.00	21.2535	22.4447	21.2583	1.59	.0022
2	40.00	18.5118	19.5346	18.5785	31.43	.0669
3	60.00	17.6378	18.7935	17.7565	42.58	.1067
4	80.00	15.5275	16.6370	15.6646	47.73	.1288
5	100.00	16.3890	16.9955	16.4645	46.33	.1297
6	120.00	13.3120	14.0500	13.4015	44.26	.1261
7	140.00	16.0044	17.4357	16.1719	42.26	.1215
8	160.00	15.7208	16.8510	15.8469	40.02	.1156
9	180.00	17.3191	18.4175	17.4295	35.81	.1037
10	200.00	16.9152	18.0172	17.0244	35.24	.1022
11	220.00	15.8135	16.8645	15.9328	40.56	.1177
12	240.00	18.1906	19.4605	18.3475	44.27	.1285
13	260.00	15.8702	17.3015	16.0103	44.37	.1288
14	280.00	16.8303	17.9205	16.9632	43.65	.1267
15	300.00	18.1345	19.1100	18.2455	40.64	.1180
16	320.00	18.4677	19.5994	18.5934	39.63	.1151
17	340.00	15.1232	16.4180	15.2622	38.25	.1111
18	360.00	19.1220	20.1750	19.2339	37.95	.1099

RUN = 16

INITIATOR = .020M/L EMULSIFIER = .010M/L MONOMER/WATER = 4/10
TEMPERATURE = 50 C RESICENCE TIME = 30.00MIN

NO	TIME	PLATE-1	PLATE-2	PLATE-3	CONVERS.	FCL.VOLUME
1	20.00	14.3950	15.7482	14.4460	26.72	.0374
2	40.00	16.9137	18.2000	17.0505	51.56	.1096
3	60.00	15.1223	16.5405	15.3520	67.41	.1686
4	80.00	15.0534	15.9535	15.2615	90.06	.2426
5	100.00	16.5892	17.9624	16.9320	93.88	.2622
6	120.00	18.4665	19.6440	18.7660	93.94	.2672
7	140.00	17.5890	18.6920	17.8670	92.19	.2646
8	160.00	13.9853	15.3572	14.3375	93.50	.2696
9	180.00	21.2518	22.6015	21.5920	91.53	.2646
10	200.00	17.6348	18.7060	17.9050	91.49	.2648
11	220.00	15.5271	16.7975	15.8480	91.56	.2652

RUN = 17

INITIATOR = .020M/L EMULSIFIER = .010M/L MONOMER/WATER = 4/10
TEMPERATURE = 50 C RESICENCE TIME = 30.00MIN

NO	TIME	PLATE-1	PLATE-2	PLATE-3	CONVERS.	FCL.VOLUME
1	20.00	16.9129	18.1500	16.9455	19.02	.0252
2	40.00	18.4677	19.7774	18.6080	51.94	.1104
3	60.00	17.5930	18.8158	17.7960	70.03	.1751
4	80.00	15.1221	16.5335	15.4555	92.06	.2480
5	100.00	13.9667	15.0215	14.2440	93.49	.2611

6	120.00	15.0535	16.4533	15.4105	94.19	.2679	
7	140.00	17.6356	18.9000	17.9610	94.18	.2703	
8	160.00	14.3950	15.6270	14.7315	94.49	.2736	
9	180.00	16.5903	17.6251	16.8575	93.82	.2712	
10	200.00	16.0032	17.3400	16.3480	93.60	.2709	
11	220.00	15.5266	16.6410	15.4160	94.19	.2728	
12	240.00	15.8127	16.8204	16.0705	92.73	.2686	
13	260.00	16.8304	18.1940	17.1210	76.96	.2227	

RUN = 18

INITIATOR = .010M/L EMULSIFIER = .060M/L MONOMER/WATER = 4/10
TEMPERATURE = 50 C RESIDENCE TIME = 30.00MIN

NO	TIME	PLATE-1	PLATE-2	PLATE-3	CONVERS.	FCL.VOLUME
1	20.00	18.1834	19.4980	18.1990	3.78	.0053
2	40.00	15.7151	17.1340	15.8070	27.59	.0583
3	60.00	17.3172	18.7555	17.4605	37.78	.0938
4	80.00	18.5100	19.7940	18.6565	40.53	.1083
5	100.00	15.6385	16.7450	15.7820	44.96	.1246
6	120.00	21.2513	22.4268	21.4096	45.97	.1297
7	140.00	15.4552	16.6260	15.6095	44.41	.1264
8	160.00	19.1034	20.2036	19.2475	43.88	.1255
9	180.00	15.8510	17.0115	16.0015	43.28	.1241
10	200.00	16.9144	18.0925	17.0650	42.52	.1220
11	220.00	17.6751	18.7567	17.8041	39.29	.1128
12	240.00	16.8966	17.9440	17.0195	38.55	.1107
13	260.00	16.8732	18.1442	17.0105	35.06	.1007
14	280.00	17.0477	18.1600	17.1620	33.08	.0951
15	300.00	16.6160	17.8980	16.7345	29.22	.0840
16	320.00	16.6851	19.9485	16.8010	28.96	.0832
17	340.00	18.1657	19.5345	18.2935	29.57	.0850
18	360.00	19.4844	20.6400	19.6035	33.19	.0954
19	380.00	17.9408	19.0000	18.0540	34.62	.0995
20	400.00	17.1305	18.3732	17.2595	33.47	.0962
21	420.00	17.1303	18.2245	17.2440	33.51	.0963

RUN = 19

INITIATOR = .010M/L EMULSIFIER = .060M/L MONOMER/WATER = 4/10
TEMPERATURE = 50 C RESIDENCE TIME = 30.00MIN

NO	TIME	PLATE-1	PLATE-2	PLATE-3	CONVERS.	FCL.VOLUME
1	20.00	16.6220	17.8780	16.6255	0.00	0.0000
2	40.00	17.1368	18.3069	17.2110	26.90	.0568
3	60.00	15.7208	16.8494	15.8480	43.44	.1079
4	80.00	18.1895	19.4900	18.3580	46.75	.1250
5	100.00	17.1323	18.3926	17.3065	48.89	.1355
6	120.00	15.4717	16.4285	15.6065	48.34	.1363
7	140.00	18.6868	19.7952	18.8390	46.50	.1324
8	160.00	15.6388	16.8192	15.7975	45.18	.1292
9	180.00	19.4858	20.8206	19.6565	43.16	.1237
10	200.00	16.9299	18.3452	17.1090	42.04	.1207
11	220.00	17.9448	19.0947	18.0905	42.07	.1208
12	240.00	21.2496	22.4635	21.4090	42.98	.1235
13	260.00	15.8666	17.0979	16.0270	43.38	.1246
14	280.00	18.5078	19.7280	18.6685	43.91	.1262
15	300.00	16.8716	18.1243	17.0345	44.49	.1278
16	320.00	19.1194	20.4315	19.2930	44.14	.1268
17	340.00	17.6502	18.9202	17.8510	43.55	.1251
18	360.00	18.1646	19.5306	18.3405	42.81	.1230
19	380.00	16.8955	18.2308	17.0705	43.67	.1255

RUN = 20

INITIATOR = .005M/L EMULSIFIER = .010M/L MONOMER/WATER = 4/10
TEMPERATURE = 50 C RESIDENCE TIME = 30.00MIN

NO	TIME	PLATE-1	PLATE-2	PLATE-3	CONVERS.	FCL.VOLUME
1	20.00	12.7521	13.9640	12.7536	0.00	0.0000
2	40.00	12.5302	13.9674	12.5820	17.05	.0363

3	60.00	15.4225	16.6400	15.5050	27.92	.0700
4	80.00	13.8126	14.9432	13.9035	30.97	.0834
5	100.00	12.7295	14.0596	12.9365	29.74	.0833
6	120.00	11.5028	12.7874	11.6020	27.97	.0798
7	140.00	16.5211	17.5233	16.5910	24.92	.0717
8	160.00	15.6716	16.8406	15.7435	21.73	.0628
9	180.00	14.2152	15.4070	14.2775	18.25	.0529
10	200.00	16.7376	17.7643	16.7840	15.54	.0451
11	220.00	10.3377	11.5906	10.3860	13.73	.0399
12	240.00	13.9847	15.1000	14.0280	13.23	.0384
13	260.00	15.5472	16.8944	15.6085	15.70	.0456
14	280.00	15.3287	16.4530	15.3905	19.20	.0558
15	300.00	14.0393	15.0675	14.0950	18.91	.0549
16	320.00	13.8232	14.9933	13.9955	18.73	.0544
17	340.00	13.6736	15.0500	13.7420	17.25	.0501
18	360.00	14.9766	16.1728	15.0310	15.69	.0456
19	380.00	14.8191	16.1566	14.8735	13.91	.0404
20	400.00	14.9598	16.2380	15.0450	12.37	.0359
21	420.00	15.1126	16.2108	15.1530	12.47	.0363
22	440.00	17.8796	19.1279	17.9335	14.84	.0431
23	460.00	16.5786	17.7890	16.6475	19.92	.0579

RUN = 21

INITIATOR = .015M/L EMULSIFIER = .010M/L MONOMER/WATER = 4/10
TEMPERATURE = 50 C RESIDENCE TIME = 30.00MIN

NO	TIME	PLATE-1	PLATE-2	PLATE-3	CONVERS.	FCL.VOLUME
1	20.00	15.7195	16.6265	15.7415	16.76	.0235
2	40.00	19.4855	20.5475	19.5425	44.30	.0942
3	60.00	15.4710	16.4690	15.5965	52.16	.1306
4	80.00	19.1195	20.2080	19.2770	55.84	.1506
5	100.00	16.9300	17.7575	17.0635	60.18	.1683
6	120.00	18.6865	19.7450	18.8645	61.65	.1755
7	140.00	17.0470	18.1710	17.2430	63.40	.1822
8	160.00	18.1650	19.1735	18.3535	67.76	.1956
9	180.00	16.8960	17.9180	17.1045	73.95	.2140
10	200.00	17.3155	18.5100	17.5905	83.59	.2422
11	220.00	16.8725	17.9000	17.1105	84.05	.2437
12	240.00	18.1880	19.4535	18.4875	85.89	.2491
13	260.00	17.1315	18.2025	17.3585	76.72	.2225

RUN = 22

INITIATOR = .015M/L EMULSIFIER = .060M/L MONOMER/WATER = 4/10
TEMPERATURE = 50 C RESIDENCE TIME = 30.00MIN

NO	TIME	PLATE-1	PLATE-2	PLATE-3	CONVERS.	FCL.VOLUME
1	20.00	15.6386	16.7892	15.6475	.23	.0003
2	40.00	17.1307	18.2977	17.2605	50.91	.1675
3	60.00	17.6903	18.8103	17.8755	65.94	.1636
4	80.00	18.5084	19.7584	18.7615	75.80	.2024
5	100.00	21.2495	22.3195	21.4885	81.04	.2243
6	120.00	15.7184	16.7367	15.9555	83.11	.2342
7	140.00	18.1655	19.1430	18.3935	81.30	.2212
8	160.00	19.4855	20.7645	19.7900	83.97	.2396
9	180.00	16.6182	17.9660	16.9415	84.33	.2415
10	200.00	17.9454	19.3193	18.2680	82.33	.2360
11	220.00	15.4717	16.6646	15.7520	82.33	.2362
12	240.00	18.1881	19.4372	18.4705	78.97	.2266
13	260.00	17.0462	18.1255	17.2845	76.90	.2207
14	280.00	16.9299	18.0791	17.1715	73.04	.2098
15	300.00	19.1196	20.2181	19.3475	71.98	.2068
16	320.00	17.3159	18.5703	17.5770	72.23	.2074
17	340.00	18.6858	19.7648	18.9105	71.98	.2066
18	360.00	16.8954	18.0611	17.1340	70.93	.2036
19	380.00	16.8723	18.2366	17.1545	71.74	.2060
20	400.00	17.1322	18.1730	17.3499	72.24	.2074

RUN = 23

INITIATOR = .005M/L EMULSIFIER = .060M/L MONOMER/WATER = 4/10
TEMPERATURE = 50 C RESICENCE TIME = 30.00MIN

NO	TIME	PLATE-1	PLATE-2	PLATE-3	CONVERS.	FCL.VOLUME
1	80.00	19.1181	20.3127	19.2320	33.31	.0891
2	100.00	17.9443	19.1774	18.0925	41.59	.1153
3	120.00	19.4850	20.5135	19.6100	41.24	.1165
4	140.00	16.9294	18.0123	17.0525	37.89	.1080
5	160.00	17.0454	18.1783	17.1635	34.15	.0978
6	180.00	16.8017	17.9143	16.8990	31.00	.0890
7	200.00	17.1311	18.4504	17.2410	26.16	.0752
8	220.00	16.6162	17.7533	16.6955	21.08	.0606
9	240.00	17.1306	18.2602	17.2139	22.09	.0635
10	260.00	21.2502	22.4787	21.3394	22.14	.0637
11	280.00	18.1651	19.2624	18.2464	22.69	.0653
12	300.00	16.8959	17.9964	16.9812	23.97	.0689
13	320.00	17.7200	18.9042	17.8125	24.19	.0696
14	340.00	17.6906	19.0050	17.7960	24.97	.0718
15	360.00	19.1263	20.3905	19.2231	23.62	.0679
16	380.00	14.1185	15.0605	14.1862	21.86	.0629
17	400.00	18.1887	19.3730	18.2798	23.75	.0683

RUN = 24

INITIATOR = .010M/L EMULSIFIER = .040M/L MONOMER/WATER = 4/10
TEMPERATURE = 50 C RESICENCE TIME = 30.00MIN

NO	TIME	PLATE-1	PLATE-2	PLATE-3	CONVERS.	FCL.VOLUME
1	20.00	17.5443	18.8203	17.5530	1.43	.0020
2	45.00	20.4972	21.7142	20.5995	36.59	.0818
3	60.00	17.8525	19.1050	18.0005	47.17	.1175
4	80.00	19.4822	20.6343	19.6400	51.07	.1370
5	100.00	18.6860	20.0459	18.8780	50.75	.1412
6	120.00	14.7949	16.0900	14.9745	48.83	.1383
7	140.00	16.8715	18.1455	17.0455	47.56	.1359
8	160.00	16.5649	17.6952	16.7135	45.41	.1304
9	180.00	18.1981	19.4189	18.3570	44.80	.1290
10	200.00	16.7732	18.1100	16.9470	44.69	.1288
11	220.00	18.7240	19.9391	18.8360	45.89	.1323
12	240.00	19.3342	20.6715	19.5130	46.02	.1327
13	260.00	12.7817	14.1727	12.9675	45.96	.1326
14	280.00	16.0884	17.4033	16.2595	44.67	.1289
15	300.00	15.4710	16.7666	15.6328	42.72	.1233
16	320.00	18.3253	19.6847	18.4947	42.61	.1230
17	340.00	17.6478	18.7413	17.7775	40.38	.1165
18	360.00	19.0531	20.3304	19.2040	40.20	.1160
19	380.00	15.2294	16.5013	15.3873	42.44	.1225
20	400.00	16.3183	17.5975	16.4771	42.44	.1225

RUN = 25

INITIATOR = .010M/L EMULSIFIER = .020M/L MONOMER/WATER = 4/10
TEMPERATURE = 50 C RESICENCE TIME = 30.00MIN

NO	TIME	PLATE-1	PLATE-2	PLATE-3	CONVERS.	FCL.VOLUME
1	20.00	19.4842	20.9307	19.4880	0.00	0.0000
2	40.00	16.5665	17.8774	16.6430	27.24	.0579
3	60.00	15.2309	16.4860	15.3625	42.81	.1071
4	80.00	16.3202	17.6678	16.4895	47.88	.1290
5	100.00	16.1988	19.3518	18.3435	46.04	.1286
6	120.00	19.3342	20.4144	19.4660	43.86	.1247
7	140.00	16.8716	17.9710	16.9855	40.43	.1160
8	160.00	17.5439	18.6660	17.6630	37.31	.1076
9	180.00	17.6484	18.9878	17.7900	34.28	.0991
10	200.00	18.6667	20.0235	18.8196	34.67	.1003
11	220.00	16.0900	17.2935	16.2200	37.84	.1096
12	240.00	15.4713	16.7243	15.6180	41.19	.1193
13	260.00	18.7243	20.0811	18.9945	44.28	.1283
14	280.00	16.9311	18.1143	17.0815	44.93	.1301

15	300.00	18.2231	19.3030	18.3605	44.94	.1302
16	320.00	18.3255	19.5161	18.4740	44.01	.1275
17	340.00	12.2287	13.4446	12.3755	42.53	.1232
18	360.00	17.8530	19.1038	18.0075	43.56	.1262
19	380.00	14.7955	15.9730	14.9355	41.85	.1213

RUN = 26

INITIATOR = .010M/L EMULSIFIER = .010M/L MONOMER/WATER = 4/10
TEMPERATURE = 50 C RESICENCE TIME = 20.00MIN

NO	TIME	PLATE-1	PLATE-2	PLATE-3	CONVERS.	FCL.VOLUME
1	15.00	15.5928	16.7416	15.6065	6.93	.0105
2	30.00	15.2154	16.2615	15.2740	25.30	.0369
3	45.00	13.2900	14.3740	13.3785	32.35	.0839
4	60.00	12.1325	13.0945	12.2047	27.77	.0766
5	75.00	13.3755	14.4148	13.4572	28.32	.0803
6	90.00	15.2538	16.4685	15.3330	22.92	.0658
7	105.00	13.7815	14.8810	13.8395	18.14	.0524
8	120.00	10.5386	11.5468	10.5795	13.56	.0393
9	135.00	16.3880	17.4955	16.4258	11.15	.0323
10	150.00	14.7365	15.7545	14.7696	10.55	.0306
11	165.00	11.9289	12.9635	11.9615	10.17	.0295
12	180.00	19.1534	20.1435	19.1902	12.27	.0356
13	195.00	16.4770	17.4532	16.5271	17.51	.0508
14	210.00	13.3090	14.4082	13.3715	19.56	.0568
15	225.00	13.9340	15.0520	13.9905	17.21	.0500
16	240.00	12.3165	13.0855	12.3545	16.80	.0488
17	255.00	13.5830	14.5145	13.6340	13.84	.0402
18	270.00	15.9985	16.9905	16.0342	11.83	.0343
19	285.00	13.0905	14.2100	13.1240	9.58	.0278
20	300.00	14.0790	15.2590	14.1191	11.08	.0322

RUN = 27

INITIATOR = .020M/L EMULSIFIER = .010M/L MONOMER/WATER = 4/10

TEMPERATURE = 50 C RESICENCE TIME = 20.00MIN

NO	TIME	PLATE-1	PLATE-2	PLATE-3	CONVERS.	FCL.VOLUME
1	15.00	16.5668	17.8684	16.5750	2.23	.0034
2	30.00	18.7250	19.9822	18.8226	34.97	.0785
3	45.00	17.8539	19.1685	18.0077	46.37	.1200
4	60.00	19.4834	20.6762	19.6383	48.52	.1335
5	75.00	18.6668	19.7734	18.8247	46.01	.1302
6	90.00	16.9315	18.1177	17.0707	41.81	.1198
7	105.00	19.3345	20.5305	19.4567	35.89	.1034
8	120.00	16.3187	17.6010	16.4215	27.60	.0798
9	135.00	15.4708	16.6152	15.5518	24.07	.0697
10	150.00	17.5432	18.6346	17.6329	28.29	.0819
11	165.00	14.7900	16.0665	14.9163	34.50	.0999
12	180.00	17.6443	18.9805	17.7675	34.76	.1007
13	195.00	18.1945	19.3118	18.2968	31.75	.0920
14	210.00	16.0853	17.2550	16.1769	26.83	.0778
15	225.00	16.8676	18.0603	16.9510	23.72	.0687
16	240.00	15.2260	16.5555	15.3327	27.55	.0798
17	255.00	18.3221	19.4575	18.4312	33.43	.0969
18	270.00	12.7783	14.0291	12.9005	34.02	.0986
19	285.00	17.3119	18.6107	17.4301	31.54	.0914
20	300.00	12.2244	13.3052	12.3115	27.64	.0802

RUN = 28

INITIATOR = .010M/L EMULSIFIER = .040M/L MONOMER/WATER = 4/10
TEMPERATURE = 50 C RESICENCE TIME = 20.00MIN

NO	TIME	PLATE-1	PLATE-2	PLATE-3	CONVERS.	FCL.VOLUME
1	45.00	14.6160	15.7494	14.6729	17.18	.0441
2	60.00	13.8447	15.1415	13.9725	34.94	.0955
3	75.00	13.8882	15.1229	14.0110	34.14	.0962
4	90.00	15.8929	17.1167	16.0155	33.93	.0966
5	105.00	14.1720	15.4364	14.2395	30.98	.0889

6	120.00	13.2017	14.3707	13.3125	28.39	.0617
7	135.00	17.2089	18.5368	17.3130	25.42	.0733
8	150.00	16.6186	17.9300	16.7132	23.07	.0665
9	165.00	16.5585	17.9825	16.6500	21.94	.0633
10	180.00	16.5632	17.7321	16.6442	22.00	.0635
11	195.00	14.9191	16.0707	15.0007	22.58	.0652
12	210.00	14.2687	15.5504	14.3910	24.17	.0697
13	225.00	14.8544	15.4020	14.9278	25.04	.0723
14	240.00	15.4509	16.6448	15.5430	24.92	.0719
15	255.00	15.1014	16.0924	15.1751	23.89	.0689
16	270.00	13.8424	15.1500	13.9368	23.06	.0666
17	285.00	15.8000	16.9900	15.8775	22.67	.0654

RUN = 29

INITIATOR = .020M/L EMULSIFIER = .040M/L MONOMER/WATER = 4/10
TEMPERATURE = 50 C RESIDENCE TIME = 20.00MIN

NO	TIME	PLATE-1	PLATE-2	PLATE-3	CONVERS.	FCL.VOLUME
1	15.00	16.9138	18.1537	16.9210	0.00	0.0000
2	30.00	17.1566	18.3932	17.1872	7.37	.0164
3	45.00	16.0030	17.1571	16.1335	42.68	.1099
4	60.00	18.5467	19.7564	18.7215	52.23	.1429
5	75.00	15.1213	16.4608	15.3300	55.04	.1547
6	90.00	17.6344	18.9468	17.8350	53.17	.1514
7	105.00	14.3938	15.6573	14.5742	49.04	.1405
8	120.00	16.8283	17.9803	16.9780	44.09	.1267
9	135.00	17.5282	18.6580	17.6645	40.55	.1166
10	150.00	13.1720	14.2572	13.3005	39.69	.1142
11	165.00	18.6619	20.0057	18.9230	40.22	.1158
12	180.00	17.2318	18.4678	17.3800	40.22	.1158
13	195.00	15.5261	16.7672	15.6763	40.64	.1170
14	210.00	15.6114	17.0217	15.9558	40.00	.1152
15	225.00	13.9842	15.0450	14.1128	40.72	.1173
16	240.00	18.4654	19.6446	18.6142	42.57	.1226
17	255.00	15.9148	17.0076	16.0584	44.51	.1282
18	270.00	17.9156	18.9572	18.0499	43.59	.1255

RUN = 30

INITIATOR = .030M/L EMULSIFIER = .010M/L MONOMER/WATER = 4/10
TEMPERATURE = 50 C RESIDENCE TIME = 20.00MIN

NO	TIME	PLATE-1	PLATE-2	PLATE-3	CONVERS.	FCL.VOLUME
1	15.00	16.5889	17.6594	16.6368	26.76	.0436
2	30.00	16.5640	17.6060	16.6978	48.66	.1090
3	45.00	18.6615	19.5948	18.7963	57.15	.1477
4	60.00	16.6198	17.8131	16.8200	62.73	.1723
5	75.00	15.9150	17.0978	16.1505	72.47	.2056
6	90.00	17.9161	19.0910	18.1900	84.70	.2422
7	105.00	20.4975	21.5732	20.7604	88.39	.2543
8	120.00	15.1207	16.3472	15.4200	88.00	.2539
9	135.00	16.9117	18.0133	17.1763	86.41	.2496
10	150.00	17.5267	18.6753	17.7930	83.29	.2408
11	165.00	15.0516	16.3500	15.3042	69.35	.2005
12	180.00	17.6564	18.9194	17.8730	60.81	.1759
13	210.00	17.2309	18.3044	17.3840	50.05	.1446
14	225.00	17.6324	18.8261	17.7887	45.65	.1320
15	240.00	17.5873	18.7663	17.7212	39.27	.1136
16	255.00	15.8110	17.1365	15.9300	30.42	.0880
17	270.00	18.5460	19.6160	18.6310	26.56	.0769
18	285.00	18.4655	19.7620	18.5914	33.15	.0959
19	300.00	16.8240	17.9205	16.9515	39.03	.1130

RUN = 31

INITIATOR = .030M/L EMULSIFIER = .010M/L MONOMER/WATER = 4/10
TEMPERATURE = 50 C RESIDENCE TIME = 20.00MIN

NO	TIME	PLATE-1	PLATE-2	PLATE-3	CONVERS.	FCL.VOLUME
1	15.00	14.6183	15.9327	14.6675	25.76	.0391

2	30.00	18.2258	19.4750	18.3595	48.41	.1085
3	45.00	15.4527	16.5700	15.6128	56.67	.1464
4	60.00	16.2438	17.6740	16.4920	64.99	.1785
5	75.00	17.2102	18.5021	17.4709	73.90	.2087
6	90.00	13.1717	14.5276	13.4990	87.81	.2511
7	105.00	13.8668	14.9961	14.1535	91.93	.2645
8	120.00	17.1562	18.2225	17.4000	82.26	.2373
9	135.00	15.1018	16.2880	15.3390	71.48	.2065
10	150.00	14.2695	15.5358	14.5065	61.92	.1787
11	165.00	14.9200	16.1586	15.1348	61.54	.1779
12	180.00	13.2036	14.4417	13.4239	63.18	.1827
13	195.00	13.9856	15.3132	14.2145	61.15	.1769
14	210.00	16.0023	17.3074	16.1955	52.08	.1506
15	225.00	15.8945	17.2735	16.0744	45.55	.1317
16	240.00	14.1736	15.4190	14.3170	39.86	.1153
17	255.00	14.8558	16.2284	15.0100	38.81	.1123
18	270.00	16.5602	17.7275	16.7115	45.24	.1308
19	285.00	13.8895	15.1207	14.0625	49.29	.1426
20	300.00	13.8436	15.1461	14.0518	56.47	.1633

RUN = 32

INITIATOR = .020M/L EMULSIFIER = .040M/L MONOMER/WATER = 4/10
TEMPERATURE = 50 C RESICENCE TIME = 20.00MIN

NO	TIME	PLATE-1	PLATE-2	PLATE-3	CONVERS.	FCL.VOLUME
1	60.00	14.3933	15.5106	14.4320	9.06	.0248
2	75.00	17.2318	18.3724	17.3915	45.64	.1283
3	90.00	17.9163	19.0248	18.0860	53.26	.1517
4	105.00	15.0929	16.2545	15.2225	48.43	.1387
5	120.00	18.4645	19.7913	18.6250	40.73	.1170
6	135.00	16.5635	17.9200	16.7085	35.41	.1019
7	150.00	15.8107	17.0118	15.9188	29.07	.0837
8	165.00	16.5456	19.7578	18.6142	16.59	.0478
9	180.00	16.6196	17.7774	16.6610	8.80	.0254
10	195.00	15.1208	16.3035	15.1500	4.67	.0134
11	210.00	18.6614	19.9413	18.6842	2.10	.0061
12	225.00	17.6332	18.8638	17.6525	1.31	.0038

RUN = 33

INITIATOR = .020M/L EMULSIFIER = .040M/L MONOMER/WATER = 4/10
TEMPERATURE = 50 C RESICENCE TIME = 20.00MIN

NO	TIME	PLATE-1	PLATE-2	PLATE-3	CONVERS.	FCL.VOLUME
1	45.00	16.5898	17.9175	16.7088	32.89	.0847
2	60.00	17.5275	18.7881	17.7079	51.70	.1414
3	75.00	17.6574	18.9904	17.8659	55.27	.1554
4	90.00	15.8104	16.8509	15.9704	53.51	.1524
5	105.00	17.6329	18.9392	17.8189	48.90	.1401
6	120.00	16.5635	17.8064	16.7278	44.85	.1288
7	135.00	17.2314	18.4426	17.3809	41.59	.1196
8	150.00	18.5454	19.7213	18.6912	41.77	.1202
9	165.00	14.3931	15.5310	14.5408	43.93	.1265
10	180.00	15.0521	16.1957	15.2074	46.16	.1329
11	195.00	17.5878	18.7808	17.7602	49.41	.1423
12	210.00	16.6191	17.9476	16.8017	46.77	.1347
13	225.00	18.6607	19.9952	18.8258	44.98	.1296

RUN = 34

INITIATOR = .025M/L EMULSIFIER = .040M/L MONOMER/WATER = 4/10
TEMPERATURE = 50 C RESICENCE TIME = 20.00MIN

NO	TIME	PLATE-1	PLATE-2	PLATE-3	CONVERS.	FCL.VOLUME
1	15.00	13.1121	14.3042	13.1305	6.06	.0092
2	30.00	14.0800	15.4017	14.2153	44.41	.0991
3	45.00	17.2919	18.5106	17.4664	54.95	.1413
4	60.00	17.3500	18.6317	17.5600	59.55	.1628
5	75.00	16.9125	18.0486	17.1095	61.47	.1727
6	90.00	15.5258	16.3664	15.6796	64.21	.1827

7	105.00	20.4978	21.6933	20.7253	66.59	.1906
8	120.00	14.5900	15.8982	14.8415	67.12	.1926
9	135.00	9.9252	11.1614	10.1665	68.12	.1958
10	150.00	12.0637	13.3219	12.3062	67.16	.1931
11	165.00	14.2138	15.2666	14.4156	66.75	.1920
12	180.00	14.0745	15.2924	14.3080	66.75	.1920
13	195.00	16.8280	18.0685	17.0531	62.91	.1810
14	210.00	14.7357	15.9047	14.9404	60.53	.1742
15	225.00	15.9152	17.1275	16.1192	57.98	.1668
16	240.00	15.2554	16.5129	15.4620	56.49	.1625
17	255.00	15.8002	16.9906	15.9991	57.53	.1655
18	270.00	11.3942	12.6400	11.6016	57.31	.1649
19	285.00	15.1945	16.4431	15.3975	55.45	.1607

RUN = 35

INITIATOR = .020M/L EMULSIFIER = .040M/L MONOMER/WATER = 4/10
TEMPERATURE = 50 C RESICENCE TIME = 20.00MIN

NO	TIME	PLATE-1	PLATE-2	PLATE-3	CONVERS.	FCL.VOLUME
1	45.00	16.7901	18.0859	16.9350	42.16	.1085
2	60.00	15.0789	16.4388	15.2800	53.58	.1466
3	75.00	15.9197	17.2748	16.1366	56.66	.1593
4	90.00	14.5025	15.7625	14.7075	55.93	.1593
5	105.00	14.2041	15.5732	14.4143	54.18	.1552
6	120.00	17.5651	18.9056	17.7645	51.13	.1469
7	135.00	15.0634	16.3244	15.2495	50.62	.1456
8	150.00	13.4982	14.7618	13.6915	52.60	.1514
9	165.00	16.5256	17.7755	16.7245	54.88	.1580
10	180.00	16.6110	17.9543	16.8326	57.05	.1643
11	195.00	11.1683	12.4565	11.3984	59.25	.1706
12	210.00	15.5312	16.7417	15.7426	60.66	.1747
13	225.00	13.8937	15.1675	14.1200	61.78	.1779

RUN = 37

INITIATOR = .020M/L EMULSIFIER = .010M/L MONOMER/WATER = 4/10
TEMPERATURE = 50 C RESICENCE TIME = 20.00MIN

NO	TIME	PLATE-1	PLATE-2	PLATE-3	CONVERS.	FCL.VOLUME
1	15.00	13.7487	15.1095	13.8775	32.89	.0953
2	30.00	14.6485	15.9014	14.8280	50.93	.1476
3	45.00	18.0548	19.2557	18.2552	59.69	.1730
4	60.00	13.2912	14.4305	13.4798	59.20	.1715
5	75.00	15.0910	16.1977	15.2645	56.47	.1637
6	90.00	15.6632	16.8492	15.8318	50.52	.1464
7	105.00	15.6680	16.8715	15.8144	42.91	.1244
8	120.00	14.5670	15.6405	14.6835	38.04	.1102
9	135.00	14.6542	15.8554	14.7944	41.08	.1191
10	150.00	15.8050	16.8226	15.9318	44.01	.1275
11	165.00	14.6341	15.5143	14.7417	43.13	.1250
12	180.00	16.8192	18.0575	16.9600	39.96	.1158
13	195.00	14.2905	15.4698	14.4099	35.34	.1024
14	210.00	11.6750	12.7830	11.7774	32.07	.0929
15	225.00	13.6310	14.8605	13.7419	31.24	.0905
16	240.00	14.2400	15.3875	14.3522	34.05	.0987
17	255.00	13.8980	15.0702	14.0220	37.02	.1073

Table III-2

RUN 15

Reaction Time in Min	Dilution Ratio	Wavelength in Å						
		6500	6000	5500	5000	4500	4000	3500
10	1/3	.150	.153	.153	.156	.154	.152	.150
20	1/6	.249	.258	.262	.264	.264	.256	.246
40	.5/250	.022	.023	.032	.043	.060	.088	.141
	1/250	.049	.064	.082	.105	.140	.192	.279
	1/100	.112	.144	.188	.248	.340	.480	.717
60	0.3/250	.031	.041	.055	.074	.101	.143	.220
	0.3/100	.093	.114	.150	.198	.267	.373	.557
80	0.3/250	.081	.110	.137	.173	.220	.294	.412
	.3/100	.168	.213	.269	.344	.456	.622	.897
100	.2/255	.060	.078	.098	.126	.165	.221	.312
	.2/100	.153	.192	.242	.309	.407	.550	.784
120	.1/250	.038	.051	.065	.080	.102	.134	.183
110	.1/250	.045	.059	.073	.090	.114	.146	.197
	.1/100	.105	.132	.164	.205	.263	.344	.471
160	.1/250	.056	.072	.090	.111	.140	.180	.243
	.1/100	.140	.174	.216	.268	.340	.441	.597
180	.1/250	.055	.070	.087	.107	.134	.172	.229
	.1/100	.138	.171	.209	.260	.329	.424	.567
200	.1/250	.066	.084	.104	.128	.159	.202	.267
	.1/100	.159	.195	.238	.295	.370	.470	.628
220	.1/250	.060	.076	.094	.115	.143	.180	.237
	.1/100	.168	.205	.250	.308	.386	.491	.648
240	.1/250	.071	.089	.108	.132	.164	.206	.270
	.1/100	.174	.212	.257	.315	.394	.501	.658
280	.1/250	.068	.084	.104	.126	.157	.199	.261
	.1/100	.161	.197	.240	.295	.371	.475	.628
320	.1/250	.060	.077	.094	.115	.143	.180	.235
	.1/100	.152	.187	.227	.280	.350	.448	.592

RUN 16

Reaction Time in Min	Dilution Ratio	Wavelength in Å						
		6500	6000	5500	5000	4500	4000	3500
20	.2/100	.009	.017	.022	.027	.034	.041	.057
	.4/100	.018	.026	.033	.042	.055	.076	.112
40	.2/250	.024	.034	.044	.057	.074	.098	.137
	.2/100	.057	.077	.100	.131	.175	.238	.345
60	.2/250	.076	.099	.124	.160	.208	.283	.404
	.2/100	.187	.236	.298	.380	.502	.688	.988
80	.2/500	.086	.109	.138	.176	.228	.300	.417
	.2/250	.172	.216	.272	.347	.452	.601	.837
	.2/100	.436	.537	.677	.861	1.117	1.476	1.957
100	.2/500	.132	.166	.205	.257	.330	.432	.592
	.2/250	.272	.335	.413	.518	.663	.867	1.167
	.2/100	.686	.838	1.032	1.284	1.614	2.006	2.335
120	.2/500	.206	.252	.310	.388	.490	.632	.846
	.2/250	.415	.508	.618	.766	.964	1.232	1.580

RUN 18

Reaction Time in Min	Dilution Ratio	Wavelength in Å						
		6500	6000	5500	5000	4500	4000	3500
40	.4/100	.031	.037	.044	.052	.065	.082	.115
	.2/100	.020	.024	.028	.032	.037	.045	.060
	1.4/100	.089	.105	.124	.151	.192	.258	.376
60	.4/100	.051	.067	.088	.116	.155	.215	.317
	.6/100	.079	.105	.135	.176	.240	.334	.494
80	.4/100	.081	.108	.140	.185	.248	.341	.504
	.2/100	.045	.062	.082	.107	.143	.195	.284
100	.4/100	.122	.157	.202	.263	.350	.484	.708
	.2/100	.065	.088	.110	.144	.140	.260	.377
120	.4/100	.155	.198	.254	.328	.439	.599	.866
	.2/100	.077	.100	.128	.164	.217	.296	.424
160	.4/100	.214	.269	.339	.435	.571	.770	1.085
	.2/100	.104	.133	.168	.217	.283	.380	.536
200	.4/100	.244	.304	.380	.482	.626	.837	1.152
	.2/100	.119	.150	.189	.240	.310	.412	.574
240	.4/100	.250	.310	.388	.490	.633	.838	1.154
	.2/100	.128	.160	.202	.254	.328	.434	.600
280	.4/100	.195	.243	.302	.383	.494	.654	.905
	.2/100	.092	.116	.146	.183	.236	.312	.429
320	.4/100	.148	.184	.231	.292	.379	.503	.702
	.2/100	.070	.091	.114	.144	.186	.244	.338
360	.4/100	.170	.214	.268	.342	.443	.592	.828
	.2/100	.085	.109	.136	.173	.224	.297	.414
400	.4/100	.174	.219	.275	.349	.454	.607	.848
	.2/100	.086	.110	.138	.177	.229	.304	.424

RUN 19

Reaction Time in Min	Dilution Ratio	Wavelength in Å						
		6500	6000	5500	5000	4500	4000	3500
40	.2/100	.08	.014	.017	.022	.026	.034	.049
	.4/100	.016	.023	.030	.037	.048	.066	.099
	.6/100	.024	.032	.040	.040	.069	.096	.146
80	.2/100	.038	.053	.072	.096	.131	.184	.272
	.4/100	.077	.104	.141	.189	.260	.367	.545
120	.2/100	.073	.097	.126	.164	.218	.301	.438
	.4/100	.158	.204	.267	.344	.461	.640	.929
160	.2/100	.042	.058	.074	.096	.126	.169	.240
	.4/100	.110	.141	.180	.232	.304	.411	.584
200	.2/100	.111	.142	.180	.289	.300	.401	.566
	.2/250	.050	.065	.082	.104	.132	.173	.259
240	.2/100	.115	.144	.184	.234	.304	.407	.568
	.3/100	.184	.231	.291	.372	.484	.649	.906
280	.2/100	.115	.147	.184	.235	.306	.408	.573
320	.2/100	.123	.156	.196	.250	.325	.436	.611
360	.2/100	.119	.152	.192	.243	.316	.422	.590
400	.2/100	.119	.152	.191	.243	.316	.421	.591
440	.2/100	.130	.164	.205	.260	.334	.444	.618

RUN 20

Reaction Time in Min	Dilution Ratio	Wavelength in Å						
		6500	6000	5500	5000	4500	4000	3500
40	.2/100	.007	.010	.013	.016	.019	.023	.032
	.4/100	.012	.018	.023	.027	.035	.046	.068
	.8/100	.023	.030	.038	.048	.063	.086	.130
80	.2/100	.041	.056	.074	.098	.130	.179	.262
	.4/100	.082	.110	.145	.192	.258	.358	.524
120	.2/100	.077	.098	.126	.162	.214	.291	.417
	.4/100	.157	.200	.256	.328	.437	.598	.858
160	.2/100	.089	.115	.146	.187	.245	.330	.450
	.4/100	.178	.225	.284	.366	.478	.641	.900
200	.2/100	.080	.102	.129	.163	.210	.275	.380
	.4/100	.172	.214	.268	.338	.435	.574	.789
240	.2/100	.095	.117	.146	.182	.230	.299	402
	.4/100	.183	.226	.279	.347	.439	.569	.764
260	.2/100	.090	.112	.140	.170	.214	.275	.367
280	.2/100	.098	.123	.152	.188	.237	.307	.414
320	.2/100	.094	.118	.146	.184	.234	.305	.416
360	.2/100	.092	.116	.144	.181	.230	.300	.410
400	.2/100	.090	.113	.140	.172	.216	.278	.372
420	.2/100	.091	.113	.139	.170	.212	.269	.358
440	.2/100	.095	.118	.146	.180	.226	.289	.386

RUN 21

Reaction Time in Min	Dilution Ratio	Wavelength in Å						
		6500	6000	5500	5000	4500	4000	3500
15	.4/100	.006	.009	.013	.015	.017	.019	.026
	1/100	.014	.018	.023	.027	.032	.041	.062
30	.2/100	.028	.039	.054	.072	.098	.138	.204
	.2/250	.011	.018	.025	.032	.042	.057	.083
45	.2/100	.079	.105	.139	.183	.244	.336	.490
60	.2/100	.140	.178	.228	.292	.386	.530	.766
75	.2/100	.227	.283	.358	.459	.604	.816	1.151
90	.2/100	.334	.414	.519	.656	.846	1.117	1.518
	.2/250	.136	.168	.212	.268	.347	.458	.633

RUN 22

Reaction Time in Min	Dilution Ratio	Wavelength in Å						
		6500	6000	5500	5000	4500	4000	3500
20	1/100	.015	.017	.020	.020	.019	.017	.016
40	.2/100	.019	.027	.035	.045	.060	.082	.123
60	.2/100	.045	.061	.081	.108	.147	.206	.304
80	.2/100	.088	.115	.150	.196	.262	.362	.536
100	.2/100	.152	.193	.247	.319	.425	.586	.849
120	.2/100	.209	.262	.332	.429	.566	.769	1.088
	.2/250	.086	.109	.137	.177	.233	.313	.448
140	.2/100	.270	.336	.422	.537	.699	.937	1.303
	.2/250	.110	.139	.175	.222	.288	.384	.538
160	.2/250	.140	.174	.218	.273	.352	.464	.641
180	.2/250	.186	.229	.282	.353	.450	.589	.798
200	.2/250	.182	.224	.275	.343	.431	.559	.749
220	.2/250	.209	.254	.310	.381	.477	.610	.809
240	.2/250	.236	.285	.346	.425	.528	.670	.875
260	.2/250	.249	.299	.361	.439	.544	.685	.883
280	.2/250	.219	.263	.317	.385	.474	.593	.760
300	.2/250	.205	.246	.296	.358	.440	.550	.703
320	.2/250	.204	.245	.295	.356	.435	.541	.691
340	.2/250	.188	.224	.272	.326	.397	.496	.631
360	.2/250	.173	.208	.250	.303	.370	.459	.589
380	.2/250	.178	.214	.257	.311	.382	.477	.612
400	.2/250	.178	.214	.259	.313	.385	.485	.625

RUN 23

Reaction Time in Min	Dilution Ratio	Wavelength Å						
		6500	6000	5500	5000	4500	4000	3500
40	2/100	.025	.030	.033	.034	.035	.036	.039
60	2/100	.014	.017	.020	.021	.020	.018	.016
80	1/100	.053	.056	.057	.056	.054	.052	.053
	2/100	.113	.115	.115	.114	.112	.111	.117
100	1/100	.089	.108	.134	.171	.229	.322	.486
120	.5/100	.079	.104	.137	.182	.247	.348	.516
140	.4/100	.084	.112	.147	.194	.261	.364	.536
160	.4/100	.104	.135	.176	.229	.306	.426	.627
180	.2/100	.062	.081	.104	.133	.176	.240	.347
200	.2/100	.063	.081	.104	.133	.175	.237	.338
220	.2/100	.058	.076	.097	.124	.161	.218	.310
240	.2/100	.048	.063	.080	.101	.132	.176	.248
260	.2/100	.041	.053	.069	.086	.112	.148	.208
280	.2/100	.034	.044	.057	.072	.092	.121	.169
300	.2/100	.035	.047	.059	.075	.095	.123	.172
320	.2/100	.036	.047	.059	.074	.093	.120	.165
340	.2/100	.030	.040	.051	.063	.080	.103	.141
360	.2/100	.032	.043	.053	.065	.083	.105	.145

RUN 24

Reaction Time in Min	Dilution Ratio	Wavelength in Å 6500	6000	5500	5000	4500	4000	3500
45	.2/100	.019	.026	.035	.043	.056	.073	.107
60	.2/100	.041	.056	.072	.093	.123	.168	.246
80	.2/100	.065	.087	.113	.147	.195	.267	.390
100	.2/100	.091	.118	.152	.195	.257	.353	.512
120	.2/100	.119	.151	.192	.245	.325	.441	.630
160	.2/100	.151	.190	.240	.306	.398	.534	.750
200	.2/100	.166	.208	.258	.327	.420	.559	.770
240	.2/100	.175	.217	.271	.340	.437	.574	.790
280	.2/100	.165	.204	.257	.317	.405	.534	.732
320	.2/100	.133	.166	.207	.260	.335	.441	.610
360	.2/100	.128	.161	.200	.253	.325	.430	.597
400	.2/100	.138	.172	.215	.270	.348	.461	.638

RUN 25

Reaction Time in Min	Dilution Ratio	Wavelength in Å 6500	6000	5500	5000	4500	4000	3500
30	3/100	.018	.022	.025	.026	.028	.029	.034
40	.2/100	.016	.022	.028	.034	.043	.054	.075
60	.2/100	.039	.054	.072	.094	.126	.171	.250
80	.2/100	.076	.100	.150	.170	.223	.306	.446
100	.2/100	.102	.132	.168	.216	.285	.391	.563
120	.2/100	.129	.163	.207	.265	.349	.474	.675
140	.2/100	.149	.188	.237	.304	.397	.533	.751
160	.2/100	.162	.203	.255	.323	.417	.556	.772
180	.2/100	.168	.209	.261	.327	.422	.557	.768
200	.2/100	.177	.218	.271	.339	.434	.569	.778
240	.2/100	.207	.254	.314	.391	.498	.650	.883
280	.2/100	.228	.279	.344	430	.547	.712	.968
320	.2/100	.248	.303	.374	.464	.590	.770	1.036
360	.2/100	.263	.320	.387	.486	.614	.795	1.064

RUN 26

Reaction Time in Min	Dilution Ratio	Wavelength in Å						
		6500	6000	5500	5000	4500	4000	3500
30	.2/100	.014	.020	.027	.035	.046	.062	.090
45	.2/100	.032	.047	.063	.084	.114	.157	.230
60	.2/100	.052	.071	.094	.123	.163	.223	.328
90	.2/100	.079	.101	.127	.161	.210	.284	.401
120	.2/100	.062	.080	.100	.125	.160	.210	.290
150	.2/100	.036	.048	.059	.072	.091	.113	.153
165	.2/100	.032	.043	.052	.063	.077	.095	.125
180	.2/100	.039	.050	.062	.076	.095	.121	.163
195	.2/100	.050	.064	.081	.102	.129	.168	.234
225	.2/100	.063	.081	.102	.128	.165	.220	.309
255	.2/100	.065	.082	.104	.130	.167	.218	.301
270	.2/100	.064	.081	.102	.127	.162	.210	.288
285	.2/100	.060	.076	.095	.119	.147	.189	.256
300	.2/100	.054	.070	.086	.106	.132	.169	.228

RUN 27

Reaction Time in Min	Dilution Ratio	Wavelength in Å						
		6500	6000	5500	5000	4500	4000	3500
30	.2/100	.019	.028	.038	.050	.068	.094	.140
45	.2/100	.059	.080	.106	.140	.189	.260	.381
60	.2/100	.110	.143	.185	.239	.317	.435	.636
75	.2/100	.140	.178	.225	.289	.383	.523	.749
90	.2/100	.180	.225	.285	.366	.481	.648	.912
120	.2/100	.167	.207	.258	.323	.414	.545	.747
135	.2/100	.185	.228	.282	.352	.448	.584	.790
150	.2/100	.189	.231	.285	.354	.448	.580	.761
165	.2/100	.189	.233	.287	.357	.452	.587	.795
195	.2/100	.163	.198	.244	.303	.386	.503	.684
225	.2/100	.174	.214	.264	.326	.413	.534	.719
240	.2/100	.179	.219	.269	.333	.419	.542	.726
255	.2/100	.187	.230	.284	.353	.447	.580	.784
270	.2/100	.194	.240	.294	.366	.466	.606	.825

RUN 28

Reaction Time in Min	Dilution Ratio	Wavelength in Å						
		6500	6000	5500	5000	4500	4000	3500
45	.6/100	.022	.025	.029	.030	.031	.034	.041
60	.2/100	.019	.027	.035	.043	.056	.074	.107
75	.2/100	.031	.043	.058	.076	.100	.137	.200
90	.2/100	.044	.060	.079	.102	.135	.183	.269
105	.2/100	.056	.074	.096	.124	.163	.221	.321
135	.2/100	.078	.100	.123	.157	.203	.272	.386
165	.2/100	.078	.099	.124	.157	.202	.266	.371
195	.2/100	.074	.095	.119	.151	.192	.253	.351
225	.2/100	.076	.097	.121	.152	.195	.257	.358
255	.2/100	.074	.095	.119	.150	.192	.253	.351

RUN 29

Reaction Time in Min	Dilution Ratio	Wavelength in Å						
		6500	6000	5500	5000	4500	4000	3500
30	.6/100	.020	.023	.025	.025	.023	.020	.019
45	.2/100	.021	.032	.043	.056	.076	.106	.160
60	.2/100	.045	.063	.085	.113	.153	.213	.376
75	.2/100	.079	.106	.139	.182	.244	.336	.494
105	.2/100	.122	.156	.198	.256	.338	.461	.661
135	.2/100	.127	.161	.204	.259	.338	.452	.639
165	.2/100	.118	.150	.190	.241	.312	.417	.582
195	.2/100	.114	.146	.185	.235	.305	.407	.573
225	.2/100	.120	.152	.192	.244	.318	.425	.599
255	.2/100	.127	.161	.203	.258	.334	.449	.627
285	.2/100	.142	.180	.230	.288	.373	.498	.697

RUN 30

Reaction Time in Min	Dilution Ratio	Wavelength in Å 6500	6000	5500	5000	4500	4000	3500
15	.2/100	.016	.012	.014	.017	.021	.030	.052
30	.2/100	.063	.074	.097	.128	.172	.239	.355
45	.2/100	.144	.175	.223	.287	.379	.522	.773
60	.2/100	.237	.286	.358	.461	.612	.832	1.180
90	.2/100	.843	1.005	1.218	1.487	1.812	2.134	2.360
	.1/100	.418	.496	.608	.749	.943	1.208	1.562
120	.1/100	.708	.829	.974	1.154	1.362	1.585	1.776
	.1/250	.275	.318	.380	.458	.560	.693	.866
150	.09/250	.295	.335	.387	.448	.522	.607	.705
180	.1/250	.212	.236	.272	.310	.355	.404	.461
225	.1/250	.145	.162	.188	.216	.252	.300	.366

RUN 31

Reaction Time in Min	Dilution Ratio	Wavelength in Å 6500	6000	5500	5000	4500	4000	3500
15	.2/100	.011	.016	.021	.024	.028	.035	.048
30	.2/100	.046	.064	.085	.113	.151	.210	.305
45	.2/100	.121	.158	.203	.262	.346	.472	.688
75	.2/250	.176	.221	.277	.351	.452	.598	.829
105	.2/250	.493	.593	.717	.876	1.086	1.356	1.676
135	.1/250	.296	.351	.417	.498	.600	.731	.897
165	.1/250	.204	.241	.283	.331	.390	.463	.550
180	.1/250	.184	.216	.253	.295	.347	.407	.482
195	.1/250	.286	.334	.390	.456	.536	.636	.758
225	.2/250	.174	.208	.246	.294	.356	.435	.550
255	.2/250	.150	.181	.217	.262	.321	.401	.520
285	.2/250	.157	.192	.232	.281	.350	.441	.579

RUN 32

Reaction Time in Min	Dilution Ratio	Wavelength in Å 6500	6000	5500	5000	4500	4000	3500
60	1/100	.036	.040	.042	.042	.040	.039	.044
75	.2/100	.027	.038	.052	.068	.092	.129	.196
90	.2/100	.051	.071	.095	.126	.171	.238	.351
105	.2/100	.072	.096	.127	.166	.220	.303	.445
135	.2/100	.082	.106	.136	.174	.229	.313	.451
165	.2/100	.046	.060	.076	.095	.122	.162	.228

RUN 33

Reaction Time in Min	Dilution Ratio	Wavelength in Å 6500	6000	5500	5000	4500	4000	3500
45	.2/100	.017	.024	.030	.036	.044	.057	.084
60	.2/100	.039	.054	.072	.095	.129	.180	.267
75	.2/100	.069	.093	.122	.160	.214	.296	.430
105	.2/100	.111	.143	.181	.232	.306	.419	.603
135	.2/100	.137	.173	.218	.278	.361	.484	.683
165	.2/100	.145	.183	.229	.290	.376	.500	.699

RUN 34

Reaction Time in Min	Dilution Ratio	Wavelength in Å						
		6500	6000	5500	5000	4500	4000	3500
15	1/100	.017	.021	.023	.024	.022	.019	.018
30	.2/100	.021	.031	.042	.054	.073	.102	.153
45	.2/100	.056	.076	.101	.134	.183	.253	.373
60	.2/100	.096	.125	.163	.213	.283	.391	.571
90	.2/100	.213	.268	.339	.434	.571	.771	1.088
120	.2/250	.152	.189	.236	.297	.379	.498	.682
	.2/100	.377	.463	.572	.718	.919	1.200	1.603
150	.2/250	.176	.217	.266	.328	.414	.534	.713
180	.2/250	.159	.194	.237	.291	.363	.463	.608
210	.2/250	.142	.174	.212	.259	.322	.410	.539
240	.2/250	.120	.148	.182	.225	.280	.358	.475
270	.2/250	.110	.136	.167	.205	.256	.328	.438

RUN 35

Reaction Time in Min	Dilution Ratio	Wavelength in Å						
		6500	6000	5500	5000	4500	4000	3500
45	.2/100	.021	.029	.038	.049	.065	.089	.133
60	.2/100	.047	.064	.085	.112	.151	.210	.309
75	.2/100	.083	.110	.143	.187	.252	.346	.510
105	.2/100	.140	.178	.227	.292	.386	.526	.755
135	.2/100	.181	.228	.286	.364	.471	.631	.882
165	.2/100	.222	.275	.343	.430	.554	.730	1.001
195	.2/100	.267	.328	.404	.503	.641	.836	1.132
	.2/250	.096	.122	.150	.185	.235	.304	.412
225	.2/250	.120	.149	.184	.226	.286	.370	.499
255	.2/250	.139	.171	.210	.258	.326	.419	.563
285	.2/250	.186	.228	.277	.339	.425	.545	.722

RUN 36

Reaction Time in Min	Dilution Ratio	Wavelength in Å						
		6500	6000	5500	5000	4500	4000	3500
30	.2/100	.016	.023	.030	.037	.049	.065	.097
45	.2/100	.038	.054	.072	.096	.131	.182	.269
60	.2/100	.072	.096	.126	.164	.219	.302	.442
90	.2/100	.154	.196	.249	.321	.422	.576	.821
120	.2/100	.224	.280	.350	.443	.573	.761	1.057
150	.2/100	.293	.360	.446	.557	.710	.927	1.246
	.2/250	.117	.146	.181	.226	.287	.374	.510
180	.2/250	.124	.154	.190	.234	.295	.379	.510
210	.2/250	.117	.149	.185	.231	.296	.383	.515
240	.2/250	.131	.160	.196	.240	.300	.384	.511
270	.2/250	.132	.162	.199	.244	.305	.392	.520

RUN 37

Reaction Time in Min	Dilution Ratio	Wavelength in Å						
		6500	6000	5500	5000	4500	4000	3500
15	.2/250	.017	.024	.030	.036	.044	.055	.076
30	.2/250	.034	.048	.063	.080	.104	.138	.198
45	.2/250	.064	.084	.106	.135	.175	.234	.338
60	.2/250	.087	.111	.139	.177	.231	.311	.438
90	.2/250	.132	.165	.206	.257	.328	.430	.590
120	.2/250	.141	.173	.212	.260	.326	.417	.556
150	.2/250	.137	.168	.205	.250	.312	.397	.524
180	.2/250	.116	.142	.174	.213	.266	.340	.453
195	.2/250	.120	.148	.180	.222	.277	.354	.470
210	.2/250	.115	.142	.174	.212	.265	.334	.442
240	.2/250	.113	.140	.169	.206	.256	.323	.423
255	.2/250	.132	.162	.198	.242	.300	.382	.506
Base Line		.006	.008	.008	.009	.008	.007	.006

APPENDIX IV

Computer Listings

Two computer listings are given in this Appendix. The first program computes the conversion, number of particles, polymer volume and total interfacial particle area from the total property population balances equations (2.40-2.43) (Comprehensive Model). The second program is used for control studies and is based on equations (2.69-2.73) (Simplified Model). This program linearizes and then discretizes the non-linear model at each sampling interval. Best estimates of the state vector are obtained by using a linear Kalman filter. Then the suboptimal stochastic control problem is solved for a linear-quadratic performance index.

The major symbols used in these programs are defined below or identified with the symbols used in the nomenclature for the different parameters and variables.

T(I)	:	Ith time interval
TNP(I)	:	number of polymer particles
TVP(I)	:	total polymer volume
TAP(I)	:	total polymer area

TXP(I)	:	monomer conversion
FSA(I)	:	free soap concentration
F(I)	:	nucleation rate
RNAD(I)	:	average number of radicals per particle
DNP(I)	:	number average diameter
DWP(I)	:	weight average diameter
XC	:	x_c
RT	:	Θ
CIF	:	$[I]_{feed}$
STF	:	S_F
TMCF	:	M_F
DM	:	d_m
DP	:	d_p
WM	:	M_w
FLTX	:	k_v
AN	:	Na
PI	:	Π
SCM	:	S_{CMC}
SA	:	a_s
DW	:	D_w, diffusion coefficient in water
RKMF	:	k_{fm}
RKP	:	k_p
E	:	ϵ
Z	:	μ

RM	:	m partition coefficient
CMWF	:	M_{wc}
RNA	:	Na
SI	:	a_s
SOLM	:	M_{wc}
RKD	:	fk_d
TH(1)	:	θ_3
TH(2)	:	θ_4
TH(3)	:	θ_0 parameters in equations (5.7-5.9)
TH(4)	:	θ_1
TH(5)	:	θ_2
STT	:	time accounting for induction period
FHMS	:	constant flow rate of a mixture of monomer, water and emulsifier, (S_1)
FHIC	:	constant flow rate of a water solution of initiator, (I_1)
FHIV	:	variable flow rate of an initiator solution, (I_2)
FHSV	:	variable flow rate of an emulsifier solution (S_2)
RTM	:	monomer volume fraction in FHMS
RTH	:	water volume fraction in FHMS
RIN1	:	initiator concentration in FHIC
RIN2	:	initiator concentration in FHIV
RS1	:	emulsifier concentration in FHMS
RS2	:	emulsifier concentration in FHSV

THETA	:	θ
SON	:	monomer concentration
ASOAP	:	free soap area
TSPL	:	sampling interval
VREC	:	reactor working volume
PHI(3,3)	:	Φ matrix in equation (7.25)
DL(3,2)	:	Δ matrix in equation (7.25)
UK1(2,1)	:	$\underline{u}$ in equation (7.25)
YK(3,1)	:	$\underline{y}$ measurements in equation (7.26)
RW(3,3)	:	R_w covariance matrix
RV(3,3)	:	R_v covariance matrix
XKK(3,1)	:	$\hat{x}(K/K)$ in equation (7.27)
GAIN(3,3)	:	K(k) in equation (7.31)
PKK(3,3)	:	P(K/K) in equation (7.29)
Q1(3,3)	:	Q in equation (7.35)
Q2(2,2)	:	R in equation (7.35)
XKD(3,1)	:	desired state vector values
UKD(2,1)	:	desired control vector values

```
      PROGRAM TST (INPUT,OUTPUT,TAPE5=INPUT,TAPE6=OUTPUT)
C*
C*    USING THE AGE DISTRIBUTION FUNCTION IN A CSTR , THIS PROGRAM
C*    COMPUTES ALL IMPORTANT EXTENSIVE PROPERTIES OF OVERALL PARTICLE
C*    POPULATION, CONVERSION, TOTAL POLYMER VOLUME, TOTAL INTERFACIAL
C*    PARTICLE AREA ,ETC. FOR THE CONTINUOUS EMULSION POLYMERIZATION
C*    OF VINYL ACETATE.
C*
      COMMON T(900), TNP(900), TVP(900), TAP(900), TXP(900), FSA(900)
      COMMON F(600), RNAD(600), DNP(600), DWF(600)
     + PI,SCM, RKD, SA, RKP, DW, RKMF,VDIF,E, Z, RM, CMMF
C*
C*    INPUT REQUIRED DATA
C*
      READ(5, 707) XC, RT, CIF, STF, TMCF, DM, DP, VM, WM, FLTX, AN, RK1,
      FLTX = 1.4
      AN = 6.023E23
      PI = 4.0*ATAN(1.0)
      RK1 = (36.*PI)**(1./3.)
      SCM = 4.E-3
C*
C*    INPUT REQUIRED VALUES FOR MODEL S PARAMETERS
C*
      SA = 3.E7
      RKP= 1.8669E7*EXP(-5606./(323.*1.987))
      RKMF = 3.7237E6*EXP(-9895./(323.*1.987))
      VDIF = .268E-15
      RKD = 5.E-6
      DW = 3.2E-7
      E = 15.
      Z = 2.58E-5
C*
C*    CALL SOLVE ROUTINE
C*
      STEP = 10.
      N = 20
      EPS = .5
      CALL SOLVE(N, STEP, EPS, IER)
      N = IER
      WRITE(6, 301)
      DO 709 I = 1, N
  709 T(I) = T(I)/60.
      WRITE(6, 302) (I,T(I),TNP(I),TVP(I),TAP(I),FSA(I),TXP(I),RNAD(I),
     + DNP(I), DWP(I), I = 1, N)
      DO 311 K = 1, N, 4
      CALL PLOTPT(T(K), TXP(K), 4)
  311 CONTINUE
      CALL OUTPLT
      WRITE(6, 305)
      DO 374 K = 1, N, 4
      CALL PLOTPT(T(K), TNP(K), 4)
  374 CONTINUE
      CALL OUTPLT
      WRITE(6, 306)
      DO 393 K = 1, N, 4
      CALL PLOTPT(T(K), FSA(K), 4)
```



```
  393 CONTINUE
      CALL OUTPLT
      WRITE(6, 401)
      DO 105 K = 1, N, 4
      CALL PLOTPT(T(K), TAP(K), 4)
  105 CONTINUE
      CALL OUTPLT
      WRITE(6, 205)
      DO 106 K = 1, N, 4
      CALL PLOTPT(T(K), DNP(K), 4)
  106 CONTINUE
      CALL OUTPLT
      WRITE(6, 206)
      DO 107 K = 1, N, 4
      CALL PLOTPT(T(K), DWP(K), 4)
  107 CONTINUE
      CALL OUTPLT
      WRITE(6, 207)
      DO 108 K = 1, N, 4
      CALL PLOTPT(T(K), RNAD(K), 4)
  108 CONTINUE
      CALL OUTPLT
      WRITE(6, 208)
C*
  301 FORMAT        (1H1, 2X, *NO*, 5X, *TIME*, 7X, *TOTAL N*, 4X,
     + *POL.VOL*, 4X, *PART. AREA*, 4X, *SOAP CON.*, 4X, *CONVERSION*,
     + 4X, *RAD./PART.*, 5X, *NUM.AV.D*, 5X, *WEIG.AV.D*, ///)
  302 FORMAT(I5, F10.2, 6E14.5)
  305 FORMAT(///, 20X, *---CONVERSION VERSUS TIME---*,)
  306 FORMAT(///, 20X, *---TOTAL NUMBER OF PARTICLES VERSUS TIME---*,)
  401 FORMAT(///,20X, *---TOTAL SOAP CONCENTRATION---*,)
  205 FORMAT(///, 20X, *    TOTAL PARTICLE AREA VERSUS TIME    *,)
  206 FORMAT(///, 20X, *    NUMBER AVERAGE DIAMETER VERSUS TIME    *,)
  207 FORMAT(///, 20X, *    WEIGHT AVERAGE DIAMETER VERSUS TIME    *,)
  208 FORMAT(///, 20X, *    AVERAGE NUMBER OF RADICALS PER PARTICLE*,)
  707 FORMAT(5F10.0)
  355 STOP
      END
```

```
      C*      SUBROUTINE SOLVE(N, STEP, EPS, IER)
      C*
      C*      ROUTINE SOLVE COMPUTES ALL EXTENSIVE PROPERTIES OF THE LATEX
      C*      BY SOLVING A SYSTEM OF FOUR INTEGRAL-DIFFERENTIAL EQUATIONS
      C*      SIMULTANEOUSLY USING AN ITERATIVE TECHNIQUE.
            DIMENSION VPHL(600)
            DIMENSION FAC(600), FGST(600)
            DIMENSION VPI(600), PNP(600), XPI(600), OI(600)
            DIMENSION TDES(600), VIG(600), AIG(600), QI(600), EK(600)
            COMMON T(600), TNP(600), TVP(600), TAP(600), TXP(600), FSA(600)
            COMMON F(600), RNAD(600), DNP(600), CNF(600)
            COMMON XC, RT, CIF, STF, TMCF, CM, DP, VM, HM, FLTX, AN, RK1,
           + PI,SCM, RKD, SA, RKP, DW, RKMF,VCIF,EM, Z, RM, CMHF

            T(1) = TNP(1) = TVP(1) = TAP(1) = TXP(1) = FSA(1) = 0.
            PNP(1) = VPI(1) = XPI(1) = QK(1) = QI(1) = TDES(1) = 0.
            VIG(1) = AIG(1) = F(1) = 0.
            RNAD(1) = CNP(1) = DNP(1) = QI(1) = FGST(1) = 0.
            FAC(1) = 1.
            VG = AG = 0.
            FI = (1.-XC)/(1.-XC*(1.-DM/DP))
            CIF = CIF/(RKD*RT + 1.)*AN/FLTX
            STF = STF*SA/FLTX
            TMCF = TMCF/FLTX
            SCM = SCM/FLTX*SA
            CMH = CMHF/FLTX
            RMPC = 4.95
            RM = RMPC/CMHF
            C1 = RM*RKD/(24.*DW*RKMF)*(6./PI)**(2./3.)
            C2 = .PKP*DM*C1**.5/(AN*DP)
            TT = 0.
            J = 1
            LITER = 59
            ICNT = 1
            ICLT = 30
            IAPLM = 40
            EPS1 = 5.E-2
            IST = 0
            CZ = 0.
            DO 1102 I = 1, N
            FAC(I) = 1.
      1102  VPI(I) = XPI(I)=0.
      C*
      C*    START SOLVING THE SYSTEM OF FOUR I-O.E
      C*
            CCL = 14.E-17
            HLP = 1.
        330 J = J + 1
            IF(TXP(J-1) .GT. XC) FI = (1.-TXP(J-1))/(1.-TXP(J-1)*(1.-DM/DP))
            IF(CZ .EQ. 1.) STEP = 90.
        331 TT = TT + STEP
            EX = 1. - EXP(-TT/RT)
            TMC = TMCF*EX
            CI = CIF*EX
            ST = STF*EX
            RI = RKD*CI
```



```
            CON1= C2*(RKD*CIF)**.5*FI/(1.-FI)**(1/3.)
            DC = 1./(C1*EX**2.)
            IF(TNP(J-1) .EQ. 0.) FG = RI
            ITER = 0
      C*
      C*    START THE ITERATIVE SOLUTION
      C*
            IST = IST - 1
            IF(IST .LT. 0) IST = 0
            F(J) = FG
            ZVG = VG
            ZAG = AG
            H = EXP(-(TT-T(J-1))/RT)
            H1 = RT*(1.-H)
        370 TNP(J) = TNP(J-1)*H + FG*H1
            TVP(J) = TVP(J-1)*H + ZVG*H1
            TAP(J) = TAP(J-1)*H + ZAG*H1
            TXP(J) = TXP(J-1)*H + DP*ZVG*H1/(TMC*MP)
            T(J) = TT
            VOR = TMC*(1.-TXP(J))*VM - TVP(J)*FI/(1.-FI) - CMH*VM
            VO1 = VOIF*(XC-TXP(J))/XC
            IF(VO1 .LT. 0.) GO TO 142
            CRD = (6.*VO1/PI)**(1./3.)*1.E9
            AD1 = (4.*PI)**(1./3.)*(3.*VO1)**(2./3.)
            IF(VOR .LE. 0.) VOR = 0.
            ORN = VOR/VO1
            AD = ORN*AD1
            GO TO 143
        142 ORN = CRD = AD = 0.
        143 AP = TAP(J)
            AM = ST - SCM - AP
            FSA(J) = AM/SA
            SUMA = 0.
            SUMX = 0.
            SUMA = 0.
            SUMV = 0.
            SPD = 0.
            SDN = 0.
            SDM = 0.
            SDM1 = 0.
            FGST(J) = STEP*F(J)
            IF(ITER .GT. 0) GO TO 1122
            DO 1124 L = 1, J
            VPHL(L) = VPI(L)
      1124  CONTINUE
      1122  DO 340 L = 2, J
            H1 = T(L-1)
            H = T(L)
            TM = T(J-1)
            FGF = F(L)
            IF(FGF .EQ. 0.) GO TO 430
            PNP(L) = FGST(L)*EXP(-(TT-H)/RT)
            SUMA = SUMA + PNP(L)
            GIN = 2.*PI*(EXP(-(TT-H1)/(RT*2.))*EXP(-(TT+H1)/(2.*RT)) -
           + EXP((TM-H1)/(RT*2.)) - EXP(-(TM+H1)/(2.*RT)))
            LTEST = 0
            IAP = 1
```

```
      SUBROUTINE SCLVE      73/74   TS TRACE
      IF(L-J) 41, 42, 42
   41 FF = FAC(L)
      CON = CON1*FF
      GO TO 79
   42 FF = FAC(L-1)
      FAC(L) = FAC(L-1)
      GO TO 43
   76 CON = CON1*FAC(L)
   78 VPO = 2.*CON*GIN/(T3*FFF**.5)
      VPI(L) = (VPHL(L)**(2./3.) + VPO)**1.5
      CI(L) = (4.*VPI(L)/PI)**(1./3.)
      AREAI = PI*DI(L)**2.*PNP(L) /(1.-FI)**(2./3.)
      IF(LTEST .EQ. 1) GO TO 79
      IAP = IAP + 1
      P1 = FAC(L)
      IF(IAP(J) .LE. 0.) GO TO 17
      FAC(L) = (AREAI/IAP(J))**.5
   17 P2 = FAC(L)
      FTES = ABS(P1**2.-P2**2.)
      IF(FTES .LE. EPS) GO TO 74
      IF(IAP .LE. IAPLM) GO TO 76
      IEP = J-1
      WRITE(6, 28)
   28 FORMAT(20X, *STOP PROGRAM*, )
      GO TO 21
   74 LTEST = 1
      GO TO 76
   79 SUMA = SUMA + AREAI
      SUMV = SUMV + VPI(L)*PNP(L)
      PMC = 1. - PT*(EXP(-H1/RT) - EXP(-TT/PT))/(TT-H1)
      PMC = PMC*TMCF
      XPI(L) = DF*VPI(L)*PNP(L)/(PMC*HP)
      SUMX = SUMX + XPI(L)
      FIN = F(L)
      PIN = FIN*EXP(-(TT-H)/PT)
      VPIN = VPI(L)
      DK(L) = DC*(VPIN/(1.-FI))**(-2./3.)
      IF(DK(L) .EQ. 0.) GO TO 425
      DI(L) = (PI/(PIN*2.*DK(L)))**.5*FAC(L)
      GO TO 426
  425 DI(L) = 0.
  426 TOES(L) = DK(L)*PIN*DI(L)
      VIG(L) = VPIN**(1./3.)*PIN**.5*CON
      AIG(L) = PIN**.5*CON
      SPO = SPO + PIN*DI(L)
      SDN = SDN + PNP(L)*DI(L)
      SDW = SDW + PNP(L)*DI(L)**4.
      SDW1 = SDW1 + PNP(L)*DI(L)**3.
      GO TO 340
  430 PNP(L)=VPI(L)=DI(L)=XPI(L)=DK(L)=CI(L)=TOES(L)=VIG(L)=AIG(L)=0.
      FAC(L) = FAC(L-1)
  340 CONTINUE
C*
      NDIM = J
      CALL TRIN(T, TOES, NDIM)
      CALL TRIN(T, VIG, NDIM)
      CALL TRIN(T, AIG, NDIM)
```

```
      SUBROUTINE SCLVE      73/74   TS TRACE                    FTN 4.6+460      78/08/22.
      AG =       (2./3.)*PK1*(1.-FI)**(-2./3.)*AIG(NDIM)*EX
      VG = VIG(NDIM)*EX
  706 TEST1 = ABS(TNP(J)-SUMN)/SUMN
      XTEST = TXP(J-1)*H + DP*VG*H1/(TMC*HM)
      F1 = RI + TOES(NDIM)
      P = 1.-AP*Z
      P = .55*P
      AM1 = AM
      IF(AM .LE. 0.) GO TO 350
      IF(P .LE. 0.) GO TO 205
      F2 = (1. + E*AP/AM1+ P/AM1)
      F3 = (1.+ E*AP/P + AM1/P)
      F(J) = F1/F2 + F1/F3
      IF(J .LE. 5) GO TO 6
      F(J) = F(J) - COL*F(J)**2.
      IF(F(J) . LT. 0.) F(J) = 0.
      IF(F(J) . LE. 0.) GO TO 135
    6 CZ = 0.
      GO TO 360
  205 F(J) = F1/(1. + E*AP/AM1)
      IF(J .LE. 5) GO TO 6
      F(J) = F(J) - COL*F(J)**2.
      IF(F(J) . LT. 0.) F(J) = 0.
      IF(F(J) . LE. 0.) GO TO 135
      CZ = 0.
      GO TO 360
  350 IF(P-.02) 135, 135, 136
  136 F(J) = F1/(1.+E*AP/P)
      IF(J .LE. 5) GO TO 6
      F(J) = F(J) - COL*F(J)**2.
      IF(F(J) . LT. 0.) F(J) = 0.
      IF(F(J) . LE. 0.) GO TO 135
      CZ = 0.
  933 GO TO 360
  135 FG = 0.
      TNP(J) = SUMN
      TEST1 = 0.
      IF(IST .EQ. 0) CZ = 1.
C*
C*    START  CHECKING FOR CONVERGENCE
C*
      TEST = ABS(XTEST-TXP(J))/XTEST
      GO TO 400
  360 TEST = ABS(FG-F(J))/F(J)
      IF(CZ .EQ. 1.) GO TO 400
      IF((TT-T(J-1)) .EQ. 10.) GO TO 400
  989 TT = TT -STEP
      J = J -1
      STEP = 10.
      FG = F(J-1)
      IST = 30
      GO TO 330
  400 IF(TEST .LE. EPS1 .AND. TEST1 .LE. EPS)  GO TO 390
      FG = F(J)
      ZVG = VG
      ZAG = AG
      ITER = ITER + 1
```

```
      SUBROUTINE SOLVE      73/74   TS TRACE

230               IF(ITER .LE. LITER) GO TO 370
                  EPS1 = EPS1*3.
                  WRITE(6, 410) J, ITER, TT, TNP(J), TXP(J), TAP(J), TVP(J), FG,
                 + FSA(J), DRN, DRO
                  WRITE(6, 635) J, ITER, TT, SUMN, SUMX, SLMA, SUMV
235               HLP = HLP + 1.
                  IF(HLP .LE. 9.) GO TO 989
                  IF(TEST1 .LE. EPS) GO TO 390
                  WRITE(6, 371)
              371 FORMAT(10X, *SOLUTION DOES NOT CONVERGE STOP PROGRAM*,)
240               IER = J-1
                  RETURN
              390 ICNT = ICNT + 1
                  IF(HLP .EQ. 1.) GO TO 391
                  EPS1 = EPS1/(3.*(HLP-1.))
                  HLP = 1.
245           391 WRITE(6, 410) J, ITER, TT, TNP(J), TXP(J), TAP(J), TVP(J), FG,
                 + FSA(J), DRN, DRO
                  WRITE(6, 635) J, ITER, TT, SUMN, SUMX, SLMA, SUMV
                  RNAC(J) = SRO/SUMN
250               DNP(J) = SCN/SUMN*1.E9
                  DWP(J) = SCW/SDW1*1.E9
                  IF(ICNT .EQ. ICLT) GO TO 520
                  GO TO 515
              520 ICNT = 1
255               DO 805 I = 1, J
                  IF(PNP(I) .LE. 0.) GO TO 805
                  WRITE(6, 415)  I, PNP(I), VPI(I),CI(I),XPI(I),DK(I),DI(I),FAC(I)
              805 CONTINUE
                  DO 525 I = 1, J
260               Y = PNP(I)/SUMN
                  IF(Y .EQ. 0.) GO TO 525
                  CALL PLOTPT(DI(I), Y, 4)
              525 CONTINUE
                  CALL OUTPLT
265               TIME = TT/60.
                  WRITE(6, 530) TIME
              515 IF(J .LT. N) GO TO 330
                  IER = J
              415 FORMAT(I10, 7E15.5)
270           410 FORMAT(3X, 2I6, F10.1, 8E13.5)
              635 FORMAT(3X,     2I6, F10.1, 4E13.5,//)
              530 FORMAT(//, 20X, *THE PARTICLE SIZE DISTRIBUTION*, 4X,
                 + *AT TIME = *, F10.4, *  MIN*,)
               21 RETURN
                  END
```

```
      SUBROUTINE TRIN       73/74   TS TRACE                FTN 4.6+460      78/09/22.

                  SUBROUTINE TRIN(X, Y, NDIM)
C*
C*    THIS ROUTINE PERFORMS THE INTEGRATION FOR A GIVEN
C*
 5  C*    GENERAL TABLE OF ARGUMENT AND FUNCTION VALUES.
                  DIMENSION X(1), Y(1)
                  SUM2 = 0.
                  IF(NDIM-1) 4, 3, 1
C*
10  C*
                  INTEGRATION LOOP
                1 DO 2 I = 2, NDIM
                  SUM1 = SUM2
                  SUM2 = SUM2 + .5*(X(I)-X(I-1))*(Y(I)+Y(I-1))
                2 Y(I-1) = SUM1
15              3 Y(NDIM) = SUM2
                4 RETURN
                  END
```

```
PROGRAM TST      73/74   TS TRACE

      PROGRAM TST(INPUT,OUTPUT,PUNCH,TAPE5=INPUT,TAPE6=OUTPUT,
     + TAPE7=PUNCH)
C*
C*****************************************************************
C*                                                               *
C* 1. COMPUTE ALL THE EXTENSIVE PROPERTIES - CONVERSION, NUMBER OF*
C*    PARTICLES, TOTAL PARTICLE INTERFACIAL AREA - OF A LATEX PRODUCT*
C*    FROM A CONTINUOUS EMULSION POLYMERIZATION REACTOR FOR VAC *
C* 2. OBTAIN A DISCRETE MODEL OF THE NONLINEAR SYSTEM            *
C* 3. FIND THE BEST ESTIMATES OF THE STATE VECTOR - KALMAN FILTER*
C* 4. SOLVE THE SUBOPTIMAL CONTROL PROBLEM FOR FEEDBACK CONTROL  *
C*                                                               *
C*****************************************************************
C*
      COMMON/TH/ RKP, RKMF, RNA, DP, DM, SMC1, XC, Z, S1, SOLM, WM,
     + RKC, TH(8), STT, FHMS, FHIC, FHIV, FHSV, RTM,RTH, RIN1, RIN2,
     + RS1, RS2, THETA, SON, RI, ASOAP, C1, E, SMC, TSPL, VREC
      COMMON/THREE/ PHI(3,3), DL(3,2), UK1(2,1), YK(3,1), PH(3,3),
     + PV(3,3), XKK(3,1), GAIN(3,3), PKK(3,3), Q1(3,3),Q2(2, 2),UOP(2,1)
      COMMON/FIVE/ XKO(3, 1), UKO(2,1), SON2, SO2, CI2, T2
C*
C*    INPUT REQUIRED DATA AND PARAMETERS VALUES
C*
      SON2 = SO2 = CI2 = T2 = 0.
      READ(5, 50) DP, DM, WM, XC
      READ(5, 50) FHMS, FHIC, FHIV, FHSV
      READ(5, 50) RTM, RTH, RIN1, RIN2
      READ(5, 50) RS1, RS2, VREC, THETA
      READ(5, 56) ((PHI(I, J), J = 1, 3), I = 1, 3)
      READ(5, 56) ((PV(I, J), J = 1, 3), I = 1,3)
      READ(5, 52) ((Q1(I, J), J = 1, 3), I = 1,3)
      READ(5, 50) ((Q2(I, J), J = 1, 2), I = 1, 2)
      READ(5, 50) UK1(1,1), UK1(2,1), UKO(1,1), UKO(2,1)
      READ(5, 54) XKO(1,1), XKO(2,1), XKO(3,1)
      READ(5, 54) (XKK(I, 1), I = 1, 3)
      READ(5, 52) ((PKK(I, J), J = 1, 3), I = 1, 3)
      RKP = 1.8669E7*EXP(-5606./(323.*1.987))
      RKMF = 3.7237E6*EXP(-9895./(323.*1.987))
      RKO = 5.046E-6
      RNA = 6.023E23
      SOLM = .34
      S1 = 3.E7
      SMC1= 3.2E-3
      Z = 2.E-5
      TH(1) = 6.301
      TH(2) = 489.9
      TH(3) = 7.2
      TH(4) = 556.6
      TH(5) = 58.03
      TH(6) = 4.735
      TH(7) = -.1245
      TH(8) = 2.E-8
      STT = 11.*60.
      TSPL = 5.
      N = 200
C*
C*    CALL SOLVE ROUTINE

PROGRAM TST      73/74   TS TRACE                    FTN 4.6+460     78/08/21. 21.2
C*
C*    CALL SOLVE(N)
C*
C*    PRINT AND PLOT RESULTS
C*
C*    CALL PRIPLT(N)
   50 FORMAT(4F10.0)
   52 FORMAT(E10.1, 8F5.0)
   54 FORMAT(3F10.0)
   56 FORMAT(E10.2, 3F5.0, E10.2, 3F5.0, E10.2)
      STOP
      END
```

```
C*    SUBROUTINE SOLVE(N)
C*
C*    ROUTINE SOLVE CALCULATES ALL EXTENSIVE PROPERTIES OF THE LATEX
C*    CALLS LINOTE - FILTER AND CONTROL ROUTINES
      DIMENSION YI(3), Y(3, 41), RN(20), XX(20), VL(20), RD(20),
     + ARA(20), RES(20), GP(20), IRE(20)
      COMMON/ONE/ T(900), RNP(900), RNAD(900), VOL(900), AREA(900),
     + X(900), FSA(900), AVD(900), FGP(900), IGEN(900)
      COMMON/THREE/ PHI(3,3), DL(3,2), UK1(2,1), XK(3,1), RW(3,3),
     + FV(3,3), XKK(3,1), GAIN(3,3), PKK(3,3), Y1(3,3),D2(2, 2),UDP(2,1)
      COMMON/TWO/ RKO, JKMF, RNA, DP, DM, SMC1, XC(7), S1, SOLN, HH,
     + FKO, TH(4), STT, FHMS, FMIC, FHIV, FHSV, GTH, FTH, RIN1, RIN2,
     + FS1, FS2, THETA, SON, PI, ASOAP, C1, E, SMC, TSPL, VREC
      COMMON/FOUR/ XKNL(3, 1), XKL1(3, 1), XKL(3, 1), PAPT
      COMMON/SEVEN/ XLIDE(200, 3), YMES(200, 3), YFILT(200, 3),
     + XNONL(200, 3), FRIN(200), FREM(300), CININ(200), CINEM(200),LOI
      EXTERNAL F
C*
      DATA N1, N3, STEP, H/3, 1, 60., 3./
      T(1) = RNP(1) = RNAD(1) = VOL(1) = 0.
      AREA(1) = FSA(1) = AVD(1) = X(1) = FGP(1) = 0.
      ALD = ARS= SED= TDES= 0.
      APEA(1) = 1.
      IGEN = 1
      DO 106 K = 1, 20
      RN(K) = XX(K) = VL(K) = RD(K) = 0.
      ARA(K) = RES(K) = GP(K) = 0.
      IRE(K) = 0
  106 CONTINUE
      XKL1(1, 1) = XKL1(2, 1) = XKL1(3, 1) = 0.
      DO 15 I = 1, 200
      DO 15 J = 1, 3
      XLIDE(I, J) = YMES(I, J)= XFILT(I, J) = 0.
   15 CONTINUE
      IGCN(1) = 1
      IRE(1) = 1
      TT = STT
      COUNT = 0.
      ITYPE = 0
      LOI = 0
      NF = 10
      WRITE(6, 301)
      CALL MEASURE(LOI, XKNL, YK)
      CALL CONTROL(LOI, NF)
      CALL ACTION(LOI, UK1)
      CALL BALANCE(TT, LOI, UK1)
C*
C*    START SOLUTION
C*
      DO 20 J = 2, N
      SRN = SXC = SAP = SVL = 0.
      SRD = DES = SGP = 0.
   75 ICNT2 = 0
      TT = TT + STEP
```



```
C*    IF(LOI .EQ. 55). ITYPE = LOI
      IGCN(J) = IGEN
  401 N2 = 1 + IFIX(STEP/H)
      DO 105 IG = 1, IGEN
      YI(1) = RN(IG)
      YI(2) = XX(IG)
      YI(3) = VL(IG)
      DO 22 I = 1, N1
      DO 22 K = 1, N2
      Y(I, K) = 0.
   22 CONTINUE
      LCH = IG
      APS = ARA(IG)
      SED = TDES -RD(IG)*RN(IG)*RES(IG)
      FAC = (ARA(IG)/AREA(J-1))
      IF(FAC .EQ. 0.) FAC = .40
      IF(IGEN .EQ. 1) FAC = 1.0
      SX= X(J-1)
      CALL RKG(F, Y, N1, N2, N3, YI, H)
      RN(IG) = Y(1, N2)
      XX(IG) = Y(2, N2)
      VL(IG) = Y(3, N2)
      RD(IG) = RAD
      APA(IG) = AR
      RES(IG) = RDE
      GP(IG) = FI
      IF(RN(IG) .LT. 0.) RN(IG) = XX(IG) = GP(IG) = 0.
  105 CONTINUE
      DO 32 IG = 1, IGEN
      SRN = SRN + RN(IG)
      SXC = SXC + XX(IG)
      SAP = SAP + APA(IG)
      SVL = SVL + VL(IG)
      SRD = SRD + RD(IG)*RN(IG)
      DES = DES + RD(IG)*RN(IG)*RES(IG)
      SGP = SGP + GP(IG)
   32 CONTINUE
      TDES = DES
      T(J) = TT/60.
      RNP(J) = SRN
      VOL(J) = SVL
      X(J) = SXC
      AREA(J) = SAP
      FGP(J) = SGP
      IF(SRN .LE. 0.) GO TO 505
      RNAD(J) = SRD/SRN
      AVD(J) = (SVL*6./(3.14*SRN))**(1./3.)*1.69
      GO TO 506
  505 RNAD(J) = VCOL= AVD(J) = 0.
  506 ALD = SAP
      SS = (ASOAP-SAP)/S1
      FSA(J) = SS
      IF(SS .LE. SMC/S1) GO TO 500
      IF(SGP .GT. 0.) GO TO 500
      ICNT2 = 1
      IGEN = IGEN + ICNT1*ICNT2
```

```
      SUBROUTINE SOLVE      73/74   TS TRACE
  115                 IRE(IGEN) = J
                      IDF = IRE(IGEN) - IRE(IGEN-1)
                      J1 = J-1
                      IF(J1 .LE. 0) J1 = 1
  120                 FPNR = RNP(J)
                      PSGN = RNP(J)/RNP(J-1)
                      IF(PSGN .LT. 1.) GO TO 906
                      IF(IDF .LE. 10 .OR. FPNR .GT. 0.) GO TO 500
  125               906 IF(IDF .LE. 10 .OR. FPNR .GT. 0.) IGEN = IGEN-1
                    500 CONTINUE
                C*
                C*    COUNT = COUNT + 1.
                      IF(COUNT - TSPL) 701, 702, 702
  130               702 LOI = LOI + 1
                      XMONL(LOI, 1) = XKNL(1, 1) + SRN
                      XMONL(LOI, 2) = XKNL(2, 1) + SVL
                      XMONL(LOI, 3) = XKNL(3, 1) + SXC
                      PART = RNP(J-5)
  135                 CALL LINOTE(SXC, SRO, SAR, DES, UK1, PHI, DL)
                      CALL MEASURE(LOI, XKNL, YK)
                C*
                C*    CALL FILTER
                C*
  140                 CALL CONTROL(LOI, NF)
                      CALL ACTION(LOI, UOP)
                703   CALL BALANCE(TT, LOI, UK1)
                      COUNT = 0.
                C*
                701   CONTINUE
                 20   CONTINUE
  145           301   FORMAT(1H1, 10X, *CONTROL PROBLEM TEST*)
                      RETURN
                      END

      SUBROUTINE F          73/74   TS TRACE                FTN 4.6+460     78/08/21. 21.2
                C*    SUBROUTINE F(XO, XP)
                C*
                C*    COMPUTES THE DN/DT, DX/DT, DV/DT DERIVATIVES FOR THE TOTAL
    5           C*    NUMBER OF PARTICLES, CONVERSION AND POLYMER VOLUME
                C*
                      DIMENSION XO(3), XP(3)
                      COMMON/TW/ RKP, RKMF, RNA, DP, CM, SMC1, XC, Z, S1, SOLM, WM,
                     + RKD, TH(4), STT, FHMS, FHIC, FHIV, FHSV, FTM,PTH, RIN1, RIN2,
   10                 + FS1, FS2, THETA, SON, RI, ASOAP, C1, E, SMC, TSPL, VREC
                      COMMON/FSOV/ VLP, RAD, AR, ALD, ARS, PDE, SED, FI ,ICNT1, ICNT2,
                     + LCH, IGEN, FAC, SX
                C*
                      RI = THETA*60.
   15                 IF(XO(1) .GT. 0.) GO TO 52
                      XP(1) = RI
                      XP(2) = 0.
                      XP(3) = 0.
                      AP = 0.
   20                 SE2 = SMC/S1
                      ICNT1 = 0
                      RAD = 0.
                      GO TO 60
                   52 IF(SX-XC) 54, 54, 55
   25              54 XC1 = XC
                      GO TO 56
                   55 XC1 = SX
                   56 RMP = (1.-XC1)*DM/(1.-XC1*(1.-DM/DP))
                      VMF = RMP/DM
                      VLP = SON*XO(2)/(DP*(1.-VMF))
   30                 R = (3.*VLP/(4.*3.14*XC(1)))**(1./3.)
                      IF(R .LE. 0.) R = 2.5E-8
                      PDE = C1/R**2.
                      AP = (36.*3.14*XO(1))**(1./3.)*VLP**(2./3.)
   35                 AP = ALD-ARS*AP
                   16 RAD = (P1/(2.*PDE*XO(1)))**.5*FAC
                      GVOL = RKP*RMP*RAD*XO(1)/(RNA*DP)
                      CONV = GVOL*DP/SON
                      TDES = SED + PDE*XO(1)*RAD
   40                 CAP = FI + TDES
                      AM = ASOAP -SMC - AP
                C*
                C*    COMPUTE THE TOTAL NUCLEATION RATE
                C*
   45              200 FI = 0.
                      GO TO 360
                   201 AM1 = ASOAP -AP
                      P = 1. - AP*2
                      IF(AM1/S1 .LE. SE2) GO TO 350
   50                 IF(P .LE. 0.) GO TO 205
                      F2 = (1. + E*AP/AM1 + P/AM1)
                      F3 = (1. + E*AP/P + AM1/P)
                      FI = CAP/F2 + CAP/F3
   55                 GO TO 360
                   205 FI = CAP/(1. + E*AP/AM1)
                      GO TO 360
                   350 IF(P-.02) 135, 135, 136

      SUBROUTINE F          73/74   TS TRACE                FTN 4.6+460     78/08/21. 21.26
                   136 FI = CAP/(1. + E*AP/P)
   60                 GO TO 360
                   135 FI = 0.
                      SE2 = 1.1*SMC/S1
                      ICNT2 = 1
                C*
   65              360 XP(1) = -XO(1)/ST + FI
                      XP(2) = -XO(2)/ST + CONV
                      XP(3) = -XO(3)/ST + GVOL
                   60 RETURN
                      END
```

SUBROUTINE BALANCE 73/74. TS TRACE

```
      SUBROUTINE BALANCE(TT, NC, UK1)
C*
C*    INITIATOR, EMULSIFIER, MONOMER BALANCES
C*
      DIMENSION UK1(2, 1)
      COMMON/ITW/ RKP, RKMF, RNA, OD, CP, SMC1, XC, Z, S1, SOLM, HM,
     + FKD, TH(4), SIT, FHMS, FHIC, FHIV, FHSV, RTM, RTM, RIN1, RIN2,
     + RS1, RS2, THETA, SON, RI, ASOAP, C1, E, SMC, ISPL, VREC
      COMMON/FIVE/ XKO(3, 1), UKO(2,1), SON2, SO2, CI2, T2
      COMMON/SEVEN/ XLIDE(200, 3), YMES(200, 3), XFILT(200, 3),
     + XNONL(200, 3), FRIN(200), FREM(300), CININ(200), CINEM(200),LOI
C*
      RMPC = 0.95
      WRITE(6, 105) NC
   22 SON1 = SON2
      SO1 = SO2
      CI1 = CI2
      T1 = T2
C*
      VTTL = FHMS + FHIC   + FHIV + FHSV
      VMON = FHMS*RTM
      VH2O = FHMS*RTM + FHIC + FHIV + FHSV
      CMF2 = VMON/VH2O
      CINF2 = (FHIC*RIN1 + FHIV*RIN2)/VH2O
      CEF2 = (FHMS*RS1*RTM + FHSV*RS2)/VH2O
      FLTX = VTTL/VH2O
      THETA  = VREC/VTTL
      UK1(1, 1) = CINF2
      IF(UK1(1, 1) .LE. 0.) UK1(1, 1) = 1.E-4
      UK1(2, 1) = CEF2
      NC1 = NC + 1
      FRIN(NC1) = FHIV
      FREM(NC1) = FHSV
      CININ(NC1) = CINF2
      CINEM(NC1) = CEF2
C*
      RM = RMPC/SOLM
      FSLP = TH(6) + TH(7)*THETA
      IF(FSLP .LE. .25) FSLP = .25
      A3 = TH(1) - TH(2)*CINF2/FSLP
      IF(A3 .LT. .5) A3 = .5
      DM = TH(8)*A3
      IF(CEF2 .LE. .02) GO TO 707
      E = EXP(TH(3) + TH(5)*(CEF2 - .02))
      GO TO 708
  707 E = EXP(TH(3) + TH(4)*(CEF2 - .02))
  708 CONTINUE
      SMC = SMC1*S1/FLTX
      T2 = TT/60.
      EX = EXP(-(T2-T1)/THETA)
      CI2 = (CINF2 - (CINF2-CI1)*EX)
      SO2 = (CEF2 - (CEF2-SO1)*EX)
      SON2 = (CMF2 - (CMF2-SON1)*EX)
      WRITE(6, 106) T2, FHMS, FHIC, FHIV, FHSV, CINF2, CEF2, CMF2,
     +THETA, DM, E, CI2, SO2, SON2
C*
      RI = RKD*RNA*CI2/FLTX
```

SUBROUTINE BALANCE 73/74 TS TRACE FTN 4.6+460 78/08/21. 21.26

```
      ASOAP = SO2*S1/FLTX
      SON = SON2*DM/FLTX
      EX1 = 1. - EXP(-T2/THETA)
      C1 = RKMF*3.*DM/(RKP*RM*EX1)
  105 FORMAT(//,11X,*FLOW RATES IN (ML/MIN)*,19X,*CONCENTRATIONS OF REAC
     +TANTS  IN(MOL/L-H2O)*/14,6X,*CONCENTRATIONS OF REACTANTS OUT*,//)
  106 FORMAT(2X, *TIME =*, F7.2,* FHMS =*, F7.4,* FHIC =*, F7.4,* FHIV =
     +*, F7.4,* FHSV =*, F7.4,* CINF2 =*, F7.4,* CEF2 =*, F7.4,* CMF2 =*,
     + F7.4,*  L/L-H2O*,/2X, *THETA =*, F6.2, * DM =*, E9.3, * E =*,
     + E9.3,  24X, * CI2  =*, F7.4,* SO2  =*, F7.4,* SON2 =*, F7.4,/)
      RETURN
      END
```

SUBROUTINE MEASURE 73/74 TS TRACE FTN 4.6+460 78/08/21. 21.26

```
      SUBROUTINE MEASURE(LOI, X, Y)
C*
C*    PROVIDES NOISY MEASUREMENTS FOR THE MODEL'S STATES
C*
      DIMENSION X(3, 1), Y(3, 1), WN(200), WV(200)
      IF(LOI .GE. 1) GO TO 20
      N = 200
      SN = .1E17
      CALL RANGAU(WN, N, 5, SN)
      SV = .01
      CALL RANGAU(WV, N, 6, SV)
   20 IF(LOI .EQ. 0) GO TO 25
      Y(1, 1) = X(1, 1) + WN(LOI)
      IF(Y(1, 1) .LT. 0.) Y(1, 1) = 0.
      Y(2, 1) = X(2, 1) + WV(LOI)
      IF(Y(2, 1) .LT. 0.0001) Y(2, 1) = 0.
      Y(3, 1) = X(3, 1) + 4.5*WV(LOI)
      IF(Y(3, 1) .LT. .1) Y(3, 1) = 0.
   25 RETURN
      END
```

SUBROUTINE FILTER 73/74 TS TRACE

```
      SUBROUTINE FILTER
C*
C*    THE KALMAN FILTER GIVES THE BEST ESTIMATES OF THE STATE
C*    VECTOR GIVEN THE OBSERVED QUANTITIES Y AND U
      DIMENSION C1(3, 1), C2(3, 1), C3(3, 3), C4(3, 3)
      DIMENSION XKK1(3,1), XK1K1(3,1), PKK1(3,3), PK1K1(3,3)
      COMMON/THREE/ PHI(3,3), DL(3,2), UK1(2,1), YK(3,1), GH(3,1),
     + FV(3,3), XKK(3,1), GAIN(3,3), PKK(3,3), IL(3,1), C2(2, 2),UDP(2,1)
      COMMON/SEVEN/ XLIDE(200, 3), YMES(200, 3), XFILT(200, 3),
     + XNONL(200, 3), FPIN(200), FPEM(200), CINEM(200), CINEM(200),LOI
C*
      N1 = 1
      N2 = 2
      N3 = 3
      DO 12 I = 1, N3
      XK1K1(I, 1) = XKK(I, 1)
      DO 12 J = 1, N3
      PK1K1(I, J) = PKK(I, J)
   12 CONTINUE
C*
C*    OBTAIN THE PREDICTION X(K/K-1) AND THE COVARIANCE P(K/K-1)
      DO 10 I = 1, N3
      C1(I, 1) = C2(I, 1) = 0.
      DO 10 J = 1, N3
      C3(I, J) = C4(I, J) = 0.
   10 CONTINUE
      CALL MATMPY(PHI, XK1K1, C1, N3, N3, N1)
      CALL MATMPY(DL, UK1, C2, N3, N2, N1)
      CALL MATADD(C1, C2, XKK1, N3, N1)
      CALL MATMPY(PHI, PK1K1, C3, N3, N3, N3)
      CALL MATMPY(C3, PHI, C4, N3, N3, N3)
      CALL MATADD(C4, RW, PKK1, N3, N3)
C*
C*    CALCULATE THE FILTER GAIN K(K)
C*
      DO 20 I = 1, N3
      C1(I, 1) = C2(I, 1) = 0.
      DO 20 J = 1, N3
      C3(I, J) = C4(I, J) = 0.
   20 CONTINUE
      CALL MATADD(PKK1, RV, C3, N3, N3)
      C4(1, 1) = 1./C3(1, 1)
      C4(2, 2) = 1./C3(2, 2)
      C4(3, 3) = 1./C3(3, 3)
      CALL MATMPY(PKK1, C4, GAIN, N3, N3, N3)
C*
C*    ESTIMATE X(K/K) AND COMPUTE THE COVARIANCE P(K/K)
      DO 30 I = 1, N3
      C1(I, 1) = C2(I, 1) = 0.
      DO 30 J = 1, N3
      C3(I, J) = C4(I, J) = 0.
   30 CONTINUE
      CALL MATSUB(YK, XKK1, C1, N3, N1)
      CALL MATMPY(GAIN, C1, C2, N3, N3, N1)
```

SUBROUTINE FILTER 73/74 TS TRACE FTN 4.6+460 78/08/21. 21.26

```
      CALL MATADD(XKK1, C2, XKK, N3, N1)
      CALL MATMPY(GAIN, PKK1, C3, N3, N3, N3)
      CALL MATSUB(PKK1, C3, PKK, N3, N3)
      DO 50 I = 1, 3
      XFILT(LOI, I) = XKK(I, 1)
      YMES(LOI, I) = YK(I, 1)
   50 CONTINUE
C*
      WRITE(6, 40)
      WRITE(6, 42) (YK(I, 1), XKK(I, 1), (GAIN(I, J), J = 1, 3),
     + (PKK(I, J), J = 1, 3), I = 1, 3)
   40 FORMAT        (//, 4X, *MEASUREMENT*, 6X, *BEST E. X(K)*, 11X,
     + *GAIN MATRIX*,24X, *COVARIANCE MATRIX*, //)
   42 FORMAT(3X, E12.4, 4X, 7E12.4)
      RETURN
      END
```

SUBROUTINE MATRAN 73/74 TS TRACE FTN 4.6+460 78/08/21. 21.26

```
      SUBROUTINE MATRAN(A, B, M, N)
C*
C*    COMPUTES THE TRANSPOSE OF A MATRIX
C*
      DIMENSION A(M, N), B(N, M)
      DO 10 I = 1, M
      DO 10 J = 1, N
      B(J, I) = A(I, J)
   10 CONTINUE
      RETURN
      END
```

SUBROUTINE MATMPY 73/74 TS TRACE FTN 4.6+460 78/08/21. 21.26

```
      SUBROUTINE MATMPY(A, B, C, M, N, L)
C*
C*    A SUBROUTINE FOR MATRIX MULTIPLICATION
C*
      DIMENSION A(M, N), B(N, L), C(M, L)
      DO 10 I = 1, M
      DO 10 J = 1, L
      C(I, J) = 0.
      DO 10 K = 1, N
      C(I, J) = C(I, J) + A(I, K)*B(K, J)
   10 CONTINUE
      RETURN
      END
```

```
      SUBROUTINE LINOTE(SX, SRO, AP, DES, CONT, FI, DL)
C*
C*    ESTABLISHES THE STRUCTURE OF A AND B MATRICES BY EFFECTIVELY
C*    FACTORING OUT X AND U FROM THE NONLINEAR FUNCTION(X,U,T)
C*    COMPUTES THE FI AND DL MATRICES OF THE CORRESPONDING DISCRETE SYSTEM
      DIMENSION FI(3, 3), DL(3, 2), CONT(2, 1), CNT(3, 1), CH(3, 1),
     + CA(3, 1)
      COMMON/TW/ PKP, PKMF, PNA, DP, CP, SMC1, XC, Z, S1, SOLM, HM,
     + PKD, TH(4), SIT, FHMS, FHIC, FHIV, FHSV, RTH, PTH, RIN1, RIN2,
     + PS1, RS2, THETA, SON, RI, ASOAP, C1, E, SMC, TSPL, VREC
      COMMON/EQUP/ XKNL(3, 1), XKL(3, 1), XKL(3, 1), PART
      COMMON/SEVEN/ XLIDE(200, 1), YMES(200, 3), YFILT(200, 1),
     + XNONL(200, 3), PAIN(200), PREM(300), CIAIN(200), CIAEN(200),LDI
C*
      N3 = 3
      RT = THETA*60.
      CNT(1, 1) = CONT(1, 1)
      CNT(2, 1) = CONT(2, 1)
      CNT(3, 1) = 0.
      IF(SX -XC) 54, 54, 55
   54 XC1 = XC
      GO TO 56
   55 XC1 = SX
   56 RMP = (1.-XC1)*DM/(1.-XC1*(1.-DP/CP))
      GVOL = RKP*RMP*SRO/(RNA*DP)
      CONV = GVOL*DP/SON
      EX = EXP(-TSPL/THETA)
      EX1 = RT*(1. - EX)
      FN = (XKNL(1,1) - PART*EX)/EX1
      IF(FN .LE. 0.) FN = 0.
C*
C*    COMPUTE THE CONSTANT MATRICES OF THE DISCRETE SYSTEM
      DO 110 I = 1, N3
      DO 110 J = 1, N3
      FI(I, J) = 0.
      IF(I .EQ. J) FI(I, J) = EX
  110 CONTINUE
      U1 = CNT(1, 1)*2.
      U2 = CNT(2, 1)*2.
      DL(1, 1) = FN/U1*EX1
      DL(1, 2) = FN/U2*EX1
      DL(2, 1) = GVOL/U1*EX1
      DL(2, 2) = GVOL/U2*EX1
      DL(3, 1) = CONV/U1*EX1
      DL(3, 2) = CONV/U2*EX1
C*
      CALL MATMPY(FI, XKL1, CH, 3, 3, 1)
      CALL MATMPY(DL, CONT, CA, 3, 2, 1)
      CALL MATADD(CH, CA, XKL, 3, 1)
      WRITE(6, 150)
      WRITE(6, 152) (XKNL(I,1), XKL(I,1), FI(I,1), FI(I,2), FI(I,3),
     + XKL1(I,1), DL(I,1), DL(I,2), CNT(I, 1), I = 1, 3)
      DO 10 I = 1, N3
      XKL1(I, 1) = XKL(I, 1)
      XLIDE(LDI, I) = XKL(I, 1)
```



```
   10 CONTINUE
  150 FORMAT(5X, "NON-LINEAR", 7X, "LINEAR X(K)", 11X, "PHI MATRIX",
     + 17X, " X(K-1)", 7X,"DL MATRIX", 7X," U(K-1) ", //)
  152 FORMAT(3X, E12.4, 4X, 6E12.4)
      RETURN
      END
```



```
      SUBROUTINE ACTION(NC, UK1)
C*
C*    SETS THE VARIABLE FLOW RATES
      DIMENSION UK1(2, 1), A(3, 3), B(3)
      COMMON/TW/ RKP, PKMF, PNA, DP, CP, SMC1, XC, Z, S1, SOLM, HM,
     + PKD, TH(4), SIT, FHMS, FHIC, FHIV, FHSV, RTH, PTH, RIN1, RIN2,
     + PS1, RS2, THETA, SON, RI, ASOAP, C1, E, SMC, TSPL, VREC
C*
      B(1)    =(FHMS*RTH + FHIC)*.01
      B(2)    = FHIC*RIN1
      B(3)    = FHMS*RS1*RTH
      A(1, 1) = .01
      A(1, 2) = A(1, 3) =-.01
      A(2, 3) = A(3, 2) = 0.
      A(2, 2) = -RIN2
      A(3, 3) = -RS2
   22 A(2, 1) = UK1(1, 1)
      A(3, 1) = UK1(2, 1)
      CALL SIMQ(A, B, 3, IER)
      WRITE(6, 885) IER
  885 FORMAT(I5)
      IF(B(2) .LT. 0.) B(2) = 0.
      IF(B(3) .LT. 0.) B(3) = 0.
      IF(B(2) .GT. 12.5) B(2) = 12.5
      IF(B(3) .GT. 12.5) B(3) = 12.5
      FHIV = B(2)
      FHSV = B(3)
   26 RETURN
      END
```



```
      SUBROUTINE MATSUB(A, B, C, M, N)
C*
C*    A SUBROUTINE FOR MATRIX SUBTRACTION
      DIMENSION A(M, N), B(M, N), C(M, N)
      DO 10 I = 1, M
      DO 10 J = 1, N
      C(I, J) = A(I, J) - B(I, J)
   10 CONTINUE
      RETURN
      END
```

```
      C*    SUBROUTINE CONTROL(NC, NF)
      C*
      C*    COMPUTE THE OPTIMAL FEEDBACK CONTROL FOR THE LINEARIZED SYSTEM
      C*    WHICH SATISFIES A LINEAR QUADRATIC PERFORMANCE INDEX
            DIMENSION CI(3, 6), CIT(6, 3), CIH(2, 6), CIHT(6, 2), Q2HT(6, 2),
           + Q2H(2, 6), DLNT(2, 6), FIN(6, 6), DLN(6, 2), PPK(6, 6),
           + CLK(2, 6), Q1H(6, 6), XH(6, 1)
            DIMENSION C1(6, 3), C2(2, 6), C3(2, 6), C4(2, 2), C5(2, 2), C6(6,6),
           + C7(6, 6), C8(6, 6), C9(6, 6)
            COMMON/THREE/ PHI(3,3), DL(3,2), UK1(2,1), YK(3,1), SW(3,1),
           + PV(3,3), XKK(3,1), GAIN(3,3), FKK(3,3), Q1(3,3),Q2(2, 2),UOP(2,1)
      C*   ,COMMON/FIVE/ XKO(3, 1), UKO(2,1), SON2, SO2, CI2, T2
            N1 = 1
            N2 = 2
            N3 = 3
            N4 = 4
            N5 = 5
            N6 = 6
      C*
      C*
      C*    CLEAR AND SET WEIGHTING MATRICES
            IF(NC .GE. 1) GO TO 20
            DO 22 I = 1, N3
            DO 22 J = 1, N3
            CI(I, J) = CIT(I, J) = 0.
            IF(I .EQ. J) CI(I, J) = CIT(I, J) = 1.
         22 CONTINUE
            DO 24 I = 1, N3
            DO 24 J = N4, N6
            CI(I, J) = CIT(J, I)= 0.
         24 CONTINUE
            CIT(N4, N3) = CI(N3, N4) = -1.
            DO 26 I = 1, N6
            DO 26 J = 1, N6
            FIN(I, J) = 0.
         26 CONTINUE
            FIN(N4, N4)=FIN(N5,N5)=FIN(N6,N6)=1.
            DO 28 I = 1, N6
            DO 28 J = 1, N2
            DLN(I, J) = 0
            CIH(J, I) = CIHT(I, J) = 0.
         28 CONTINUE
            CIHT(N5,N1)=CIHT(N6,N2)=CIH(N1,N5)=CIH(N2,N6) = -1.
            CALL MATMPY(CIT, Q1, C1, N6, N3, N3)
            CALL MATMPY(C1, CI, Q1H, N6, N3, N6)
            DO 12 I = 1, N2
            DO 12 J = 1, N2
            I1 = I + N4
            J1 = J + N4
            Q1H(I1, J1) = Q2(I, J)
         12 CONTINUE
            CALL MATMPY(CIHT, Q2, Q2HT, N6, N2, N2)
            CALL MATMPY(Q2, CIH, Q2H, N2, N2, N6)
            XH(N4, N1) = -XKO(N1, N1)
            XH(N5, N1) = -UKO(N1, N1)
```

SUBROUTINE CONTROL 73/74 TS TRACE FTN 4.6+460 78/05/21. 21.

```
            XH(N6, N1) = -UKO(N2, N1)
         20 CONTINUE
            IF(NC .EQ. 0) GO TO 475
      C*
      C*    FORM THE AUGMENTED MATRICES FIN AND DLN
            DO 32 I = 1, N3
            XH(I, 1) =-XKK(I, 1)
            DO 32 J = 1, N3
            FIN(I, J) =PHI(I, J)
         32 CONTINUE
            DO 36 I = 1, N3
            DO 36 J = 1, N2
            DLN(I, J) = DL(I, J)
         36 CONTINUE
      C*
      C*    GENERATE THE CONTROL MATRIX CLK BY SOLVING THE RECURSIVE SET
      C*    OF MATRIX EQUATIONS
            DO 40 I = 1, N6
            DO 40 J = 1, N6
            PPK(I, J) = Q1H(I, J)
         40 CONTINUE
            NH = NF - 3
            WRITE(6, 470)
            DO 42 L = 1, NF
            CALL MATRAN(DLN, DLNT,N6, N2)
            CALL MATMPY(DLNT, PPK, C3, N2, N6, N6)
            CALL MATADD(C8, Q2, C5, N2, N2)
            CALL MATINV(C5, C4, N2)
            CALL MATMPY(C3, FIN, C2, N2, N6, N6)
            CALL MATADD(Q2H, C2, C3, N2, N6)
            CALL MATMPY(C4, C3, CLK, N2, N2, N6)
      C*
            CALL MATMPY(DLN, CLK, C6, N6, N2, N6)
            CALL MATSUB(FIN, C6, C7, N6, N6)
            CALL MATRAN(FIN, C8, N6, N6)
            CALL MATMPY(C9, PPK, C9, N6, N6, N6)
            CALL MATMPY(C9, C7, C9, N6, N6, N6)
            CALL MATMPY(Q2HT, CLK, C9, N6, N2, N6)
            CALL MATSUB(Q1H, C9, C7, N6, N6)
            CALL MATADD(C9, C7, PPK, N6, N6)
            IF(L .LE. NH) GO TO 42
            WRITE(6, 445) L, ((CLK(I, J), J = 1, 6), I = 1, 2)
         42 CONTINUE
      C*
      C*    COMPUTE THE OPTIMAL FEEDBACK SETTINGS
            CALL MATMPY(CLK, XH, UOP, N2, N6, N1)
            WRITE(6, 446) UOP(1, 1), UOP(2, 1)
            WRITE(6, 44)
         44 FORMAT(//, 1(2X, *---------*))
        445 FORMAT(12X, I5, 6E12.4,/17X, 6E12.4,//)
        446 FORMAT (/, 15X, *OPTIMAL INLET CONCENTRATIONS*//, 19X,*INITIATOR*,
           + 2X, *EMULSIFIER*, //18X, 2E12.4)
        470 FORMAT(//, 40X, *FEEDBACK CONTROL MATRIX*,/1.X, *ITER.*,/ )
        475 RETURN
            END
```

```
SUBROUTINE PRIPLT     73/74    TS TRACE
      C*    SUBROUTINE PRIPLT(N)
      C*
      C*    PRINTS AND PLOTS RESULTS
            COMMON/ONE/ T(900), PNP(900), PNAC(900), VCL(900), AREA(900),
           * X(900), FSA(900), AVD(900), FGP(900), IGCN(900)
            COMMON/SEVEN/ XLIDE(200, 3), YMES(200, 3), XFILT(200, 3),
           * XMGNL(200, 3), FSIN(200), FREM(300), CININ(200), CINEM(200),LDI
      C*    DATA SSIN, SSEM, FSSIN, FSTEM, XCONS/.0100,.010,4.29,.09,.75/
            WRITE(6, 301)
            DO 550 J = 1, N
            WRITE(6, 300) J, T(J), PNP(J), VCL(J), AREA(J), FSA(J), X(J),
           * PNAC(J), AVD(J), FGP(J), IGCN(J)
        550 CONTINUE
            DO 311 K = 1, N, 2
            TT = T(K)
            X1 = X(K)
            CALL PLOTPT(TT, X1, 4)
        311 CONTINUE
            CALL OUTPLT
            WRITE(6, 305)
            DO 374 K = 1, N, 2
            TT = T(K)
            R = PNP(K)
            CALL PLOTPT(TT, R, 4)
        374 CONTINUE
            CALL OUTPLT
            WRITE(6, 306)
            DO 393 K = 1, N, 2
            TT = T(K)
            R = FSA(K)
            CALL PLOTPT(TT, R, 4)
        393 CONTINUE
            CALL OUTPLT
            WRITE(6, 401)
            DO 600 K = 1, N, 2
            CALL PLOTPT(T(K), AREA(K), 4)
        600 CONTINUE
            CALL OUTPLT
            WRITE(6, 601)
            DO 602 K = 1, N, 2
            CALL PLOTPT(T(K), AVD(K), 4)
        602 CONTINUE
            CALL OUTPLT
            WRITE(6, 603)
            DO 373 K = 1, N, 2
            TT = T(K)
            R = PNAC(K)
            CALL PLOTPT(TT, R, 4)
        373 CONTINUE
            CALL OUTPLT
            WRITE(6, 307)
      C*
            I = 1
            DO 835 K = 1, LDI
            I = I + .5
```

```
SUBROUTINE PRIPLT     73/74    TS TRACE                    FTN 4.6+460        78/08/21. 21

            TT = T(I)
            CALL PLOTPT(TT,RNP(I), 4)
            CALL PLOTPT(TT,XLIDE(K, 1), 2)
            CALL PLOTPT(TT,YMES(K, 1), 1)
        835 CONTINUE
            CALL OUTPLT
            WRITE(6, 935)
            I = 1
            DO 836 K = 1, LDI
            I = I + 5
            TT = T(I)
            CALL PLOTPT(TT,RNP(I), 4)
            CALL PLOTPT(TT,XFILT(K, 1), 2)
        836 CONTINUE
            CALL OUTPLT
            WRITE(6, 936)
            I = 1
            DO 836 K = 1, LDI
            I = I + 5
            TT = T(I)
            CALL PLOTPT(TT,VCL(I), 4)
            CALL PLOTPT(TT,XLIDE(K, 2), 2)
            CALL PLOTPT(TT,YMES(K, 2), 1)
        836 CONTINUE
            CALL OUTPLT
            WRITE(6, 936)
            I = 1
            DO 839 K = 1, LDI
            I = I + 5
            TT = T(I)
            CALL PLOTPT(TT,VCL(I), 4)
            CALL PLOTPT(TT,XFILT(K, 2), 2)
        839 CONTINUE
            CALL OUTPLT
            WRITE(6, 939)
            SUMPE = 0.
            SUMXX = 0.
            I = 1
            DO 837 K = 1, LDI
            I = I + 5
            TT = T(I)
            CALL PLOTPT(TT,X(I), 4)
            CALL PLOTPT(TT,XLIDE(K, 3), 2)
            CALL PLOTPT(TT,YMES(K, 3), 1)
            SUMPE = SUMPE + (XCONS - YMES(K, 3))**2.
            SUMXX = SUMXX + (XCONS - X(I))**2.
        837 CONTINUE
            CALL OUTPLT
            WRITE(6, 937)
            SUMFL = 0.
            I = 1
            DO 840 K = 1, LDI
            I = I + 5
            TT = T(I)
            CALL PLOTPT(TT,X(I), 4)
            CALL PLOTPT(TT,XFILT(K, 3), 2)
            SUMFL = SUMFL + (XCONS - XFILT(K, 3))**2.
```

```
      SUBROUTINE PRIPLT     73/74   TS TRACE
  115           940 CONTINUE
                    CALL OUTPLT
                    WRITE(6, 940)
                C*
  120               SUMEM = 0.
                    SUMIN = 0.
                    I = 1
                    DO 105 K = 1, LOI
                    I = I + 5
                    IT = T(I)
  125               CALL PLOTPT(IT,FRIN(K), 4)
                    CALL PLOTPT(IT,FREM(K), 2)
                    SUMEM = SUMEM + (FREM(K)-FREM(K))**2.
                    SUMIN = SUMIN + (FRIN(K)-FRIN(K))**2.
  130           105 CONTINUE
                    CALL OUTPLT
                    WRITE(6, 110) SUMXX, SUMME, SUMFL, SUMIN, SUMEM
                    I = 1
                    DO 106 K = 1, LOI
  135               I = I + 5
                    WRITE(7, 108) K, FRIN(K), FREM(K), X(I), XFILT(K, 3), PNP(I),
                   + XFILT(K, 1)
                C*  106 CONTINUE
  140               108 FORMAT(I4, 2F10.4,.4E12.4)
                    110 FORMAT(//, 5E12.4)
                    300 FORMAT(I5, F10.4, 4E14.5, I3)
                    301 FORMAT
                   +    (1H1, 2X, *NO*, 5X, *TIME*, 7X, *TOTAL N*, 9X,
  145              +*POL.VOL*, 4X, *PART. AREA*, 5X, *SOAP CON.*, 4X, *CONVERSION*,
                   +4X, *RAD./PART.*,5X,*AVE. DIA. *, 4X, *PAR. GENERATION*, ///)
                    305 FORMAT(//, 20X, *---CONVERSION VERSUS TIME---*,)
                    306 FORMAT(//, 20X, *---TOTAL NUMBER OF PARTICLES VERSUS TIME---*,)
                    401 FORMAT(//,20X, *--- FREE SOAP CONCENTRATION---*,)
                    601 FORMAT(//, 20X, *  TOTAL PARTICLE AREA VERSUS TIME   *,)
  150               603 FORMAT(//, * AVERAGE PARTICLE DIAMETER *,)
                    307 FORMAT(//, 20X, *---AVERAGE NUMBER OF RADICALS  VERSUS TIME---*, )
                    325 FORMAT(1H1, 5X, *MONOMER CONCENTRATION  *, 5X, *EMULSIFIER CONCEN
                   +TRATION*, 5X, *INITIATOR CONCENTRATION *, 5X, *RESIDENCE TIME*,//
                   + 16X, * L/L-H2O*, 23X, *MOL/L-H2O*, 19X, *MOL/L-H2O*, 16X, *SEC*,
  155              + //, 3(16X, F10.3, 4X), 4X, F10.1, //)
                    709 FORMAT(8F10.0)
                    935 FORMAT(//, 10X, *--NUMBER OF PARTICLES VERSUS TIME--
                   + DISCRETE MEASUREMENT RESPONSE*)
                    938 FORMAT(//, 10X, *--NUMBER OF PARTICLES VERSUS TIME--
  160              + FILTERED RESPONSE*)
                    936 FORMAT(//, 10X, *--POLYMER VOLUME VERSUS TIME--
                   + DISCRETE MEASUREMENT RESPONSE*)
                    939 FORMAT(//, 10X, *--POLYMER VOLUME VERSUS TIME--
                   + FILTERED RESPONSE*)
  165               937 FORMAT(//, 10X, *--CONVERSION VERSUS TIME--
                   + DISCRETE MEASUREMENT RESPONSE*)
                    940 FORMAT(//, 10X, *--CONVERSION VERSUS TIME--
                   + FILTERED RESPONSE*)
                    RETURN
                    END
```

NONLINEAR

NONLINEAR

NONLINEAR

NONLINEAR

NONLINEAR

NONLINEAR

```
      SUBROUTINE MATINV     73/74   TS TRACE                FTN 4.6+460        78/08/21. 21.
                C*    SUBROUTINE MATINV(SS, INVRSE, N)
                C*
                C*    A   SUBROUTINE  FOR  MATRIX  INVERSION
                C*
  5             C*    REAL S(10, 20), SS(N,N), INVRSE(N, N)
                      DO 1 I = 1, N
                      DO 1 J = 1, N
                    1 S(I, J) = SS(I, J)
  10                  J1 = N + 1
                      J2 = 2 * N
                      DO 2 I = 1, N
                      DO 2 J = J1, J2
  15                2 S(I,J) = 0.0
                      DO 3 I = 1, N
                      J = I + N
                    3 S(I, J) = 1.0
                C*
  20            C*    START  THE  PIVOTIAL  CONDENSATION
                C*
                      DO 610 K = 1, N
                      KP1 = K + 1
                      IF(K .EQ. N) GO TO 500
                      L = K
  25                  DO 400 I = KP1, N
                  400 IF (ABS(S(I,K)) .GT. ABS(S(L,K))) L = I
                      IF (L .EQ. K) GO TO 500
                      DO 410 J = K, J2
  30                  TEMP = S(K, J)
                      S(K, J) = S(L, J)
                  410 S(L, J) = TEMP
                  500 DO 501 J = KP1, J2
                  501 S(K, J) = S(K, J) / S(K, K)
  35                  IF (K .EQ. 1) GO TO 600
                      KM1 = K-1
                      DO 510 I = 1, KM1
                      DO 510 J = KP1, J2
                  510 S(I, J) = S(I, J) - S(I, K) * S(K, J)
  40                  IF (K .EQ. N) GO TO 700
                  600 DO 610 I = KP1, N
                      DO 610 J = KP1, J2
                  610 S(I, J) = S(I, J) - S(I, K) * S(K, J)
                  700 DO 701 I = 1, N
  45                  DO 701 J = 1, N
                      K = J + N
                  701 INVRSE(I, J) = S(I, K)
                      RETURN
                      END
```

```
      SUBROUTINE MATADD     73/74   TS TRACE                FTN 4.6+460        78/08/21. 21.
                C*    SUBROUTINE MATADD(A, B, C, M, N)
                C*
                C*    A SUBROUTINE FOR MATRIX ADDITION
                C*
  5                   DIMENSION A(M, N), B(M, N), C(M, N)
                      DO 10 I = 1, M
                      DO 10 J = 1, N
                      C(I, J) = A(I, J) + B(I, J)
  10                10 CONTINUE
                      RETURN
                      END
```

24 FLOW RATES IN (ML/MIN)

TIME = 151.00 FHMS =25.7100 FHIC =10.0000 FHIV = 4.1388 FHSV = 0.0000 INF2 = .0096 CEF2 = .0101 CMF2 = .4020 L/L-H2O
THETA = 30.11 OW = .305E-07 E = .517E+01 CONCENTRATIONS OF REACTANTS IN(MOL/L-H2O)
CONCENTRATIONS OF REACTANTS OUT CI2 = .0092 SO2 = .0109 SON2 = .4011

NON-LINEAR

.4125E+16
.8544E-01
.3941E+00

LINEAR X(K)

.4125E+16 .8470E+00
.8461E-01 0.
.3803E+00 0.

PHI MATRIX

0. 0. 0.
0. .8470E+00 0.
0. 0. .8470E+00

X(K-1)

.4870E+16
.8499E-01
.3846E+00

DL MATRIX

.6659E+04 .6367E+04 .9610E-02
.6565E+00 .6277E+00 .1005E-01
.2837E+01 .2713E+01 0.

U(K-1)

MEASUREMENT

.8376E+16
.7804E-01
.3509E+00

BEST E. X(K)

.1081E+17
.4095E-01
.3638E+00

.1403E+00
0.
0.

GAIN MATRIX

0. 0. 0.
0. .3262E+00 0.
0. 0. .3295E+00

COVARIANCE MATRIX

.8980E+33 0. 0.
0. .3262E-04 0.
0. 0. .6590E-03

ITER. FEEDBACK CONTROL MATRIX

8 0. 0. .5693E-02 -.6626E-02 -.9790E+00 -.2009E-01
0. 0. .2722E+00 -.3263E+00 .1005E+01 -.3942E-01

9 0. 0. .5693E-02 -.6626E-02 -.9790E+00 .2009E-01
0. 0. .2722E+00 -.3263E+00 .1005E+01 -.3942E-01

10 0. 0. .5693E-02 -.6626E-02 -.9790E+00 .2009E-01
0. 0. .2722E+00 -.3263E+00 .1005E+01 -.3942E-01

OPTIMAL INLET CONCENTRATIONS

INITIATOR EMULSIFIER

.9907E-02 .5540E-02

0

29 FLOW RATES IN (ML/MIN)

TIME = 155.00 FHMS =25.7100 FHIC =10.0000 FHIV = 4.2123 FHSV = 0.0000 INF2 = .0094 CEF2 = .0100 CMF2 = .4009 L/L-H2O
THETA = 30.06 OW = .297E-07 E = .504E+01 CONCENTRATIONS OF REACTANTS IN(MOL/L-H2O)
CONCENTRATIONS OF REACTANTS OUT CI2 = .0093 SO2 = .0108 SON2 = .4011

NON-LINEAR

.3493E+16

LINEAR X(K)

.3493E+16 .8468E+00

PHI MATRIX

0. 0.

X(K-1)

.4125E+16

DL MATRIX

0. 0.

U(K-1)

.9756E-02